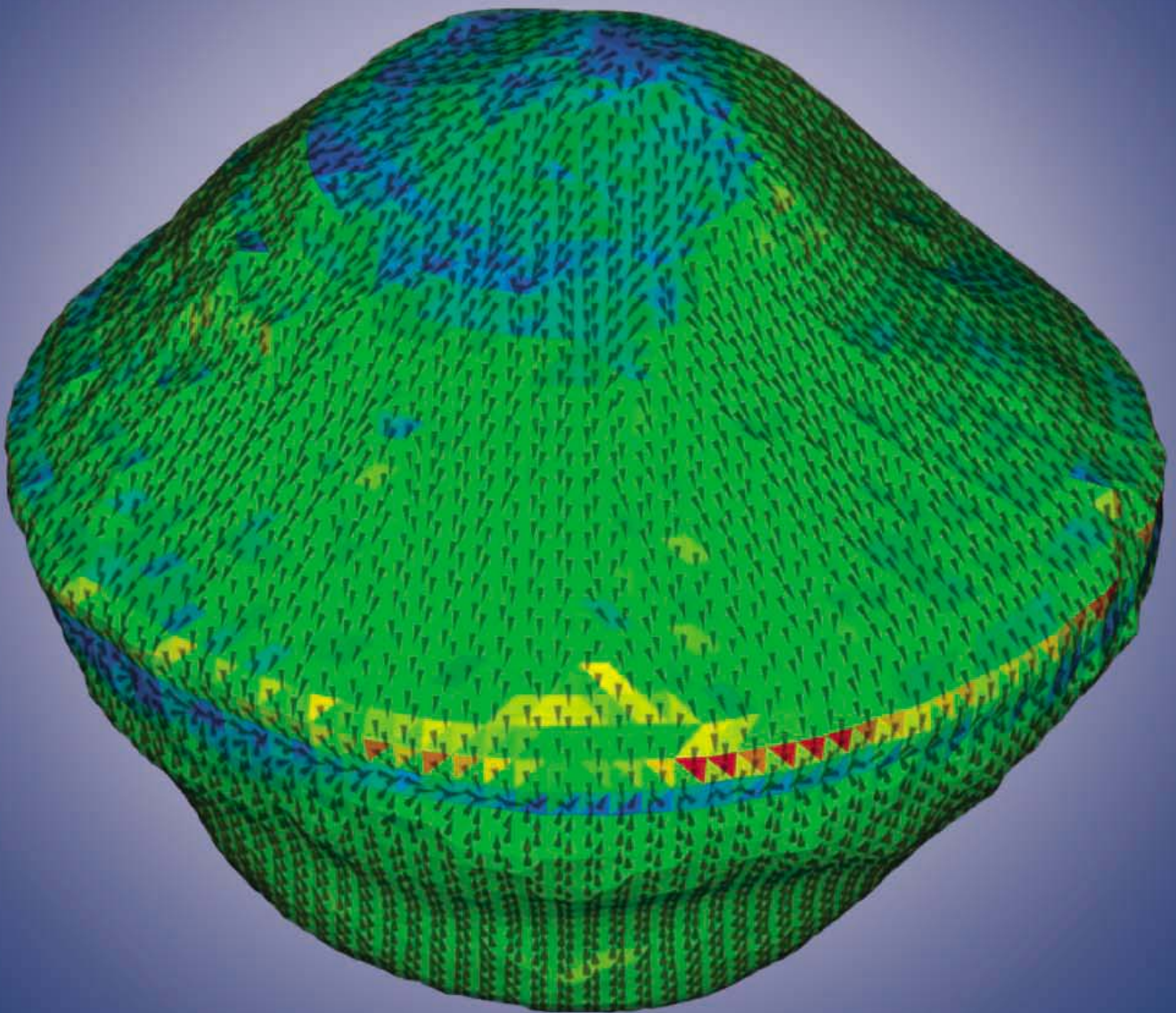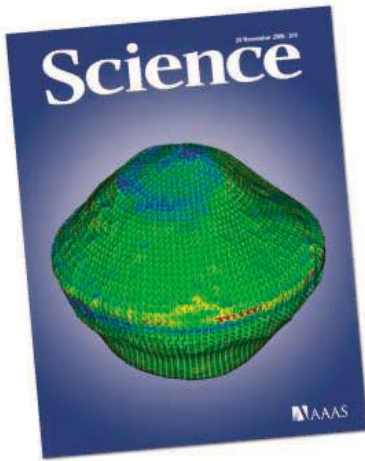# Science

COVER

A radar-derived model of Alpha, the larger half of the binary near-Earth asteroid (66391) 1999 KW4. Alpha is an unconsolidated aggregate 1.5 kilometers in diameter; its effective slope ranges from zero (blue) to 70° (red). Its rapid 2.8-hour rotation induces material to flow (arrowheads) from both the northern and southern hemispheres toward the equator. See pages 1276 and 1280.

Image: NASA/JPL

DEPARTMENTS

EDITORIAL

NEWS OF THE WEEK

NEWS FOCUS

1232

LETTERS

BOOKS *ET AL.*

EDUCATION FORUM

PERSPECTIVES

1244

Science

SCIENCE EXPRESS

www.scienceexpress.org

TECHNICAL COMMENT ABSTRACTS

REVIEW

1248 & 1267

BREVIA

RESEARCH ARTICLES

REPORTS

REPORTS *CONTINUED...*

1252, 1295, & 1298

AAAS
ADVANCING SCIENCE, SERVING SOCIETY

Wireless energy transfer in action.

SCIENCENOW

www.sciencenow.org DAILY NEWS COVERAGE

Dark Energy Made an Early Entry
The strange space-stretching stuff has been around for most of the universe's history.

The Ultimate "Flash Photography"
A burst of x-rays reveals the structure of a tiny object—before obliterating it.

Outlets Are Out
Researchers conceptualize a way to recharge electronic devices wirelessly.
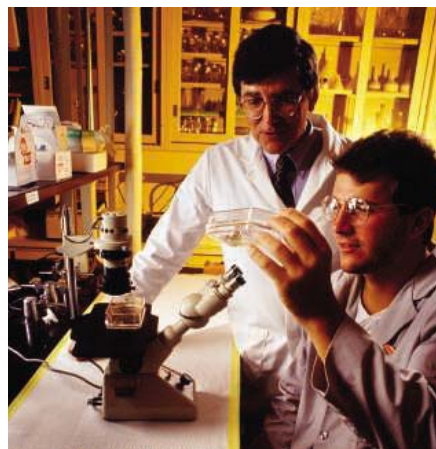
Spotting a good mentor.

SCIENCE CAREERS

www.sciencecareers.org CAREER RESOURCES FOR SCIENTISTS

GLOBAL: Mind Matters—Get Yourself Mentored
I. S. Levine
Learn how to spot a good mentor and cultivate a relationship to improve your prospects.

US: Saving Languages, Sustaining Communities
A. Sasso
Linguistics professor Melissa Axelrod works with Native American communities to rescue and revitalize languages.

US: Profile—Melanie Sanford
J. Austin
A series of fortunate events led this chemist to contribute to Nobel Prize–winning work, but her success is no accident.

GRANTSNET: International Funding Index
GrantsNet Staff
Read about the latest funding opportunities from Europe, Asia, and the Americas.
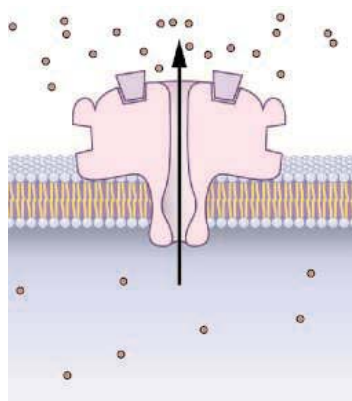
IP_3R releasing calcium.

SCIENCE'S STKE

www.stke.org
SIGNAL TRANSDUCTION KNOWLEDGE ENVIRONMENT

REVIEW: The Inositol 1,4,5-Trisphosphate Receptor (IP_3R) and Its Regulators—Sometimes Good and Sometimes Bad Teamwork
C. Choe and B. E. Ehrlich
Numerous cytosolic and endoplasmic reticular proteins interact with and regulate the IP_3R.

EVENTS
Browse through this calendar to find meetings or sessions focused on cell signaling.

SCIENCEPODCAST

Listen to the 24 November *Science* Podcast to hear about antipoaching measures in the Serengeti, questions surrounding carbon emission trading schemes, the population genetics of the typhoid bacterium, and more.
www.sciencemag.org/about/podcast.dtl

Separate individual or institutional subscriptions to these products may be required for full-text access.
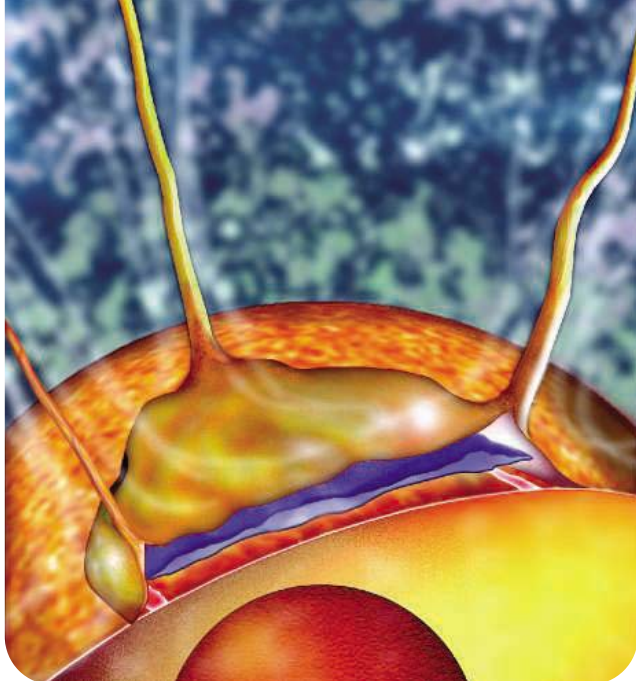
Heat Flow Below

Heat transfer across the core-mantle boundary (CMB) regulates not only the Earth's magnetic field through the geodynamo but also the style of mantle convection. Measuring heat transfer at such great depth is difficult, but mineral transitions within the mantle, which can be detected seismically, can provide insights. Post-perovskite (pPv) is the most extreme polymorph of per-ovskite, the primary mineral of the lower mantle, and may be abundant near the CMB. **Lay et al.** (p. 1272), have located a lens of material just a few hundred kilometers above the CMB beneath the Pacific Ocean that may be pPv. The heat flow in this region could be deduced by measuring the depth of the pPV lens seismically and by knowledge of pPv's mineral properties. Temperature gradients yield a heat flux comparable to the average at the Earth's surface as well as a lower limit to the heat flow.

Lessons of the Past

Conservation biology and practice are typically based on contemporary ecological information. **Willis and Birks** (p. 1261) review the need for a perspective that stretches further back in time, and discuss the potential contributions of paleoecological research to conservation biology.

Complex Behavior in Ruthenate Superconductor

The superconductor strontium ruthenate (Sr_2RuO_4) is a rather complex material with an unconventional (non–s-wave) pairing symmetry. Unlike other unconventional superconductors, such as the d-wave cuprates, theory suggested and experiments hinted at a p-wave symmetry and a pairing of triplet spins. Theorists also suggested the possibility of a complex p-wave symmetry that breaks time reversal symmetry. **Kidwingiri et al.** (p. 1267, published online 26 October; see the Perspective by **Rice**) use phase-sensitive Josephson junction interferometry to confirm the complex p-wave order parameter symmetry in Sr_2RuO_4, and also present direct evidence for the existence of coexisting chiral superconducting domains.

Seeing Alpha and Beta

Of the various binary objects in space, binary asteroids are the smallest, as well as the closest for observation. **Ostro et al.** (p. 1276, published online 12 October; see the cover) used radar to map the binary Earth-approaching asteroid (66391) 1999 KW4 and deduce its physical properties. Alpha, the main component, is an unconsolidated aggregate and spins on its axis every 2.8 hours. The smaller companion, Beta, is elongated and denser than Alpha. **Scheeres et al.** (p. 1280, published online 12 October) model the coupled orbital and rotational dynamics of the system. Alpha is spinning at a rate near its break-up speed, and the authors suggest that the system may have been put into its excited state by a close pass with the Sun or Earth. The binary asteroid may have ultimately originated from the disruption of a rubble-pile precursor.

Reevaluating Greenland Ice Sheet Melting

The rate at which Greenland Ice Sheet is melting appears to be accelerating. **Luthcke et al.** (p. 1286, published online 19 October; see the Perspective by **Cazenave**) report results from an analysis of data collected by GRACE (Gravity Recovery and Climate Experiment), the pair of satellites launched in 2002, that can follow melting by measuring tiny variations in gravity caused by the redistribution of Earth's mass. Like other recent studies, they find that Greenland is losing ice at an alarming rate, 101 ± 16 gigatons (Gt) of ice per year from 2003 to 2005, compared to the average of about 12 Gt of ice per year for the decade between 1992 and 2002, and they see that ice sheet appears to be losing mass along its southern edges and gaining slightly in its interior. However, the rate they have calculated is much less than other recent estimates, which are closer to 240 Gt of ice per year for the same period. Why the method used in this estimate is so much less than in other stories, and which estimate is correct, has yet to be resolved.

Not Getting Any Younger

Organic carbon in soils is the second largest active reservoir on Earth and exerts a key influence on the concentration of atmospheric CO_2, and about half of soil organic carbon is refractory organic carbon. **Smittenberg et al.** (p. 1283) compare the radiocarbon ages of terrestrial vascular plant waxes found in marine sediments with those of the surrounding sediments, and find that they become increasingly older throughout the course of the Holocene. They conclude that in soils that have developed since the last deglaciation, accumulation of refractory organic has continued for the duration of the Holocene and is ongoing.

Changes in the Deep

It is becoming increasingly possible to describe the history of biodiversity in ecological as well as taxonomic terms. **Wagner et al.** (p. 1289; see the Perspective by **Kiessling**) provide evidence for a marked change in the ecological structure of marine benthic communities after the largest of the mass extinctions, the end Permian. Using data from a large, open-source repository of fossil occurrence data, they chart the shifts in relative abundances in fossil communities during the Phanerozoic. Before the mass extinction, communities were dominated by sessile, suspension-feeding organisms, whereas afterward, there was a shift to communities dominated by mobile creatures.
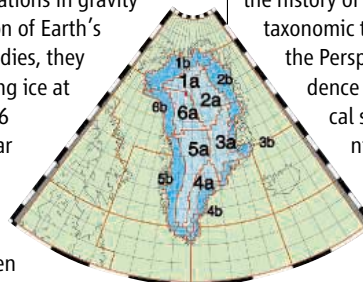
Expand Long Range dNTPack

Long Range PCR Products —
Now Within Reach

22 kb fragment from the human tPA gene

14.8 kb fragment from the mouse β-Globin gene
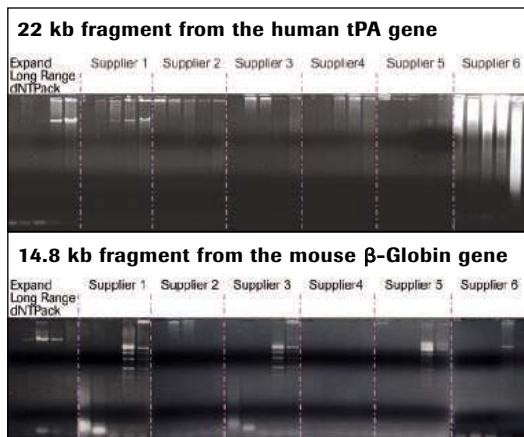
Result: Only Expand Long Range dNTPack enabled the highly specific amplification of both fragments from human and mouse genomic DNA.

Choose the new **Expand Long Range dNTPack** as your complete solution for the consistent amplification of PCR products of **5 to 25 kb** from genomic DNA. Order a single catalog number to obtain a sophisticated DNA polymerase blend, newly optimized buffer system, and ultrapure PCR-grade nucleotides.

- **Robust**: Amplify templates that other polymerases can't.

- **Specific**: Generate more of the product you want, less of what you don't want.

- **Time-tested**: Rely on this next-generation system from the company that pioneered long-template PCR with the launch of the Expand Long Template PCR System.

Request a free sample today!
Obtain the long PCR products your research requires by **requesting a free sample*** of Expand Long Range dNTPack at *www.long-range-pcr.com*

* Some conditions apply. Samples are limited. See website for details.

Roche Diagnostics

Roche Diagnostics GmbH
Roche Applied Science
68298 Mannheim
Germany

A Deadly Complement

So-called Dobzhansky-Muller genes interact to produce hybrid sterility. **Brideau *et al*.** (p. 1292; see the news story by **Pennisi**) have identified, cloned, and characterized the *Lethal hybrid rescue* (*Lhr*) gene in *Drosophila simulans,* which encodes a protein that localizes to heterochromatic regions of the genome. The proteins encoded by *Lhr* and *Hybrid male rescue (Hmr)* form a pair of Dobzhansky-Muller hybrid incompatibility genes, which appear to cause hybrid lethality only in a hybrid genetic background.

Mobilizing Nutrients into Wheat

Iron is a critical nutrient for plants as much as for the humans who eat them. In plants, iron is required for photosynthesis and respiration, but too much iron can be toxic (see the Perspective by **Gitlin**). **Kim *et al*.** (p. 1295, published online 2 November) provide insight into how plants collect and store iron while avoiding its toxic effects. Analysis of the vacuolar iron transport gene in *Arabidopsis* shows that the cellular vacuole is used for storage of iron. **Uauy *et al*.** (p. 1298) have identified the *TaNAM* gene, which regulates senescence, as well as the mobilization of nitrogen, zinc, and iron, from leaves to the developing grain. Cultivated wheat varieties have a nonfunctional copy of the *TaNAM-B1* gene. Introduction of the functional allele increases grain protein, Zn, and Fe, potentially improving the nutritional content of wheat.

Amateur Pathogen

Typhoid fever is caused by *Salmonella enterica* serovar Typhi, which mostly affects impoverished populations in the Southern Hemisphere. Notoriously, it can be carried asymptomatically by individuals who shed large quantities of bacteria. **Roumagnac *et al*.** (p. 1301) analyzed 105 strains from around the world and discovered a population structure best explained by neutral genetic drift in which the pre-Neolithic ancestral strain and intervening mutations still exist. Various haplotypes were probably distributed globally during acute epidemics followed by prolonged persistence in the gall bladder of asymptomatic carriers.

CREDIT: ROUMAGNAC ET AL.

Brain Versus Brawn

The clock genes that control circadian rhythms in mammals also contribute to other aspects of physiology, behavior, and health. One such clock gene, *Bmal1*, encodes a transcription factor whose inactivation in mice causes disturbances in circadian rhythms and alterations in activity level, body weight, and other physiological functions. By reexpressing the *Bmal1* gene in selective tissues in *Bmal1*-deficient mice, **McDearmon *et al*.** (p. 1304) show that the transcription factor exerts distinct tissue-specific functions. Circadian rhythmicity in the mutant mice was normalized only when *Bmal1* was expressed in the brain, whereas normalization of the animals' activity level and body weight required *Bmal1* expression in muscle.

Bacterial Assist for Chemotherapy

A major challenge in cancer chemotherapy is delivering cytotoxic drugs to tumors in sufficient quantities to kill the malignant cells while sparing normal cells. One promising strategy for tumor-targeted drug delivery involves encapsulation of drugs within liposomes. **Cheong *et al*.** (p. 1308) find that they can markedly enhance the efficacy of liposomal doxorubicin in mouse tumor models by prior injection of the mice with spores of *Clostridium novyi-NT*, an anaerobic bacterium that selectively infects tumors. *C. novyi-NT* encodes a secreted protein, "liposomase," that ruptures liposomes and promotes release of their cytotoxic cargo into the tumor.

Predicting What Comes Next

How does the brain make the perceptual decisions that lead to object recognition? Using functional magnetic resonance imaging, **Summerfield *et al*.** (p. 1311) observed predictive neural signals in the frontal cortex, which suggests that predictive coding accounts for perceptual inference. Moreover, direction-specific functional connectivity between the frontal and visual cortices was observed during perceptual decision-making.

Carbon Trading

William H. Schlesinger is dean of the Nicholas School of the Environment and Earth Sciences, Duke University, Durham, NC.

ENTHUSIASM IS SPREADING FOR CAP-AND-TRADE SYSTEMS TO REGULATE THE AMOUNT of CO_2 emitted to Earth's atmosphere. In 1990, the U.S. Environmental Protection Agency set a limit on SO_2 emissions from obvious point sources and allowed those who emit less than their quota to trade excess allowances. As a result, regional acid deposition was dramatically reduced. Can the world do the same for CO_2?

Fundamental differences in the biogeochemistry of SO_2 and CO_2 suggest that establishing a comprehensive, market-based cap-and-trade system for CO_2 will be difficult. For SO_2, anthropogenic point sources (largely coal-fired power plants), which are relatively easy to control, dominate emissions to the atmosphere. Natural sources, such as volcanic emanations, are comparatively small, so reductions of the anthropogenic component can potentially have a great impact, and chemical reactions ensure a short lifetime of SO_2 in the atmosphere. CO_2, in contrast, comes from many distributed sources, some sensitive to climate, others sensitive to human disturbance such as cutting forests. It is thus impossible to control all of the potential sources.

Human-derived emissions from fossil fuel combustion are one of the smaller components of the atmospheric flux of CO_2, which is dominated by exchange between forests and the oceans. During most of the past 10,000 years, the uptake and loss of CO_2 from forests and the oceans must have been closely balanced, because atmospheric CO_2 showed little variation until the start of the Industrial Revolution. CO_2 from coal, oil, and natural gas combustion now comes from many segments of society, including electric power generation, industry, home heating, and transportation. Unbalanced by equivalent anthropogenic sinks for carbon, fossil fuel emissions account for the vast majority of the rise of CO_2 in Earth's atmosphere. Caps on emissions, like those instituted for SO_2, will be difficult to institute if the burden of reducing CO_2 is to be borne equally by all emitters.

Because land plants take up CO_2 in photosynthesis and store the carbon in biomass, forests and soils seem to be attractive venues to store CO_2. Market-based schemes propose substantial payments and credits to those who achieve net carbon storage in forestry and agriculture, but these projected gains are often small and dispersed over large areas. We will need to net any such carbon uptake against what might have occurred without climate-policy intervention. Conversely, will Canada and Russia be billed for incremental CO_2 releases that stem from the warming of cold northern soils as a result of global warming from the use of fossil fuels worldwide?

If credit is given to those who choose not to cut existing forests, the increasing total demand for forest products will shift deforestation to other areas. Frequent audits will be needed to determine current carbon uptake, insurance will be necessary to protect past carbon credits from destruction by fire or windstorms, and payments will be necessary if the forest is cut. All these efforts will be costly to administer, diminishing the value of the rather modest carbon credits expected from forestry and agriculture.

Many environmental economists recognize that a tax or fee on CO_2 emission from fossil fuel sources is the most efficient system to reduce emissions and spread the burden equitably across all sources: industrial and personal. A tax on emissions of fossil fuel carbon could replace the equivalent revenue from income taxes, so the total tax bill of consumers would be unchanged. A higher tax on gasoline would preserve the personal right to drive a larger car or drive long distances, but it would also motivate decisions to do otherwise. A tax on emissions from coal-fired power plants, manifest in monthly electric bills, would motivate the use of alternative energies and energy-use efficiencies at home and in industry.

The biogeochemistry of carbon suggests that both emissions taxes and cap-and-trade programs will work best if restricted to sources of fossil fuel carbon. Other net sources and sinks of carbon in its global biogeochemical cycle are simply too numerous and usually too small to include in an efficient trading system. Simple, fair, and effective must be the hallmarks of policies that will wean us from the carbon-rich diet of the Industrial Revolution, and we must begin soon if we are to have any hope of stabilizing our climate.

– **William H. Schlesinger**

PSYCHOLOGY

Managing Terror

Our awareness that we exist exposes us, unfortunately, to the inescapable terror of dying. Jonas and Fischer have explored the role of religious beliefs in allowing people to manage their terror in situations where mortality is made salient. In particular, they focus on the distinction between extrinsic (searching for safety and solace) and intrinsic (searching for meaning and value) religious beliefs. Just after the November 2003 bombings in Istanbul, customers in a Munich coffee shop were more likely to rise in defense of their cultural worldview (to disagree with newspaper articles that were inconsistent with their own assessments of the likelihood of an attack in Germany) if they scored low on an intrinsic religiousness scale than if they scored high; this difference in behavior dissipated with time as the reminder of death became less salient. In follow-up experiments involving students from a Jesuit school and a local university, they found that intrinsically religious people did not think more about dying when reminded of mortality (in contrast to extrinsically oriented individuals) and that this capacity to buffer one's state of mind contributed to their not having to mobilize terror management defenses in the face of death. —— GJC

J. Pers. Soc. Psychol. **91**, 553 (2006).

BIOMEDICINE

Gastric Distress for Obestatin

In a developed world suffering an obesity epidemic, new reports of molecules that regulate appetite and body weight inevitably attract broad interest, and the secreted peptide obestatin (Zhang *et al.*, Research Articles, p. 996, 11 November 2005) was no exception. Derived from the same precursor as ghrelin (a peptide that promotes food intake and obesity in rodent models), obestatin was shown to have activities that oppose the effects of ghrelin: It suppressed food intake, delayed gastric emptying, and decreased body weight gain in rodents. These intriguing effects were mediated by its interaction with a G-protein–coupled receptor called GPR39.

Subsequent experiments in other laboratories suggest that obestatin may be regulating energy balance in a manner distinct from that originally proposed and/or that its effect on food intake is subtle. Moechars *et al*. found that mice genetically deficient in GPR39, the putative receptor for obestatin, gain weight more readily than their wild-type littermates, but they attributed this to the inhibitory effects of GPR39 on gastrointestinal motility rather than appetite, as food intake was similar for the mutant and wild-type mice. Nogueiras *et al*. injected rats with obestatin obtained from three different suppliers and found that obestatin had no effect on food intake, body weight, or other physiological parameters involved in energy balance. Importantly, neither group was able to detect expression of the GPR39 gene in the hypothalamus, the region of the brain targeted by most hormones associated with appetite control. — PAK

Gastroenterology **131**, 1131 (2006); *Endocrinology* 10.1210/en.2006-0915 (2006).

MATERIALS SCIENCE

Small and Strong

The intricate silica cell walls fabricated by the unicellular algae known as diatoms are highly porous and are produced with high fidelity. Diatoms have therefore been viewed as a possible platform for nanostructured materials synthesis. Hildebrand *et al.* have probed cell wall synthesis in the nanostructured form of *Thalassiosira pseudonana,* an organism whose genome has recently been sequenced. They studied a series of structural intermediates to unravel the chemical formation sequence and to ascertain when certain proteins come into play. At the earliest
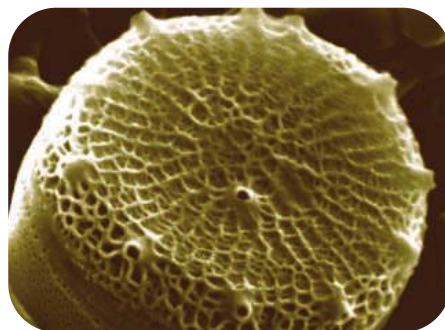
***T. pseudonana* cell wall.**

stages, they observed an outline of the valve with silica ribs radiating from the center. The rim structure then thickens, followed by a thickening of the rest of the valve structure. As the ribs form and fuse together, they give rise to a nanoporous structure with larger, more irregular pores than those formed earlier in the process. These observations confirm that the structure of *T. pseudonana* has been optimized to maximize strength with minimized material requirements, all the while allowing for the uptake and efflux of metabolites during this process. The authors hope in the long term to replicate and control many of these features through modification of the genome or through mixing of an appropriate array of polypeptides and polyamines to foster silica polymerization in vitro. — MSL

J. Mater. Res. **21**, 2689 (2006).

GEOCHEMISTRY

Postdiluvian Pb

Lead contamination of exposed soils in residential areas is a strong concern because of the danger that ingestion of the heavy metal can pose to children's health. One promising remediation strategy is the addition of a clean soil layer to the surface. Before Hurricane Katrina in August 2005, Mielke *et al.* had undertaken a study in which they were monitoring soil lead levels at 25 contaminated New Orleans properties after treatment with 15 cm of clean alluvium drawn from the Mississippi River. They now report the impact of flooding caused by the hurricane on these lead

levels. Although erosion and soil mixing might have been expected to substantially elevate surface lead levels, the authors found that the general increase on the flooded properties was relatively small, and consistent with a steady but slow rise observed in the series of measurements before the hurricane. Median lead levels were reduced from 1051 to 6 mg/kg by the treatment, subsequently rose to 10 mg/kg before the flooding, and were elevated after the hurricane to 16 mg/kg. The authors attribute this steady rise to resuspension and deposition of lead-bearing dust across the city. — JSY

Environ. Sci. Technol. **40**, 10.1021/es061294c (2006).

ATMOSPHERIC SCIENCE
Clean Competition

Concern has arisen about air quality during planning for the August 2008 Olympic Games in Beijing, China, as so many of the scheduled competitions are intensely aerobic, and summer pollution levels in Beijing can be high. Both the national and municipal governments there have introduced a range of measures to reduce locally generated air pollution, a strategy almost certain to have a positive effect. However, air pollution can also arise

View of Beijing.

from remote generation sources, and thus local mitigation efforts may not be sufficient to meet the stated objectives of the Chinese officials toward air quality improvement. Streets *et al.* assess the importance of outside sources as contributors of two significant regional and urban air pollutants: fine particulate matter and ozone. Using a combination of emissions data and modeling, they conclude that sources far from the city exert a substantial influence on air quality in Beijing, and that fine particulate matter and ozone could exceed healthful levels in the unfortunate event of unfavorable meteorological conditions, even if local sources were eliminated entirely. The authors suggest that additional emission control measures in Beijing's populous, industrialized neighboring provinces should be considered. — HJS

Atmos. Environ. 10.1016/j.atmosenv.2006.08.046 (2006).

IMMUNOLOGY
Strengthening A Weak Choice

The cell surface co-receptors CD8 and CD4 define two classes of T cells and facilitate the recognition of antigens presented by the class I and class II major histocompatibility complex (MHC) proteins, respectively. They are also critical in the development and selection of T cells in the thymus. One model proposes that in double-positive thymocytes (those expressing both CD4 and CD8), the stronger signals delivered by CD4 direct T cells toward a single positive CD4 fate, whereas weaker signals emanating from CD8 contribute to class I recognition, resulting in a program of continued CD8 expression and loss of CD4. Erman *et al.* generated transgenic mice in which a chimeric CD8 protein carrying the intracellular CD4 domain was expressed under the normal CD8 regulatory elements. The increase in signal strength via the co-receptors in class I–restricted thymocytes did not alter lineage choice; rather, an increase in the number of cells entering the single positive CD8 T cell pool was seen. Hence, the more potent (in terms of downstream Lck kinase activation) intracellular CD4 domain could explain the familiar bias in the number of CD4 over CD8 T cells seen in the mammalian thymus. — SJS

J. Immunol. **177**, 6613 (2006).

BIOCHEMISTRY
Grabbing a Helping Strand

Helicases are a highly conserved class of enzymes that use ATP to unwind or destabilize DNA and RNA double helices. These enzymes are thought to latch onto a single-stranded (ss) region of the duplex, the "loading strand," and then to motor along the strand, either in the 5' or 3' direction, peeling apart the duplex as they go. Puzzlingly, some RNA helicases can unwind duplexes regardless of which strand they start from. Yang and Jankowsky have analyzed the unwinding activity of the yeast RNA helicase Ded1, which is involved in translation initiation. Although Ded1 cannot unwind DNA-DNA duplexes, it can load onto ssDNA (of either polarity), "travel" across a short region of double-stranded DNA (without unwinding it), and tease apart a DNA-RNA duplex on the far side. Indeed, the loading strand need only be nearby and not necessarily covalently linked to the target duplex. Thus, the loading strand may serve to increase the concentration of Ded1 in the vicinity of the target. An unwinding mechanism in which the enzyme doesn't travel extensively may be well suited for local conformational changes in protein–nucleic acid complexes, something this class of helicases specializes in. — GR

Nat. Struct. Mol. Biol. **13**, 981 (2006).

SILENT FLIER

Engineers with a transatlantic think tank, the Cambridge-MIT Institute (CMI), this month declared success at designing a superquiet passenger jet.

The 215-seater, called the SAX-40, shown in a computer model above, would be so quiet you would scarcely hear its landing noise above the traffic if you were standing near the airport boundary, say the design team of 40 students and engineers. Plus, they claim, it would burn 25% less fuel than a comparable plane today.

The key to the SAX-40's low profile is its use of a "flying wing" design rather than the traditional cylinder with fins. This gives it strong lift at low speed, reducing the distance and power needed for takeoff and landing—and also reducing fuel requirements, says Alexander Quayle, a Ph.D. candidate at the University of Cambridge who worked on smoothing the undercarriage. In addition, the engine intakes are mounted on top to send noise skyward, and edges are smoothed to reduce noisy airflow fluctuations.

The U.K. government sank about $4.4 million into the project, mainly to give CMI students a chance to work with industry people. But whether SAX-40 ever gets off the ground will depend on how promising it looks to the private sector. "We got a very warm welcome from Boeing," says Quayle. The Seattle, Washington–based company is one of about 30 backers who made in-kind contributions to the 3-year project, using its software to test the airframe in simulated flight.

UNDERCOVER FROG >>

A 3-centimeter tree frog that resembles a splotch on a leaf makes its scientific debut this month in *Memoirs of the Queensland Museum.* Named *Litoria richardsi* after one of its discoverers, herpetologist Stephen Richards of the South Australian Museum in Adelaide, it was found near a swamp in Papua New Guinea. Herpetologist Michael Cunningham of the University of the Free State in Bloemfontein, South Africa, says the amphibian—one of only two such frogs found— lives high in the rainforest canopy and probably glides through the air using its highly webbed feet.

Homage to Washday

It's easy to overlook mundane scientific accomplishments, but the American Chemical Society (ACS) remembers. This year, its "Landmarks of Chemistry" project is honoring a humble laundry detergent: Tide.

Introduced 60 years ago last month, Procter and Gamble's Tide was the first synthetic detergent that could clean really dirty clothes in hard or soft water without, like soap, leaving scummy residues.

Both synthetic detergents and soap contain molecules that bond to water on one end and fats at the other, pulling oil and

1946 Tide ad.

grease off clothes into water. But unlike soap, such detergents are not derived from animal or vegetable fats, relying instead on a synthetic molecule. The first product, Dreft, was so-so as a cleaner. But with Tide, scientists learned to balance surfactants, which let water penetrate clothes, and "builders," which help the surfactants reach embedded dirt. In early attempts, the chemicals in hard water reacted with builders to stiffen clothes—"Your clothes were clean, but you couldn't walk," says Landmarks project manager Judah Ginsberg. After further tinkering, Tide was launched in 1946, the same year the automatic washing machine was introduced. It was a smash hit, becoming the century's best-selling laundry detergent.

An ACS landmark "has to have had an impact on both the public and chemistry," says retired ACS executive Michael Bowen. "[Tide] was an excellent piece of chemical development."

NETWATCH >>
Crop Circles

Very like a Paul Klee painting, this satellite image of an area south of Garden City, Kansas, depicts where wheat is grown with center-pivot irrigation that creates circle-shaped fields. Reddest areas are crops that reflect near-infrared wavelengths. Light-colored areas are fallow or harvested fields.

The wheat snapshot is one of 41 dazzling, zoomable satellite images from the last 30 years put together by the Smithsonian Institution Traveling Exhibition Service. The Web site also contains an explanation of how remote sensing works and links to teaching materials for grades 5 through 12. >> www.earthfromspace.si.edu

Q What's the quickest link to advances in the world of science?

AAAS

AAAS Advances—the free monthly e-newsletter exclusively for AAAS members.

Each month, AAAS members keep up with the speed of science via a quick click on the newsletter Advances.

Look for the next issue of Advances delivered to your inbox mid month. Look up archived issues at aaas.org/advances.

Features include:

- A special message to members from Alan Leshner, AAAS CEO
- Timely news on U.S. and international AAAS initiatives
- Just-released reports and publications
- Future workshops and meetings
- Career-advancing information
- AAAS members-only benefits

All for AAAS members only.

aaas.org/advances

Science
AAAS

Advances

AAAS

Advances – The Monthly Newsletter for AAAS Members

Message to Members: R&D Funding Trends
AAAS in Action: News to Note
AAAS at Work: Programs at the Forefront
AAAS Science Careers: Events, Tools, Advice
AAAS Announcements: Items of Interest
Read On, Online: Science Sites

Message to Members
R&D FUNDING TRENDS

Dear AAAS Member,
As a continuing service to scientists, engineers, a ers, AAAS provides timely, comprehensive, and i analyses of R&D funding in the U.S. federal budg A new AAAS analysis of the proposed Fiscal Yea shows that R&D funding for most nondefense a jected to decline significantly over the next five a few will in fact increase.. Funding for the phys NSF, the Department of Energy, and the Nation ence and Technology will increase, as will wea and space exploration. At the same time, the of Health budget is slated to continue a decli year. For continuously updated coverage of b the U.S. Congress and Executive Branch, go A book-length report on R&D in the FY 2007 released at the AAAS Forum on S&T Policy AAAS continues to speak out, both directly in public forums, urging sound science pol investment in critical areas such as the ph health, and energy resources, which is ne innovation to benefit global society. We th supporting these critical actions.

Sincerely,
Alan I. Leshner, CEO, AAAS

P.S. Symposium proposals are due 8 M Meeting, "Science and Technology for February in San Fra

Pioneers

STEM CELL ANGELS. Many relatives of diabetes patients support an expansion of stem cell research. Two New York women whose sons have the illness have gone a step further by starting a stem cell foundation.

Susan Solomon (above, right), a lawyer and management consultant, and Mary Elizabeth Bunzel, a journalist, were asked by the Juvenile Diabetes Research Foundation to serve on a task force aimed at getting New York to adopt a stem cell initiative similar to California's Proposition 71. But Solomon concluded that "life is too short" to pursue that obstacle-ridden course. So the two women, tapping an array of contacts in business, medicine, and the arts, set about generating support for a private initiative that heart researcher Kenneth Chien of Massachusetts General Hospital in Boston calls an "Olympic Village" for researchers conducting work not eligible for federal funding.

The New York Stem Cell Foundation has already set up a private lab—location undisclosed—in Manhattan where researchers from Harvard and Columbia universities are currently at work. And last month, the foundation held its first conference—on translational stem cell research—at Rockefeller University. Future plans include the awarding of four 3-year postdoctoral fellowships.

NONPROFIT WORLD

CANCER NETWORK. While building his corporate empire, U.S. shipping magnate and billionaire Daniel Ludwig relied heavily on getting smart people to work together. Now, 14 years after his death, his foundation is getting cancer researchers from different universities to collaborate more closely with one another.

Last week, the Ludwig Fund for Cancer Research announced gifts of $20 million each to six institutions around the country: Harvard, Stanford University in Palo Alto, California, the Massachusetts Institute of Technology in Cambridge, Johns Hopkins University in Baltimore, Maryland, the Memorial Sloan-Kettering Cancer Center in New York City, and the University of Chicago. The money will go toward the establishment of cancer centers, which will also receive a portion of the foundation's real estate stock and $2 million every year for the next 7 years. The foundation is offering additional funding for projects that are hatched by two or more centers, as well as work done in collaboration with the Ludwig Institute for Cancer Research.

The gift represents a wonderful boost at a time when federal funding for biomedical research is stagnating, says George Demetri, who will head the Ludwig center at Harvard's Dana-Farber Cancer Institute in Boston. "The money will help us take some risks," he says. In previous years, the foundation has provided the six institutions with $53 million.

MOVERS

CHANGE AT THE SALK. Richard Murphy has decided to retire as president and CEO of the Salk Institute for Biological Studies in San Diego, California. The 62-year-old cell biologist and his wife will move to the East Coast next summer to be closer to their children and grandchild. No successor has been announced.

The $160 million that Murphy helped raise during his 6-year tenure enabled the institute to start new research groups and facilities. It now plans further expansion into disciplines such as biophotonics and metabolic diseases.

Milestones

THE GEOLOGY GENE. A Ph.D. earned last month from the University of Washington, Seattle, marked more than the launch of Jennifer Kay's career in the earth sciences. It continued a Kay family tradition. Her great-grandfather, George Frederick Kay, was one of the founders of soil science early in the last century. Grandfather Marshall Kay (below) was the leading authority on geosynclines, the central concept of midcentury continental geology. Father Robert Kay (bottom, with Jennifer) pursues the geochemistry of oceanic volcanic rocks at Cornell University. And the newly minted researcher has been delving into a more watery corner of the earth sciences: the behavior of snow, ice, and clouds.

Immersion is the key to maintaining a long-running tradition, says Jennifer's mother, Suzanne Kay, herself a geoscientist at Cornell. That's unlikely to present a challenge: With assorted other relatives in the natural sciences, Suzanne says, Kay family gatherings could double as small scientific conferences.

Got a tip for this page? E-mail people@aaas.org

GLOBAL WARMING

U.N. Conference Puts Spotlight on Reducing Impact of Climate Change

NAIROBI—For the past 6 years, Louis Verchot has had a ringside seat for Lake Victoria's ecological decline. Intense rainstorms pounding down on degraded land have swept in millions of tons of phosphorus-laden sediments from the Nyando River, transforming the lake from a nutrient-limited ecosystem into one with a gross excess of nutrients. On a visit last spring, says Verchot, a soil specialist at the World Agroforestry Centre in Nairobi, the water was so choked with an algal bloom that a glass of it "looked like spinach soup."

Verchot can't do anything about the torrential rains. But to help communities in western Kenya's Lake Victoria Basin mitigate the damage, he's spearheading a project with the Kenyan Agricultural Research Institute, funded by the Global Environment Facility (GEF), to reforest denuded land with acacias and other indigenous trees and to help farmers switch to sustainable agricultural practices. It will be a long haul, says Verchot, "but we think we will be able to help them out."

Victoria's downward spiral is a stark example of how climate change—shifting patterns of rainfall in this case—and poor resource management have conspired to create an ecological nightmare. The countries most vulnerable to these effects are also those least able to adapt to the changes, U.N. Secretary-General Kofi Annan told the U.N. Climate Change Conference in Nairobi last week. "Innumerable African communities have suffered climate-related disasters in recent years," he said. "For them, adaptation is a matter of sheer survival."

One clear message from the Nairobi meeting is that the need to adapt to climate change is finally being taken seriously on the world stage. Until now, the debate on climate change has been dominated by the epic dispute over how to stem greenhouse gas emissions, says Jon Barnett, an environmental sociologist at the University of Melbourne, Australia. "But we know that
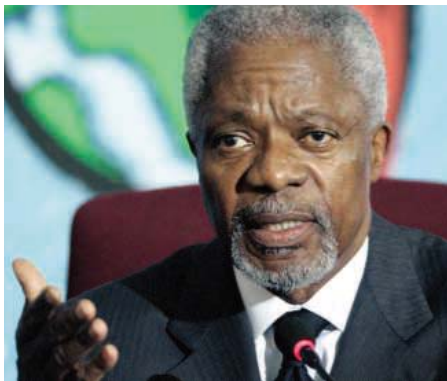
Adapt or perish. Unusually heavy rainfall and unsustainable resource management are accelerating erosion around Lake Victoria (*above*). Poor countries are least able to adapt, says Kofi Annan (*top*).

even if we completely stopped emissions tomorrow, there are already enough [greenhouse gases] in the atmosphere that more global warming is inevitable," he says.

Here at the annual U.N. conference of nations that have ratified the landmark 1990 Kyoto Protocol, which binds parties to sharp limits on greenhouse gas emissions, delegates fleshed out an Adaptation Fund that will funnel assistance—

eventually amounting to hundreds of millions of dollars—to developing countries that bear the brunt of climate change. But disagreement over who will control the money—GEF or the countries that the fund is designed to help—will delay implementation until next year's meeting at the earliest. "This will be one of the most important debates that the next conference will have," says Ian Noble of the World Bank.

The fund could be a huge boost to nascent efforts to adapt to climate change. Emerging problems run the gamut from shifting disease patterns and droughts to coastal erosion from rising sea levels. Without adaptation, the World Bank forecasts that climate-change impacts in vulnerable developing countries could cost up to $100 billion per year over the coming decades.

One new initiative described at the meeting aims to build climate adaptation into global public health. The World Health Organization (WHO) estimates that climate change is already causing at least 150,000 excess deaths per year. One major killer is malaria. Here in Kenya, some 20 million people are at risk as warmer average temperatures allow the mosquito that transmits malaria to spread into the highlands, says Solomon Nzioka of Kenya's Ministry of Health. "We've established that we have something to be concerned about," says WHO's Diarmid Campbell-Lendrum. "Now we're at the critical point: telling people what to do about it." For malaria spread, measures could include more aggressive mosquito control at higher altitudes and stepped-up vaccine R&D.

WHO and the U.N. Development Programme have launched a pilot project in seven countries—Barbados, Bhutan, China, Fiji, Jordan, Kenya, and Uzbekistan—with different health vulnerabilities to climate change. Last month, for example, Chinese officials agreed to explore ways to reduce fatalities from heat waves, which are estimated to cause between 225,000 and 890,000 excess deaths per year from strokes and heart attacks in China, says Jin Yinlong, director general of the National Institute for Environmental Health and Engineering in Beijing. "We will be judged on how well we protect people's lives as climate change evolves," says Campbell-Lendrum.

Scores of other projects are getting off

CREDITS (LEFT TO RIGHT): ANTONY NJUGUNA (KENYA)/REUTERS; LOUIS V. VERCHOT

FOCUS

China's gene-
therapy push
1232

Molecular
gastronomy
1235

Why hybrids
usually fail
1238

the ground. The World Bank is spending about $50 million on adaptation projects, and bilateral programs have committed $110 million to more than 50 projects in 29 countries. Even the United States, which has not ratified the Kyoto Protocol, is getting in on the adaptation action: The U.S. Agency for International Development has promised $2 million for such projects over the next 5 years. Still, "we are orders of magnitude underfunded," says Alf Wills, South Africa's

chief climate negotiator at the conference.

Globe-spanning adaptation efforts are necessary, says Barnett, but there are also immediate priorities on a very local scale. Take the Pacific island nation of Niue, the smallest in the world. Intensification of tropical cyclones and rising sea levels "could wipe the nation off the map within decades in the worst-case scenario," Barnett says. Luckily, he says, some quick-fix adaptations could make a big difference. "For a start, half the

population needs to be relocated to higher ground," he says. That, along with improvements in infrastructure to help islanders cope with climate-related problems, "comes to a ballpark figure of $60 million." Considering that what is at stake is an entire nation with its own unique language and culture, says Barnett, "this is incredibly cheap."

–RICHARD STONE AND JOHN BOHANNON

DEVELOPMENTAL BIOLOGY

Teams Identify Cardiac 'Stem Cell'

Like many organs, the heart is a patchwork of cell types, from smooth muscle that pulses blood through arteries to endothelial cells lining vessels. These pieces, varied as they are, were long considered distant cousins born of different parent cells. But two new studies have uncovered a primitive type of heart cell in mice that can give rise to the heart's main cell lineages. If the finding holds up, it will make the heart one of very few organs, along with the blood, known to grow largely out of a single type of cell; it may also ease the introduction of embryonic stem cell treatments in cardiac patients.

"It's surprising that so much can come from" just one type of heart cell, says Timothy Kamp, who studies cardiovascular regenerative medicine at the University of Wisconsin, Madison. "You have essentially a type of cardiac stem cell."

Although they took different approaches, the two groups that found the heart progenitor cells both identified overlapping genetic markers to define their progenitor population, and both found that the cells could differentiate into cardiac muscle and blood vessel cells, the principal building blocks of the heart. The first paper, led by Gordon Keller, a stem cell biologist at Mount Sinai School of Medicine in New York City, was published earlier this month in *Developmental Cell*; the second appeared this week in *Cell*. That work was led by a husband-and-wife team, Karl-Ludwig Laugwitz and Alessandra

Moretti, at the Technical University of Munich in Germany, and Kenneth Chien at Massachusetts General Hospital in Boston.

The Chien team found that mouse embryonic stem cells developing into heart cells first entered an intermediate state that could be monitored by tracking expression of three different genes. Those intermediates, which the scientists called "triple positive cells," gave rise only to heart cells. To confirm that these triple positive progenitor cells, grown under artificial conditions, exist in an animal, the researchers examined mouse embryos at different points in their development. Around day 8, they detected them.

Although Keller's team did not use all the same markers as Chien's to characterize the cells it found, both groups found that their cells could differentiate into the same cardio-

vascular cell types. "We're arriving at a similar progenitor," says Keller, also adding that "it's still pretty early days."

To prove that these progenitor cells can become functioning, specialized heart cells, the scientists need to inject them back into an animal to see whether they give rise to the different cardiac tissue types, Moretti notes. That is also a key experiment to determine whether these master ancestor cells can repair a damaged heart. Keller's group has begun precisely this experiment, inserting the progenitor cells it identified into mice whose hearts resemble those of humans following a heart attack.

Chien notes that "we have not formally proven that that cell can make a whole heart." Still, says Kamp, the work could ease one of the most worrying concerns about using embryonic stem cells in patients: that, left alone to form whatever cell type they fancy, they'll develop into tumors. "If you can have a more committed cell population that can only give rise to limited progeny," Kamp says, "that's going to dramatically reduce the risk." And the cells might still be flexible enough to form, say, a coronary artery, which includes different cell types. Still, admits Laugwitz, that "remains to be proven." Both groups, in the United States and Germany, are working with human embryonic stem cells to see whether the mouse patterns will hold.

–JENNIFER COUZIN

CREDIT: MORETTI *ET AL.*, *CELL* (2006)
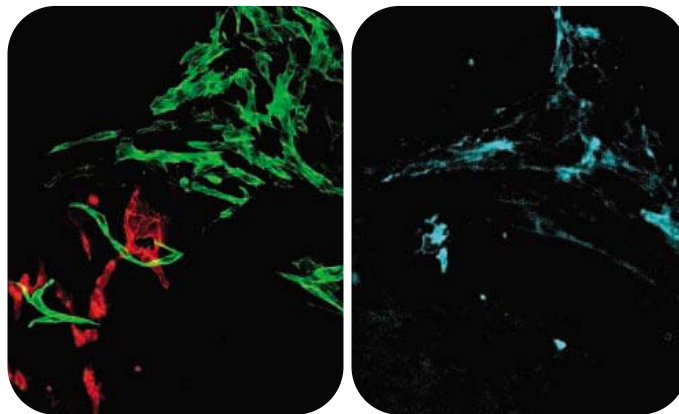
Versatile. The same cells from an early mouse embryo give rise to the heart's endothelial cells (red) in blood vessels, contracting heart muscle cells (green), and smooth muscle cells (blue, *right image*).

FUSION

Scientists Reap ITER's First Dividends

Japanese researchers were disappointed when they lost a bid last year to host the $12 billion International Thermonuclear Experimental Reactor (ITER) project. But they should be cheered by the consolation prize: In an agreement due to receive provisional approval this week, some $870 million will be spent on fusion-related facilities in Japan, with equal contributions from Japan and the European Union. European researchers are happy too, as most of Europe's contribution will be in-kind, and the whole effort will speed the work toward a commercial fusion power reactor. The need to compensate the runner-up "has turned necessity into advantage for the fusion program," says

Reactor reborn. Japan will remove the core of its JT-60 reactor and rebuild it with superconducting magnets to aid the ITER project.

CREDIT: JAPAN ATOMIC ENERGY AGENCY

Günter Janeschitz, head of fusion at Germany's Karlsruhe research center.

The origins of the deal lie in the frantic diplomacy in 2004 and 2005 during which the then–ITER partners—China, the European Union, Japan, South Korea, Russia, and the United States—tried to decide between sites at Rokkasho in Japan and Cadarache in France. In an effort to win support for their sites, both Japan and the E.U. upped their offers to pay as much as 50% of the total ITER cost if they were host. "There was a lot of money on the table," says Chris Llewellyn Smith, director of the U.K. Atomic Energy Authority's Culham Laboratory.

The idea emerged that this extra money could be used to build the International Fusion Materials Irradiation Facility. IFMIF uses neutrons similar to those inside a fusion reactor to test and validate materials that would be used in a commercial prototype that comes after ITER, dubbed DEMO. Building IFMIF now rather than later would speed the transition to DEMO.

Once the ITER site deal was completed in June 2005 and negotiations on what is known as the "Broader Approach" began, there was not as much money on the table—not enough to build IFMIF, anyway. And Japan had other priorities: It wants to rebuild its existing fusion reactor, the JT-60, with superconducting magnets. This would create a mini-ITER where operational scenarios could be tested and refined. Japan also wants to build an International Fusion Energy Research Center at Rokkasho, which will house a supercomputer for simulations and lead the effort to design DEMO.

According to an E.U. official involved in the negotiations, Europe's only requirement was that the Broader Approach contain an engineering design effort for IFMIF so that construction could start about 6 years from now. In the agreement presented this week, $190 million is earmarked for IFMIF design. But according to the E.U. official, in an official letter Japan made clear that even though it would lead the design effort, it did not necessarily want to host the machine. The E.U. offered to be the host if no others came forward. "Personally, I'm very happy with this result," says Llewellyn Smith. "IFMIF is on the road."

Following this week's initialing of the Broader Approach agreement, both sides will check it through, aiming to sign it by the end of the year. Also up for signing this week is the main ITER agreement, which will mark the creation of the international organization that will build the machine.

–DANIEL CLERY

Controversy on the Brain

The Nobel Prize–winning director of a neuroscience center at the Massachusetts Institute of Technology (MIT) is stepping down in December in the wake of a controversy over the abortive hiring of a young female biologist in June. Earlier this year, Susumu Tonegawa, who leads the Picower Institute for Learning and Memory, discouraged a young brain scientist from taking a job with a rival institute at MIT.

A panel examining the incident released a report 2 November that criticized the conduct of Tonegawa and other faculty members involved. It said their behavior illuminated the lack of a clear mission for the school's many-faceted neuroscience effort and turf battles between its parts (Science, 10 November, p. 913). Tonegawa, who said last week that he would remain at MIT but would focus solely on research, has declined comment. But Stanford University neuroscientist Ben Barres, who has closely followed the controversy, called the resignation "an important step forward" to foster "a more collaborative and supportive environment" for MIT neuroscience.

–ANDREW LAWLER

Cell Scanning and Shuffleboard

Germany's Max Planck Society is considering opening an outpost in the Sunshine State. This month, society President Peter Gruss visited South Florida to discuss joining the Scripps Research Institute, the Burnham Institute, and several other high-profile research organizations that Governor Jeb Bush has lured to Florida (Science, 1 September, p. 1219). Scripps President Richard Lerner introduced Bush and Gruss during a Bush-led trade mission to Europe last year and has pushed the idea of Germany's premier research organization joining the Florida research pack. If the deal goes through, says Enno Aufderheide, chief of Max Planck's external relations, as many as three of the society's top scientists could take up residence in Palm Beach County. Aufderheide says the new institute would focus on bioimaging to complement the biochemistry, cancer research, and translational medicine research Scripps plans to do at its new campus in Palm Beach Gardens. The deal, worth several hundred million dollars, hinges on financing from state and local sources. No German taxpayer money would fund the new institute, Aufderheide says. The idea is "very attractive but far from a final decision," he says.

–GRETCHEN VOGEL

Kicking the tires. Representative Sherry Boehlert (*right*) with Senator John McCain at the South Pole.

INTERVIEW: SHERWOOD BOEHLERT

Explaining Science to Power: Make It Simple, Make It Pay

After 24 years of serving a House of Representatives district in upstate New York, including the last six as chair of the House Science Committee, Sherwood "Sherry" Boehlert will retire next month from the U.S. Congress. A self-proclaimed "cheerleader for science" on a panel that lacks the power of the purse strings, the moderate Republican sought common ground among both conservatives within his party and Democrats across the aisle on a range of issues including tougher environmental standards and undergraduate science education.

The 70-year-old Boehlert is uncertain about his next step—ruling out an afterlife as a Washington lobbyist but hoping to remain active on national science and environmental issues. But before packing up, he sat down last week with *Science*'s Jeffrey Mervis in his Capitol Hill office to reflect on the nature of government and what role scientists can play.

Q: How well do scientists get their message across to politicians?
On the 24 years I've been on the House Science Committee, I'd say they've gone from a D-minus to a solid B. They're beginning to appreciate that politics is a different realm. …

When you talk to Congress, you have to appeal to the interests of the audience that you're dealing with. To talk about some great advance in pure scientific terms isn't enough. What does it do to strengthen the economy, or enhance competitiveness, or provide more jobs?

I'm a typical congressman, with a bachelor's degree in public relations and no science background, yet I ended up on the science committee. And I say that's the perfect place for me because I ask the obvious questions: Why can't we do this? Why won't this work? I make them think in more practical terms.

Q: How important is the economic argument, and does every project have to have one?
You have to remember that this is representative government, and I'm sent here to exercise my best judgment on the important issues of the day. So if you want me to exercise my best judgment, then you have to prove to me that it has some public benefit besides a bunch of Ph.D.s sitting in a laboratory coming up with something that they can publish that no one can understand. I mean, what's the real benefit?

Q: What would it take for scientists to get an A?
You have to do more advocacy, and the people who are good at it have to train their colleagues. … I have a theory that to be an eminent scientist, you have to invest a lot of time and resources in getting a good education, including a Ph.D., and then you publish a lot of papers. Then suddenly, one day, you have arrived, and people who are aware of your vast knowledge begin to beat a path to your door. And they want to listen to you, so the scientists get used to giving tutorials. But then they want to come to Congress and give tutorials. That doesn't work. We don't have time for tutorials. They need to get right to the point: "This is why it's important. I know there are a lot of competing interests, but here's why we should be at the head of the line. And here's what it means for society."

Q: Some scientists are starting to endorse candidates and raise money for individual campaigns. Good idea?
I don't think that's the way to go. A lot of scientists don't even want to get involved in politics because they think that it's dirty.

I'll bet you that if you look at all the new freshmen, you won't find a single one, from either party, who campaigned on something like the American Competitiveness Initiative, or more resources for NSF [National Science Foundation], or greater investment in science and math education. I'll bet you won't find one. And that's a failure by the scientific community.

Why aren't they more involved? It's not about raising money—although there's certainly a lot of money in politics. Why aren't they visiting candidates and explaining to them, on their home turf at the university in their district, why they should be really interested in their agenda? I tell scientists that their new best friends should be these new congressmen. Don't just visit them in Washington with a lobbyist. Invite them to come to the university in their district, not to a technical presentation that they probably can't understand, but to a general discussion of what's going on and what it means. … I think that the scientific community will be an abject failure if, when these new freshmen start campaigning for reelection, at least a few of them don't have a science component in their platform.

Q: If you became a lobbyist, with professional societies as your clients, what would you tell them to do, and where would you take them?
Of course I would come to the Hill, and to the Science Committee, and to the appropriations committees. But I'd also tell them to get their people back home to come here. Because a person from North Dakota coming to see a congressman from upstate New York is not nearly as persuasive as someone from his district.

Q: What science agencies are most effective at getting their message across, and how do they do it? For example, does it work when the National Science Foundation invites legislators and their staffs to Antarctica?

You're damn right it does. Because there's no substitute for kicking the tires. I've had two trips to Antarctica, and in the last one [January 2006], I was part of a bipartisan group of 10 members. Of that 10, there were probably two who shared my view that global climate change was real and that we damn well better do something about it. The rest were skeptical or neutral. But after we got back, every one of them had a heightened interest in the subject.

Why? Because down at the South Pole, they heard from scientists about how their experiments related to global climate change. The same thing happened at the Great Barrier Reef in Australia, where we heard how this great treasure was being damaged because of something called global change. And the next time there's a floor vote on the budget of some science agency supporting research on climate change—and I won't be around—I'll bet that

A bipartisan farewell. Boehlert is congratulated by Bart Gordon, his expected successor as science committee chair, as well-wishers mark the unveiling of his portrait.

this group will be a more receptive audience because they've seen it firsthand.

What are we supposed to do—sit in our offices and read these reports? Like hell. We need to get out in the field and see the facilities. McMurdo Station is not a place I'd suggest as a vacation spot. But we spent 5 days on the ice, and we learned a lot.

Q: Over your career, which science agency heads were the best at getting their message across?

One of the best is Mike Griffin, the current NASA administrator. He understands his audience. I don't need a translator to deal

with him, even though I'm a generalist and he's a distinguished scientist.

[Former NSF Director] Erich Bloch is another, without question. In each case, they clearly know their stuff. They know how to make their argument and explain why it's deeply and intensely important to them in a way that is important to the nation. It doesn't do any good if the intended recipient doesn't understand what you're talking about and is looking at their watch, wondering about their next appointment. ... To this day, when people think of the ideal NSF director, Erich is who they talk about.

Q: Is the president well-served by his current science adviser, and is science being coordinated effectively across all federal agencies?

Here's the problem. The president has a lot of people vying for his attention. And quite honestly, whether it's this president or Bill Clinton before him, science isn't given the attention it deserves because there's not the sense of urgency that the secretary of defense or the secretary of state bring to the table. And [George W. Bush] has a natural passion for education, which gives the secretary of education an edge. So while we've had capable and fine people as directors of OSTP [Office of Science and Technology Policy], it's not considered a top-tiered adviser to the president, and the director doesn't get the face time that the other secretaries receive. ...

So yes, I think that the science adviser should have greater access to the president. But there have been improvements in this Administration. For example, when Mitch Daniels was [Office of Management and Budget] director, for the first time the science adviser was brought into the budget negotiations with all the science agencies. I think that was an important step.

Q: Speaking of budgets, do you think that the next Congress will curb academic earmarks?

I think so. I think you'll see less rather than more, and that trend is good.

Q: Voluntarily?

Are you kidding? You're going to ask the people who benefit from this practice to stop voluntarily? But I think there's general agreement that earmarks have gotten out of hand, and that something needs to be done.

Sought: Reruns of *The Office*

With Democrats assuming control of Congress, Representative Rush Holt (D–NJ) is hoping its Office of Technology Assessment (OTA) will be revived. Holt says Congress needs the one-stop think tank, which the Republicans gutted after taking power in 1995, to help explain a variety of issues from electronic voting to nanotechnology, and that it could be reconstituted for $30 million a year. Holt hasn't yet asked for the support of Democratic leaders, but Representative Bart Gordon (D–TN), in line to become chair of the House Science Committee, likes the idea. Last summer, at a hearing on the topic, Gordon said, "We could use a service like OTA" to help legislators assess conflicting expert opinion. But the retiring chair of that panel, Representative Sherwood Boehlert (R–NY), thinks OTA is "desirable but not essential" and that Congress is not lacking in objective data.
–JEFFREY MERVIS

Cloning Ban Imperiled

Australia's 2002 ban on the cloning of human embryonic cells may soon be lifted if a bill to repeal it gets a majority in the House after clearing the Senate this month. Mal Washer, the Liberal Party member behind the House bill, predicts a large margin of victory. But Family First Party leader Steve Fielding, who supports the ban, says it's too early to tell, noting that repeal passed the Senate by one vote. If approved, the new bill would forbid the making of sperm-fertilized embryos for research and the implantation of a cloned embryo into a woman's uterus. It would also bar the transfer of a human nucleus into an animal egg. The bill would allow human somatic cell nuclear transfer and narrow the definition of embryo to cover only entities surviving the first mitotic division.   **–ELIZABETH FINKEL**

Assessing the Assessment

The Bush Administration is breaking a 1990 law that requires a quadrennial assessment of how climate change affects the United States, a lawsuit filed last week alleges. The last such assessment was published in 2000, and the Bush Administration says 21 specialized reports on climate topics follow the law's intent. The suit was filed by environmental groups in a northern California federal court. In a statement supporting the suit, Senator John Kerry (D–MA) condemned what he called the Administration's "foot-dragging." A Kerry aide says that next year's Democratic majority in Congress may try to compel compliance through spending measures or new laws. "All options are on the table," she says.   **–ELI KINTISCH**

U.S. INTELLECTUAL PROPERTY

Patent Experts Hope High Court Will Clarify What's Obvious

Thomas Deuel thought his 1990 discovery of the purified DNA sequences that code for a cellular growth factor called pleiotrophin was sufficiently new and different to deserve a patent. The U.S. Patent and Trademark Office (PTO) respectfully disagreed. Citing "the routine nature of cloning techniques," PTO concluded that what the cell biologist had done in his lab at Washington University School of Medicine in St. Louis—purify, characterize, and obtain the DNA that codes for a protein—was "prima facie obvious." But Deuel appealed and won, with a special federal court declaring in 1995 that the patent office's view of what was common knowledge was based on "speculation and an impermissible hindsight."

Determining what is not obvious—one of the four tests that U.S. inventors must meet to receive a patent—has always been an inexact science, and for nearly 2 centuries, PTO's examiners had wide latitude to disqualify patents on that basis. But in the past 3 decades, the Court of Appeals for the Federal Cir-

cuit has restricted their scope with cases such as Deuel's. Next week, the U.S. Supreme Court will hear oral arguments on a landmark case, *KSR International Co.* v. *Teleflex Inc.*, that could decide whether the current high standard for rejecting a patent based on obviousness should be lowered.

The U.S. high-tech community is deeply divided over the issue. Most computing and technology firms hope the high court will back a broad definition of obviousness, which would give PTO more leeway to reject what the companies consider to be undeserv-

A head of its time? A pumpkin-shaped leaf bag is different enough from other bags to deserve a patent, a federal appeals court ruled in 1999.

ing patent applications. In the past, they argue, such patents have led to expensive court battles and unpleasant business surprises. In contrast, the biotech and pharma sectors want the court to maintain what they see as a continued flow of legitimate innovations to preserve a healthy biomedical industry. Three dozen groups, as diverse as AARP and the Michelin tire company, have filed briefs on one or another side of the debate.

Law professor John Duffy of George Washington University in Washington, D.C., who represents KSR, calls nonobviousness "the heart of what is a patent." To win patent protection, an idea or object must be new, useful, and properly described. The law also requires that a patentable idea would not have been obvious at the time of invention to a hypothetical "person having ordinary skill in the art."

Making that call is one of the toughest decisions that an examiner faces. It's not because of ignorance. All of PTO's 282 biotech examiners have advanced science degrees to inform their decisions; 63% have Ph.D.s. Yet federal judges, as in the Deuel case, have steadily narrowed definitions of obviousness, making it harder for the examiners to apply their expertise. "We had been rejecting those kinds of claims," says Esther Kepplinger, who was a supervisor in the biotechnology examiner corps when Deuel submitted his application. She says that the examiners were ▶

Government Questions Sequencing Patent

A decades-old patent application could rewrite the history of who invented the automated DNA sequencer.

Last week, the U.S. Patent and Trademark Office (PTO) decided that a 1982 application from Enzo Biochem, a small New York biotech company, covers the same invention named in a 1998 patent awarded to former California Institute of Technology biologist Leroy Hood and colleagues. Hood's patent, owned by the California Institute of Technology (Caltech) in Pasadena, covers sequencing using gel electrophoresis—the technology currently underpinning the $7 billion DNA sequencing industry.

PTO's decision to begin what's called an interference procedure follows decades of efforts by Enzo's lawyers to win a patent. At stake are presumed millions of dollars in royalty income for Caltech and the fiscal health of sequencing giant Applied Biosystems in Foster City, California, which licensed Hood's technology in a majority of its machines. Applied Biosystems, with fiscal 2006 sequencing-machine revenue of $540 million, has previously fought off other attacks on the intellectual property it owns or licenses.

Attorneys say the announcement itself marks a victory for Enzo, which last fiscal year recorded losses of $15.7 million. But the company's chances of success are hard to determine. Caltech's attorneys, who declined to comment on the matter, are expected to claim that PTO erred in deciding that Enzo's application covers Hood's invention, although a copy of the typed 1982 version does mention the procedure. At some point, the two sides will also bicker over who invented what first—with the answer hinging on yet-to-be-disclosed lab notebooks and calendars.

The whole process, which could include a subsequent trial and appeal, could last 5 years or longer, says interference specialist R. Danny Huntington of Bingham McCutchen LLP in Washington, D.C. Caltech's patent expires in 2015. If Enzo wins and receives a patent with a later expiration date, Applied Biosystems would have to pay additional royalties to use the technology. At the same time, a patent on gel electrophoresis could be less important by then, notes George Church of Harvard Medical School in Boston, because scientists are steadily moving toward new methods of sequencing DNA. Techniques include using pores or solid surfaces to cut costs or sequence genes faster (*Science*, 17 March, p. 1544). **–ELI KINTISCH**

"startled that the court would have said this was not obvious."

More than common sense
The question before the high court next week began as a standard infringement case. In 2002, Limerick, Pennsylvania–based Teleflex, a manufacturer, sued KSR, an Ontario, Canada–based firm that makes brake pedals, for patent infringement. It won before the federal circuit court, and KSR appealed to the Supreme Court, which decided earlier this year to take the case. At issue is whether Teleflex's 2001 patent, which combines an adjustable and electric pedal, was obvious and should not have been granted.

In a 1966 precedent-setting case involving plow parts, the high court gave examiners the power to "ascertain" or "determine" obviousness without much definition of the term. Patent lawyers say that gave examiners wide latitude to issue rejections. But since its 1982 founding, the federal circuit has established more direct instructions to PTO: An existing specific teaching, suggestion, or motivation for a combination of elements is required to declare a patent claim obvious.

"Common sense" does not "substitute for authority," the court said in 2002. Two years later, a federal court ruled that a patent on a drug combining the painkillers Vicodin and ibuprofen was invalid as obvious. But the federal circuit reversed that decision because there was "no record of evidence … suggesting the enhanced biomedical effect of the combination."

Critics say such decisions have driven PTO to issue bad patents that hurt consumers and innovators alike. "Anyone who's been sick knows you can put two analgesics together to fight pain," says Jeffrey Light of Washington, D.C.–based Patients not Patents, which joined with AARP on KSR's side. Such patents, says Light, "lead to higher costs" for consumers and choke competition. And they hurt truly innovative scientists, adds Duffy, who represents KSR: "Follow-on patents can rob the pioneering patents of their just rewards."

Defenders of the status quo, including the Biotechnology Industry Organization in Washington, D.C., say the high court shouldn't jeopardize a reliance "on factual findings" that has allowed the U.S. research enterprise to flourish. And Kevin

Noonan, a patent attorney with McDonnell Boehnen Hulbert & Berghoff LLP in Chicago, Illinois, fears giving examiners, whose expertise varies greatly, too much say in the obviousness call. "Do we really want whether someone gets a patent to be based on what examiner they get by the luck of the draw?" he asks.

The federal circuit itself may even be rethinking the issue. Last month, in what its critics welcome as a new tack, it declared that its obviousness standards are "quite flexible" and require "consideration of common knowledge and common sense."

Last year, the high court avoided taking any dramatic steps to overhaul the patent system in cases dealing with the patentability of scientific concepts and the legal power of a granted patent. But critics are hopeful that the nine justices will now act forcefully to fix a flaw they think is more central to patent quality. "Obviousness is getting closer to the root of the problem," says Josh Lerner of Harvard Business School in Boston, an outspoken opponent of the current regime. "*KSR* is potentially huge."

–ELI KINTISCH

U.S. SCIENCE POLICY

Resignations Rock Census Bureau

Knowledgeable observers of the U.S. Census Bureau are shaking their heads over the sudden resignations last week of Director Louis Kincannon and his deputy and chief census statistician, Hermann Habermann.

It's "time for me to retire," wrote Kincannon in a 14 November letter to President George W. Bush, who appointed him to the post in 2002. But there are widespread rumors that the men were pushed out. The resignations come amid stepped-up preparations for the 2010 Census, the first one that will use only a short form. The agency is also facing a possible $58 million cut in its 2007 budget, which is still pending in Congress, that would jeopardize the new American Community Survey, ongoing monthly sampling designed to substitute for the old long form in the decadal census.

The 66-year-old Kincannon told *Science* he's leaving as soon as his successor is in place because he wants to spend more time with his grandchildren in Tennessee. But in other news reports, he noted that his relationship with his bosses at the Department of Commerce had deteriorated since the departure last year of Donald Evans as Commerce secretary. Habermann declined to comment.

Commerce spokesperson Dan Nelson says, "It was mutually agreed that the time was right" for the departures. But Edward Spar, director of the Council of Professional Associations on Federal Statistics, says he is certain

Out the door. Census chief Louis Kincannon and his deputy have resigned.

that Kincannon was asked to resign and that Habermann, a "consummate statistician" whom he sees regularly, "had no plans to leave January 3 [his stated departure date]. … I still don't understand the actual reason."

A former Census official who asked not to be quoted by name believes that some Republicans in Commerce and on Capitol Hill are concerned that Democrats will revive efforts to adjust census numbers to make allowance for undercounts of poor people—who are likely to vote Democratic. To counter that attempt, he says, those officials want compliant leadership at the bureau.

But former census director Kenneth Prewitt, now a professor at Columbia University, says those fears are unfounded. "I am absolutely certain that the current [Census Bureau] leadership does not want to adjust the census," asserts Prewitt. A House Republican staffer told *Science* he is satisfied that no one wants to revive the idea of an adjustment, which the bureau formally rejected in 2003. Other sources say Habermann, who is responsible for day-to-day operations, was the primary target after resisting pressure to appoint partisans to career posts.

–CONSTANCE HOLDEN

Chinese researchers have been the first to put cancer gene-therapy products on the market, but critics question the data behind the success stories

Splicing Out The West?

上层: 碱 液
下层: 培养液

BEIJING—Maria Corina Roman, a Danish surgeon, made international news when she decided to seek treatment for her breast cancer using the world's first commercial gene therapy. Disappointed with standard cancer treatment, Roman flew to China in 2004 to try Gendicine, a Chinese product that contains a virus with a human tumor suppressor gene (*p53*) spliced into its DNA. Just days after the first injection, Roman reported that she had regained energy and appetite. Gendicine's maker, SiBiono GeneTech Co. in Shenzhen, spread the word. Encouraging reports about this gene therapy appeared in the Financial Times, Business Week, and China Daily.

This fall, however, Roman's tumor has returned, SiBiono acknowledges. The company's chief executive, Peng Zhaohui, says nevertheless that the drug has proved to have "good efficacy," adding that Roman, SiBiono's most famous client, "should continue to treat with Gendicine."

Peng's advice is based on more than optimism; it reflects national policy. China's State Food and Drug Administration (SFDA) approved Gendicine for clinical use in October 2003 and licensed its commercial production in spring of 2004. Last year, SFDA approved a second genetically engineered anticancer

product: a modified virus, dubbed H101, designed to infect and kill cells containing mutated versions of the *p53* gene. The maker, Sunway Biotech Co. in Shanghai, says it expects to strike a licensing deal by the end of this year with Genzyme Corp. in Cambridge, Massachusetts, to run clinical trials of a Genzyme gene-therapy product in China and possibly test H101 in the United States.

As these projects advance in China, gene therapies in North America and Europe are struggling to complete premarket clinical tests. After a U.S. patient died in a 1999 gene-therapy trial and two children in French trials developed leukemia in 2002, the U.S. Food and Drug Administration (FDA) tightened controls on experiments, says James Norris, head of the U.K.-based International Society for Cell & Gene Therapy of Cancer. Western companies say they are making progress but have not yet brought a single gene therapy to market.

Some see this as a sign that China is catching up with, or even surpassing, the West. "I think the future of gene therapy will be in China," says Andre Lieber, a gene-therapy researcher at the University of Washington (UW), Seattle. But he warns that recent claims of success should be read

with caution. There is a "problem" with interpreting clinical studies done in China, Lieber says. Often the primary data are published only in Chinese—raising a barrier to nonspeakers—and even when they appear in English, critical information may be missing (see sidebar, p. 1233).

Intellectual-property rights may be problematic, too. Some researchers in the West have questioned claims of independent innovations made by Chinese drug companies; this could limit sales outside China. Finally, critics argue that the Chinese regulatory system is not rigorous and that Gendicine, for one, was approved with scant evidence of efficacy. With drugs to treat cancer, "the bar is a lot lower than in the United States to get approval," says Frank McCormick, director of the University of California, San Francisco, Comprehensive Cancer Center.

High hopes

On a plot of land in the outskirts of Shenzhen stands an empty building with opaque windows, a site where owners hope a biotech bonanza will blossom. Starting next year, this newly constructed plant will begin producing 1.5 million vials of Gendicine per year, seven times the capacity of SiBiono's current facility,

Great leap forward. With a boost from the government, SiBiono GeneTech in Shenzhen has jumped to the front ranks of China's biotech industry.

according to SiBiono's Peng. *Science* visited Peng in his office in May and spoke with him last month by phone.

A hallway at the company's headquarters is plastered with clippings from Chinese and international media describing how Gendicine has helped cancer patients. Peng said SiBiono aims to spearhead the sale of gene-therapy products in China with Gendicine. It was given its Chinese name—*jin you sheng*, "born again today"—by China's Vice President Zeng Qinghong when he made a ceremonial visit to the company a month before SFDA cleared the drug for market.

SFDA approved Gendicine as a treatment for head and neck cancer based on small clinical trials showing that more patients had tumors disappear with Gendicine plus radiotherapy (64%) than with radiotherapy alone (19%). Peng has called these "phase II/III" trials, an unusual term that combines safety (phases I and II) with proof of efficacy (phase III).

In 2005, SFDA approved Sunway's H101, also designed for treatment of head and neck cancer, after a 160-patient phase III clinical trial showed that 74% of patients receiving H101 plus chemotherapy experienced a reduction in the size of tumors compared to 40% of patients receiving chemotherapy alone.

Gendicine has now been given to more than 4000 patients to treat not just head and neck tumors but also 50 different cancers, Peng claims. The venture thus far has received about $6 million in grants and government start-up funds as well as $6 million from private investors.

Peng projected in 2004 that 50,000 patients would have received Gendicine treatment by the end of 2006. Demand is far short of that target, but if the drug works—and if patients can afford the high price of treatment, costing $1680 to $3360 per cycle—the market could eventually be huge. "Having 1.3 billion potential patients compared to 300 million in the United States makes a successful drug very lucrative in China," says Norris.

Imitation or innovation?
Doubts persist, however, about China's future as a gene-therapy powerhouse. Some U.S. companies allege that China's commercial products are spinoffs of Western inventions with relatively minor modifications. Introgen Therapeutics in Austin, Texas, for example, claims that SiBiono's Gendicine is similar to its own experimental product, a recombinant adenovirus containing the human *p53* gene (rAd-*p53*).

Wei-Wei Zhang, president and CEO of San Diego-based GenWay Biotech, published the first paper on rAd-*p53* while working at the University of Texas M. D. Anderson Cancer Center in Houston in 1994. He holds U.S. patents on the viral construct and related processes. M. D. Anderson negotiated a license with Introgen, which has spent more than $70 million to develop a product based on Zhang's rAd-*p53*, trademarked Advexin. It has been in clinical trials since 1994. The company's ongoing phase III trial using Advexin to treat head and neck cancer is under review for "accelerated approval" by FDA.

Introgen's 106-patient phase II trial in 2005 showed a 10% "tumor response rate," defined by at least 30% reduction in tumor

Gendicine's Efficacy: Hard to Translate

Clinical data supporting China's advances in gene therapy often appear in Chinese-language journals—which are inaccessible to many Western readers. To bridge the gap, James Wilson, editor of *Human Gene Therapy* (*HGT*), last year solicited a review in English summing up published clinical evidence behind China's first gene-therapy product, Gendicine, by Peng Zhaohui, CEO of SiBiono GeneTech in Shenzhen, the company that put Gendicine on the market (see main text).

Peng's review in the September 2005 issue of *HGT* has been cited at least a dozen times by experts as a definitive view of Chinese clinical trial results. However, Marshall Posner, medical director of the Head and Neck Oncology Program at the Dana-Farber Cancer Institute in Boston, says that, after reading translations of the original reports, the findings are hard to evaluate. The trials "were not done with a high degree of structure, and it is not clear what protocols were followed or how patients were randomized," Posner says. Others question the quality of the data.

Comparing Peng's summary with original Chinese-language reports, *Science* found that the summary did not include some information in the originals. For example, Peng described patients in a phase I (safety) clinical trial of Gendicine as having "advanced" cancers. But a Chinese-language report said seven of the 12 participants in this trial had limited primary tumors that had not spread to lymph nodes. Although the original paper reported that all 12 patients received surgery along with gene therapy, Peng's summary of therapeutic effects mentioned only treatment with Gendicine, noting that 11 patients who received it had a remission of cancer lasting more

Man of the moment. Peng Zhaohui, CEO of SiBiono GeneTech, summarized gene-therapy data in English.

than 3 years. In a telephone interview, Peng said that he had inadvertently omitted data on the surgeries.

Peng's review discussed so-called phase II/III trials of Gendicine in 2001–2002, citing three primary publications. But the primary papers reported only phase II trials—relatively modest ones that had enrolled a total of 124 patients. (Phase III trials are larger and demonstrate efficacy.) Another flaw, says Anthony Chan, chair and chief of service of the Department of Clinical Oncology at Prince of Wales Hospital in Hong Kong, is that these trials—which compared Gendicine plus radiotherapy to radiotherapy alone for head and neck cancer—is that "the definition of complete response … was not provided," even though it is especially difficult to define in such cases.

China's State Food and Drug Administration (SFDA) approved Gendicine for production in 2004 without data from a standard phase III trial. Peng's explanation: SFDA did not require such trials for new drug approvals before May 1999, and because "our clinical trials were approved before 1999, we were not required to do phase III trials." Peng adds that this is "okay" because "the SFDA approved our drug on safety and efficacy." **–HAO XIN**

With reporting by Jerry Guo.

size, in patients who received Advexin alone. Introgen Vice President Robert Sobol says phase III trials are going well.

Meanwhile, Introgen CEO David Nance claims that Gendicine is a "derivative" of his company's product. In an August 2006 filing with the U.S. Securities and Exchange Commission, Introgen claims that Gendicine infringes on a 1994 patent filed in China but concedes that "enforcement of patents in China is unpredictable, and we do not know if monetary damages could be recovered from SiBiono."

Peng disputes these statements. In a phone interview, he said that Gendicine is "very different" from Introgen's product, and that the only similarity is the use of *p53*.

Sunway acknowledges that its product, H101, was inspired by U.S. research but says it developed H101 independently—a claim that is not disputed. According to Sunway officials and other observers, H101 is similar to a product called Onyx-015, made by Onyx Pharmaceuticals Inc. in San Francisco. Onyx-015 and H101 both use a modified adenovirus to target probable cancer cells that have a deficient or mutated *p53* gene. This so-called oncolytic virus, which has been tested in U.S. phase I and II clinical trials, is designed to replicate in target cells and kill them.

Onyx never filed for a patent on Onyx-015 in China. Nevertheless, Sunway CEO Hu Fang says that in developing H101, "we followed almost everything Onyx did in clinical trials. … We modified the virus, very little, for patent purposes."

Sheer numbers. Companies that want to develop a new idea for treating cancer are attracted by China's low costs and huge market.

Although Onyx-015 has shown in phase II trials that it also can achieve local shrinkage of head and neck tumors of about 60% to 70%, McCormick, a co-founder of Onyx, says this was not enough to win FDA approval. Regulators wanted more evidence, specifically data showing that Onyx-015 prolonged survival. Onyx ended a phase III trial when the main backer pulled out in 2005.

At this point, Sunway obtained exclusive worldwide rights from Onyx to use the 015 modified virus in H101. "We bought the patent from Onyx because now we want to put our drug in Europe, the United States, and

Japan," says Hu. The distribution network will be ready soon, and Hu expects 2000 patients to sign up in the first year. The company is working on an improved version, H103, that includes a heat shock protein designed to attack metastatic tumors by inducing an immune response.

Different standards

The Chinese government is both an investor in and a regulator of biotech projects such as the ventures that produced Gendicine and H101. Some observers, including Norris, are concerned that the government's dual role could weaken its vigor as an enforcer of standards. He notes that "backers of these companies are high-level government officials." From 2001 to 2005, the Ministry of Science and Technology (MOST) provided $106 million to innovative drug development, some of which went to SiBiono.

SiBiono's Peng also helped write a regulatory guidebook for SFDA on evaluating cancer gene-therapy products. Leaning forward in his executive chair, Peng proudly shows off a thin pamphlet. "It's the most systematic guidelines in the world, and I was the main framer," Peng exclaims. There's an appearance of a conflict of interest in this, Norris says, although the government's acceptance of help with regulatory guidelines may reflect a wish to catch up quickly with standards in developed countries.

Peng acknowledges that SiBiono has government support and confirms that the application for Gendicine was sped "through a special channel." The data from the Gendicine trials were submitted to SFDA in March 2003; the drug was approved 7 months later. Sunway also "pushed" to get its H101 application through in 10 months, Hu confirms. But companies can also apply for accelerated review at the U.S. FDA, and Peng argues that Chinese companies must comply with strict regulations, just like their counterparts in the West.

Yin Hongzhang, SFDA's chief of biological products, says the agency has "special policies" to approve a drug on the fast track if an initial technical review looks fine. "But we would require the manufacturer to do further research and collect more data on efficacy to submit" after approval, he says. Earlier this year, he asked SiBiono to send the required follow-up data; when he spoke with *Science* he was still waiting for the data.

China's regulatory framework differs in another way. Whereas the U.S. FDA often requires that novel cancer drugs extend the life

Selected Chinese Cancer Gene-Therapy Drugs			
Company	**Founded**	**Products**	**Status**
Shenzhen SiBiono GeneTech Co.	1998	● Recombinant adenovirus encoding human tumor suppressor gene *p53* (rAd-*p53* or Gendicine)	Approved in 2003
Shanghai Sunway Biotech Co.	1999	● Recombinant oncolytic adenovirus (H101 or Oncorine)	Approved in 2005
		● Genetically modified adenovirus encoding heat shock protein HSP70 gene (H103)	In phase I
Shenzhen Tiandakang Gene Engineering Co.	2001	● Recombinant adenovirus–herpes simplex virus encoding thymidine kinase (AdV-TK)	Finished phase I
Guangzhou Doublle Bioproduct Inc.	2001	● Recombinant adenovirus encoding human endostatin (Ad-rhE)	Entered phase II
		● Recombinant adenovirus encoding human interferon-γ (Ad-rhIFN)	Applied for phase I
Chengdu Hoist Inc.	1998	● Recombinant adenovirus encoding human interleukin-2	In phase I

of the patient to be judged a success, SFDA approved both Gendicine and H101 on the basis of tumor shrinkage.

Sunway's Hu says his company intends to show that H101 increases survival as well as shrinks tumors. "Survival time for patients is very important," says Hu. In a retrospective study, he says the company has found that H101 can provide a 7-month survival benefit, but the results were not significant. They are now repeating phase III trials with a bigger sample size and more treatment cycles designed to maximize survival benefit.

There is good reason to expect that Chinese biotechnology will have a bright future. Companies in China "have excellent pro-

duction facilities, a lot of money, and a lot of good people," says UW's Lieber. Zhang adds that Chinese bioscientists deserve credit for picking up U.S. pioneers' work in cancer gene therapy.

At least a half-dozen Chinese gene-therapy drugs are in clinical trials at the moment, says Savio Woo, past president of the American Society of Gene Therapy. "Before the end of this decade, they should have more drugs. I will be surprised if they didn't," he says. China also may draw significant outside investment to the field. Genzyme, for example, is negotiating to have Sunway run a phase II gene-therapy clinical trial in China. The U.S. company is testing a modified adenovirus construct (Ad2/HIF-1α) to promote angiogenesis

in patients with peripheral arterial disease, an immobilizing condition that decreases blood flow to the muscles. Already, Genyzme has enrolled 300 patients in Europe and the United States. "The climate in China is changing, with more innovative companies not just focused on manufacturing," says Genzyme Vice President Earl Collier Jr. "We want to participate."

Zhang nevertheless worries about "media hype" that could "mislead patients, officials, and investors and cause significant damage to the further development of China's biotech industry." He hopes China can avoid repeating the mistakes that set back gene therapy in the West.

–JERRY GUO AND HAO XIN

Jerry Guo is a writer in New Haven, Connecticut.

Chef-scientist. Hervé This wants to rid cookbooks of thousands of useless old wisdoms.

CREDIT: COURTESY OF INRA

PROFILE: HERVÉ THIS

The Joy of Evidence-Based Cooking

Molecular gastronomist Hervé This is trying to demystify cooking in a country whose cuisine is famous worldwide

PARIS—Is it true that pears turn red in covered copper pans lined with tin? Do you always have to whip cream in the same direction? Does the skin of suckling pigs really get more crackling when the head is cut immediately after roasting? What of the old French wisdom that mayonnaise, a delicate emulsion of oil and water, will fail when prepared by menstruating women?

Such are the questions that occupy the mind of French celebrity scientist Hervé This, who studies the science of cooking. This (pronounced "Teess"), who has dual appointments at the National Institute for Agronomic Research (INRA) and the Collège de France, wants to know whether common rules of cooking are science-based or

just bogus. (The answers to the above questions, in case you are wondering, are no, no, yes, and no, respectively.)

This is the most prominent spokesperson of a small but growing research field known as "molecular gastronomy," or, as famed food science writer Harold McGee from Palo Alto, California, puts it, "the science of making delicious things." He studies what happens in pots, pans, and ovens to create that divine flavor and texture. And in the process, he's trying to give cooking a more solid scientific basis, which means getting rid of some age-old wisdoms.

That may seem like a hard sell in a country where tradition reigns, especially in matters relating to food. Yet This has been

remarkably successful. A series of books, columns, and TV appearances, as well as his close ties to some famous chefs, have made him a household name in France; his efforts to introduce science into culinary schools and to acquaint children with science through cooking have met with enthusiasm. Even those who criticize his scientific output concede that This has been a remarkably effective spokesperson for both science and culinary innovation.

Although trained as a physical chemist, This, 51, started his career in 1981 as an editor at *Pour la Science*, a popular science magazine. But he was crazy about cooking, had his own lab at home, and very often wrote about food. In 1995, chemist and Nobel laureate Jean-Marie Lehn asked This to join his chemistry lab at the Collège de France, a job This initially combined with his work at the magazine. But when he was offered a job at INRA as well in 2000, he quit his editing job to become a full-time researcher.

Although the science of cooking has existed for centuries, the field matured, and unmistakably picked up cachet, thanks to a series of now-legendary annual gatherings between 1992 and 2003 at a resort in Erice, Sicily. This organized the meetings with physicist Nicholas Kurti, a pioneer in cooking research at Oxford University who died in 1998. Participants would discuss the science behind food preparation, occasionally cook, and invariably eat and drink well for about 4 days. "It was a place where Nobel scientists and three-star chefs came together, indulging in a hobby, if you will," says Anthony Blake, a retired flavor expert who attended several times.

Kurti and This coined the term molecular gastronomy as they prepared the first meeting, in part because it sounded modern and sexy. Since then, the name has stuck as a way to distinguish the small group of researchers who study restaurant and home cooking from the larger, older, and less glamorous field of industrial food chemistry. But McGee—another frequent guest at Erice—considers it a misnomer, because scientists in this field don't study the interaction of individual molecules like molecular biologists do; it's just food chemistry, he says. (This disagrees.)

To add to the confusion, the term molecular gastronomy is also widely used to describe the cuisine at some creative top restaurants that have their own labs, such as elBulli, 2 hours from Barcelona, which was named the world's best restaurant by *Restaurant* magazine this year. Actually, elBulli chef Ferran Adrià has invented most of his revolutionary techniques—such as the use of hydrocolloids and agar-agar to create new textures—without the help of scientists, says McGee. And Adrià resents the fact that so many press stories link him to the scientific field; scientific curiosity is just one of the many elements of his cooking, his says.

Deconstructing stock

On a recent afternoon at his Collège de France lab, one of This's co-workers was making a carrot stock. Stocks may be commonplace in the kitchen, This explains, but they are still something of a scientific mystery. This has studied exactly which compounds come out of the carrot to give the liquid its flavor—sugars and amino acids, mostly—but he also wants to know how this happens. Are they released as cells in the carrot burst open? Or do they simply diffuse out of the channels in the carrot? And does it make a difference whether you simmer for 2 or 20 hours?

One of This's obsessions is that chefs, despite knowing so little about science, have developed such elaborate laws. Over the years, he has meticulously collected more than 25,000 instructions, called *précisions* in French, from cookbooks, many of which are useless, he says. So where do they come from? "Our parents love us. Why are they teaching us all these rules that make no sense?" His hypothesis: Cooks, using trial and error, remembered the circumstances in which they created a successful dish, even if they were irrelevant, and made them part of the recipe.

If that's true, he says, then dishes prone to fail—such as mayonnaise—should have

Show-and-tell. This, who studies the science of cooking, often livens up lectures with demonstrations.

accumulated more *précisions* than the easy ones; in other words, there should be an inverse relation between what This calls the recipe's "robustness" and the number of *précisions*. Testing the theory for a number of different dishes, This did indeed find the predicted relation—although there was one outlier, meat stock, which is hard to blow yet surrounded with *précisions*. (This chalks it up to stocks' extraordinary importance in French culinary culture.)

This's ambition is to do away with all unnecessary instructions and the wasted time they entail. If each of France's 500 culinary schools tested four *précisions* a year, an idea he is now promoting, the job could be done in just over 10 years, he says. Not everybody is equally fascinated. "I'm not sure I'd spend so much time studying misunderstandings of the past," says McGee. But food scientist Erik van der Linden of Wageningen University in the Netherlands says investigating these old wisdoms is "hugely important" because it can lead to new scientific questions.

Resistance from the culinary world can be strong, however: For instance, several chefs balked when This told them that it's useless to throw cooked haricots verts into

ice water to preserve the fresh green color. "They thought that the cold fixated the chlorophyll," says This. "Chemically, that doesn't mean anything."

In another attempt to bring rigor to the messy process of cooking, This has developed a system for "classification of dispersed systems," which describes each dish as a formula, based on the state of its ingredients (gas, liquid, or solid) and the preparation process. (In this system, puff pastry becomes $((S_1/S_2)_{0.5} \sigma ((W/O)/S_3)_{0.5})^{\sigma729}$.) The formulas—a bit like those Lavoisier developed to describe chemical reactions—can be used not only to classify dishes, This says, but to invent new ones as well. "He's the first one ever to try that, and it's something to be proud of," says Van der Linden.

Although he says he's more interested in research than in cooking, This does have close ties with a three-star chef, Pierre Gagnaire of the eponymous restaurant in Paris. Every month, This sends him an idea from the lab—for instance, an egg cooked at 65°C, which is far less rubbery than those cooked at 100°—which Gagnaire then turns into a recipe. (The entire collection is available on Gagnaire's Web site.)

Meanwhile, This is tirelessly campaigning to promote his field. His CV lists 600 interviews and press conferences—until he stopped keeping track. His lectures are enormously popular—"I've always thought of him more as a showman than a scientist," Blake says—and his columns are published in 11 journals and magazines in France and abroad. At the request of former culture minister Jack Lang, This developed a science and cooking class for schoolchildren in 2001, which is still running. ("A great way to make them love chemistry," he says.) He has just started a Foundation for Food Science and Culture at the prestigious Académie des Sciences.

"He is really effective and wonderful as a popularizer, and that's very important," says McGee. And if more chefs follow This's lead and become a tad less loath to forgo tradition, he adds, France might have less trouble fending off newcomers such as Spain and the United Kingdom that are threatening its position as the world's best country for eating. **–MARTIN ENSERINK**

SCIENCE FUNDING

Italy's Research Crunch: Election Promises Fade

Critics say no-growth agenda could leave Italian science isolated in Europe

Italy's researchers are bracing for a tough year ahead. The 2007 national finance bill, which is creeping through the legislature and is due for signature by 31 December, would provide no growth for cash-starved universities and research centers. Indeed, some centers are facing cuts as deep as 13%. But the bill does create new research jobs and makes small allocations to selected research budgets, mainly in response to protests. Also included are administrative "reforms," which have been greeted with both hope and suspicion.

Researchers are feeling the pinch because the center-left government of Prime Minister Romano Prodi, elected in May, is under pressure to reduce the country's deficit. The chief of the university and research ministry, Fabio Mussi, who says he is trying to avert a crunch, has warned already that 2007 will be "a lean year for everyone." Appeals for more funds are coming from students, university rectors, institute heads, and eminent scientists. In a widely reported plea for new research positions, Nobel laureate Rita Levi-Montalcini said during a recent debate: "Italy is poor in raw material but rich in human capital. If it's destroyed, Italy can't help but sink." In response, the government came up with a small hike to cash already earmarked for 2000 new posts over the next 3 years.

But the finance bill is a huge disappointment to scientists. During the election, Prodi's team campaigned on a pledge to hike research spending from the current level of 1.1% of gross domestic product to 3% by 2010. Such a boost would have put Italy in line with European Union (E.U.) goals for creating a knowledge economy (*Science*, 7 April, p. 37). Mussi has now set his sights lower: "reaching 1.5% within 5 years." Fabio Pistella, head of the National Research Council (CNR), says that the "incredible" cuts of 13% he is facing will mean the council can't even cover salaries. "Italian research runs the risk of being completely left out of the E.U.'s Framework 7 initiatives," he warns, and Piero Benvenuti, chief of the National Institute for Astrophysics, fears the loss of "the predominant role that Italian astrophysics has created for itself in the world."

The institutional reforms in the bill, Mussi insists, are designed to improve transparency and remove "party politics." A U-turn would restore autonomy to institutions such as the National Institute for the Physics of Matter, which was incorporated into CNR by former science minister Letizia Moratti. Another change has already separated the education and research ministries, reversing a merger carried out by the previous government.

The bill also includes a radical measure to remove research institution heads—viewed by many as political appointees—and set up committees to search for replacements on merit. Some scientists grumble that this measure would only increase government control. But others are encouraged. Carlo Bernardini, a physicist at the University of Rome "La Sapienza," says the measures are a "gulp of oxygen" that could help science recover from the "business mentality" of the previous government. Along with other scientists, he is pleased that the government is backing a shift toward autonomy and accountability in research institutions. The Italian Space Agency is already being overhauled (*Science*, 10 November, p. 903).

In pushing for new research posts, Mussi recognized that the workforce needs rejuvenation, not just expansion. The average age of a newly appointed university *ricercatore* (researcher in the first career step) is almost 36, whereas the average age of all *ricercatori* is about 50. Only half the nation's estimated 108,000 academic staff have tenure, and 30,000 will be retiring in the next few years.

The academic appointment system itself is in for overhaul too. Currently, selection competitions—known as the *concorsi*—are run by individual universities. Under the new regulations, universities would still advertise their posts, but evaluation would follow national criteria. Procedures would be established to ensure transparency and speed up selections, and members of selection committees would be drawn from outside a university making an appointment. Successful candidates would be cleared for specific universities only on the go-ahead of a new assessment agency, ANVUR. This long-debated independent organ would have broad authority to evaluate the merit of research produced by institutions as the basis for distribution of new resources. Academic leaders are wary. Mussi has only sketched out his plan; members of the Accademia dei Lincei, an independent scholarly society, want to see the details. They are concerned about delays and paperwork inherent in centralized systems of review.

What's missing in the bill, says Aldo Schiavone, law faculty head at Florence University, is "a plan or list of priorities" for reforming the universities, a sentiment echoed by head of state Giorgio Napolitano, who has called for a "courageous reform" of the entire university system. But that's not in the cards this year.

–SUSAN BIGGIN
Susan Biggin is a writer in Trieste, Italy.

Political drama. After an emotional appeal from Nobelist Rita Levi-Montalcini (*inset*), research chief Fabio Mussi increased funds for research posts.

EVOLUTION

Two Rapidly Evolving Genes Spell Trouble for Hybrids

Evolutionary geneticists are pinning down pairs of genes that help promote speciation; these genes are rapidly evolving, but not in response to ecological pressures

New species arise when populations become separated and evolve along different paths until, eventually, their members can no longer breed successfully with each other. That was Darwin's revolutionary insight, and it has shaped our understanding of the natural world. But the underlying mechanism has been hard to pin down. Why, for example, do even closely related species have difficulty producing viable offspring? Hybrids, if they survive at all, tend to be less fit than their parents. And therein lies the crux of speciation.

Now, one group has nailed down a 70-year-old theory about why hybrids are usually doomed to failure. On page 1292, Daniel Barbash, a geneticist at Cornell University, and his colleagues report the identification of a pair of genes that are key to making two closely related fruit fly species reproductively incompatible. Other groups are closing in on genes that cause problems for hybrids in monkeyflowers and marine invertebrates called copepods. In each case, the genes appear to be evolving rapidly, implying that they are under selective pressure. It's the "beginning of a new phase in speciation research, where we can get at both the specific genetic mechanisms and [the] interactions underlying one of the most fundamental questions in evolutionary biology," says Mohammed Noor of Duke University in Durham, North Carolina.

This work supports a theory first proposed in 1937 by Theodosius Dobzhansky and independently a few years later by Hermann Joseph Muller. They suggested that the root cause of hybrid failure is that pairs of genes whose proteins interact with each other—for instance, an enzyme and the protein it breaks down—evolve along different paths after populations split. In each population, the gene pairs evolve in concert so that their protein products continue to work together. But, said Dobzhansky and Muller, eventually the proteins in the individuals in one population will have changed so much that they no longer work properly with their former partners in the other population. When mixed back together in hybrids, these proteins are incompatible—an enzyme from one population will no longer break down the target protein from the other, for example—and potentially lethal problems arise: Hybrids may be sterile or may not survive at all.

Hybrid hypothesis. Independently, Theodosius Dobzhansky (*top*) and Hermann Joseph Muller proposed that incompatible genes could kill hybrids, speeding speciation.

The Dobzhansky-Muller model gained wide acceptance. "It's really our best general model of how mutations can accumulate to cause reproductive isolation," says Hopi Hoekstra, an evolutionary biologist at the University of California, San Diego. Confirming the details, however, has been challenging. "The problem is really, really hard because what you are trying to do is genetics between species," says H. Allen Orr, an evolutionary geneticist at the University of Rochester in New York.

Over the years, researchers have found evidence supporting parts of the Dobzhansky-Muller model but not all of it. Typically, researchers find one gene but not its putative partner. For example, for decades, researchers

have known that crossing two aquarium fish—a platyfish and a swordtail—has dire consequences. The offspring develop large black spots, and crossing the hybrid back to a parent often results in lethal skin tumors. Cancer researcher Manfred Schartl of the University of Würzburg, Germany, tracked down a causative gene, *Xmrk2*, on the X chromosome. He knows that it interacts with a "suppressor" gene that keeps *Xmrk2* in check and suspects that *Xmrk2* and the suppressor have diverged across the two species so they no longer interact effectively. However, to this day, the true identity of the suppressor remains unknown.

Drosophila researchers were also stumped for a long time. They could produce offspring by mating *D. melanogaster* with *D. simulans*, *D. mauritiana*, or *D. sechellia*, but too few offspring survived for researchers to carry out additional breeding experiments. Takao Watanabe came to the rescue in the 1970s when he discovered a mutant strain of *D. simulans* that could hybridize quite successfully with *D. melanogaster*. Watanabe, a geneticist at the National Institute of Genetics in Mishima, Japan, surmised that somewhere in its genome, the *D. simulans* strain carried a mutant gene that interacts successfully with a partner in *D. melanogaster*. He called the unidentified gene *lhr* for "lethal hybrid rescue." The finding "jump-started the field," says Barbash.

In the late 1980s, Michael Ashburner and Pierre Hutter of the University of Cambridge uncovered evidence for a similar gene in *D. melanogaster*, calling it *hmr* for "hybrid male rescue." They didn't know the exact location or identity of this gene, but crosses between *hmr* mutant strains and *D. simulans* worked just fine. With these strains in hand, researchers were able to produce viable hybrids, and they began modifying the genomes of the parents further to track down the specific genes involved in hybrid sterility and lethality.

On to the genes

Barbash picked up where Watanabe and Ashburner and their colleagues left off. In 2003, he and his colleagues pinpointed and sequenced the *D. melanogaster hmr* gene and discovered that it was a transcription factor. A year later, he and Philip Awadalla of North Carolina State University in Raleigh and colleagues demonstrated that the *hmr* genes had indeed diverged functionally between the two species. When they put an intact copy of *D. melanogaster hmr* into the *hmr* mutant strain, hybrids with *D. simulans* died as larvae. But when they repeated the experiment

with an intact *hmr* from *D. simulans*, hybrids survived, Barbash reported. When they compared the differences in 250 genes between the two species, they found that *hmr* was one of the most rapidly evolving.

With one gene that fulfilled Dobzhansky and Muller's expectations in hand, Barbash began to chase down its partner. He focused on *lhr*, as several earlier studies suggested that *lhr* and *hmr* worked as a pair. The rough location of *lhr* was already known but not its identity. With the help of the newly generated genome sequence data for *D. simulans*, Nicholas Brideau, Jun Wang, and Heather Flores in Barbash's lab looked for genes whose sequence indicated that their proteins could interact with the hmr protein. They concentrated on one that had not only diverged quite a bit from its counterpart in *D. melanogaster* but is also mutated in Watanabe's *D. simulans* strain.

Brideau, Wang, and Flores designed an ingenious experiment to test whether they had the correct gene. They put the candidate *lhr* gene from *D. simulans* into *D. melanogaster* and mated the resulting fruit flies with Watanabe's *D. simulans* strain. If the candidate gene was indeed *lhr*, its presence in *D. melanogaster* should override the mutant *lhr* in *D. simulans* and result in dead hybrids. It did. Barbash's group has confirmed that the lhr and hmr proteins interact. "We don't understand the mechanistic or molecular basis of the interaction," Barbash says, "but both genes in combination are required to kill the hybrid."

Scores of other incompatible gene pairs have likely evolved over the millions of years that fruit flies have diverged. Daven Presgraves, an evolutionary geneticist at the University of Rochester, is well on his way to pinning down a second pair. In 2003, after devising a way to screen for hybrid lethality genes, he turned up with one called *Nup96*, which codes for a protein that is part of the nuclear pore in eukaryotes. To begin to track down *Nup96*'s partner, he and Wolfgang Stephan of the University of Munich, Germany, took a close look at five of the 30 other fruit fly pore proteins to see how they differed between *D. melanogaster* and *D. simulans*. To their surprise, all five are evolving quite fast, they reported online 20 October in *Molecular Biology and Evolution*. The screen Presgraves used to identify *Nup96* detects only those genes whose interacting partner is on the X chro-

Look-alikes not alike. Although nearly identical —researchers rely on the cuticle (*near right*) of *Drosophila melanogaster* (*top*) and the cuticle (*far right*) of *D. simulans* (*bottom*) to tell these fruit flies apart—the two species rarely produce viable young.
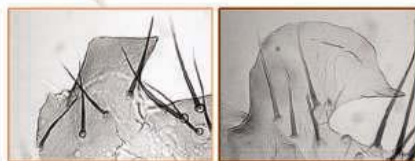
mosome. Only one of the five other pore proteins, called Nup153, has that genomic address. "We are certainly hot on the trail" of pinning down *Nup96*'s incompatible partner, says Presgraves.

Although much of the progress in identifying Dobzhansky-Muller gene pairs comes from fruit fly studies, researchers are starting to track down these genes in other species. In the monkeyflower, for instance, they have narrowed the search to relatively small chromosomal regions. In other cases, such as copepods, two genes are in hand, but their relationship is known primarily through test-tube studies and not through genetic analyses.

While a graduate student with John Willis at Duke University, Andrea Sweigart tracked down the cause of hybrid sterility in two closely related species of monkeyflower. One, *Mimulus guttatus*, is pollinated by insects, while the other, *M. nasutus*, is self-fertilizing. Both species occur in western North America but tend to grow in different habitats. Hybrids do form where they coexist,

but the species maintain distinct identities, says Sweigart, now at the University of Rochester.

In 2001, Lila Fishman, now at the University of Montana, Missoula, and Willis showed that second-generation hybrids suffer from male sterility, suggesting genetic incompatibilities were at work. From extensive breeding and genetic mapping studies between the two species and between hybrids and the parental lines, Sweigart and Willis identified two places in the genome, called hms1 and hms2, where the incompatible genes are located, they reported in the April issue of *Genetics*.

Ronald Burton of the Scripps Institution of Oceanography in San Diego, California, has found two interacting genes that may be helping to isolate different populations of copepods, a Californian intertidal invertebrate. He and his students have found that the gene for the protein cytochrome c, which is important for electron transport and energy generation, varies across copepod populations. Test-tube studies indicate that these variations affect the efficiency of the protein's reaction with cytochrome c oxidase, suggesting that these two could be genetically incompatible in hybrids.

Selective pressures

These new findings have thrown up some surprises. In particular, the genes behind hybrid lethality are evolving and adapting at an unusual pace compared to the rest of the genome. "Almost all these genes have a strong signature of natural selection," says Hoekstra. Yet the genes seem unlikely candidates for rapid evolution. The lhr protein is associated with heterochromatin, the parts of chromosomes containing lots of repetitive DNA, and nuclear pores are conserved from yeast to humans. "You just don't expect those genes to evolve rapidly," says Presgraves.

The fact that nucleoporin genes evolved quickly in species that are widely separated geographically suggests that ecological factors are not at the root of those gene changes, Presgraves adds. Indeed, notes Jerry Coyne, an evolutionary biologist at the University of Chicago in Illinois, "where the action is going to be is to [learn] what kind of natural selection is acting on these genes." The answer is unlikely to take another 70 years. **–ELIZABETH PENNISI**

Bad match. Sister species, the platyfish (*top left*) and the swordtail (*top right*) can interbreed, but hybrids (*bottom*) often develop deadly melanoma tumors.

Q

Who's helping bring the gift of science to everyone?
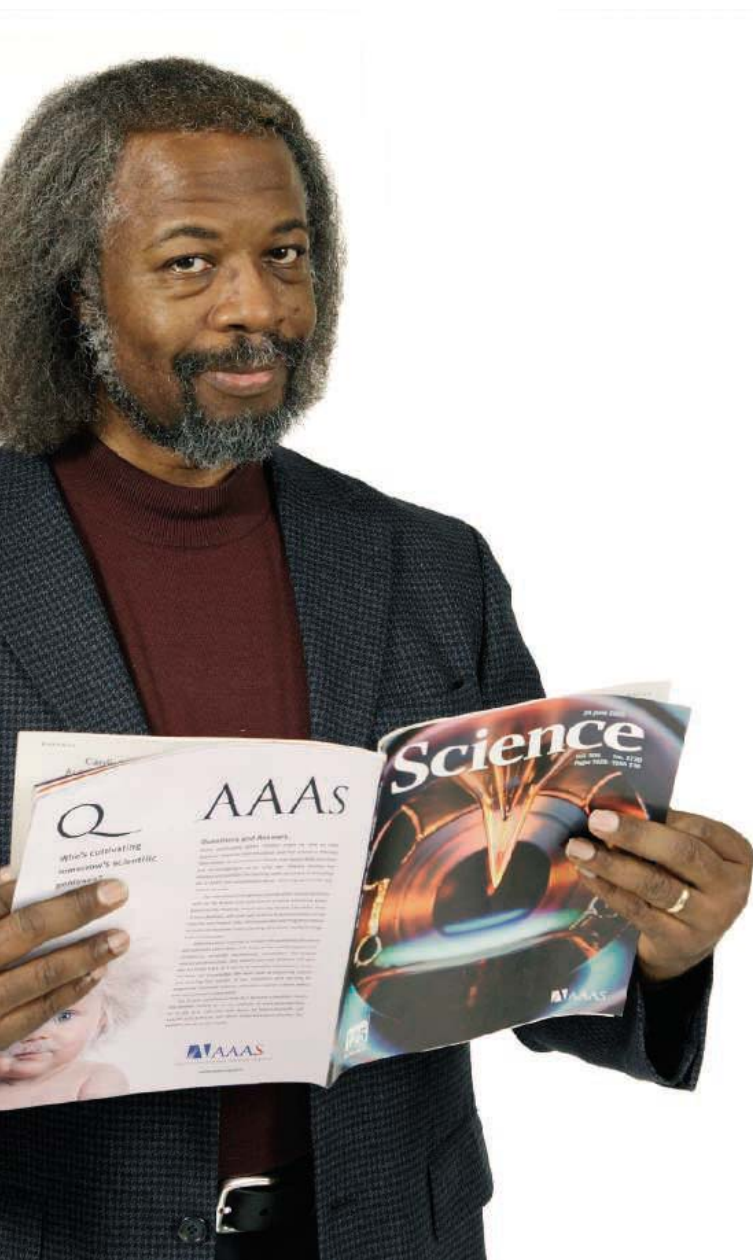
AAAs

" As a child I got very interested in space travel. When I was six my father gave me some books on rockets and stars. And my universe suddenly exploded in size because I realized those lights in the sky I was looking at were actually places.

I wanted to go there. And I discovered that science and technology was a gift that made this possible. The thrill of most Christmas presents can quickly wear off. But I've found that physics is a gift that is ALWAYS exciting.

I've been a member of AAAS for a number of years. I think it's important to join because AAAS represents scientists in government, to the corporate sector, and to the public. This is very vital because so much of today's science is not widely understood.

I also appreciate getting *Science* because of the breadth of topics it covers. It gives me a great grounding for many activities in my professional life, such as advising government agencies and private corporations. "

Jim Gates is a theoretical physicist and professor at the University of Maryland. He's also a member of AAAS.

See video clips of this story and others at
www.aaas.org/stories

S. James Gates Jr., Ph.D.
Theoretical physicist
and AAAS member

AAAS

ADVANCING SCIENCE, SERVING SOCIETY

LETTERS

edited by Etta Kavanagh

A Debate Over Iraqi Death Estimates

JOHN BOHANNON'S ARTICLE "IRAQI DEATH ESTIMATES CALLED TOO high; methods faulted" (News of the Week, 20 Oct., p. 396) contains several errors that require comment.

Bohannon fails to appreciate that cluster sampling is a random sampling method. Sampling for our study was designed to give all households an equal chance of being included. In this multistage cluster sampling, random selections were made at several levels ending with the "start" house being randomly chosen. From there, the house with the nearest front door was sampled until 39 consecutive houses were selected. This usually involved a chain of houses extending into two or three adjacent streets. Using two teams of two persons each, 40 houses could be surveyed in one day. Of our 47 clusters, 13 or 28% were rural, approximating the UN estimates for the rural population of Iraq.

Bohannon states that Gilbert Burnham did not know exactly how the Iraqi team conducted its survey. The text sent to Bohannon, which he fails to cite, said, "As far as selection of the start houses, in areas where there were residential streets that did not cross the main avenues in the area selected, these were included in the random street selection process, in an effort to reduce the selection bias that more busy streets would have." In no place does our *Lancet* paper say that the survey team avoided small back alleys. The methods section of the paper was modified with the suggestions of peer reviewers and the editorial staff. At no time did Burnham describe it to Bohannon as "oversimplified."

Those who work in conflict situations know that checkpoints often scrutinize written materials carried by those stopped, and their purpose may be questioned. Unique identifiers, such as neighborhoods, streets, and houses, would pose a risk not only to those in survey locations, but also to the survey teams. Protection of human subjects is always paramount in field research. Not including unique identifiers was specified in the approval the study received from the Johns Hopkins Bloomberg School of Public Health Committee on Human Research. At no time did the teams "destroy" details, as Bohannon contends. Not recording unique identifiers does not compromise the validity of our results.

Concerning mortality estimates, Michael Spagat may be content, as Bohannon claims, with mortality data collected barely 1 year into an escalating 3.5-year war. Others might not find these so helpful.

GILBERT BURNHAM AND LES ROBERTS

Department of International Health, Johns Hopkins Bloomberg School of Public Health, Baltimore, MD 21205, USA.

An Iraqi woman collapses after learning of the death of a relative in a bomb attack on a police car.

Response

I DO APPRECIATE THAT CLUSTER SAMPLING relies on random samples. It is indeed the very bone of contention. "Sampling for our study was designed to give all households an equal chance of being included," Burnham and Roberts write. But according to their methods as published in *The Lancet*, that is not the case.

My article reports the concerns of Sean Gourley and Neil Johnson, who point out that the starting house was always on a street "randomly selected from a list of residential streets crossing the main street." This excludes all the smaller streets—including back alleys—that do not cross a main street. Maps of Iraqi cities, freely available at www.earth.google.com, show that many residential areas would be excluded by this survey protocol. People living in those underrepresented households, Gourley and Johnson argue, are less likely to be exposed to the violence—car bombs, drive-by shootings, airstrikes—that accounts for most of the reported deaths.

When I asked Burnham by e-mail about this possible source of bias, he replied that "in areas where there were residential streets that did not cross the main avenues in the area selected, these were included in the random street selection process, in an effort to reduce the selection bias that more busy streets would have." When I asked him why the published methods leave out this wiggle room, he replied that "in trying to shorten the paper from its original very large size, this bit got chopped, unfortunately." I used the term "oversimplified" to describe this discrepancy.

I stated that "the details about neighborhoods surveyed were destroyed." The details in question are the "scraps" of paper on which streets and addresses were written to "randomly" choose households, and as Burnham and Roberts explained to me, that record has indeed been destroyed. I appreciate the difficulty of conducting a study in a combat zone and also the researchers' desire to protect the survey team and respondents. At the same time, scientists concerned about the true number of Iraqi casualties want to know which method was used to select households and whether sample bias can explain the high number of violent deaths reported by Burnham *et al*. But without a clear and explicit methodology or raw data to independently examine, it is impossible to know.

JOHN BOHANNON

CREDIT: SLAHALDEEN RASHEED/REUTERS

A Nonprotein Amino Acid and Neurodegeneration

RESEARCH ON β-METHYLAMINO-L-ALANINE (BMAA) and neurodegenerative disease among the Chamorro people of Guam lost momentum when M. W. Duncan reported BMAA levels in washed cycad flour far lower than those reported to generate acute neurotoxicity in primates (1, 2). We hypothesized that the Chamorros may be exposed to increased levels of cycad neurotoxins, including BMAA, when they eat flying foxes and other animals that forage on cycad seeds (3). Two new findings—selective neurotoxicity of BMAA to motor neurons at low concentrations (4) and alternative inputs of BMAA in the Chamorro diet (5)—have brought renewed attention to BMAA. M. W. Duncan and A. M. Marini's Letter "Debating the cause of a neurological disorder" (22 Sept., p. 1737) needs clarification, as the authors may have been unaware of recent literature that supports the link between BMAA and neurological disease.

Cycad seeds
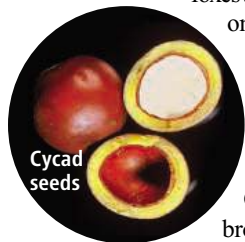
Their suggestion that BMAA "is not very neurotoxic" needs updating in light of evidence that 30 µM BMAA selectively kills motor neurons (4). Duncan and Marini express concern about the three flying fox specimens analyzed in our 2003 paper (6), but we subsequently reported BMAA in an additional 21 specimens (7). They question the specificity of the assay we used, but 6-aminoquinolyl-N-hydroxy-succinimidyl carbamate, developed as a stable high-performance liquid chromatography fluorescent tag for hospital analysis of amino acids (8, 9), is more reliable than the less modern methods used by Montine et al. (10).

Questions about Chamorro consumption of flying foxes ignore evidence that hunting contributed to significant declines in flying fox populations (11). Over 220,000 dead flying foxes were imported within a 15-year period to meet resultant consumer demand (12). We have also found that high levels of BMAA occur

in protein fractions of cycad flour (13), which updates Duncan's earlier report (2).

The discovery that BMAA is produced by diverse taxa of cyanobacteria opens the possibility of human exposure far from Guam (14). Our blinded analysis of BMAA in control and diseased tissues, however, does not prove causality. The real question is not whether BMAA is present, but whether exposure to BMAA can produce progressive neurodegeneration. That question deserves a second look.

PAUL A. COX[1] AND SANDRA A. BANACK[2]
[1]Director, Institute for Ethnomedicine, Jackson Hole, WY 83001, USA. [2]Associate Professor of Biological Science, California State University, Fullerton, CA 92834, USA.

References

1. P. S. Spencer et al., Science 237, 517 (1987).
2. M. W. Duncan, Adv. Neurol. 56, 301 (1991).
3. P. A. Cox, O. W. Sacks, Neurology 59, 1664 (2002).
4. S. D. Rao, S. A. Banack, P. A. Cox, J. H. Weiss, Exp. Neurol. 201, 244 (2006).
5. P. A. Cox, S. A. Banack, S. J. Murch, Proc. Natl. Acad. Sci. U.S.A. 100, 13380 (2003).
6. S. A. Banack, P. A. Cox, Neurology 61, 387 (2003).
7. S. A. Banack, S. J. Murch, P. A. Cox, J. Ethnopharmacol. 106, 97 (2006).
8. S. A. Cohen, D. P. Michaud, Anal. Biochem. 211, 279 (1993).
9. P. Fürst, L. Pollack, T. A. Graser, H. Godel, P. Stehle, J. Chromatogr. 499, 557 (1990).
10. T. J. Montine, K. Li, D. P. Perl, D. Galasko, Neurology 65, 768 (2005).
11. M. E. Wheeler, CAL-NEVA Wildl. Trans. 1979, 149 (1979).
12. G. J. Wiles, U.S.Fish Wildl. Serv. Biol. Rep. 90, 53 (1992).
13. S. J. Murch, P. A. Cox, S. A. Banack, Proc. Natl. Acad. Sci. U.S.A. 101, 12228 (2004).
14. P. A. Cox et al., Proc. Natl. Acad. Sci. U.S.A. 102, 5074 (2005).

Plants, RNAi, and the Nobel Prize

IN JENNIFER COUZIN'S RECENT PIECE ON THE Nobel Prize that was awarded to Andy Fire and Craig Mello, an anonymous RNA interference (RNAi) researcher was quoted as saying "plants got screwed" ("Method to silence genes earns loud praise," News of the Week, 6 Oct., p. 34). As an early participant in the plant RNA silencing field, I take exception with this view. I feel that the Nobel committee's decision to focus on the central role of double-stranded RNA (dsRNA) was quite appropriate; it was this specific discovery that broke an obscure field wide open and brought it to the attention of all biologists. The publication of RNAi (1) catalyzed new interactions between plant and animal geneticists that led directly to all kinds of discoveries about the mechanisms underlying and related to RNAi. The impact on biological research from understanding that dsRNA is a key intermediate in triggering RNAi has been huge. dsRNA is used as a tool to silence genes in a significant percentage of all papers on eucaryotic biology (for instance, "RNA interference" was mentioned in more than 20% of

all research articles published this year in the journal I edit, The Plant Cell, the leading primary research journal in plant biology). Of course, there were also many other very important discoveries in the RNAi field, by researchers working in plants, animals, and fungi, but none of them had the same catalytic impact on biology as did Fire and Mello's key insight and elegant experimentation. The Nobel committee decided to keep the award simple and straightforward for good reason.

The Nobel Prize is not really about making scientists famous—it is about making science interesting and accessible to the public. RNAi is a wonderful vehicle for communicating the importance and potential of basic research. Many more people will now understand the value of fundamental research because of the RNAi story, and that is fantastic news for all scientists.

Congratulations, Andy and Craig, and thank you for your tremendous contribution to science! **RICH JORGENSEN**
Editor in Chief, The Plant Cell, Department of Plant Sciences, University of Arizona, Tucson, AZ 85721–0036, USA.

Reference

1. A. Fire et al., Nature 391, 806 (1998).

WE CONGRATULATE ANDREW FIRE AND CRAIG Mello on their Nobel Prize for the discovery of RNA interference (RNAi). Their experiments identified double-stranded RNA as a reliable trigger of gene silencing and attracted the interest of animal biologists. However, as plant scientists who were involved in some of the earliest work on gene silencing, we want to correct the impression conveyed in Jennifer Couzin's article "Method to silence genes earns loud praise" (News of the Week, 6 Oct., p. 34) that plant biologists made puzzling findings that were not tied together in any way. The general principle developed by plant biologists was "homology-dependent gene silencing," in which various combinations of "homologous" sequence interactions between DNA and/or RNA induce silencing at either the transcriptional or posttranscriptional level (1). This concept, which was novel at the time, underlies our current understanding of RNAi-mediated silencing pathways in both the cytoplasm and the nucleus. Epigenetic modifications induced by homologous sequence interactions, including RNA-directed DNA methylation (2), were identified in some of the earliest plant studies and paved the way for the discovery of RNAi-mediated heterochromatin formation in fission yeast. Connections between homology-dependent gene silencing and transposon control, virus resistance, and development were made early on by plant scientists (1, 3, 4) and are now considered, at least in part, to be

RNAi-mediated processes. Double-stranded RNA as an intermediate in the silencing pathway in plants was proposed in models (*4*, *5*) and directly tested in plant systems (*6*). Thus, plant research leading up to the discovery of RNAi in *C. elegans* cannot be regarded as a set of diffuse observations that lacked a unifying theme, nor did plant scientists fail to recognize the broader implications of their work.

MARJORI MATZKE AND ANTONIUS J. M. MATZKE

Gregor Mendel Institute of Molecular Plant Biology, Austrian Academy of Sciences, Vienna A-1030, Austria.

References
1. M. Matzke, A. Matzke, *Plant Physiol.* **107**, 679 (1995).
2. M. Wassenegger *et al.*, *Cell* **76**, 567 (1994).
3. R. Flavell, *Proc. Natl. Acad. Sci. U.S.A.* **91**, 3490 (1994).
4. J. Lindbo *et al.*, *Plant Cell* **5**, 1749 (1993).
5. M. Metzlaff *et al.*, *Cell* **88**, 845 (1997).
6. P. Waterhouse *et al.*, *Proc. Natl. Acad. Sci. U.S.A.* **95**, 13959 (1998).

TECHNICAL COMMENT ABSTRACTS

COMMENT ON Papers by Chong *et al.*, Nishio *et al.*, and Suri *et al.* on Diabetes Reversal in NOD Mice

Denise L. Faustman, Simon D. Tran, Shohta Kodama, Beatrijs M. Lodde, Ildiko Szalayova, Sharon Key, Zsuzsanna Toth, Éva Mezey

Chong *et al.*, Nishio *et al.*, and Suri *et al.* (Reports, 24 March 2006, pp. 1774, 1775, and 1778) confirmed that treating nonobese diabetic (NOD) mice with an immune adjuvant and semisyngenic spleen cells can reverse the disease but found that spleen cells did not contribute to the observed recovery of pancreatic islets. We show that islet regeneration predominately originates from endogenous cells but that introduced spleen cells can also contribute to islet recovery.

Full text at www.sciencemag.org/cgi/content/full/314/5803/1243a

RESPONSE TO COMMENT ON Chong *et al.* on Diabetes Reversal in NOD Mice

Anita S. Chong, Jikun Shen, Jing Tao, Dengping Yin, Andrey Kuznetsov, Manami Hara, Louis H. Philipson

We failed to detect transdifferentiation of spleen cells into β cells following diabetes reversal in nonobese diabetic (NOD) mice, thus contradicting a key finding of a 2003 report. We respond to Faustman *et al.* by justifying the use of mouse insulin promoter–green fluorescent protein transgenic mice as an appropriate system for detecting spleen-derived β cells in the islets of cured NOD mice.

Full text at www.sciencemag.org/cgi/content/full/314/5803/1243b

RESPONSE TO COMMENT ON Nishio *et al.* on Diabetes Reversal in NOD Mice

Junko Nishio, Jason L. Gaglia, Stuart E. Turvey, Christopher Campbell, Christophe Benoist, Diane Mathis

Contrary to previous findings, we found no significant differentiation of splenocytes into pancreatic islet cells in nonobese diabetic (NOD) mice treated with an immune adjuvant and allogenic spleen cells. We show that our single-nucleotide polymorphism assay has the requisite sensitivity to support our contention. The experiments of Faustman *et al.* lack adequate controls, and we maintain that no evidence of islet regeneration has been presented.

Full text at www.sciencemag.org/cgi/content/full/314/5803/1243c

RESPONSE TO COMMENT ON Suri *et al.* on Diabetes Reversal in NOD Mice

Anish Suri and Emil R. Unanue

Faustman *et al.* present no new information to explain why three independent laboratories failed to reproduce their previous results implicating spleen cell transdifferentiation in the reversal of murine type 1 diabetes. Modulation of the immunological process in nonobese diabetic (NOD) mice has been accomplished by many laboratories using different protocols and does not represent a novel finding in their work.

Full text at www.sciencemag.org/cgi/content/full/314/5803/1243d

---

POLITICAL SCIENCE

Learning to Become a "Good" Citizen

André Blais

The principal claim David Campbell advances in *Why We Vote* is that an internalized sense of civic duty is a crucial factor motivating people to vote and that this sense of duty is nourished in homogeneous communities with strong civic norms. Campbell, a political scientist at the University of Notre Dame, proposes a dual-motivations theory of public engagement. People become involved to fulfill a sense of duty or to protect their interests. The two motivations exist among different types of people but also sometimes within the same individual. Both affect the decision to vote or not to vote, although sense of duty matters more. Sense of duty dominates in "civic"-minded forms of engagement such as volunteering, whereas interest is prominent in activities such as protest or partisan work.

> **Why We Vote**
> How Schools and Communities Shape Our Civic Life
>
> *by David E. Campbell*
>
> Princeton University Press, Princeton, NJ, 2006. 283 pp. $39.50, £26.95. ISBN 0-691-12525-2.

The author performs a myriad of complementary analyses of voting in U.S. counties or metropolitan areas, which establish the following patterns: (i) There is a u-shaped relationship between community heterogeneity and turnout. People are more likely to vote in both the most politically homogeneous and the most heterogeneous communities (because of their sense of duty in the former, and because of greater competition in the latter). (ii) Volunteerism increases in more homogeneous communities, whereas protest and electoral activism thrive in more heterogeneous settings. (iii) Those with more politically homogeneous social networks are more inclined to vote. (iv) Adolescents who live in more homogeneous counties are more likely to do volunteer work. (iv) Adolescents who volunteer are more inclined to vote when they become adults. (v) The strength of civic norms within one's high school (the prevalence of the belief that to be a good citizen one must vote) increases the probability that one will vote (and do volunteer work) 15 years later.

The reviewer is in the Départment de sciences politiques, Université de Montréal, Case Postale 6128, succursale Centre-ville, Montreal, Quebec H3C 3J7, Canada. E-mail: andre.blais@umontreal.ca

In short, Campbell argues that whether one votes or not in an election hinges very much on social norms and most strongly on the feeling that it is a citizen's moral obligation to vote, and that this norm is usually acquired before adulthood. Sense of civic duty, like all social norms, develops more strongly in homogeneous settings—where people are more likely to arrive at a consensus about what is right and wrong, to recognize the legitimacy of the other members of the community to enforce the norm, and to interact with these other members (this last condition facilitating the actual implementation of the norm).

One of the book's important findings is that what matters for the development of civic norms is political homogeneity. Previous research has focused on the consequences of economic, racial, or ethnic heterogeneity. Campbell argues that shared political preferences constitute a significant indicator of common ground among people. And indeed he shows that while political homogeneity has powerful effects on public engagement, the impact of social or economic heterogeneity is weak and inconsistent.

This is an impressive study. Each piece of the puzzle is examined rigorously, and specific pieces of evidence are marshaled to support each argument. The empirical tests are compelling. The appropriate control variables are incorporated into the analyses. It is difficult to see how and why the relationships that are uncovered could be spurious. And the author does a wonderful job of linking the various results into a coherent story.

Instilling civics.

Nonetheless, there remain some ambiguities or inconsistencies. The author starts with a dual-motivations theory, but by the end of the analyses, duty has become the predominant consideration and interest has been relegated to the sidelines. If different types of communities and schools nurture different types of motivations, we should expect civic climate to be positively correlated with volunteering but also to be negatively correlated with other forms of engagement such as electoral activism and political voice. The data Campbell analyzes confirm the former prediction but not the latter (there is no negative correlation with political activism).

I find the book extremely compelling and provocative. The big questions that remain are: How much does sense of duty explain turnout? And how much does political homogeneity explain sense of duty?

Campbell provides some indications as to the answers. Everything else being equal, the probability of voting in 1980 was 10 percentage points higher for someone whose high school civic climate was strongest in 1965 than for someone whose high school civic climate was weakest. The size of the impact is of the same magnitude as the effects of education and parental political involvement. This justifies the claim that sense of civic duty ought to be included in a comprehensive model of turnout. But we still do not have a good grasp of how many people vote primarily because they feel it is their duty to do so.

Campbell finds that the impact of political heterogeneity on youth volunteering is of the same magnitude, again comparable to the effects of parental education and parental volunteering. These results suggest, however, that the family is at least as important as the school and the community in shaping civic norms. This seems to be forgotten by the author, who is perhaps too focused on the debate about the consequences of social heterogeneity. My reading of the evidence is that families shape civic norms at least as much as schools and communities.

Lastly, *Why We Vote* challenges us to think seriously about the role of schools in society. Schools are meant to produce intel-

CREDIT: CORBIS

ligent citizens but also "responsible" ones. Campbell's study shows that schools matter. It may not be clear what should and can be done to foster the development of civic norms in the schools. But clearly we must think hard about which aspects of the existing system facilitate or hinder the attainment of that objective.

10.1126/science.1135672

SCIENCE CAREERS

An Unpredictable Future Should Not Stop You from Planning

Dmitrii F. Perepichka

Building a successful career in science or in any other endeavor is a long and difficult journey, where a few decisions—right or wrong—can profoundly change your future. Walking into the local bookstore or even a university library, you can find a plethora of career counseling literature, some of which may remind you of wilderness survival recommendations. Many of these titles are intended for business students, salespeople, and financial managers, and it seems next to impossible to find a good, comprehensive book that would help a beginning researcher. This scarcity is not because the scientific environment is inherently less hostile than the business world. In fact, scientists face a competitive environment in which only the fittest persist and are more likely to succeed with a better guide than trial and error.

With *Survival Skills for Scientists*, Federico Rosei and Tudor Johnston (an experimentalist in surface science and a theoretician in plasma physics, respectively, at the University of Quebec's Institut National de la Recherche Scientifique Enérgie, Matériaux, et Télécommunications) aim to fill this information vacuum. The book poses questions about careers that, although not forbidden, graduate students often leave

The reviewer is in the Department of Chemistry, McGill University, 801 Sherbrooke Street West, Montreal, Quebec H3A 2K6, Canada. E-mail: dmitrii.perepichka@mcgill.ca

unasked. Progressing from undergraduate studies to graduate school, through postdoctoral fellowship to their first real job, only a few young scientists can rely entirely on the advice of a good older friend or a mentor, a person who they would not hesitate to ask and whose opinion they can trust. How do you choose a field, a school, and a professor? Why should you continue on for a postdoc? Where and how do you publish your results? At the end of your training, how do you get the job you desire and how do you secure funding for your research? The authors address these and many concomitant issues through the prism of understanding of a younger professor (Rosei), rectified with the time-tested opinion of his senior colleague (Johnston).

Although largely based on the authors' personal experiences, the book is amazingly multifaceted. Unlike other similar publications (of which there are only a few), *Survival Skills* is not limited to a single career choice. Instead, it discusses scientific life in academia, industry, and government labs as well as in different parts of the world. The authors should be congratulated for the depth of their analysis of challenges facing the modern researcher. Most of the observations and recommendations of these two physics professors are quite general and would apply in almost any area of the natural sciences, engineering, and, to a lesser extent, the biomedical sciences. The specific circumstances in the social sciences are very different, although some parts of the book will be universally helpful.

I found the book thought provoking and packed with information, yet amusing and in most places easy to read. The anecdotes in the "Diversions" and Rosei's collection of "Cautionary Tales" are both humorous and to the point. The book's main message is that even for an unpredictable future, planning ahead is a better strategy than simply going along with the flow. Although no text can substitute for first-hand experience, an intelligent person should be able to learn from others' mistakes. Reading and reflecting on the ideas presented in *Survival Skills* early in your career could save a

> **Survival Skills for Scientists**
>
> *by Federico Rosei and Tudor Johnston*
>
> Imperial College Press, London, 2006. 227 pp. $38, £22. ISBN 1-86094-640-2. Paper, $24, £14. ISBN 1-86094-641-0.

Providing guidance. Inukshuk, structures made by piling unworked, local stones, offer the Inuit of the Canadian Arctic guidance on the best paths to take and hazards to avoid.

lot of time and frustration. Best of all, you do not actually have to agree with all the specific advice the authors give. (I don't, and even the authors do not always agree with one another.) But their arguments will certainly help you to work out your own line of behavior.

One criticism: The authors overemphasize their categorization of scientists as alpha (those who like to manage the research) or beta (those who like to do the research). That leaves the impression that the prime goal of any ambitious person should be to ascend the career ladder, as quickly as possible starting to manage research and forgetting "how to turn the knobs." To the contrary, many recent science pioneers have been leaders at both alpha and beta tasks. Donald Cram (who shared a 1987 Nobel Prize for molecular recognition and supramolecular chemistry) is said to have greeted each new assistant professor in UCLA's chemistry department by showing his palms and saying: "Look at these hands. That's how I made my first 20 papers." Thus, it is not the lack of desire to work in the lab that differentiates a scientific leader from a follower.

The regrettable truth, however, is that in today's world the manager's qualities are becoming an ever larger component of a personality of a successful scientist. Knowing this should make you a better player—whether you count yourself as a pragmatist (as perhaps are the authors of this book) or you are more romantically motivated (as I like to think of myself). And that is just one of the many useful lessons *Survival Skills for Scientists* imparts.

10.1126/science.1134999

MENTORING

Volunteers Bring Passion to Science Outreach

Moriah R. Beck,[1,2]* Elizabeth A. Morgan,[1] Stephanie S. Strand,[1,2] Thomas A. Woolsey[1,3]

Partnerships between graduate students and high school students in St. Louis benefit both groups, and bring real laboratory experiences to the high school students.

Scientists in the United States have been called upon to help reform science and math education by engaging in "effective equal partnerships" with primary and secondary schools (*1*). Such partnerships are often developed as part of research proposals to establish a "broader impact" component. A highly successful program at Washington University in St. Louis, Missouri, shows that such partnerships are valuable not only to the schools but also to the participating scientists.

Many universities have initiated successful science outreach programs that involve professional educators and full-time staff. In contrast, the Young Scientist Program (YSP) at Washington University in St. Louis is led and staffed almost entirely by graduate and medical student volunteers, who as scientists bring enthusiasm directly from the laboratory to the classroom. YSP is a partnership between the university and nearby school systems that improves science education in high schools and also attracts young students to scientific careers.

YSP was founded by two Washington University M.D./Ph.D. students, Jim McCarter and Matt Schreiber, in 1991. They recognized that students often lose interest in science during high school and hypothesized that exposure to hands-on research would attract young students to careers in science (*2*). They launched a program to bring high school students into biomedical laboratories at Washington University for summer research internships. The program continues to focus on nearby public schools that include
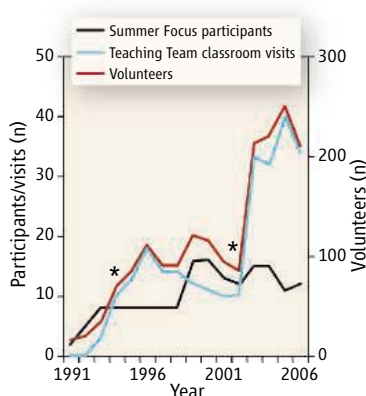
Growth of the YSP program. The number of Summer Focus participants (black line), teaching team classroom visits (blue line), and total number of volunteers (red line) per year highlight how the program has developed since inception. Volunteers typically participate in several activities over several years; values approximate the numbers of volunteers participating in any given year. Asterisks mark years when a part-time, and later full-time, coordinator was hired.

children from disadvantaged backgrounds.

Structure

YSP is run by volunteers who participate for many reasons, including dedication to community outreach, a love of teaching, and a commitment to increase the participation of underrepresented groups in science. Involvement ranges from fundraising to curriculum development and teaching to directing the entire YSP program [see supporting online material (SOM)]. The volunteers—currently about 150 graduate and medical students, postdoctoral fellows, and residents—receive no pay or academic credit.

Schools for the city of St. Louis (population 360,000) and the surrounding metropolitan region of Missouri and Illinois (population 2.7 million) serve about 34,000 students (including kindergarteners to 12th graders), 82% of whom are African American (compared with the Missouri average of 18%) (*3*). Most of these students are from low-income families. Only 57% of entering freshmen complete high school (compared with the Missouri average of 86%), and of these only 41% enroll in college (Missouri's average is 64%). Despite efforts toward improvement of the St. Louis schools, the Missouri School Improvement Program currently gives the St. Louis school district only provisional accreditation (*4*), whereas elsewhere in Missouri, 97% of public school districts have earned full accreditation.

Programs

YSP volunteers have developed several programs (see SOM) to supplement the educational experience of high school students and their teachers. Successful implementation, continued funding, and institutional support have allowed the program to expand both the number of volunteer opportunities and the number of students reached (see figure, left).

Teaching Teams. YSP volunteers develop and lead interactive, inquiry-driven science exercises in local public high school science classes and after-school programs for off-site conferences and during field trips. The team members provide all necessary equipment and reagents and work in groups of three to seven volunteers with student groups of 10 to 200. Teaching-team activities are modified in collaboration with teachers, integrating classroom curriculum and state standards. Teaching teams have interacted directly with more than 5000 students since 1993.

Summer Focus. From 80 to 100 high school student applicants each year, 30 are interviewed and 12 finalists are chosen as Summer Focus Scholars. Each Scholar is mentored by a volunteer graduate student or postdoctoral fellow, completes an independent research project, and writes a formal research paper during an eight-week internship. Projects are related to the research of the mentors and address real scientific questions. Scholars also meet with individual tutors and participate in laboratory technique workshops, weekly seminars, journal clubs, and a science-writing course. More than 165 local students have participated in Summer Focus.

Teacher and Researcher Partnership. YSP initiated this program in 2001 to provide summer research and curriculum enrichment experiences for three to six public school teachers each year. Nearly half of the teachers who apply are selected each year to work with scientists on an individual research project and curriculum develop-

[1]The Young Scientist Program, [2]Department of Molecular Microbiology, [3]Department of Neurological Surgery, Washington University School of Medicine, St. Louis, MO 63110, USA.

*To whom correspondence should be addressed. E-mail: mrwillia@artsci.wustl.edu

ment activities for their own classrooms. Teachers earn professional development credits and receive a stipend and funds for classroom supplies.

Mad Scientist Network (MadSci). YSP's Web site (*5*), launched in 1995, includes MadSci (*6*), a forum designed to answer science questions submitted via the internet. MadSci has evolved into an international resource promoting global science literacy at all education levels. YSP volunteers still serve as moderators, although MadSci was recently incorporated as an independent nonprofit organization under the direction of its creator and former YSP volunteer Lynn Bry.

Benefits and Outcomes

YSP asks its participants to evaluate programs shortly after participation. Retrospective evaluations are undertaken every 5 years, most recently in 2002 (see SOM). Thus, both the immediate and long-term effectiveness of YSP programs are assessed.

YSP has had a substantial impact on its volunteers. YSP volunteers become more aware of educational disparities in urban areas and gain a variety of skills that are not formally taught during graduate and post-graduate training. In the 2002 retrospective evaluation, past volunteers ranked teaching, mentoring, and communication as the most valuable skills acquired through YSP participation (see figure, above right). Results showed that 44% of respondents selected the group-teaching experience as one of the greatest benefits (fig. S7). The retrospective evaluation also showed that a third of former volunteers who are no longer at Washington University participate in community outreach at their new locations. Thus, YSP has brought to a cadre of young scientists the resolve, experience, and skills to continue this outreach to the public throughout their careers.

The ultimate objective of YSP is to enrich the scientific experience of local high school students and teachers. Teaching teams reach the most students, primarily during visits to local classrooms. Through hands-on experimentation and small-group discussions, students explore science in an informal but structured setting under the direction of bright and compelling role models. A survey of more than 200 students participating in the neuroscience teaching team at the 2006 Spring Brain Conference demonstrated that the students had a better understanding of the nervous system after participating and they enjoyed the experience (*7*). Similar data from teaching team visits to St. Louis public schools confirm

that this approach is a viable way to increase science content knowledge in specific subject areas (fig. S3).

For students and teachers participating in the Summer Focus and Teacher and Researcher Partnership programs, the benefits are even greater. Participants experience a professional scientific atmosphere and see the risks and rewards of science. By retrospective evaluation, 65% of former Scholars indicated that the Summer Focus experience confirmed their commitment to a career in science or medicine (fig. S6). Past Scholars (2002 evaluation) ranked laboratory techniques, application of the scientific method, and writing ability as the most important skills acquired through YSP (see figure, right). Partnership teachers benefit as they discuss scientific concepts, share experiences about teaching and connecting with students, and develop new curricula. Once Scholars and teachers get to know Washington University and its faculty, they continue to use this resource after their summer internships.

Support

YSP's current annual budget (*8*) is $53,500 plus the salary of one full-time coordinator, paid for by the university. The program is now building an endowment. A faculty adviser meets monthly with the student director and the coordinator. YSP convenes past participants, community members, and Washington University faculty and volunteers twice a year to solicit feedback and ideas.

The Future

YSP was established on the premise that science literacy and access to science-based careers are improved by the active involvement of professional scientists in the education of the local community. Since 1991, more than 350 Washington University volunteers have worked directly with students and teachers from nearby high schools, with a measurably positive impact. A key strength is that YSP is organized and run by volunteers whose commitment to the program springs from a love of teaching and mentoring future scientists. A full-time coordinator, a faculty adviser, and community advisory board allow for evolution, innovation, and growth through successive generations of volunteer leadership.

In the 15 years since its inception, YSP has firmly established its role at Washington University and the St. Louis high schools. YSP's methods and exercises have been dis-
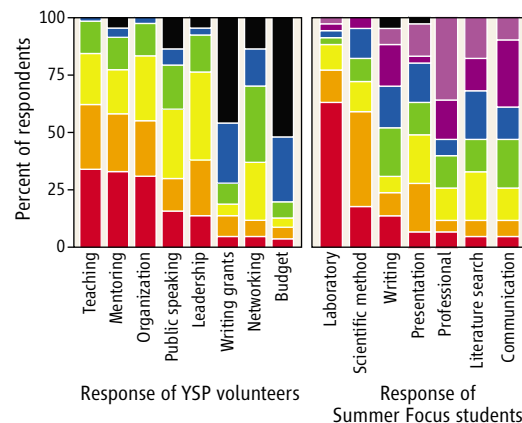
Skills gained through YSP activities. In 2002, YSP volunteers (*n* = 58) (**left**) and Summer Focus students (*n* = 28) (**right**) completed a retrospective evaluation in which they ranked the value of specific skills acquired during participation in YSP. Likert scale categories are represented by the colors of the rainbow, with red indicating most valuable and purple indicating least valuable; black, not applicable.

seminated by former volunteers and faculty via the internet and at outreach seminars in conjunction with national meetings. As YSP continues to adapt and grow, it remains committed to enriching the scientific experience of underserved populations one student at a time.

References and Notes

1. R. R. Colwell, E. M. Kelly, *Science* **286**, 237 (1999).
2. Committee on Science, Engineering, and Public Policy, *Rising Above the Gathering Storm: Energizing and Employing America for a Brighter Economic Future* (National Academies Press, Washington, DC, 2006); available online (http://fermat.nap.edu/execsumm_pdf/11463.pdf).
3. Missouri Department of Elementary and Secondary Education, *Missouri School District Profiles* (Missouri Department of Elementary and Secondary Education, Jefferson City, MO, 2006); available online (http://dese.mo.gov/planning/profile/115115.html).
4. Saint Louis Public Schools, *An Annual Report to the Community 2003–2004* (Saint Louis Public Schools, St. Louis, MO, 2004); available online (www.slps.org/districtinformation/index.htm).
5. The Young Scientist Program (www.medicine.wustl.edu/~ysp).
6. The Mad Scientist Network (www.madsci.org).
7. S. R. McIver, C. LaPash, *2006 Brain Awareness Week Report* (Society for Neuroscience, Washington, DC, 2006); available online (www.sfn.org/baw/bawreport2006).
8. This work was supported in part by grants from the Howard Hughes Medical Institute (51000177 and 51000126); Washington University's Medical Scientist Training Program, Office of Diversity Programs, Medical Center Alumni Association, Genome Sequencing Center (NIHGR grant), and the Division of Biology and Biomedical Sciences; Pfizer, Inc.; and the American Association of Anatomists. YSP has also received other small grants and gifts.
9. We thank J. Mosher, J. McCarter, A. Grillo-Hill, M. Bradley, S. Elgin, V. May, G. Frey, and P. Balcerzak.

PHYSICS

Superconductivity with a Twist

A material related to high-temperature superconductors exhibits mobile regions of twisted symmetry much like ordered magnetic regions in magnets.

Maurice Rice

Cuprate oxides, which were found to be superconducting at relatively high temperatures about 20 years ago, have several less well-known cousins. One of the most intriguing of these "unconventional" materials, strontium ruthenate (Sr_2RuO_4), was observed to be a superconductor in 1994 (*1*). Now, two reports, one by Kidwingira *et al.* on page 1267 of this issue (*2*) and the other by Xia *et al.* in *Physical Review Letters* (*3*), provide detailed insights into how this material superconducts.

Soon after the discovery of superconductivity in Sr_2RuO_4 came proposals that it should be an unconventional superconductor like the cuprates, but with a crucial difference (*4*). Current flows freely in a superconductor because the electrons form pairs that travel unhindered through the material. In Sr_2RuO_4, the electron pairs that form in the superconducting state should have parallel rather than antiparallel spins. (The states of a parallel spin pair are called triplets, and antiparallel spins are singlets.)

This difference has consequences for the orbital part of the electron pair wave function, a matter of fundamental importance in sorting out the various possible superconducting mechanisms. Electrons belong to the class of particles called fermions and thus obey some special rules—namely, that only odd orbital states are allowed for these triplet pairs, the lowest of which is called a p-wave state (where "odd" in this case means odd values of angular momentum: $L = 1, 3$, etc.).

Since the discovery of superconductivity in Sr_2RuO_4, much evidence has accumulated in support of the proposed triplet pairs (*5*), culminating in an elegant proof by Liu and co-workers (*6*) of the odd orbital character of the pairs. But this does not answer all the questions: The electron pairs in unconventional superconductors with non–s-wave pairing may or may not have an actual orbital moment. An orbital moment appears when the pair has a net angular momentum, but, particularly in a crystal, the angular momentum can be quenched by the lower symmetry. In the cuprates the pairs do not have net angular momentum, but the ruthenates always seemed more promising and early measurements were supportive (*7*).

The author is at the Institut für Theoretische Physik, Eidgenössische Technische Hochschule Zürich, 8092 Zürich, Switzerland. E-mail: maurice.rice@itp.phys.ethz.ch

Kidwingira *et al.* and Xia *et al.* have directly established the presence of an orbital moment in Sr_2RuO_4. They find that this superconductor has some similarities to a magnet—in technical terms, it breaks time-reversal symmetry. What this means quantum mechanically is that its pair wave function is inherently complex (that is, having real and imaginary parts), with a phase that twists through 2π as one follows the relative wave vector of the electrons around the Fermi surface (the constant-energy surface in momentum space of the highest occupied states). Sr_2RuO_4 is therefore the first chiral superconductor.

P-wave pairing has long been established in the fermionic superfluid ^3He, but the so-called chiral A-phase of the superfluid is restricted to a small region of the phase diagram near the high-pressure transition to the solid. The case for chiral pairing in strontium ruthenate comes from its layered structure, which leads to a cylindrical rather than a spherical Fermi surface. A chiral p-wave electron pair with an orbital moment has a wave function that is a function of the combination $k_x + ik_y$ (where k_x and k_y are the components of the electron momentum in the x and y directions, respectively). This combination has a constant modulus on a circle (in the xy plane) but not on a sphere (which includes the z axis). Because the energy gap determined by the modulus is constant on a circular Fermi cylinder but not on a Fermi sphere, chirality occurs already in weak coupling in layered materials, whereas strong coupling is required for a liquid such as ^3He. In practice, other effects contribute, such as deviations from a circular cross section in the key Fermi surface sheet in Sr_2RuO_4 and spin-orbit coupling. All this makes a direct confirmation of the earlier signs of chiral superconductivity in Sr_2RuO_4 a desirable goal.

Kidwingira *et al.* examined the magnetic field response of a Josephson junction made from a Sr_2RuO_4 crystal cleaved along a crystal axis in the basal plane and a conventional

Chiral superconductivity. Cross section of a domain wall separating two superconducting domains related by time-reversal symmetry. The domain wall lies in the yz plane with countercurrents J_y flowing in the y direction. These currents result in a magnetization dipole B_z polarized in the z direction. Experimental verification of these effects will be a further confirmation of the chiral nature of superconductivity in strontium ruthenate.

s-wave lead superconductor. The critical current passing through this junction often displayed the same pattern as conventional Josephson junctions with increasing field strength. But for other junctions of the same type, and even for thermal cycling of the same junction, Kidwingira *et al.* found completely different and random patterns. They explain this dichotomy through the presence of domain walls separating superconducting domains related by time reversal (that is, the relation between the combinations $k_x + ik_y$ and $k_x - ik_y$).

The key point is that for junctions with electron-pair transmission dominated by the k_x component, the superconductor looks coherent, whereas for those with a dominant k_y component, there is a phase change of π upon passing through each domain wall, which disrupts the standard pattern. These domains are analogous to domains with reversed magnetization in a ferromagnet, and they also split in energy when a magnetic field is applied. This can lead to formation of a single domain for samples cooled in a field, and also to noise and hysteresis generated by domain wall motion when a field is applied at low temperature to multidomain samples. Both effects are clearly demonstrated in their experiments.

Xia *et al.* (*3*) looked for rotation of the polarization direction of a reflected linearly polarized light beam with normal incidence on superconducting layers (the Kerr effect). Again, the analogy with a ferromagnet and the well-known magneto-optic Kerr effect is apt. Here the difficulty lies in the smallness of the rotation, which required a novel apparatus with very high resolution. Xia *et al.* observed the development of Kerr rotation as samples were cooled into the superconducting phase. The sign of the Kerr rotation could be positive or negative for samples cooled in zero field but was fixed for field-cooled samples by the direction of the field. Kerr rotation requires an antisymmetric term in the frequency-dependent dielectric tensor, which immediately implies broken time-reversal symmetry in the superconducting state.

The study of domains and domain walls has a long tradition in magnetism, and these experiments open this field to the study of chiral superconductors. Volovik and Gor'kov (8) were the first to study the theory of these kinds of superconducting domain walls. They found that the domains should contain counterflowing supercurrents along the wall that generate a perpendicular magnetic dipole (see the figure). All this remains to be verified experimentally, as does another effect predicted by Sigrist et al. (9): A novel magnetic vortex should accompany a singu-larity on a domain wall analogous to a Bloch line in magnetism. The observation of such a vortex with a fractional magnetic flux is a challenge to this emerging field, but it will not be easy in view of the short charac-teristic length scales that Kidwingira et al. deduce from their experiments. Confirmation of these exotic predictions will be a clear test of our understanding of these intriguing superconductors.

References
1. Y. Maeno et al., Nature **372**, 532 (1994).
2. F. Kidwingira, J. D. Strand, D. J. Van Harlingen, Y. Maeno, Science **314**, 1267 (2006); published online 26 October 2006 (10.1126/science.1133239).
3. J. Xia et al., Phys. Rev. Lett. **97**, 167002 (2006).
4. T. M. Rice, M. Sigrist, J. Phys. Condens. Matter **7**, L643 (1995).
5. A. P. MacKenzie, Y. Maeno, Rev. Mod. Phys. **75**, 657 (2005).
6. K. D. Nelson, Z. Q. Mao, Y. Maeno, Y. Liu, Science **306**, 1151 (2004).
7. G. M. Luke et al., Nature **394**, 558 (1998).
8. G. E. Volovik, L. P. Gor'kov, Sov. Phys. JETP **61**, 843 (1985).
9. M. Sigrist et al., Phys. Rev. Lett. **63**, 1727 (1989).

NEUROSCIENCE

The Brain's Dark Energy

Marcus E. Raichle

Much of the brain's enormous energy consumption is unaccounted for by its responses to external stimuli. What is this energy used for, and how do we study it?

Since the 19th century, and possibly longer, two perspectives on brain func-tions have existed (1). One view posits that the brain is primarily reflexive, driven by the momentary demands of the environment; the other, that the brain's operations are mainly intrinsic, involving the maintenance of information for interpreting, responding to, and even predicting environmental de-mands. While neither view is dominant, the former has motivated most neuroscience research. But technological advances, partic-ularly in neuroimaging, have provoked a reassessment of these two perspectives.

Human functional neuroimaging, first with positron emission tomography (PET) and now largely with functional magnetic resonance imaging (fMRI), allows the brain's responses to controlled stimuli to be studied by measuring changes in brain circulation and metabolism (energy consumption). Surprisingly, these studies have revealed that the additional energy required for such brain responses is extremely small compared to the ongoing amount of energy that the brain normally and continu-ously expends (2). The brain apparently uses most of its energy for functions unaccounted for—dark energy, in astronomical terms. What do we know about this dark energy?

The adult human brain represents about 2% of the body weight, yet accounts for about 20% of the body's total energy consumption, 10 times that predicted by its weight alone. What fraction of this energy is directly related to brain function? Depending on the approach used, it is estimated that 60 to 80% of the energy budget of the brain supports communi-cation among neurons and their supporting cells (2). The additional energy burden associ-ated with momentary demands of the environ-ment may be as little as 0.5 to 1.0% of the total energy budget (2). This cost-based analysis implies that intrinsic activity may be far more significant than evoked activity in terms of overall brain function.

Consideration of brain energy may thus provide new insights into questions that have long puzzled neuroscientists. For example, researchers have sought to explain the relative disproportion of connections (i.e., synapses) among neurons that appear to perform func-tions intrinsically within the cerebral cortex. Take the visual cortex, whose primary func-tion is to respond to external input to the retina. Less than 10% of all synapses carry incoming information from the external world (3)—a surprisingly small number. From a brain energy perspective, however, the cortex may simply be more involved in intrinsic activities.

What is this intrinsic activity? One possi-bility is that it simply represents unconstrained, spontaneous cognition—our daydreams or, more technically, stimulus-independent thoughts. But it is highly unlikely to account for more than that elicited by responding to controlled stimuli, which accounts for a very small fraction of total brain activity.
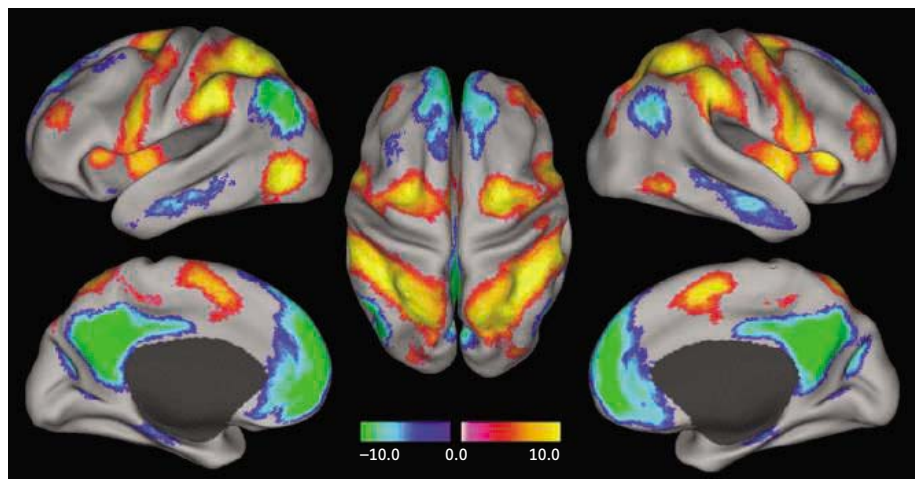
At rest, but active. fMRI images of a normal human brain at rest. The images reveal the highly organized nature of intrinsic brain activity, represented by correlated spontaneous fluctuations in the fMRI signal. Correlations are depicted by an arbitrary color scale. Positive correlations reside in areas known to increase activity during responses to controlled stimuli; negative correlations reside in areas that decrease activity under the same conditions. **(Left)** Lateral and medial views of the left hemisphere; **(center)** dorsal view; **(right)** lateral and medial views of the right hemisphere. [Reprinted from (12)]

The author is in the Department of Pediatrics, Washington University School of Medicine, St. Louis, MO 63110, USA. E-mail: gitlin@kids.wustl.edu

Another possibility is that the brain's enormous intrinsic functional activity facilitates responses to stimuli. Neurons continuously receive both excitatory and inhibitory inputs. The "balance" of these stimuli determines the responsiveness (or gain) of neurons to correlated inputs and, in so doing, potentially sculpts communication pathways in the brain (4). Balance also manifests at a large systems level. For example, neurologists know that strokes that damage cortical centers that control eye movements lead to deviation of the eyes toward the side of the lesion, implying the preexisting presence of "balance." It may be that in the normal brain, a balance of opposing forces enhances the precision of a wide range of processes. Thus, "balance" might be viewed as a necessary enabling, but costly, element of brain function.

A more expanded view is that intrinsic activity instantiates the maintenance of information for interpreting, responding to, and even predicting environmental demands. In this regard, a useful conceptual framework from theoretical neuroscience posits that the brain operates as a Bayesian inference engine, designed to generate predictions about the future (5). Beginning with a set of "advance" predictions at birth (genes), the brain is then sculpted by worldly experience to represent intrinsically a "best guess" ("priors" in Bayesian parlance) about the environment and, in the case of humans at least, to make predictions about the future (6). It has long been thought that the ability to reflect on the past or contemplate the future has facilitated the development of unique human attributes such as imagination and creativity (7, 8).

fMRI provides one important experimental approach to understanding the nature of the brain's intrinsic functional activity without direct recourse to controlled stimuli and observable behaviors. A prominent feature of fMRI is that the unaveraged signal is quite noisy, prompting researchers to average their data to reduce this "noise" and increase the signals they seek. In doing this, it turns out that a considerable fraction of the variance in the blood oxygen level–dependent (BOLD) signal of fMRI in the frequency range below 0.1 Hz, which reflects fluctuating neural activity, is lost. This activity exhibits striking patterns of coherence within known networks of specific neurons in the human brain in the absence of observable behaviors (see the figure).

Future research should address the cellular events underlying spontaneous fMRI BOLD signal fluctuations. Studies likely will cover a broad range of approaches to the study of spontaneous activity of neurons (9,

10). In this regard, descriptions of slow fluctuations (nominally <0.1 Hz) in neuronal membrane polarization—so-called up and down states—are intriguing (4, 10). Not only does their temporal frequency correspond to that of the spontaneous fluctuations in the fMRI BOLD signal, but their functional consequences may be relevant to an understanding of the variability in task-evoked brain activity as well as behavioral variability in human performance.

William James presciently suggested in 1890 (11) that "Enough has now been said to prove the general law of perception, which is this, that whilst part of what we perceive comes through our senses from the object before us, another part (and it may be the larger part) always comes (in Lazarus's phrase) out of our own head." The brain's energy consumption tells us that the brain is never at rest. The challenge of neuroscience is to understand the functions associated with this energy consumption.

References

1. R. Llinas, *I of the Vortex: From Neurons to Self* (MIT Press, Cambridge, MA, 2001).
2. M. E. Raichle, M. Mintun, *Annu. Rev. Neurosci.* **29**, 449 (2006).
3. A. Peters, B. R. Payne, J. Budd, *Cereb. Cortex* **4**, 215 (1994).
4. B. Haider, A. Duque, A. R. Hasenstaub, D. A. McCormick, *J. Neurosci.* **26**, 4535 (2006).
5. B. A. Olshausen, in *The Visual Neurosciences*, L. M. Chalupa, J. S. Werner, Eds. (MIT Press, Cambridge, 2003), pp. 1603–1615.
6. D. H. Ingvar, *Hum. Neurobiol.* **4**, 127 (1985).
7. D. Gilbert, *Stumbling on Happiness* (Knopf, New York, 2006).
8. J. Hawkins, S. Blakeslee, *On Intelligence* (Holt, New York, 2004).
9. D. A. Leopold, Y. Murayama, N. K. Logothetis, *Cereb. Cortex* **13**, 422 (2003).
10. C. C. H. Petersen, T. T. G. Hahn, M. Mehta, A. Grinvald, B. Sakmann, *Proc. Natl. Acad. Sci. U.S.A.* **100**, 13638 (2003).
11. W. James, *Principles of Psychology* (Henry Holt & Company, New York, 1890), vol. 2, p. 103.
12. M. D. Fox et al., *Proc. Natl. Acad. Sci. U.S.A.* **102**, 9673 (2005).

ATMOSPHERE

How Fast Are the Ice Sheets Melting?

Anny Cazenave

Remote-sensing data suggest that ice sheets currently contribute little to sea-level rise. However, dynamical instabilities in response to climate warming may cause faster ice-mass loss.

If the ice sheets covering Greenland and Antarctica were to melt completely, they would raise sea level by about 65 m. But even a small loss of ice mass from the ice sheets would have a great impact on sea level, particularly on low-lying islands and coastal regions. New satellite observations, including those reported by Luthcke *et al.* on page 1286 of this issue (1), now allow estimates of the mass balances of the ice sheets and their evolution through time.

For the past 3000 years, global sea level has remained stable, but since the end of the 19th century, tide gauges have detected global sea-level rises [~1.8 mm/year on average over the past 50 years (2, 3)]. Satellite altimetry data document a rate of ~3 mm/year since 1993 (4). However, it remains unclear whether the recent rate increase reflects an accelera-

tion in sea-level rise or a natural fluctuation on a decadal time scale.

Present-day sea-level rise has several causes. During the past decade, ocean warming has contributed roughly half of the observed rate of sea-level rise (5), leaving the other half for ocean-mass increase caused by water exchange with continents, glaciers, and ice sheets (6). The contribution of mountain glaciers and small ice caps to sea-level rise in the past decade is estimated to be ~0.8 mm/year (7). These figures constrain the contribution from ice sheets to less than 1 mm/year in the past decade.

Since the early 1990s, remote-sensing data based on airborne laser and satellite radar altimetry, as well as the space-borne Synthetic Aperture Radar Interferometry (InSAR) technique, have provided the first observations of ice sheet mass balance (8–13). These observations indicate accelerated ice-mass loss in recent years in the coastal regions of southern Greenland. In contrast, slight mass gain is reported in central high-elevation regions. Over Antarctica, remote sensing indicates

The author is at the Observatoire Midi-Pyrenees, 31400 Toulouse, France. E-mail: anny.cazenave@cnes.fr
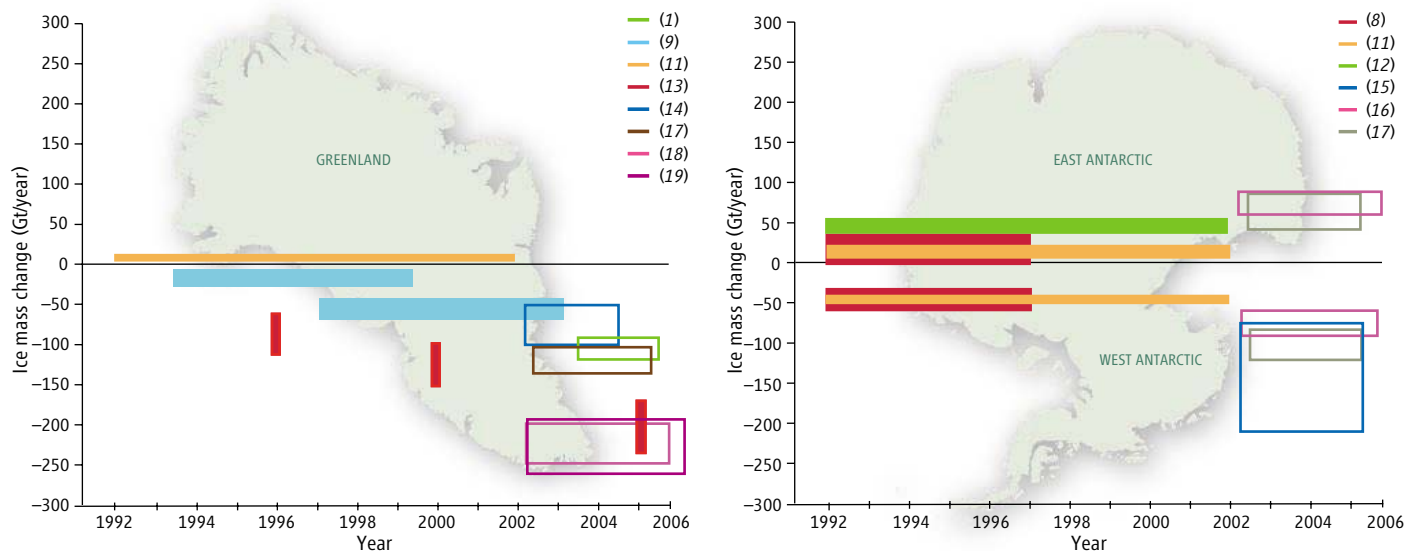
Ice-sheet mass change estimated by different remote-sensing techniques. (**Left**) Greenland. (**Right**) West and East Antarctica. The ice sheet mass change is given in gigatons per year. The numbers refer to different investigations as quoted in the reference list. Open bars correspond to GRACE results, filled bars to results from other techniques. The estimate from (*15*) is an average over the whole of Antarctica. On the right, positive values are for East Antarctica and negative values for West.

accelerated mass loss in the western part of the continent (*10*), whereas the eastern part is gaining some mass as a result of increased precipitation (*11, 12*).

Because of these contrasting behaviors—mass loss in coastal regions and mass gain in elevated central regions—ice-sheet mass loss exceeds mass gain only slightly. Thus, according to the recent mass-balance estimates, the ice sheets presently contribute little to sea-level rise. However, great uncertainty remains, mainly because of incomplete coverage by remote-sensing surveys, spatial and temporal undersampling, measurement errors, and perturbation from unrelated signals. In addition, each technique has its biases. For example, radar altimetry misses narrow coastal glaciers because of inadequate ground resolution, and ice elevations measured by the radar are much less reliable over steep, undulated surfaces than over flat high-elevation surfaces. Another uncertainty arises because conversion of elevation change to mass change requires assumptions about the surface density of snow or ice to be made.

Since 2002, the NASA/DLR Gravity Recovery and Climate Experiment (GRACE) satellite mission has provided a new tool for precise measurements of ice-sheet mass balance, with nearly complete coverage of the high-latitude regions up to 89°N/S. GRACE measures the spatiotemporal change of Earth's gravity field. Over the ice sheets, this change can be converted into ice-mass change, assuming that the gravity change results from a change in surface mass.

Several studies have reported estimates of Greenland and Antarctica ice-mass change from GRACE (*14–19*). The GRACE results confirm those from other remote-sensing techniques, that is, net ice-mass loss from Greenland and West Antarctica and a slight ice-mass gain over East Antarctica (see the figure). The GRACE results over Greenland also suggest accelerated ice-mass loss since 2002, in agreement with InSAR results (*13*).

However, the GRACE-based mass-balance estimates are highly scattered (see the figure). One reason is the short time span of the analyses (2 to 4 years, depending on the study). Over Greenland, ice mass varies widely from year to year. Because the analyses do not overlap exactly in time, different trend estimates are to be expected.

Another cause of scatter is contamination from geodynamic processes related to Earth's response to ice melt from the last deglaciation. This effect, which depends on poorly known parameters, is mainly available from modeling, with important differences between models. Moreover, over Antarctica, this effect is of the same order of magnitude as present-day ice-mass change.

A third source of uncertainty is the coarse resolution (400 to 600 km) of most GRACE results (*14–19*). As a result, the estimated ice-sheet mass change includes contributions not only from small isolated glaciers in the vicinity of the ice sheets, but also from other gravity signals (of oceanic, hydrologic, and tidal origin) from surrounding regions. These perturbing signals are still poorly known, and therefore difficult to be corrected for.

To improve the GRACE resolution, Luthcke *et al*. have applied a new approach over Greenland: They determined mass concentrations at a local scale from appropriate processing of the GRACE observations. This approach differs from the standard method, in which global solutions of the time-varying gravity field are computed, and a regional filter is then applied to extract the mass signal over the area of interest. The new approach minimizes the contamination from signals unrelated to the ice-sheet mass balance and provides results of finer resolution.

Luthcke *et al*. computed ice-mass change in six drainage basins of the Greenland ice sheet, ranging from coastal low-elevation to central elevated regions. They find ice-mass increase in high-elevation regions of northern Greenland, as suggested by satellite altimetry (*11*), and ice depletion at the margins of southern Greenland, in agreement with InSAR-based glacier discharge estimates (*13*). The results confirm accelerated ice flow in coastal regions of southeast Greenland. However, the trend is smaller than reported by some other recent GRACE-based studies (*18, 19*). Over the 2-year period of investigation, Luthcke *et al*.'s estimate of Greenland's contribution to sea-level rise amounts to ~0.3 mm/year.

However, further research is needed to improve estimates of Greenland and Antarctica mass balance (see the figure) and their contribution to sea level. Besides extending the time series of observations and reducing internal errors, it is important to reconcile estimates from different techniques and to eventually use them in synergy.

The greatest uncertainty in sea-level projections is the future behavior of the ice sheets. In recent years, the velocities of outlet glaciers in coastal regions of Greenland and Antarctica have accelerated, showing that a large fraction of ice-mass loss occurs through dynamical processes

rather than surface melting (*9*, *10*, *13*). The dynamical response of the ice sheets to present-day climate forcing may thus play a much larger role than previously assumed. Future dynamical instabilities of the ice sheets is of major concern, given their potential impact on sea level (*20*), yet comprehensive modeling of such dynamical effects is in its infancy.

Improved mass-balance estimates from remote-sensing observations, such as those reported by Luthcke *et al.*, will inform on the ongoing behavior of the ice sheets and help to validate models. This goal requires long time series of satellite observations,

and hence continuity of space missions.

References
1. S. B. Luthcke *et al.*, *Science* **314**, 1286 (2006); published online 19 October 2006 (10.1126/science.1130776).
2. J. A. Church *et al.*, *J. Climate* **17**, 2609 (2004).
3. S. Holgate, P. Woodworth, *Geophys. Res. Lett.* **31**, L07305 (2004).
4. A. Cazenave, R. S. Nerem, *Rev. Geophys.* **42**, RG3001 (2004).
5. S. Levitus, J. I. Antonov, T. P. Boyer, *Geophys. Res. Lett.* **32**, L02604, (2005).
6. A. Lombard *et al.*, *Ocean Dyn.*, in press.
7. M. Dyurgerov, M. F. Meier, INSTAAR, Univ. of Colorado, Boulder, CO, 2005; available at http://instaar.colorado.edu/other/occ_papers.html.
8. E. Rignot, R. Thomas, *Science* **297**, 1502 (2002).
9. W. Krabill *et al.*, *Geophys. Res. Lett.* **31**, L24402 (2004).
10. R. Thomas *et al.*, *Science* **306**, 255 (2004).
11. H. J. Zwally *et al.*, *J. Glaciol.* **51**, 509 (2005).
12. C. H. Davis *et al.*, *Science* **308**, 1898 (2005).
13. E. Rignot, P. Kanagaratnam, *Science* **311**, 986 (2006).
14. I. Velicogna, J. M. Wahr, *Geophys. Res. Lett.* **32**, L18505 (2005).
15. I. Velicogna, J. M. Wahr, *Science* **311**, 1754 (2006).
16. J. L. Chen, C. R. Wilson, D. D. Blankenship, B. D. Tapley, *Geophys. Res. Lett.* **33**, L11502 (2006).
17. G. Ramillien *et al.*, *Global Planet. Change*, in press.
18. J. L. Chen, C. R. Wilson, B. D. Tapley, *Science* **313**, 1958 (2006).
19. I. Velicogna, J. M. Wahr, *Nature* **443**, 329 (2006).
20. R. B. Alley *et al.*, *Science* **310**, 456 (2006).

PLANT SCIENCE

Distributing Nutrition

New insights into how plants store and mobilize nutrients, such as iron, can help in the fight against world hunger.

Jonathan D. Gitlin

Hunger claims the lives of 20,000 children a day. Worldwide, one of every three children is underweight and malnourished (*1*). Eradication of malnutrition and associated childhood mortality is a major mission of the United Nations Millennium Development Goals and will require a shared vision of conservation as well as improvements in agriculture that include increasing the nutritional value of staple crops (*2*). Advances in basic plant sciences applied to agriculture will be critical for success (*3*). Strong endorsement of this idea comes from two studies on pages 1295 and 1298 of this issue that provide insight into the mechanisms of nutrient distribution in plants (*4*, *5*). This work reminds us that any effort to enrich the nutritional content of plants requires knowledge of the mechanisms of acquisition and distribution of these nutrients throughout the component parts of the crops that are the dietary staple.

Kim *et al.* (*4*) combine mutational analysis and imaging to demonstrate an essential role for iron in seedling development—specifically, iron localized to an intracellular compartment called the vacuole in the model plant *Arabidopsis thaliana*. Although abundant, iron is relatively insoluble, and the challenge for all organisms is to acquire adequate amounts while avoiding toxicity (*6*). Iron is essential for oxygen transport throughout an organism and for cellular (mitochondrial) res-

The author is in the Department of Pediatrics, Washington University School of Medicine, St. Louis, MO 63110, USA. E-mail: gitlin@kids.wustl.edu

Dietary crops. A market, or *tianguis*, in Huauchinango, Mexico, with indigenous Mexicans and typical crop-based diets.

piration. Iron deficiency is common, affecting 500 million children in populations with crop-based diets. Infants are at greatest risk because brain growth can quickly outpace dietary availability, resulting in long-term neurocognitive impairment (*7*). Understanding iron homeostasis in plants is therefore essential to any effort intended to increase the iron content of staple foods as an approach to preventing iron deficiency.

In most organisms, iron that is stored in cells is bound to ferritin, a cytoplasmic protein. Unlike humans, but similar to yeast, plant cells contain vacuoles that function as reservoirs for ions and metabolites and could also serve as sites of iron storage (*8*). Kim *et al.* identify VIT1 as the *Arabidopsis* ortholog of a vacuolar iron transporter, CCC1, previously

identified in yeast. They show that this protein rescues the iron-sensitive phenotype of a yeast mutant that lacks CCC1, mediates iron sequestration into yeast vacuoles, and is highly expressed in developing seeds—an important food source worldwide. However, there is no difference in the total iron content of seeds or shoots between wild-type *Arabidopsis* plants and mutant plants that lack the gene encoding VIT1 (*vit1*). So is VIT1 required for plant iron homeostasis?

In an imaging tour de force, Kim *et al.* use x-ray fluorescence microtomography to demonstrate a dramatic loss of iron in germinating seeds that lack VIT1, specifically in provascular cells of the hypocotyl, radicle, and cotyledon embryonic seed tissues. This finding implicates the vacuole of provascular cells as critical to iron storage in wild-type seeds. Consistent with this idea, *vit1* seedlings germinate poorly under conditions that limit iron availability from the soil. These findings highlight the need to understand nutrient distribution in assessing homeostasis, as well as the importance of noninvasive, three-dimensional quantitative element analysis in living samples. Such approaches will find broad application to issues of nutrient homeostasis in living organisms.

In a related study, Uauy *et al.* (*5*) characterize *Gpc-B1* from wild emmer wheat as a simple Mendelian quantitative trait locus (genomic DNA that is associated with a particular trait that varies continuously across a population) that is associated with accelerated senescence and increases in grain zinc, iron, and protein content. This wheat is ancestral to

cultivated pasta wheat and is a potential source of genetic variation that could affect nutritional crop content (9). The authors identify the gene for this trait as *NAM-B1* and demonstrate that it encodes a member of the NAC transcription factor family whose members are widely distributed plant-specific transcription factors (10).

Uauy *et al.* show that the wheat genome contains three *NAM* genes, and transcript analysis reveals a parallel increase in expression of all these genes in flag leaves (the uppermost leaf on a stem) at grain maturity. Abrogating expression of these *NAM* genes by RNA interference transgenesis results in delayed whole-plant senescence and a >30% reduction of grain zinc, iron, and protein content, suggesting a quantitative contribution from each *NAM* gene. This delay in senescence and decrease in grain nutrients is associated with increased residual nitrogen, zinc, and iron in the flag leaf, thereby demonstrating a role

for *NAM* genes in nutrient redistribution to the developing grain during leaf senescence. By establishing a direct link between senescence and nutrient distribution, Uauy *et al.* provide new insight into homeostatic mechanisms of grain nutrient acquisition.

Like all good science, these studies provoke more questions. What are the signals that mobilize iron from vacuoles to distant sites along the developing plant vasculature? If there a specific set of transcripts—a "transcriptome"—regulated by the *NAM* genes that defines nutrient redistribution to the grain? Is so, what are the proteins they encode and how do they function? Understanding the regulation of vacuolar iron content could result in new approaches to iron enrichment in seeds. The cloning of *NAM-B1* illustrates the utility of defining quantitative trait loci that can permit breeding for nutritional traits on the basis of mechanistic insight.

Political and spiritual leader Mahatma

Gandhi considered hunger the greatest violence against children. These elegant new studies reinforce the inherent value of basic science for improving the lives of those youngest among us who remain without a voice in this world.

References
1. I. Serageldin, *Science* **296**, 54 (2002).
2. G. Conway, *The Doubly Green Revolution* (Penguin, London, 1997), pp. 163–182.
3. W. Danforth, *Science* **314**, 223 (2006).
4. S. A. Kim *et al.*, *Science* **314**, 1295 (2006); published online 2 November 2006 (10.1126/science.1132563).
5. C. Uauy, A. Distelfeld, T. Fahima, A. Blechl, J. Dubcovsky, *Science* **314**, 1298 (2006).
6. M. W. Hentze, M. C. Muckenthaler, N. C. Andrews, *Cell* **117**, 285 (2004).
7. B. Lozoff *et al.*, *Nutr. Rev.* **64**, S34 (2006).
8. V. Lanquar *et al.*, *EMBO J.* **24**, 4041 (2005).
9. J. Peng *et al.*, *Proc. Natl. Acad. Sci. U.S.A.* **100**, 2489 (2003).
10. A. N. Olsen, H. A. Ernst, L. L. Leggio, K. Skriver, *Trends Plant Sci.* **10**, 79 (2005).

10.1126/science.1136251

ATMOSPHERE

Global Change in the Upper Atmosphere

The upper atmosphere is cooling and contracting as a result of rising greenhouse gas concentrations. These changes are likely to affect the orbital lifetimes of satellites.

J. Laštovička, R. A. Akmaev, G. Beig, J. Bremer, J. T. Emmert

Life on Earth is affected more directly by climate change near the surface than in the upper atmosphere. However, as the story of Earth's ozone layer illustrates, changes higher up in the atmosphere can also be important. In 1989, Roble and Dickinson (1) predicted that rising greenhouse gas concentrations should affect atmospheric climate in the highest reaches of the atmosphere. Since then, upper atmospheric data have been combed for evidence of long-term trends. A coherent pattern is now beginning to emerge.

The upper atmosphere consists of the mesosphere (~50 to 90 km) and thermosphere (~90 to 800 km) (see the figure). The ionized part of the upper atmosphere, the ionosphere (~60 to 1000 km), is embedded within these regions. The thermosphere is the operating environment of many satellites. The drag

J. Laštovička is at the Institute of Atmospheric Physics, 14131 Prague, Czech Republic. E-mail: jla@ufa.cas.cz R. A. Akmaev is at CIRES, University of Colorado, Boulder, CO 80309, USA. G. Beig is at the Indian Institute of Tropical Meteorology, Pune-411 008, India. J. Bremer is at the Leibnitz-Institute of Atmospheric Physics, 18225 Kühlungsborn, Germany. J. T. Emmert is at the Naval Research Laboratory, Washington, DC 20375, USA.

exerted by the thermosphere is proportional to the ambient density. Therefore, satellite trajectories and orbital lifetimes are sensitive to long-term trends in atmospheric density at their flight altitude (although their active lifetime is at present mostly determined by the lifetime of their energy sources, by instrument failures, and by the capacity of satellite operation centers). Changes in the ionosphere affect

Ionospheric electron density ($\log_{10}$ cm^{-3})

the propagation of radio waves and hence the performance of the Global Positioning System (GPS) and other space-based navigational systems.

The increase in global surface air temperature during the 20th century has been attributed mainly to the increasing atmospheric concentrations of greenhouse gases. In the upper atmosphere, the radiative effects of greenhouse gases, particularly CO_2, become more pronounced and produce a cooling rather than a warming effect (2, 3). This effect is demonstrated by the CO_2–dominated atmosphere of Venus, where the troposphere is more than twice as warm as Earth's and the

Structure and trends in Earth's atmosphere. Atmospheric layers (orange, right) are defined by the temperature profile. Ionospheric layers (purple, left) are defined by the electron density profile (shown here at midnight at the equator). Arrows denote the direction of observed changes in the past 3 to 4 decades: Red, warming; blue, cooling; green, no temperature change; black, changes in maximum electron density (horizontal) and the height of ionospheric layers (vertical). Most spacecraft fly at altitudes above 300 km. The aircraft and satellite shown are not to scale.

thermosphere is 4 to 5 times as cold (4). The cooling should cause the upper atmosphere to contract; we may thus expect a substantial decline in thermospheric density, as well as a downward displacement of ionospheric layers (5).

The primary quantity directly affected by the changing concentration of greenhouse gases is temperature. The first comprehensive review of temperature trends at heights of about 50 to 100 km (6) reveals, after slight updating, the following trends: (i) moderate negative trends of about 2 to 3 K per decade at heights of 50 to 70 km, with the largest magnitude in the tropics; (ii) slightly larger cooling trends at heights of 70 to 80 km in the low and middle latitudes; (iii) essentially zero temperature trends between 80 and 100 km. Modeling studies agree reasonably well with the observed vertical and latitudinal structure of the thermal response (3).

Over the past three decades, the global temperature at Earth's surface has increased by 0.2 to 0.4°C, compared with a 5 to 10°C decrease in the lower and middle mesosphere. Summer-winter differences of mid-latitude land-surface temperatures are comparable in magnitude to the seasonal and 11-year solar cycle variability of mid-latitude mesospheric temperatures. Thus, the signal-to-noise ratio of the trends is much higher in the mesosphere than at Earth's surface.

No direct information on thermospheric temperature trends is available. However, estimated ion temperatures (7) at heights near 350 km reveal a negative trend of about −17 K per decade (8). Because ion temperature is strongly coupled to thermospheric temperature, these trends are qualitatively consistent with the expected thermospheric cooling.

Temperature directly affects atmospheric density. At altitudes between about 200 and 800 km, atmospheric drag causes measurable decay of the orbits of satellites and space debris. Routine satellite tracking data have been used to derive long-term changes in thermospheric density. The results (9, 10) indicate that thermospheric density has declined during the past several decades at an overall rate of 2 to 3% per decade; these density trends increase with height (9). This behavior is qualitatively consistent with model predictions (2). Model simulations also show that, in addition to the effects of greenhouse gas increases, the impact of long-term changes in stratospheric ozone and water vapor on atmospheric density may extend well into the thermosphere (11).

Thermal contraction of the upper atmosphere should result in a downward displacement of ionospheric layers (5). Laštovička and

Bremer (12) reviewed long-term trends in the lower ionosphere and found a positive trend in electron density at fixed heights, consistent with downward displacement. The maximum electron density of the E-layer and the F1-layer increased slightly (see the figure), and the height of the electron density maximum of the E-region decreased slightly (13), in qualitative agreement with model predictions (2). These ionospheric trends accelerated after 1980, providing support for their anthropogenic origin (14).

The trends described above form a consistent pattern of global change in the upper atmosphere at heights above 50 km (see arrows in the figure). The upper atmosphere is generally cooling and contracting, and related changes in chemical composition are affecting the ionosphere. The dominant driver of these trends is increasing greenhouse forcing, although there may be contributions from anthropogenic changes of the ozone layer and long-term increase of geomagnetic activity throughout the 20th century. Thus, the anthropogenic emissions of greenhouse gases influence the atmosphere at nearly all altitudes between ground and space, affecting not only life on the surface but also the space-based technological systems on which we increasingly rely.

References and Notes
1. R. G. Roble, R. E. Dickinson, *Geophys. Res. Lett.* **16**, 1441 (1989).
2. H. Rishbeth, R. G. Roble, *Planet. Space Sci.* **40**, 1011 (1992).
3. R. A. Akmaev, *Phys. Chem. Earth* **27**, 521 (2002).
4. S. W. Bougher, R. G. Roble, *J. Geophys. Res.* **96**, 11045 (1991).
5. H. Rishbeth, *Planet. Space Sci.* **38**, 945 (1990).
6. G. Beig *et al.*, *Revs. Geophys.* **41**, 1015 (2003).
7. Because the thermospheric density is very low, the temperatures of the neutral atmosphere, the ions, and the electrons differ. The ion temperature is easiest to estimate.
8. S. Zhang *et al.*, Paper SA52A-03, Spring AGU Meeting, New Orleans (2005).
9. J. T. Emmert, J. M. Picone, J. L. Lean, S. H. Knowles, *J. Geophys. Res.* **109**, A02301 (2004).
10. F. A. Marcos, J. O. Wise, M. J. Kendra, N. J. Grossbard, B. R. Bowman, *Geophys. Res. Lett.* **32**, L04103 (2005).
11. R. A. Akmaev, V. I. Fomichev, X. Zhu, *J. Atmos. Solar-Terr. Phys.*, in press; available online 12 May 2006, doi: 10.1016/j.jastp.2006.03.008 (2006).
12. J. Laštovička, J. Bremer, *Surv. Geophys.* **25**, 69 (2004).
13. J. Bremer, *Adv. Space Res.* **28**, 997 (2001).
14. J. Bremer, *Adv. Space Res.* **35**, 1398 (2005).

PALEOECOLOGY

Life's Complexity Cast in Stone

Wolfgang Kiessling

The fossil record shows that since the end of the Paleozoic era, the structure of marine communities has become more complex.

There is no doubt that the complexity of life has increased through the ages, both in the structure of individual organisms and in the ecological structure of communities (1, 2). But to trace the complexity of living systems, we need objective measurements. Species diversity is often regarded as a rough proxy of complexity in local communities, because the more species coexist in a community, the more ecological interactions between species and complex food webs are to be expected (3). However, a comprehensive picture cannot emerge when the diversity information is reduced to single numbers such as species richness or measures of how evenly species are distributed in a community. Communities with the same number of species and identical evenness values may still differ substantially in their ecological complexity.

The author is at the Museum für Naturkunde, Humboldt-Universität, 10115 Berlin, Germany E-mail: wolfgang.kiessling@museum.hu-berlin.de

On page 1289 of this issue, Wagner *et al.* (4) explore the shape of relative abundance distributions in ancient marine communities to track the evolution of ecological complexity through the past 540 million years. They separate communities whose abundance distributions simply suggest superior access to resources versus those that succeed in their own smaller niche (see the figure). In simple abundance distributions, the relative abundances of species drop rather steadily, which implies that few factors—such as the preemption of resources by dominant species—structure the community. Complex distributions are essentially those in which the dominant taxa add ecological opportunities, and complex niche partitioning is suggested by similar abundances for many species. The big surprise in their analysis is a major difference between Paleozoic (older than 250 million years) and younger communities. In older assemblages, complex and simple distributions are

about equally common, but complexly structured assemblages are substantially more common in more recent times.

With so many paleobiologists looking at local, regional, and global diversity patterns through time, how could this striking pattern have escaped our attention for so long? Previous studies (i) recorded a temporal increase in community diversity but found this to be largely confined to the past 25 million years (*5*–*7*), (ii) argued for a gradual increase (*8*), or (iii) found no distinct trend in particular ecosystems (*9*). I see three explanations for why Wagner *et al.* came out with different results: First, previous analyses usually were designed to find a trend rather than to examine its detailed trajectory. Second, the new study could take advantage of a comprehensive set of fossil communities by mining the Paleobiology Database (*10*), which is arguably the largest database of ancient life. Third, and most important, the previous studies relied on simple diversity metrics such as species richness and evenness, whereas the new analysis uses the shape of abundance distributions of ancient communities and thus goes beyond single numbers. Wagner *et al.* managed to reliably separate abundance distributions, which are usually not as distinctive as depicted in the figure and are notoriously difficult to differentiate by visual inspection or standard statistical tests (*11*).

There is still a chance that the new results are biased. All paleontological studies are plagued by incomplete preservation, and the preservation of anatomical details is usually worse in older rocks. Shells with an unstable aragonitic mineralogy also tend to be much rarer in the Paleozoic than later on (*12*). However, even if preservational bias had affected abundance distributions systematically over time, this should lead to a gradual increase in perceived complexity, rather than the distinct break recorded by Wagner *et al.*

What caused the abrupt change in complexity? The turning point seems to be the most severe mass extinction documented in
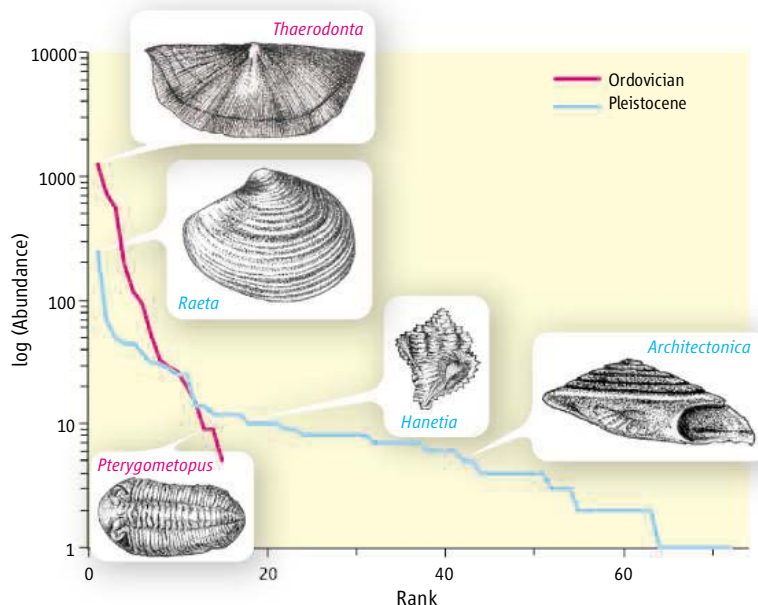
Gaining complexity. Fossil marine communities of the Paleozoic (542 to 251 million years before the present) differ from younger communities in the partitioning of relative abundances. Although about half of the Paleozoic communities are characterized by simple abundance distributions (red curve, a paleocommunity from the Late Ordovician of Minnesota), Mesozoic and Cenozoic communities predominantly exhibit complex distributions (blue curve, a paleocommunity from the Pleistocene of Ecuador).

the fossil record, the double end-Permian mass extinction some 250 million years ago (*13, 14*). This pair of extinction events, separating the Paleozoic from the Mesozoic, has apparently altered the ecological structure of communities until the present day. But how could end-Permian crisis change the ecological structure of communities so durably?

The most plausible scenario involves preferential extinction of those Paleozoic clades that predominantly lived in ecologically simple communities. Indeed, the Paleozoic seas were dominated by organisms such as brachiopods (lamp shells) and sea lilies, which lived anchored to a surface and exclusively relied on suspended organic material for feeding. These taxa were strongly affected by the end-Permian extinctions and never recovered fully. Other Paleozoic clades, such as trilobites, which were mobile and fed on organic detritus, vanished completely. Clams, snails, and sea urchins rapidly gained dominance in the Mesozoic and proliferate on today's seafloors. The diverse feeding modes of this "modern fauna" and the capability of many species to dig deeply into substrates suggest a broad range of niche exploitation. Complexly structured communities were obviously present in the Paleozoic as well, but they were not more common than the simple communities and only gained dominance after the decline of the Paleozoic fauna.

One is tempted to compare this pattern to what happened on land nearly 200 million years later, when the mammals diversified only after the incumbent dinosaurs became extinct. The ruling taxa in Paleozoic marine ecosystems may have prevented the spread of taxa that were able to construct complex communities, just because they mastered the established communities by niche preemption. Further studies on the ecology of dominant taxa in respective community types are clearly required to test this hypothesis. Additional valuable insights could also be achieved by applying the methods of Wagner *et al.* to ancient terrestrial ecosystems or plankton assemblages. Are there similar patterns, or is the evolution of complexity different in each major habitat?

A second scenario could involve the evolution of predators. Predatory organisms are known to regulate food web complexity and prevent the monopolization of communities by individual species (*15*). Proportional diversities of predators relative to all marine animals suggest a distinct rise at the beginning of the Mesozoic (*16*), which agrees with the idea that increased predation pressure altered the structure of marine communities. Unfortunately, the particularly poor fossil record of predators prevents conclusive statements, but modeling approaches might bring some progress.

References

1. A. H. Knoll, R. K. Bambach, *Paleobiology* **26** (suppl.), 1 (2000).
2. S. B. Carroll, *Nature* **409**, 1102 (2001).
3. K. Havens, *Science* **257**, 1107 (1992).
4. P. J. Wagner, M. A. Kosnik, S. Lidgard, *Science* **314**, 1289 (2006).
5. R. K. Bambach, *Paleobiology* **3**, 152 (1977).
6. M. G. Powell, M. Kowalewski, *Geology* **30**, 331 (2002).
7. A. M. Bush, R. K. Bambach, *J. Geol.* **112**, 625 (2004).
8. M. Kowalewski et al., *Paleobiology* **32**, 533 (2006).
9. W. Kiessling, *Nature* **433**, 410 (2005).
10. Paleobiology Database, http://paleodb.org.
11. A. E. Maguran, *Measuring Biological Diversity* (Blackwell, Oxford, 2004).
12. J. Madin et al., *Science* **312**, 897 (2006).
13. D. H. Erwin, *Extinction: How Life on Earth Nearly Ended 250 Million Years Ago* (Princeton Univ. Press, Princeton, NJ, 2006).
14. S. M. Stanley, X. Yang, *Science* **266**, 1340 (1994).
15. R. T. Paine, *Am. Naturalist* **100**, 65 (1966).
16. R. K. Bambach, in *The Fossil Record of Predation,* M. Kowalewski, P. H. Kelley, Eds. (Paleontological Society Special Publications, New Haven, 2002), vol. 8, pp. 319–351.

SCIENCE AND ENVIRONMENT

Abelson Seminar: It's "Time for Microbes to Have Their Due"

A visitor to Earth during most of the planet's history would have been greeted only by microbes, and those ubiquitous organisms continue to help shape both the planet's destiny and ours, according to researchers who spoke at the Philip Hauge Abelson Advancing Science Seminar at AAAS.

"It's definitely time for microbes to have their due," said David Stahl, a professor of environmental engineering and science at the University of Washington. "We live on the planet of the microbes," he said, with very large numbers of those organisms controlling the key cycles of planetary chemistry that produce such essentials to life as oxygen and organic forms of carbon and nitrogen.

But in many cases, he said, scientists still don't know which populations of bugs are in control of specific cycles. There have been surprising discoveries just within the past few years. An anaerobic organism that digests ammonia, first described in 1999, represents a major part of the nitrogen cycle that had been missed during a century of investigation, according to Stahl. Another bug, discovered in 1992, accounts for about 20% of the bacterial component of the plankton that drifts in ocean waters.

Speakers at the symposium told how genomics, microbiology, mineralogy, geochemistry, and materials science have provided new insights on the history of microbes and their potential for such practical applications as cleaning up polluted sites, mitigating the effects of climate change, or producing electricity.

The 26 October seminar "Microbes, Minerals and the Environment" honored the late Philip Abelson, editor of *Science* for 22 years and then senior adviser to AAAS. He founded and sponsored the seminar series to encourage participants to think about where science is going, not where it has been.

"We're so lucky to work on a diverse group of organisms that we know so little about," said Anna-Louise Reysenbach, a professor of microbial biology at Portland State University who has been studying the heat-loving microbes found around hydrothermal vents,

seafloor geysers that spew superhot, mineral rich water. She showed an image of one organism, which she calls the "devilheterotrophventblob," whose cell wall had formed two horn-like structures. It turns out to be the first truly acid-loving microbe in the neighborhood of such hydrothermal vents.

Microbiologist Derek R. Lovley; human microbiota *Lactobacillus,* which produces lactic acid (right).

The durability and variety of microbes continue to astonish researchers. Keynote speaker Derek R. Lovley, a microbiologist at the University of Massachusetts, Amherst, mentioned Strain 121, a deep-sea organism discovered in 2003 that survives at $121°C$ ($250°F$). That is the highest temperature at which life is known to exist—equivalent to the heat in autoclaves used to sterilize surgical instruments.

Species of bacteria called *Geobacter* are of interest because of their novel abilities to transfer electrons. They can harvest electricity from aquatic environments and may prove useful as power sources for underwater monitoring instruments, Lovley said. It is likely that fuel cells can be made from pure cultures of *Geobacter* organisms, he added, perhaps initially to power electronic gadgets like cell phones.

There are other practical applications on the horizon, speakers said, including use of *Geobacter* species and other microbes to bind uranium, plutonium, and other metals in polluted groundwater or soils. Bruce Hungate, an ecologist at Northern Arizona University, offered a cautionary note, however, on one proposed "biological fix" for rising carbon dioxide levels in the atmosphere. While plants may

grow more in response to elevated carbon dioxide levels, Hungate said, microbes in the soil apparently have a reverse effect, limiting the amount of carbon that the soils can sequester.

Paul Falkowski, a professor in the Institute of Marine & Coastal Sciences and the Department of Geological Sciences at Rutgers University, was wary of human tinkering with natural cycles. "We are messing with something we don't really know much about," he said. "We have, in the last 150 to 200 years, so critically altered the carbon, phosphorus, sulfur, nitrogen, water cycles," Falkowski said, that society is on a path toward unsustainable development.

Falkowski urged reductions in carbon dioxide and sulfur emissions and in the use of nitrogen-containing fertilizers so that we can return to a world "where microbes basically are taking care of the cycles for us, because we cannot take care of the cycles for ourselves."

—*Earl Lane*

EDUCATION

Digital Architects Ponder the Library of the Future

The emergence of the Internet over the last decade as an everyday data and communication tool has created enormous possibilities in science education, but also inefficiencies and distractions. If you doubt it, go to your favorite Internet search engine and type in v-e-n-u-s.

What do you get? Not just the second planet from the Sun, but a line of women's clothing, the Roman goddess of love and beauty, and an e-zine about women in the arts.

For the past 11 years, the U.S. National Science Foundation (NSF) and a corps of visionaries funded by NSF have been building a library that sharpens the focus of the Internet and makes it an effective, efficient tool of 21st-century education for science, technology, engineering, and mathematics (STEM). It's called the National Science Digital Library (go to your search engine and type in n-s-d-l). Nearly 200 of the library's architects—including representatives from industry, major universities, and government—gathered at AAAS 18 to 20 October to consider its future.

"You know all the reports that are out now about the conditions of the STEM disciplines in the United States and how few kids are going into them, the whole pipeline issue," said Kaye Howe, executive director of NSDL Core Integration. "We would really like to be part of the solution on this, both by creating a community

and by giving that community the material, the tools, and the services it needs in order to master these very important areas that are sometimes difficult to master."

Aside from providing services to the average science classroom, Howe said, the NSDL might be crucial in providing education support in poor states where textbooks are in short supply, or in areas like New Orleans where schools have been devastated by natural disasters. And, she said, it might provide a critical connection to science for a student who is otherwise bored and inclined to drift away from STEM fields.

Since the NSDL was conceived 11 years ago, NSF has funded over 200 related projects. Among them is the AAAS-managed BiosciEdNet (BEN) portal, which offers more than 4500 reviewed resources covering 77 biological sciences topics.

"AAAS is involved with the NSDL because of its mission related to science literacy for all and increasing public understanding of science," said Yolanda George, deputy director of Education and Human Resources at AAAS. "Also, the NSDL provides an opportunity for AAAS to work with its affiliated organizations to strengthen teaching and learning in the biological sciences."

Before the Internet, a library was evaluated in part on the number of volumes on its shelves, Howe said. But with "the growth of information on the Internet, material itself was no longer scarce. What did begin to happen very quickly was that finding that material and finding material that you could trust, and use—that really became the great exercise."

Today, the NSDL works as a more discerning version of Google. Type in v-e-n-u-s and you get nearly 2000 up-to-date resources about every aspect of Earth's neighboring planet, all carefully reviewed by experts, suitable for students and teachers at various levels from kindergarten through undergraduate studies.

But behind that seemingly simple service is a stream of interests working to refine a futuristic science of collecting, storing, and distributing data. From a process of constant evaluation and reevaluation, NSF and the NSDL have developed a system of "pathways"—collaborative administration centers which oversee the collection, management, and organization of the material.

The BEN Collaborative is one such pathway. Founded in 1999 by AAAS with 11 other professional societies and coalitions, it has since grown to 25 partners. Educational e-resources from all the collaborators are aggregated into a one-stop, searchable catalog at the BEN portal. In 2005, BEN was awarded a 4-year, $2.8-million NSF grant that would allow it to increase its collection to more than 27,000 scientific papers, illustrations, images, lab exercises, and other materials deemed helpful for teachers in the biological sciences.

AAAS, NASA Team Up on Solar System Book

With NASA's MESSENGER spacecraft streaking past Venus on its way to Mercury, AAAS has joined with the space agency to publish *Exploring the Inner Solar System: Expecting the Unexpected,* a book designed to inspire student interest in space sciences.
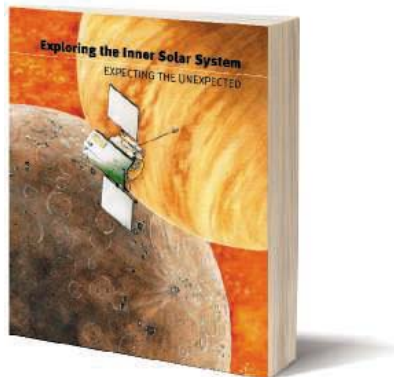
The 72-page book, aimed at science educators and students, focuses on the Moon and the solar system's four terrestrial planets: Mars, Earth, Venus, and Mercury. It features dozens of pictures and detailed discussion of both past missions and future expectations for MESSENGER, which is due to make its first Mercury flyby in January 2008.

"Millions of people, from professional scientists to science-engaged citizens, first got excited about science by following NASA space missions," said Bob Hirshon, AAAS senior project director. "The MESSENGER mission to Mercury is a chance to excite a new generation of budding scientists."

Mercury is the planet closest to the Sun; it is the hottest planet and it has the oldest surface. More than 35 years have passed since NASA's Mariner 10 craft sent the most recent images of Mercury's terrain. NASA hopes that MESSENGER will provide extraordinary images—along with new insights into how Earth was formed.

"We're trying to put the MESSENGER mission to Mercury in a broader context by showing how we reached our current understanding of the inner solar system," said the book's author, Justin Warner, who serves as a reporter for AAAS's daily Science Update radio program.

Exploring the Inner Solar System is being distributed through the MESSENGER Educator Fellows program, an initiative training 30 science educators to conduct national outreach workshops on the mission. To date, NASA estimates over 3800 teachers have been trained by the Fellows.

As a key partner in the MESSENGER education and outreach campaign, AAAS also was asked to produce other education materials for the mission, including Web sites with engaging, game-like interactive modules for students and detailed lesson plans for teachers. K-12 teachers and other educators interested in receiving copies of the book should contact bhirshon@aaas.org.

After three flybys, MESSENGER is scheduled to enter Mercury's orbit in 2011.

—*Benjamin Somers*

Role Models with Disabilities Sought for AAAS Directory

Scientists and engineers with disabilities are invited to be listed in and to nominate others for inclusion in the AAAS Resource Directory of Scientists and Engineers with Disabilities. The fourth edition of the directory, now under development, will be used as a source of experts and role models for educators, journalists, and others.

Individuals with disabilities who hold graduate or undergraduate degrees in fields of science, technology, engineering, mathematics, social and behavioral sciences, or economics can submit a listing at http://ehrweb.aaas.org/resource. The directory will be available upon request in print and CD-ROM formats, but participants' information will not be posted to the Internet.

The project is funded by the U.S. National Science Foundation. For more information, contact Tesa Leon at tleon@aaas.org or (202) 326-6582 (v/tdd).

A Call for Nominations

AAAS members may suggest nominees (including themselves) for president-elect and the Board of Directors for election in the fall of 2007. For a list of this year's candidates, see AAAS News and Notes in the 28 July 2006 issue of *Science*; for a list of current Board members, see the masthead page of any recent issue of *Science*.

Please send the suggested nominee's curriculum vitae no later than 30 December to Gretchen Seiler, AAAS Executive Office, 1200 New York Avenue, N.W., Washington, DC 20005. Suggested nominees will be considered by the AAAS Committee on Nominations at their winter meeting.

AAAS Members Elected as Fellows

In October, the AAAS Council elected 449 members as Fellows of AAAS. These individuals will be recognized for their contributions to science and technology at the Fellows Forum to be held on 17 February 2007 during the AAAS Annual Meeting in San Francisco. The new Fellows will receive a certificate and a blue and gold rosette as a symbol of their distinguished accomplishments. Presented by section affiliation, they are:

Section on Agriculture, Food, and Renewable Resources

Robert E. Davis, United States Department of Agriculture • Paul E. Fixen, Potash and Phosphate Institute • Jacqueline Fletcher, Oklahoma State University • David R. Gealy, United States Department of Agriculture • Robert L. Gilbertson, University of California, Davis • Tissa H. Illangasekare, Colorado School of Mines • Molly Jahn, Cornell University • Richard L. Lindroth, University of Wisconsin • Karen Ann Kuenzel Moldenhauer, University of Arkansas • Joseph G. Morse, University of California, Riverside • William A. Payne, Texas A&M University • Ian L. Pepper, University of Arizona • Pamela C. Ronald, University of California, Davis • Cynthia Rosenzweig, NASA Goddard Institute for Space Studies • Coby Schal, North Carolina State University • David Warren Stanley, United States Department of Agriculture • Chris van Kessel, University of California, Davis • Joachim von Braun, International Food Policy Research Institute

Section on Anthropology

Marina Cords, Columbia University • Christine Ward Gailey, University of California, Riverside • Terry Harrison, New York University • Clark Spencer Larsen, Ohio State University • William Leonard, Northwestern University • Jonathan M. Marks, University of North Carolina at Charlotte • Margaret C. Nelson, Arizona State University • Alfred L. Rosenberger, Brooklyn College, CUNY • Margaret J. Schoeninger, University of California at San Diego • Jeffrey H. Schwartz, University of Pittsburgh • Elwyn Laverne Simons, Duke University • Olga Soffer, University of Illinois • Carol V. Ward, University of Missouri

Section on Astronomy

Steven V. W. Beckwith, Space Telescope Science Institute • France A. Cordova, University of California, Riverside • Philip E. Kaaret, University of Iowa • Kwok-Yung Lo, National Radio Astronomy Observatory • Rosaly M. C. Lopes, Jet Propulsion Laboratory • David J. McComas, Southwest Research Institute • William B. McKinnon, Washington University • Jean L. Turner, University of California, Los Angeles • William R. Ward, Southwest Research Institute

Section on Atmospheric and Hydrospheric Sciences

Paulo Artaxo, Universidade Sao Paulo, Brazil • James Alexander Coakley Jr., Oregon State University • Franco Einaudi, NASA Goddard Space Flight Center • Michael C. Gregg, University of Washington • William R. Holland, National Center for Atmospheric Research • Eugenia Kalany, University of Maryland, College Park • Ray Franklin Weiss, University of California, San Diego • Hugh Edward Willoughby, Florida International University

Section on Biological Sciences

Michael Edwin Akam, University of Cambridge • Robert R. H. Anholt, North Carolina State University • Barbara A. Baird, Cornell University • Dipak K. Banerjee, University of Puerto Rico • David A. Baum, University of Wisconsin • Stewart H. Berlocher, University of Illinois Urbana-Champaign • Katherine A. Borkovich, University of California, Riverside • George Timothy Bowden, Arizona Cancer Center • Wlodzimierz Marian Bujalowski, University of Texas • Sydney A. Cameron, University of Illinois, Urbana-Champaign • Akira Chiba, University of Illinois, Urbana-Champaign • Vincent L. Chiang, North Carolina State University • John S. Condeelis, Albert Einstein College of Medicine of Yeshiva University • William E. Conner, Wake Forest University • M. Fevzi Daldal, University of Pennsylvania • Julie Sloan Denslow, USDA Forestry Service • Shou-wei Ding, University of California, Riverside • Evan Eichler, University of Washington • Shelagh M. Ferguson-Miller, Michigan State University • Malcolm J. Fraser Jr., University of Notre Dame • James K. Fredrickson, Pacific Northwest National Laboratory • David Michael Geiser, Pennsylvania State University • Gregory C. Gibson, North Carolina State University • Pamela J. Green, Delaware Biotechnology Institute • Patrick L. Green, Ohio State University • Joanna Groden, Ohio State University • James R. Halpert, University of Texas • John J. Harada, University of California, Davis • Gerhard J. Haas, Fairleigh Dickinson University • Nyla A. Heerema, Ohio State University • Jodie S. Holt, University of California, Riverside • Barry Honig, Columbia University • Arthur Horwich, Yale University • Tim Hui-Ming Huang, Ohio State University • Barbara L. Illman, USDA Forest Service • John Jaenike, University of Rochester • Mark Johnson, Washington University • Barbara B. Kahn, Beth Israel Deaconess Medical Center • Leonard Katz, Kosan Biosciences, Inc. • Kenneth Keegstra, Michigan State University • Thomas J. Kelly, Sloan-Kettering Institute •

Bruce E. Kemp, St. Vincent's Institute of Medical Research • Judith Kimble, University of Wisconsin • Donald T. Krizek, U.S. Department of Agriculture • James W. Kronstad, University of British Columbia • Raju Kucherlapati, Harvard University • Kyung J. Kwon-Chung, NIAID/NIH • Ulrich L. Laemmli, Université de Genève • Amy S. Lee , University of Southern California • Bai-lian Li, University of California, Riverside • Howard B. Lieberman, Columbia University • Jennifer J. Loros, Dartmouth College • Scott William Lowe, Cold Spring Harbor Laboratory • Arthur J. Lustig, Tulane University Health Sciences Center • Paul T. Magee, University of Minnesota • Lynne E. Maquat, University of Rochester • Kenneth J. Marians, Memorial Sloan-Kettering Cancer Center • Steven L. McKnight, University of Texas • Thomas Melendy, State University of New York at Buffalo • Janet E. Mertz, University of Wisconsin • Kenneth R. Miller, Brown University • G. Wayne Minshall, Idaho State University • Mark E. Nelson, University of Illinois, Urbana-Champaign • Carol S. Newlon, University of Medicine and Denistry of New Jersey • Timothy W. Nilsen, Case Western Reserve University • Howard Ochman, University of Arizona • Scott O'Neill, The University of Queensland • Stephen A. Osmani, Ohio State University • Deborah S. Parris, Ohio State University • John C. Priscu, Montana State University • Robert R. Reisz, University of Toronto at Mississauga • William Robertson IV, Andrew W. Mellon Foundation • F. James Rohlf, Stony Brook University • Forest Rohwer, San Diego State University • Oliver A. Ryder, Zoological Society of San Diego • Coby Schal, North Carolina State University • Oswald Joseph Schmitz, Yale University • Olaf Schneewind, University of Chicago • Julian I. Schroeder, University of California, San Diego • Lawrence J. Shimkets, University of Georgia • Sandra Shumway, University of Connecticut • Shauna Somerville, Stanford University • David Lawrence Stern, Princeton University • Ann M. Stock, Center for Advanced Biotechnology and Medicine • Jack Szostak, Harvard Medical School • William A. Toscano Jr., University of Minnesota • Hans D. Van Etten, University of Arizona • Elizabeth Van Volkenburgh, University of Washington • Inder M. Verma, The Salk Institute • Jean-Philippe Vielle-Calzada, CINVESTAV • P. Kirk Visscher, University of California, Riverside • Robert Carsten von Borstel, University of Alberta • Daniel F. Voytas, Iowa State University • Barbara T. Wakimoto, University of Washington • Teresa S. F. Wang, Stanford University • Clifford F. Weil, Purdue University • William B. Whitman, University of Georgia • Juergen K. Wiegel, University of Georgia • Susan L. Williams, University of California, Davis • Jeffrey J. Wine, Stanford University • Mariana F. Wolfner, Cornell University •

H. Boyd Woodruff, Soil Microbiology Associates, Inc. • Eleanore T. Wurtzel, Lehman College, The City University of New York • Shizhong Xu, University of California, Riverside • Ning-Sun Yang, Academia Sinica • Martin Yanofsky, University of California, San Diego • Marylynn Yates, University of California, Riverside

Section on Chemistry
Hector D. Abruna, Cornell University • Joanna Aizenberg, Lucent Technologies • Louie J. Allamandola, NASA Ames Research Center • Philip Anfinrud, National Institutes of Health • Eric V. Anslyn, University of Texas, Austin • Andreja Bakac, Iowa State University • Barbara A. Baird, Cornell University • David Penfield Ballou, University of Michigan Medical School • Rudy M. Baum, American Chemical Society • Guy Bertrand, University of California, Riverside • Rafael P. Bruschweiler, Florida State University • Stephen Z. D. Cheng, University of Akron • Geoffrey William Coates, Cornell University • M. Bonner Denton, University of Arizona • Joseph M. DeSimone, University of North Carolina, Chapel Hill • Olof Einarsdottir, University of California, Santa Cruz • Jonathan Ellman, University of California, Berkeley • Carol Ann Fierke, University of Michigan • Gregory C. Fu, Massachusetts Institute of Technology • Joseph A. Gardella Jr., University of Buffalo, SUNY • Robert E. Gawley, University of Arkansas • Wayne L. Gladfelter, University of Minnesota • Craig Hill, Emory University • Keith O. Hodgson, Stanford University • Angela M. Hoffman, University of Portland • Catherine T. Hunt, Rohm and Haas Chemicals LLC • Kenneth Allen Johnson, University of Texas, Austin • Kenneth David Jordan, University of Pittsburgh • Pravin T. P. Kaumaya, Ohio State University • Mary M. Kirchhoff, American Chemical Society • Jack F. Kirsch, University of California, Berkeley • James M. Lisy, University of Illinois, Urbana-Champaign • Thomas E. Mallouk, Pennsylvania State University • Todd J. Martinez, University of Illinois, Urbana-Champaign • James A. Miller, Sandia National Laboratories • Odayan Mohanty, Boston College • Gaetano T. Montelione, Rutgers University • David W. Oxtoby, Pomona College • Reginald M. Penner, University of California, Irvine • William F. Polik, Hope College • Buddy D. Ratner, University of Washington • Mary Fedarko Roberts, Boston College • Peter J. Rossky, University of Texas, Austin • William R. Roush, The Scripps Research Institute of Florida • Steven J. Sibener, University of Chicago • Richard D. Smith, Pacific Northwest National Laboratory • Brian Stoltz, California Institute of Technology • Steven R. Tannenbaum, Massachusetts Institute of Technology • Shelby Freland Thames, University of Southern Mississippi • David M. Tiede, Argonne National Laboratory • Peter A. Tipton, University of Missouri-

Columbia • Douglas J. Tobias, University of California, Irvine • William B. Tolman, University of Minnesota • Albert F. Wagner, Argonne National Laboratory • Roderick E. Wasylishen, University of Alberta, Edmonton • David F. Wiemer, University of Iowa • Christian P. Whitman, University of Texas, Austin • Alec N. Wodtke, University of California, Santa Barbara • Kurt W. Zilm, Yale University

Section on Dentistry and Oral Health Sciences
Mary MacDougall, University of Alabama • David T. Wong, University of California, Los Angeles

Section on Education
Jan Blacher, University of California, Riverside • Melanie Margaret Cooper, Clemson University • Goery Delacote, At-Bristol, United Kingdom • Carol Dwyer, Educational Testing Service • Bat-Sheva Eylon, Weizmann Institute • Michael Feuer, National Academy of Sciences • Maria Alicia Lopez Freeman, University of California, Los Angeles • George Hammons, Philander Smith College • Jack G. Hehn, American Institute of Physics • Paul Horwitz, Concord Consortium • Shirley Ann Jackson, Rensselaer Polytechnic Institute • Mary Nakhleh, Purdue University • Nancy Nersessian, Georgia Institute of Technology • Su-Seng Pang, Louisiana State University • Nancy Songer, University of Michigan • Barbara S. Spector, University of South Florida

Section on Engineering
Reza Abbaschian, University of California, Riverside • Dereje Agonafer, University of Texas at Arlington • Kristi S. Anseth, University of Colorado • Norman Augustine, Retired President and CEO, Martin Marietta Aerospace • David D. Awschalom, University of California, Santa Barbara • Supriyo Bandyopadhyay, Virginia Commonwealth University • Ray M. Bowen, Texas A&M University • Linda J. Broadbelt, Northwestern University • Robert J. Budnitz, Lawrence Livermore National Laboratory • Wilfred Chen, University of California, Riverside • Marc Deshusses, University of California, Riverside • Yasuhiko Fujii, Tokyo Institute of Technology • Alice P. Gast, Lehigh University • Chris T. Hendrickson, Carnegie Mellon University • Linda P. B. Katehi, University of Illinois, Urbana-Champaign • Mujid S. Kazimi, Massachusetts Institute of Technology • Robert M. Kelly, North Carolina State University • Chaitan Khosla, Stanford University • Gyungho Lee, University of Illinois, Chicago • Sang Yup Lee, Korea Advanced Institute of Science and Technology • Mark S. Lundstrom, Purdue University • Susan McCahan, University of Toronto • Robert G. Parker, Ohio State University • Victor G. J. Rogers, University of California, Riverside • A. David Rossin, Stanford University • Kirk H. Schulz, Mississippi

State University • Krishna Shenai, Utah State University • Michael L. Shuler, Cornell University • William H. Steier, University of Southern California • S. K. Sundaram, Pacific Northwest National Laboratory • Thomas George Thundat, Oak Ridge National Laboratory • Fawwaz T. Ulaby, The University of Michigan • Usha Varshney, National Science Foundation • Zhong Lin Wang, Georgia Institute of Technology • Richard C. Warder Jr., University of Memphis • Charles Wyman, University of California, Riverside

Section on General Interest in Science and Engineering
Edwin M. Brogie, Laurel Senior High School • Marilee A. Long, Colorado State University • Dennis L. Meredith, Duke University • Joan Messer, Mississippi Academy of Science • Donna Gerardi Riordan, California Council on Science and Technology • Jocelyn D. Steinke, Western Michgan University • William J. Valdez, U.S. Department of Energy

Section on Geology and Geography
Timothy Beach, Georgetown University • Robert Bodnar, Virginia Polytechnic Institute and State University • Gregor Paul Eberli, University of Miami • Lucy E. Edwards, U.S. Geological Survey • Glen MacDonald, University of California, Los Angeles • Marcus E. Milling, American Geological Institute (deceased) • Samuel B. Mukasa, University of Michigan • M. Duane Nellis, Kansas State University • Bernardus A. van der Pluijm, University of Michigan • Douglas J. Sherman, Texas A&M University • Nobumichi Shimizu, Woods Hole Oceanographic Institution • Richard H. Sibson, University of Otago • Lars Stixrude, University of Michigan • Peter K. Swart, University of Miami • Stephen Walsh, University of North Carolina-Chapel Hill • Pinxian Wang, Tonji University • John Zachara, Pacific Northwest National Laboratory

Section on History and Philosophy of Science
James R. Bartholomew, Ohio State University • Sandra Herbert, University of Maryland Baltimore County • Robert Pennock, Michigan State University • William C. Wimsatt, University of Chicago

Section on Industrial Science and Technology
Manuel Gomez, University of Puerto Rico, Rio Piedras • Boris Mizaikoff, Georgia Institute of Technology

Section on Information, Computing, and Communication
Hsinchun Chen, University of Arizona • Susan J. Eggers, University of Washington • Ronald Fagin, IBM Almaden Research Center • Tio

Jiang, University of California, Riverside • Michael Jordan, University of California, Berkeley • Henry A. Kautz, University of Washington • Vipin Kumar, University of Minnesota • David D. Lewis, David D. Lewis Consulting, LLC • Michael Rung-Tsong Lyu, The Chinese University of Hong Kong • Sanjay Ranka, University of Florida • Daniel A. Reed, University of North Carolina, Chapel Hill • Terrence J. Sejnowski, The Salk Institute • Marc Snir, University of Illinois, Urbana-Champaign • Robert F. Sproull, Sun Microsystems Laboratories • Albert Y. Zomaya, The University of Sydney

Section on Linguistics and Language Sciences
Brian Daniel Joseph, Ohio State State University • Bjorn Lindblom, University of Texas, Austin • Kenji Hakuta, University of California, Merced • Johanna Nichols, University of California, Berkeley

Section on Mathematics
Amy Cohen, Rutgers University • Evans M. Harrell II, Georgia Institute of Technology • Warren Page, Retired Professor, Yeshiva University • Alan S. Perelson, Los Alamos National Laboratory

Section on Medical Sciences
James Allison, Memorial Sloan-Kettering Cancer Center • Nancy Andrews, Children's Hospital Boston • Arleen D. Auerbach, Rockefeller University • Sanford H. Barsky, Ohio State University • Charles C. Capen, Ohio State University • Martin A. Cheever, National Cancer Institute/NIH • George Q. Daley, Children's Hospital Boston • Beverly Davidson, University of Iowa • Betty Diamond, Columbia University • Paul E. DiCorleto, Cleveland Clinic Lerner Research Institute • Richard W. Dutton, Trudeau Institute • Michael Aaron Edidin, Johns Hopkins University • Serpil C. Erzurum, Cleveland Clinic • Alan Ezekowtiz, Massachusetts General Hospital • Raif Geha, Children's Hospital Boston • Philip D. Greenberg, Fred Hutchinson Cancer Research Center • Randal J. Kaufman, University of Michigan • Elliott Dan Kieff, Brigham and Women's Hospital • Norman L. Letvin, Beth Israel Deaconess Medical Center • Joseph S. Lipsick, Stanford University • JoAnn Manson, Brigham and Women's Hospital • Nina A. Mayr, Ohio State University • Dimitrios Morikis, University of California, Riverside • Hugo Wolfgang Moser, Kennedy Krieger Institute • Kenrad E. Nelson, Johns Hopkins University • Alison Davis O'Brien, Uniformed Services University of Health Services • Anne O'Garra, National Institute for Medical Research • Richard A. Rudick, Cleveland Clinic Foundation • Charles E. Samuel, University of California, Santa Barbara • Philippe Joseph Sansonetti, Unité de Pathoge-nie Microbienne Moléculaire • Andrew I. Schafer, University of Pennsylvania • Alan L. Schwartz, Washington University • Ronald N. Schwartz, NIAID/NIH • Arlene H. Sharpe, Harvard University • Susan L. Swain, Trudeau Institute • Dennis J. Thiele, Duke University • Bert Vogelstein, Johns Hopkins University • Christopher M. Walker, Columbus Children's Hospital Research Institute • Thomas E. Wellems, NIAID/NIH • Mary Ellen Wewers, Ohio State University

Section on Neuroscience
Cornelia Bargmann, Rockefeller University • John R. Carlson, Yale University • Vivien A. Casagrande, Vanderbilt University • Susan Fitzpatrick, James S. McDonnell Foundation • Lloyd A. Green, Columbia University • Duane E. Haines, University of Mississippi • Nathaniel Heintz, Rockefeller University • Thomas M. Jessel, Columbia University • Eugene M. Johnson, Washington University • Carol A. Mason, Columbia University • William C. Mobley, Stanford University • Robert Y. Moore, University of Pittsburgh • John H. Morrison, Mount Sinai School of Medicine • Henry J. Ralston III, University of California, San Francisco • Robert L. Sprague, University of Illinois, Urbana-Champaign • Susumu Tonegawa, Massachusetts Institute of Technology

Section on Pharmaceutical Sciences
William T. Beck, University of Illinois, Chicago • Charles Chavkin, University of Washington School of Medicine • Charles N. Falany, University of Alabama, Birmingham • Alan Douglas Kinghorn, Ohio State University • H. George Mandel, George Washington University

Section on Physics
Daniel N. Baker, University of Colorado, Boulder • Alan Reginald Bishop, Los Alamos National Laboratory • Steven M. Block, Stanford University • Felix Hans Boehm, California Institute of Technology • Aviva Brecher, DOT Volpe Center • Joseph I. Budnick, University of Connecticut • Moses Chan, Pennsylvania State University • Robert F. Christy, California Institute of Technology • Gordon T. Danby, Polytechnic University • Sara L. Dawson, Brookhaven National Laboratory • Stuart J. Freedman, University of California, Berkeley • Roy W. Gould, California Institute of Technology • Deborah S. Jin, University of Colorado • V. Alan Kostelecky, Indiana University • Dennis Kovar, U.S. Department of Energy • Vasudevan Lakshmi-narayanan, University of Missouri, Saint Louis • Steven G. Louie, University of California, Berkeley • Derek I. Lowenstein, Brookhaven National Laboratory • Aden Baker Meinel, University of Arizona • Umar Mohideen, University of California, Riverside • Roberto Peccei, University of California, Los Angeles • Martin Perl, Stanford Linear Accelerator Center • Robert J. Perry, Ohio State University • Peter Pesic, St. Johns College • Jorge Pullin, Louisiana State University • Daniel Rugar, Almaden Research Center • Sashi Satpathy, University of Missouri • Arthur L. Smirl, University of Iowa • Antoinette J. Taylor, Los Alamos National Laboratory • John M. Tranquada, Brookhaven National Laboratory • Karl A. Van Bibber, Lawrence Livermore National Laboratory • Evgeny Pavlovich Velikhov, Russian Research Center "Kurchatov Institute" • Tassilo Andreas Reisenegger von Oepen, Pontificia Universidad Catolica de Chile • Gwo-Ching Wang, Rensselaer Polytechnic Institute • William J. Weber, Pacific Northwest National Laboratory • Jory A. Yarmoff, University of California, Riverside

Section on Psychology
Jeffrey Reiss Alberts, Indiana University • Judy S. Deloache, University of Virginia • Martha Julia Farah, University of Pennsylvania • Klaus A. Miczek, Tufts University • Peter Shizgal, Concordia University • Michael Tanenhaus, University of Rochester • Janet F. Werker, University of British Columbia

Section on Social, Economic, and Political Sciences
Henry Brady, University of California, Berkeley • Richard B. Freeman, Harvard University • Douglas S. Massey, Princeton University • Constance Nathanson, Columbia University • Harold Shapiro, Princeton University

Section on Societal Impacts of Science and Engineering
Frederick M. Bernthal, Universities Research Association, Inc. • Matthew Bunn, Harvard University • Vary Coates, Journal of the Washington Academy of Sciences • John de la Mothe, University of Ottawa • Barry D. Gold, The Gordon and Betty Moore Foundation • Henry T. Greely, Stanford University • Andrew A. Rosenberg, University of New Hampshire • Daniel Sarewitz, Arizona State University • Robert M. Simon, Committee on Energy and Natural Resources, U.S. Senate • Caroline Wagner, George Washington University • Chris G. Whipple, ENVIRON International

Section on Statistics
William G. Cumberland, University of California, Los Angeles • Marie Davidian, North Carolina State University • Joseph F. Heyse, Merck Research Laboratories • Edward L. Korn, National Cancer Institute/NIH • David J. Marchette, Naval Surface Warfare Center • Hans-Georg Muller, University of California, Davis • Javier Rojo, Rice University • Peter H. Westfall, Texas Tech University • S. Stanley Young, National Institute of Statistical Sciences

What Is Natural? The Need for a Long-Term Perspective in Biodiversity Conservation

K. J. Willis[1]* and H. J. B. Birks[2]

Ecosystems change in response to factors such as climate variability, invasions, and wildfires. Most records used to assess such change are based on short-term ecological data or satellite imagery spanning only a few decades. In many instances it is impossible to disentangle natural variability from other, potentially significant trends in these records, partly because of their short time scale. We summarize recent studies that show how paleoecological records can be used to provide a longer temporal perspective to address specific conservation issues relating to biological invasions, wildfires, climate change, and determination of natural variability. The use of such records can reduce much of the uncertainty surrounding the question of what is "natural" and thereby start to provide important guidance for long-term management and conservation.

Paleoecological records (e.g., fossil pollen, seeds and fruits, animal remains, tree rings, charcoal) spanning tens to millions of years provide a valuable long-term perspective on the dynamics of contemporary ecological systems (1). Such studies are increasingly becoming part of community and landscape ecological research (2). In contrast, conservation-related research largely ignores paleoecological records. For example, there are no temporal records spanning more than 50 years included in any of the key biodiversity assessments published over the past 7 years (3). Paleoecological records have been considered too descriptive and imprecise, and therefore of little relevance to the actual processes of conservation and management. Such criticisms may have been valid 30 years ago, but there is now a wealth of information in paleoecological records providing detailed spatial and temporal resolutions (1, 4–7) that match in detail most records currently used in conservation research.

The potential of paleoecological records in conservation biology has been highlighted several times, including their application to biodiversity maintenance, ecosystem naturalness, conservation evaluation, habitat alteration, changing disturbance regimes, and invasions [e.g., (8–14)]. Conservation of biodiversity in a changing climate (15) and the relevant temporal and spatial scales for ecological restoration (16) have also been considered to warrant a longer-term temporal perspective. Most of these studies are descriptive and provide little practical application. A number of recent applied paleoecological studies, however, have begun to provide direct management information for biodiversity conservation at local, regional, and global scales. These include recommendations relating to biological invasions, wildfires, climate change, and conservation management within thresholds of natural variability. The overriding message from these studies is that such temporal perspectives are essential for meaningful modeling, prediction, and development of conservation strategies in our rapidly changing Earth.

Biological Invasions

Biological invasions are of critical concern to conservation organizations worldwide, with a general perception that many invasives are responsible for widespread community change and even extinctions (17). At the Rio Earth Summit Convention on Biological Diversity in 1992, for example, binding signatories were made "to prevent the introduction of, control or eradicate those alien species which threaten ecosystems, habitats or species" (18). However, biological invasions are complex. Some regions are more prone to invasion, certain species are more successful invaders than others, and sometimes it is even unclear whether a species is alien or native. The importance of the historical record in improving our ability to predict the outcome of

non-native introductions has been acknowledged [e.g., (13, 14)], but several recent paleoecological studies provide direct guidelines for the identification and management of invasives.

The distinction between what is native and what is not is often unclear. A species is usually classified as either native or exotic according to whether it is located in its presumed area of evolutionary origin and/or whether human agency is responsible for its current distribution. In the absence of a temporal record to assess a species history, the distinction can often become blurred (16). For example, in a reexamination of the British flora, several discrepancies between published records were found, with the same species being classified as "alien" or "native" depending on personal interpretation (19) (Table 1). There is also the question of how far back one takes "human" activity in determining whether a species is native or alien. When using evidence of first occurrences of species based on paleoecological records to reassess "doubtful natives" in the British flora, Preston et al. (19) determined that at least 157 plant species had been introduced to Britain by humans, intentionally or unintentionally, from the start of the Neolithic period (about 4000 years ago) to 500 years ago, yet the terminology used for their classification according to different floras is highly variable (Table 1). Preston et al. proposed that such species should be classified separately as "archaeophytes." They acknowledged, however, that this causes problems with their conservation status because this "non-native" label excludes them from the British Red Data Book of threatened or near-extinct species, and automatically deems them to be of lower conservation value—even though some are in serious decline and have been part of the British flora for at least 500 years.

A similarly conflicting conservation message was reached in an applied paleoecological study on the origin of an invasive form of the common reed (Phragmites australis) in the marshes of the inland wetlands of Lake Superior, North America (20) (Fig. 1). Over recent decades, P. australis populations have expanded rapidly throughout the coastal wetlands of North America, creating substantial changes in community structure and composition. In this study, paleoecological and genetic analyses were used to determine when the common reed became established in this region and whether the source was from a native or non-native

[1]Long-Term Ecology Laboratory, Oxford University Centre for the Environment, South Parks Road, Oxford OX1 3QY, UK. [2]Ecological and Environmental Change Research Group, Department of Biology, and Bjerknes Centre for Climate Research, University of Bergen, N-5007 Bergen, Norway, and Environmental Change Research Centre, University College London, London WC1E 6BT, UK.

*To whom correspondence should be addressed. E-mail: kathy.willis@ouce.ox.ac.uk

Table 1. Classification of 157 species of British plants that were probably introduced more than 500 years ago (archaeophytes) according to three published floras (54–56).

Published flora	Native	Doubtful native	Introduced	Probably introduced	Uncertain or untreated	Total
Dunn, 1905 (54)	31	—	103	—	23	157
Clapham et al., 1952 (55)	85	19	30	10	13	157
Stace, 1991 (56)	77	27	39	14	0	157

population. A 4000-year paleoecological record indicated that reeds were not part of the local flora until very recently (several decades), and that their recent expansion was probably linked to changes in water levels in the wetlands and human-induced changes to the landscape. The simple conservation message from this study is therefore to eradicate or control reed populations, because the expansion was recent and is likely to cause serious changes to the wetlands community. However, genetic data from these reed populations add another level of complexity because they indicate that the reeds are a native variety, raising the question of whether this is an exotic or natural invasion.

Fig. 1. Native (?) common reed (*Phragmites australis*) growing in Bark Bay Slough on Lake Superior, North America [photo: E. A. Lynch]; rattlesnake (*Crotalus mitchellii stephensi*) in the warm desert of western North America [photo: Blake L. Thompson]; wood grouse or western capercaillie (*Tetrao urogallus*) in the Cantabrian Mountains, northern Spain [photo: E. Menoni].

Oceanic islands are particularly liable to invasions, and it is often difficult to assess whether particular species are native or introduced. The invasive ornamental club moss *Selaginella kraussiana*, for example, is widely planted in the Neotropics, southern United States, Australasia, and western Europe. It is common on the Azores Islands in a range of habitats, but is it native there? Paleoecological records (*21*) (Fig. 2) clearly show that *S. kraussiana* had been present on Flores in the Azores for several thousand years before Portuguese discovery and Flemish settlement in the 15th century, thereby establishing beyond doubt its native status on Flores Island. Paleoecology again helped here to resolve a question in biodiversity conservation.

Another key question is whether invasive species are the triggering mechanism for ecosystem change, or merely opportunists taking advantage of environmental change caused by other biotic or abiotic factors? Also, are there particular factors that make a habitat more susceptible to invasion? A study of the colonization and spread of invasive shrubs in native shrublands and early successional forests in the northeastern United States, for example, found that prevalence of agricultural fields (historic and present-day) was the most influential factor affecting the colonization and spread of invasive shrubs (*22*). These native shrublands and early successional forests currently have high conservation status because of their diversity of terrestrial vertebrates. By considering the temporal dimension, the authors argue that it should be possible to identify those early successional habitats that may be especially prone to exotic invasion and ought to be of higher conservation

Fig. 2. Simplified pollen diagram from Lagoa Rasa, Flores Island, Azores, for the past 3000 years showing the percentage of tree, shrub, and herb pollen and of *Selaginella kraussiana* spores before and after human occupation of the island. [Modified from (*21*)]

priority. This study used only 40 years of temporal data, but studies incorporating longer temporal time scales have also illustrated persistent legacies of ancient land use that may influence the vulnerability of a site to invasion (*12*), including differences in soil pH, C, and N values. These imprints can last for decades to centuries. The identification of former land use by paleoecological records can thus be a tool for understanding and determining a habitat's vulnerability to invasion.

Introductions of non-native species often appear to fail a number of times before they eventually succeed; therefore, there is a lag between first colonization and population expansion of the invasive species (*23*). The reasons for resistance to invasion are complex and can have as much to do with environmental variables and extreme events as with demographic and biotic factors (*6*, *7*). A study using paleoecological records has shown that consideration should be given to biological inertia (*24*), whereby a native community occurs where environmental conditions are no longer optimal but will remain in situ without any triggering mechanism (e.g., hurricanes, windthrow, etc.) to "remove" this resident population. Thus, the life history characteristics and biology of the resident species, and not the properties of the invading species, are responsible for invasion lags. This phenomenon is particularly apparent in forest ecosystems. In many current old-growth forests in western North America, paleoecological studies have shown that these stands were established during the cooler and moister climate of the Little Ice Age (about 650 to 150 years ago) and therefore reflect recruitment responses to former climate conditions (*25*). Such information about ecological legacies (*1*) is directly relevant to conservation because such forests may be at a critical threshold and may be particularly vulnerable to invasion after a disturbance event, either natural or human-induced.
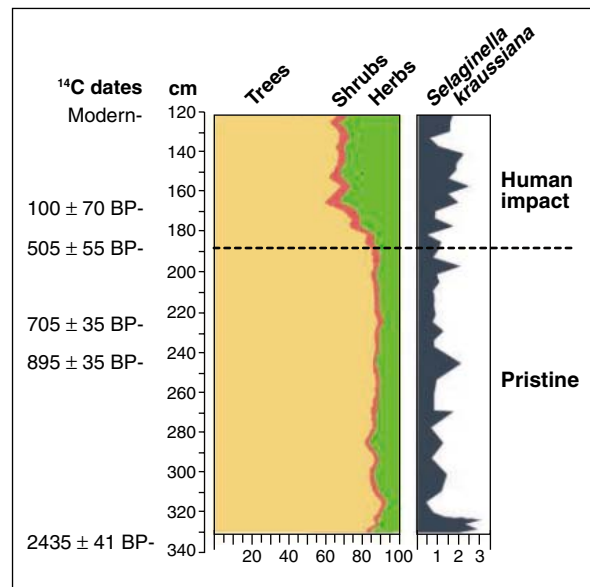
Wildfires

Wildfires have been important in shaping the structure and function of fire-prone communities throughout Earth's history (*26*). Of particular concern to conservationists, however, are changes in the frequency, severity, and extent of burning from those perceived as the "norm" (*27*). What processes are driving this change (human or climate)? How will it affect the composition of plants and animals in ecosystems, in particular those already identified as vulnerable? And are there particular management techniques

that can be implemented to alter fire regimes? Fundamental to these questions is establishing the natural variability of wildfires so that this can be used as a benchmark against which to evaluate contemporary conditions and future alternatives (28). Assessments based on short-term records (<50 years) can easily lead to misguided management plans (29).

Although climate change and human activities have long been acknowledged as drivers of wildfires, results from recent paleoecological studies show that these relationships are complex. For example, although it is not unreasonable to assume that an increase in aridity would result in more fires, several studies indicate otherwise. In the Alaskan boreal forest, fires occurred more frequently under wetter climatic conditions (30). A similar conclusion was reached in a paleoecological study of fire cycles in the Northern Great Plains grasslands of North America (31). Here, the highest charcoal flux occurred during past moist intervals when grass cover was extensive and fuel loads were high. Shifts in fuel quantity and quality can cause changes in fire regimes. Both studies show that there is a complex climate-fuel-fire relationship determining the variability of wildfires (32). Such studies (33) should be taken into account when predicting future ecosystem change within climate change conservation strategies.

Prehistoric and historic human-induced wildfires are often assumed to have caused changes in ecosystem structure and degradation, especially in tropical forests where natural fires are rare and tend to be limited in extent. Management plans to control such fires are usually implemented, however, without paleoecological evidence to confirm such an assumption. One such example is in the tropical dry forests of the southern Ratanakiri Province, northeastern Cambodia (34). Here, regional conservation policy is based on the premise that burning by humans has degraded the dense forests and resulted in the present open forest–savanna mosaic. However, a paleoecological study shows that present-day fire activity is now lower than it has been for the past 9300 years (Fig. 3). Rather, the forest-savanna shift is probably a consequence of monsoonal activity, and the high-frequency but low-intensity fires caused by humans may, in fact, conserve forest cover. In this case, the current conservation management plan is clearly at odds with evidence from the paleoecological record.

Interesting conclusions have also emerged from studies examining ecosystem composition in response to fire regimes. One of the main

findings of the work on the North American grasslands described above, for example, is that fire is not necessarily a universal feature of this ecosystem but oscillates through time with climate (31). The impact of such variability in burning regimes through time on ecosystem composition can have conservation implications. This is well illustrated in a study on the long-term record of fire and open canopy in a forest in southern Sweden that contains an exceptionally large number of endangered species of beetle (35). Of the 105 beetle species recorded at this site living on or in rotting wood that are in the Swedish Red Data Book of threatened or near-extinct species, many are associated with open forest, forest fires, or structures created by fire. Yet a site-scale paleoecological study indicates that the forest is more closed today than at any time in the past 2500 years; although
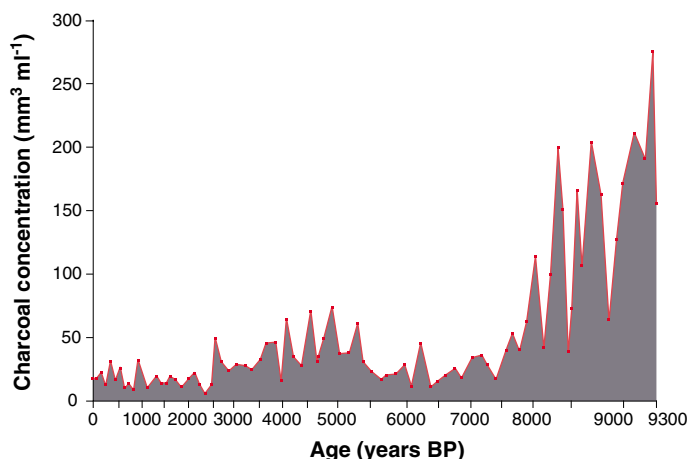
Fig. 3. Reconstructed fire regimes in northeastern Cambodian monsoonal forests over the past 9300 years, using microfossil charcoal concentration from a dated sedimentary sequence (34). The record indicates that present-day charcoal input is the lowest of the entire period. Conservation policies that suggest that human burning has increased and resulted in the open forest–savanna mosaic in this region are clearly misguided, as are management recommendations for fire suppression.

there had been a significant amount of burning in the past, there has been a large reduction in fires over the past 200 years. The authors concluded that openness of the site in the past as a consequence of burning is an important explanation for the high conservation value of the site today (35). To conserve the diverse beetle assemblage of this site, they suggested that open forest conditions needed to be restored and that prescribed burns would be the most appropriate way to achieve this.

Climate Variability

Most conservation organizations have developed climate change conservation strategies [as described in (36)] designed to conserve biodiversity in a changing climate. Two questions central to current conservation strategies arise. Where will biota move to in response to future climate change? Which species and regions are

most at risk from future climate change? Underlying these questions are key management and planning issues—for example, ensuring that reserve boundaries allow for potential species-range shifts (37) and that the species and regions most at risk are identified and protected (38).

In the evaluation of predictive models to determine the biogeographic effects of climate change, several studies have used paleoecological records for backward prediction (hindcasting) to assess errors potentially inherent in species-envelope bioclimatic modeling (39). This involves running models for past intervals of time, using present-day species data but modeling the species' response to climate change against paleoclimatic data as opposed to present-day climatic data. The predicted distributions are then tested against the distribution of the species apparent in the fossil record for the time interval covered by the paleoclimatic data to assess model robustness (40). In a study of 23 extant mammal species in the United States (39), for example, an ecological niche model was run backward for the time interval of the Last Full Glacial (14,500 to 20,500 years before the present) and predicted distributions were compared to actual distribution records obtained from the FAUNMAP fossil database (41). The model was also run in reverse (i.e., using fossil data and paleoclimatic data to predict present distributions) and similar comparisons were made. Results indicated that for nine species the model was able to predict accurately the Pleistocene distributions from the present-day data, and vice versa. Not only did this confirm that the model was robust for these species, it also provided a test for the underlying assumption of these models that the species' ecological niche characteristics have remained constant through time. A similar pattern was recently found for several North American plant species (42). The remaining species, however, either had significant predictions only one way but not the other (nine species) or were not significant in either direction (five species).

The question of why some species' distributions cannot be accurately predicted by species-climate modeling can also be answered, at least for some species, from paleoecological studies. A study of the spread of *Picea abies* (spruce) and *Fagus sylvatica* (beech) over the past 4000 years in southern Scandinavia, for example, showed that at the local-stand scale the spread of *Picea* closely tracked the changing area of suitable regional climate, whereas the spread of *Fagus* was more directly linked to anthropogenic activities and disturbance by fire (43). Thus, caution may be needed in using the results of

predictive species-envelope models in conservation planning, because the distributions of some species today or in the past may be poorly predicted.

Bioclimatic models are particularly relevant to conservationists in determining and understanding the dynamics of the leading edge of species-range margins and the potential space that will be needed for future reserve boundaries (40). There is also a considerable literature on modeling to determine which species will go extinct [e.g., (38)]. However, there are few studies of the likely fate of rear-edge populations, that is, the source populations from which the leading-edge populations migrate (Fig. 4) (44). A key conservation objective should be the preservation of conditions necessary for speciation (45). Evidence from paleoecological and genetic records indicates that the maintenance of populations in these rear-edge regions could, in fact, be critical for conservation of long-term genetic diversity (44). Evidence also suggests that these regions tend to be where plants and animals were geographically and genetically isolated in refugia during the cold stages of the Pleistocene. In Europe, for example, refugial localities have been recognized in Iberia, the Balkans, and Italy and in mountain ranges such as the Carpathians (46–48).

With the use of a combination of paleoecological and genetic evidence, other such regions have been identified, and this information is feeding into conservation policy. For example, in a study on Eurasian populations of western capercaillie (grouse)—a keystone species of Palearctic boreal and high-altitude coniferous forests (49)—a combined genetic and temporal record enabled the identification of two regions that should be classified as ecologically significant units (ESUs) because of the genetic distinctiveness of the populations within them from the rest of Europe. The distinctiveness of the populations in these ESUs, located in the Pyrenees and Cantabrian Mountains (Fig. 1), is almost certainly related to their Pleistocene refugial isolation. Similar historically related genetic patterns have been identified in these two regions for a number of plants and animals, and this knowledge is now leading to international recognition of the conservation importance of these areas (49).

In the United States, a similar approach using a molecular and deep-time historical perspective as a primary mechanism to frame biodiversity reserves (50) has been applied to a number of groups of plants and animals. Distinctive patterns of genetic diversity related to geological events in deep time (Pliocene/Miocene) and to Pleistocene refugial isolation have been demonstrated, for example, in four rattlesnake species (Fig. 1; genus *Crotalus*) in the warm deserts of western North America (50). Here it is argued that an approach that seeks to understand the causation of genetic patterns would be more effective in encapsulating biodiversity than

current measures (based on the use of geological features as a surrogate for diversity) and that such studies should be routinely used in developing integrated regional conservation policies (50).

Determination of Thresholds Within Natural Variability

Variability through time is an inherent part of ecosystem behavior. It is thus essential to incorporate variability into management policies. To do this reliably in our rapidly changing world requires answers to several questions. What are the baseline or "reference" conditions before recent times? What is the range of natural variability? Under what conditions do negative impacts become apparent? How can thresholds be determined beyond which specific management plans should be implemented?

Gillson and Duffin (51) used paleoecological records from savannas in Kruger National Park, South Africa, to determine the natural variability of woody vegetation cover during the past 5000 years. They used this information to address whether woody cover has decreased below 80% of its "highest ever value"—a threshold set by ecosystem managers to define the upper and lower level of accepted variation in this ecosystem. Paleoecological results indicated that during the past 5000 years, the estimated woody vegetation cover had remained at about 20% of its "highest ever value," and therefore that management intervention in this part of the park is unnecessary at present.

Other examples where paleoecological records have been used to identify where natural thresholds have recently been exceeded include river ecosystems in Australia (52) and Colorado (53). The large deep billabongs in the middle reaches of the Murray River, Australia, for example, do not currently support submerged mac-

rophyte beds. Yet paleoecological analyses indicate that these were an important part of the ecosystem before the arrival of Europeans (52). In the Colorado delta ecosystem (53), paleoecological studies suggest that there has been a decline of up to 94% of shelly benthic macroinvertebrates over the past 75 years. This decline is probably associated with a reduction of fresh water and nutrients resulting from the diversion of the Colorado River by dams and irrigation projects. Both studies provide quantitative assessments of the relative health (4) of these river ecosystems and indicate thresholds that have been exceeded—information that is critical to their restoration and long-term conservation.

Conclusions

Conservation biology and nature management are primarily concerned with the present and increasingly with the future. Paleoecology primarily considers the past but can provide a historical perspective to the present (1). It can also contribute to key questions in conservation and management such as habitat naturalness, biological invasions, disturbance regimes, natural variability, and ecosystem health. With increasing amounts of paleoecological data of a high spatial and/or temporal resolution (4, 5), there is potential for synergy between conservation biology and paleoecology. There are, however, several research needs and challenges that need to be met before an effective synergy can fully develop. These include the following:

1) Paleoecological studies in biodiversity hotspots with a high density of species. At present there are few studies from these critical areas.

2) Improved taxonomic resolution of the fossils found, because improved resolution invariably enhances the biological value of fossil records (5, 21).
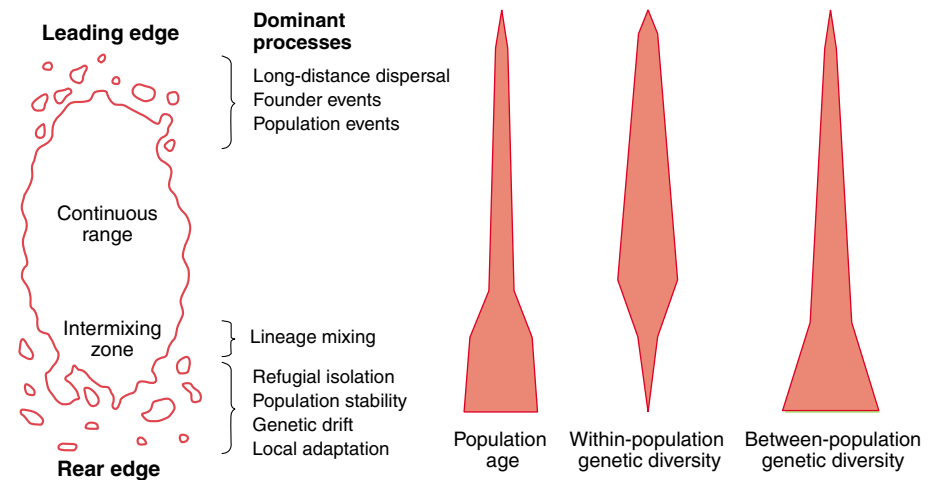
Fig. 4. Schematic representation of the leading and rear-edge populations in response to climate change (44). Paleoecological and genetic evidence suggests that the rear-edge populations may be extremely important in the conservation of long-term genetic diversity and that more attention must be given to modeling the impacts of future climate change on these populations and their protection.

3) Assessing terrestrial paleoecological data in terms of "ecosystem health" to provide an ecosystem's health history (*4*). Some taxa in paleoecological records are "indicators" of particular ecological conditions that can provide useful "symptoms" about the ecosystem's health. Paleolimnologists (*4*) have effectively applied the concept of ecosystem health to lakes in relation to critical loads of pollutants. The same concept could be usefully applied to forests, heathlands, grasslands, wetlands, tundra, and savannas.

4) Greater discussion and collaboration between paleoecologists and conservation biologists, so that the most pertinent and urgent research questions are addressed together and the most relevant paleoecological data are collected at the spatial and temporal scales of direct concern in conservation.

Paleoecology provides a historical perspective that can help put present and future conservation and management policies into context. The time is ripe for the two disciplines to work more closely together and to develop a common agenda for biodiversity conservation.

References and Notes

1. National Research Council, *The Geological Record of Ecological Dynamics: Understanding the Biotic Effects of Future Environmental Change* (National Academies Press, Washington, DC, 2005).
2. L. Graümlich, S. Sugita, L. B. Brubaker, V. M. Card, *Ecology* **86**, 1667 (2005).
3. K. J. Willis, L. Gillson, T. Brncic, B. Figueroa-Rangel, *Trends Ecol. Evol.* **20**, 107 (2005).
4. J. P. Smol, *Pollution of Lakes and Rivers—A Paleoenvironmental Approach* (Arnold, London, 2002).
5. H. J. B. Birks, *Grana* **44**, 1 (2005).
6. M. E. Lyford, S. T. Jackson, J. L. Betancourt, S. T. Gray, *Ecol. Monogr.* **73**, 567 (2003).
7. S. T. Gray, J. L. Betancourt, S. T. Jackson, R. G. Eddy, *Ecology* **87**, 1124 (2006).
8. H. J. B. Birks, *J. Veg. Sci.* **7**, 89 (1996).
9. P. B. Landres, P. Morgan, F. J. Swanson, *Ecol. Appl.* **9**, 1179 (1999).
10. T. W. Swetnam, C. D. Allen, J. L. Betancourt, *Ecol. Appl.* **9**, 1189 (1999).
11. L. Gillson, K. J. Willis, *Ecol. Lett.* **7**, 990 (2004).
12. D. R. Foster *et al.*, *Bioscience* **53**, 77 (2003).
13. G. M. MacDonald, *Adv. Ecol. Res.* **24**, 67 (1993).
14. S. T. Jackson, in *Assessment and Management of Plant Invasions*, J. O. Luken, J. W. Thieret, Eds. (Springer-Verlag, New York, 1997), p. 37.
15. L. Hannah *et al.*, *Conserv. Biol.* **16**, 264 (2002).
16. J. B. Calicott, *J. Biosci.* **27**, 409 (2002).
17. J. Gurevitch, D. K. Padilla, *Trends Ecol. Evol.* **19**, 470 (2004).
18. S. Henderson, T. E. Dawson, R. J. Whittaker, *Prog. Phys. Geogr.* **30**, 25 (2006).
19. C. D. Preston, D. A. Pearman, A. R. Hall, *Bot. J. Linn. Soc.* **145**, 257 (2004).
20. E. A. Lynch, K. Saltonsall, *Wetlands* **22**, 637 (2002).
21. J. F. N. Van Leeuwen *et al.*, *Neobiota* **6**, 27 (2005).
22. V. S. Johnson, J. A. Litvaitis, T. D. Lee, S. D. Frey, *For. Ecol. Manage.* **228**, 124 (2006).
23. D. F. Sax, J. H. Brown, *Glob. Ecol. Biogeogr.* **9**, 363 (2000).
24. B. Von Holle, H. R. Delcourt, D. Simberloff, *J. Veg. Sci.* **14**, 425 (2003).
25. C. I. Millar, W. B. Woolfendon, *Ecol. Appl.* **9**, 1207 (1999).
26. W. J. Bond, J. E. Keeley, *Trends Ecol. Evol.* **20**, 387 (2005).
27. D. McKenzie, Z. Gedalof, D. L. Peterson, P. Mote, *Conserv. Biol.* **18**, 890 (2004).
28. P. Z. Fulé, W. W. Covington, M. M. Moore, *Ecol. Appl.* **7**, 895 (1997).
29. C. Whitlock, *Nature* **432**, 28 (2004).
30. J. A. Lynch, J. L. Hollis, F. Sheng Hu, *J. Ecol.* **92**, 477 (2004).
31. K. J. Brown *et al.*, *Proc. Natl. Acad. Sci. U.S.A.* **102**, 8865 (2005).
32. J. S. Clark, P. D. Royall, C. Chumbley, *Ecology* **77**, 2148 (1996).
33. J. S. Clark, E. C. Grimm, J. Lynch, P. G. Mueller, *Ecology* **82**, 620 (2001).
34. A. L. Maxwell, *J. Biogeogr.* **31**, 225 (2004).
35. M. Lindbladh, M. Niklasson, S. G. Nilsson, *Biol. Conserv.* **114**, 231 (2003).
36. L. Hannah, G. F. Midgley, D. Millar, *Glob. Ecol. Biogeogr.* **11**, 485 (2002).
37. M. B. Araújo, M. Cabeza, W. Thuiller, L. Hannah, P. H. Williams, *Glob. Change Biol.* **10**, 1618 (2004).
38. C. D. Thomas *et al.*, *Nature* **427**, 145 (2004).
39. E. Martínez-Meyer, A. Townsend Peterson, W. W. Hargrove, *Glob. Ecol. Biogeogr.* **13**, 305 (2004).
40. M. B. Araújo, C. Rahbek, *Science* **313**, 1396 (2006).
41. FAUNMAP Working Group, *Illinois State Mus. Sci. Pap.* **25** (1994).
42. E. Martinez-Meyer, A. Townsend Peterson, *J. Biogeogr.* **33**, 1779 (2006).
43. R. H. W. Bradshaw, M. Lindbladh, *Ecology* **86**, 1679 (2005).
44. A. Hampe, R. J. Petit, *Ecol. Lett.* **8**, 461 (2005).
45. D. Jablonski, *Nature* **427**, 589 (2004).
46. K. D. Bennett, P. C. Tzedakis, K. J. Willis, *J. Biogeogr.* **18**, 103 (1991).
47. P. C. Tzedakis, I. T. Lawson, M. R. Frogley, G. M. Hewitt, R. C. Preece, *Science* **297**, 2044 (2002).
48. K. J. Willis, J. C. McElwain, *The Evolution of Plants* (Oxford Univ. Press, Oxford, 2002).
49. O. Duriez *et al.*, *Conserv. Genet.*, in press.
50. M. E. Douglas, M. R. Douglas, G. W. Schuett, L. W. Porras, *Mol. Ecol.* **15**, 3353 (2006).
51. L. Gillson, K. I. Duffin, *Philos. Trans. R. Soc. London Ser. B*, in press.
52. M. A. Reid, R. W. Ogden, *River Res. Appl.* **22**, 167 (2006).
53. M. Kowalewski, G. E. A. Serrano, K. Flessa, G. A. Goodfriend, *Geology* **28**, 1059 (2000).
54. S. T. Dunn, *Alien Flora of Britain* (West Newman, London, 1905).
55. A. R. Clapham, T. G. Tutin, E. F. Warburg, *Flora of the British Isles* (Cambridge Univ. Press, Cambridge, 1952).
56. C. A. Stace, *New Flora of the British Isles* (Cambridge Univ. Press, Cambridge, 1991).
57. We thank K. D. Bennett, S. Bhagwat, and H. H. Birks for helpful comment and discussion on this manuscript, and E. A. Lynch, M. E. Douglas, and O. Duriez for help in finding suitable photographic images. This is publication A147 from the Bjerknes Centre for Climate Research.

Effective Enforcement in a Conservation Area

Ray Hilborn,[1]* Peter Arcese,[2] Markus Borner,[3] Justin Hando,[4] Grant Hopcraft,[3,7] Martin Loibooki,[4] Simon Mduma,[5] Anthony R. E. Sinclair[6]

There are two primary approaches to wildlife conservation, the generation of economic benefits from wildlife to local communities, so that protecting wildlife is in their interest, and the enforcement of protected areas. Outside of protected areas, community-based conservation must be the cornerstone of protection (1). However, within protected areas there is debate as to whether enforcement can maintain wildlife and even whether protected areas as wildlife reserves are realistic or morally justified (2). Here, we present the history of illegal harvesting in Serengeti National Park (SNP), Tanzania; estimate the amount of antipoaching activity by park staff; and show how the level of funding for antipoaching has affected the trends in abundance of three severely affected species: African buffalo, elephant, and black rhino.

The primary form of poaching in the SNP and surrounding areas is snaring by local villagers (3), but targeted trophy hunting for elephants and rhinos occurred in the 1970s and 1980s. Park staff conduct antipoaching patrols by driving on roads and across country and foot patrols. In 1977, Tanzania closed its borders. The Tanzania economy went into a rapid decline, park budgets and resources collapsed, and it is widely acknowledged that poaching increased markedly. Beginning in the late 1980s, park budgets expanded and antipoaching patrols increased greatly, becoming a higher priority in the annual budgets.

We used the capture of poachers per patrol as our index of poaching intensity. The number of poachers arrested per year has been recorded since 1957 (fig. S1A) in the SNP; antipoaching effort, measured as ranger patrols per day was available in some years (Fig. 1A) (4, 5); and the relative poaching effort was estimated by the ratio of arrests to patrols. (Fig. 1B). Poaching was low before 1977, increased between 1977 and 1986, and declined rapidly between 1984 and 1988.

Buffalo (Fig. 1C), elephant (fig. S1C), and black rhino (fig. S1D) abundance all show a rapid decline after 1977, low numbers for several years, and then (for buffalo and elephant) a recent increase. The fitted curves come from a simple population dynamics model (6) that assumes the illegal harvest rate is proportional to the intensity of poaching. Buffalo were also affected in 1993 by a severe drought that killed 40% of the population. The model matches closely the census data for buffalo, indicating that the decline and increase in numbers is accounted for by changes in illegal hunting. Both elephants and rhinos were targeted for the high-value ivory and rhino horn trade, and the increase in poaching was probably stimulated by particularly high prices in the late 1970s. The fast increase in elephants in the 1990s was helped by the reduction in the world price of ivory due to a CITES (Convention on International Trade in Endangered Species of Wild Fauna and Flora) ban on ivory trading.

All three data sets support the basic contention that poaching after 1977 was severe and caused major declines in abundance, whereas since 1993 poaching has been reduced enough to allow populations to rebuild. Estimates of poaching intensity in recent years depend on the assumption that arrests per patrol are a linear index of poaching intensity. Patrol efficiency may have increased with better training, more resources, and development of informant networks, or, possibly, poachers may be better able to avoid patrols as they developed more experience.

Since 2000, SNP has contributed about U.S.$100,000 per year to community development projects (7), augmented by additional funds from nongovernmental agencies. However, the main decline in poaching effort occurred well before the community conservation programs were initiated; hence, the decline in poaching can be attributed primarily to the increase in antipoaching effort. Therefore, we can conclude that antipoaching is effective for the protection of the species of interest if there are sufficient resources for a professional national park service.

References and Notes

1. W. A. Newmark, J. L. Hough, *Bioscience* **50**, 585 (2000).
2. M. W. Muphree, in *Parks in Transition*, B. Child, Ed. (Earthscan, London, 2004), pp. 217–232.
3. P. Arcese, J. Hando, K. Campbell, in *Serengeti II: Dynamics, Management and Conservation of an Ecosystem*, A. R. E. Sinclair, P. Arcese, Eds. (Univ. Chicago Press, Chicago, 1995), pp. 506–533.
4. H. T. Dublin, A. R. E. Sinclair, J. McGlade, *J. Anim. Ecol.* **59**, 1147 (1990).
5. H. Hofer, M. East, in *Serengeti II: Dynamics, Management and Conservation of an Ecosystem*, A. R. E. Sinclair, P. Arcese, Eds. (Univ. Chicago Press, Chicago, 1995), pp. 332–363.
6. Materials and methods, including model descriptions, are available as supporting material on *Science* Online.
7. S. Thirgood et al., in *Serengeti III: Human Impacts on Ecosystem Dynamics*, A. R. E. Sinclair, C. Packer, S. Mduma, J. Fryxell, Eds. (Univ. Chicago Press, Chicago, in press).
8. This work was supported by NSF Biocomplexity grant BE-0308486.

[1]School of Aquatic and Fishery Sciences, Box 355020, University of Washington, Seattle, WA 98195, USA. [2]Center for Applied Conservation Research, University of British Columbia, Vancouver, British Columbia VLT 1Z4, Canada. [3]Frankfurt Zoological Society, Post Office Box 14935, Arusha, Tanzania. [4]Tanzania National Parks, Post Office Box 3134, Arusha, Tanzania. [5]Tanzanian Wildlife Research Institute, Box 661, Arusha, Tanzania. [6]Center for Biodiversity Research, University of British Columbia, Vancouver, British Columbia VLT 1Z4, Canada. [7]Community and Conservation Ecology, University of Groningen, Post Office Box 14, 9750AA, Haren, Netherlands.

*To whom correspondence should be addressed. E-mail: rayh@u.washington.edu
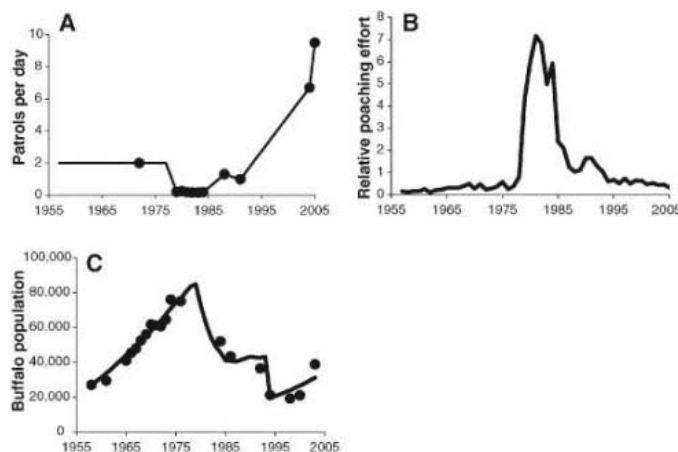
Fig. 1. (A) Number of antipoaching patrols per day: dots represent data, and lines represent interpolated values. **(B)** Estimated amount of poaching effort measured as poachers arrested per patrol day. **(C)** Observed abundance of African buffalo (dots) and model predictions (solid line).

Dynamical Superconducting Order Parameter Domains in Sr$_2$RuO$_4$

Francoise Kidwingira,[1] J. D. Strand,[1] D. J. Van Harlingen,[1]* Yoshiteru Maeno[2]

We present direct evidence for complex p-wave order parameter symmetry and the presence of dynamical chiral order parameter domains of the form $p_x \pm ip_y$ in the ruthenate superconductor Sr$_2$RuO$_4$. The domain structure creates differences in the magnetic field modulation of the critical current of Josephson junctions fabricated on orthogonal faces of Sr$_2$RuO$_4$ single crystals. Transitions between the chiral states of a domain or the motion of domain walls separating them generates telegraph noise in the critical current as a function of magnetic field or time and is responsible for hysteresis observed in field sweeps of the critical current. The presence of such domains confirms the p-wave triplet spin and complex (broken time-reversal symmetry) nature of the superconducting pairing state in Sr$_2$RuO$_4$.

S$\,$ince the ruthenate superconductor Sr$_2$RuO$_4$ (SRO) was discovered to be superconducting a decade ago (1), its pairing symmetry has been an intensely debated topic (2). On the basis of ferromagnetism in related compounds and similarities between the normal-state properties of SRO and those of superfluid ^{3}He, a p-wave order parameter was proposed (3). Early experiments revealed the extreme fragility of the superconductivity in this material, as demonstrated by a strong suppression of the transition temperature with impurities (4), raising suspicions of unconventional superconductivity. Nuclear magnetic resonance measurements showed evidence for spin-triplet Cooper pairing (5) and muon spin resonance experiments (6) revealed a spontaneous magnetization consistent with broken time-reversal symmetry. The originally proposed complex p-wave order parameter of the form $p_x + ip_y$ was fully gapped, with a phase that evolves continuously with the angle in k-space. It was later found to be inconsistent with numerous reports of excess quasi-particles at low temperature (7–10). Different scenarios were proposed to account for the discrepancy, most suggesting nodes on the z axis or in only some of the three Fermi surface sheets. In the following, we use the $p_x + ip_y$ notation to indicate a general ($p_x + ip_y$)-like order parameter with phase winding continuously with angle in k-space and broken time-reversal symmetry.

Although never directly observed, a chiral order parameter domain structure in which regions of order parameter $p_x + ip_y$ would co-exist with regions of order parameter $p_x - ip_y$ has been proposed (11) and discussed theoretically (12–14). This is analogous to the domain

structure found in ferromagnetic materials. Chiral domains have been postulated to explain phenomena otherwise not understood, such as the rate of vortex creep dynamics in unconventional superconductors (14, 15), but attempts at magnetic imaging of spontaneous currents induced by the chirality have yielded null results (16).

Determining unconventional superconductivity. Unconventional pairing is determined using the phase-sensitive Josephson interferometer technique. In this approach, a superconducting quantum interference device (SQUID) formed by fabricating Josephson junctions on different faces of a single crystal is used to measure the phase difference between different real-space tunneling directions, hence mapping the phase anisotropy of the superconducting order parameter. The quantity measured is the modulation of the critical current as a function of applied magnetic field, the so-called diffraction pattern. In materials with even spatial parity (spin singlet), this method gives a direct and unambiguous determination of the pairing symmetry as the real-space tunneling direction (normal to the junction interface) uniquely probes the corresponding k-space direction. It was a series of such experiments on the high-temperature superconductor YBa$_2$Cu$_3$O$_{7-x}$ (YBCO) that verified the pairing symmetry to be $d_{x^2-y^2}$, and therefore an unconventional superconductor (17). Before these experiments, a similar technique had been proposed (18) to test the symmetry of the heavy fermion superconductors such as UPt$_3$, suspected then (and now) to be an odd-symmetry p-wave or f-wave superconductor. The SQUID interferometer technique is considerably less definitive in this case because of the parity mismatch between the s-wave and p-wave superconductors that should suppress first-order Josephson tunneling (19). In fact, a Josephson supercurrent is expected only if a mechanism exists to break the parity

mismatch, such as spin-flip processes, interfacial magnetic impurities, or magnetic surface states. The dominant sign of the order parameter probed, and thus the outcome of phase-sensitive measurements, then depends on details of the symmetry-breaking. We will assume that the symmetry breaking that allows us to observe supercurrent is a property of the interface and is not responsible for the dynamics we observe.

A recent SQUID interferometry experiment on SRO single crystals (20) showed evidence for a sign change in the order parameter between opposite directions. These experiments required careful attention to the complicating effects of critical current asymmetry and trapped magnetic flux known from the earlier experiments on d-wave superconductors (21). Despite these issues, a compelling case for odd-symmetry pairing in SRO was made. We use the phase sensitivity of Josephson interferometry to probe not only the spatial symmetry of the order parameter but also time-reversal symmetry and the existence and dynamics of chiral order parameter domains.

Josephson interferometry on SRO. We report only on measurements made on single junctions fabricated on flat faces of high-quality SRO single crystals grown by the floating-zone method as described (22). Their superconducting transition temperatures T_c are between 1.37 K and 1.43 K, depending on the batch. Although the critical current of most of the junctions studied vanished above 1.5 K, a few exhibited a tail in the critical current extending to temperatures as high as 3 K, perhaps suggesting trace amounts of the 3 K phase at the crystal surface (23). We did not observe any qualitative difference in the interferometry data from junctions that may have this high-temperature phase.

Fabrication and measurement methods were as described (23). A picture of a sample is shown in Fig. 1A. The measurements were carried out in a ^{3}He refrigerator with a base temperature of ~325 mK. The junctions exhibit resistively shunted current-voltage characteristics (Fig. 1B) as expected for superconductor–normal metal–superconductor junctions. The critical current diffraction patterns, however, are unusual and anomalous. Their most striking feature is that different junctions—and even the same junction upon successive thermal cycling—can exhibit qualitatively different behavior. Although none of the junctions exhibit the expected Fraunhofer diffraction pattern for a perfectly uniform junction with a single phase difference, some (roughly 20% of 28 junctions studied) are very close with a central tall peak, a series of side lobes, and even symmetry with respect to the applied field direction (Fig. 2A). In contrast, others show the heavily disordered patterns characteristic of interference arising from multiple

[1]Department of Physics, University of Illinois, Urbana, IL 61801, USA. [2]Department of Physics, Kyoto University, Kyoto 606-8502, Japan.

*To whom correspondence should be addressed. E-mail: dvh@uiuc.edu

regions with different phase drops across the junction (Fig. 2, B and C), as typically observed in faceted grain boundary junctions (24, 25); some of these junctions exhibit field polarity asymmetry. The strongly modulated junctions exhibit lower critical current magnitudes. They do not have a definite period of modulation or the Fraunhofer envelope expected from a simple SQUID configuration or other multiply connected geometry. Upon thermal cycling above the transition temperature of SRO (~1.5 K), the patterns are not always identical but often remain qualitatively similar (Fig. 2D).

One intriguing feature of the diffraction patterns is the hysteresis loops observed when the magnetic field is ramped beyond a certain value (Fig. 3A). Once induced, the hysteresis loops are stable and reasonably symmetric with respect to field, and could be annealed out by returning to a smaller field scan (23). This is in sharp contrast to previous measurements we made on the cuprates, in which abrupt changes in the diffraction patterns produced by large fields were generally asymmetric and could only be eliminated by thermal cycling.

Another unexpected feature is the presence of abrupt jumps in the critical current at specific fields (Fig. 3B). These jumps are reproducible, occurring within a narrow field range in the forward and reverse field sweep directions. Upon thermal cycling above the superconducting transition temperature, the jumps sometimes disappear but more often reappear in a similar field range. The switches are not always symmetric with field direction, and the magnitude of the field at which they occur varies from junction to junction, as does the size of the jump. In a few cases, the jumps have the form of telegraph-like switching noise between two metastable critical current states, both as the magnetic field is swept and as a function of time at a fixed field (Fig. 3, C and D). The noise as a function of applied field has a signature behavior for a given thermal cycle: As long as the junction remains cold, all diffraction patterns measured show qualitatively similar switching behavior, although individual switches do not appear at the same field values, nor are they symmetric for positive and negative fields. Switching noise as a function of time appears only after a field sweep and is observed both at zero and finite fields. The time scale of the switches varies but can be remarkably slow, often with characteristic lifetimes of several seconds. In some cases, the voltage only shows one or two jumps and then remains constant, aside from small temperature and instrumentation drifts.

Modeling. Let us now consider the critical current we expect to measure for a Josephson junction on a face of a single crystal with chiral symmetry. We define the large face of the crystal (c axis) to be along the z direction and the junction tunneling direction to be along the

x direction. We assume that the local supercurrent density follows the usual Josephson relation $J = J_c \sin(\phi)$, where J_c is the local critical current density and ϕ is the local gauge-invariant phase difference across the junction. J_c can vary across the junction face as a result of spatial variations of the barrier thickness, changes in the order parameter symmetry of the superconductors arising either from faceting (which changes the local tunneling direction) or domains (which introduces a phase that is dependent on the order parameter orientation and chirality). To maintain phase coherence across the junction and through the superconducting electrodes, a magnetic field threading the junction will induce changes in ϕ along the junction face relative to the phase at the center of the junction ϕ_0. The effective magnetic thickness of the junction barrier is $t = d_{Cu} + \lambda_{SRO} + \lambda_{Pb}$, where d_{Cu} is the Cu barrier layer thickness and λ_{SRO} and λ_{Pb} are the penetration depths of the SRO and Pb electrodes. For an applied magnetic field $\mathbf{B} = B\hat{z}$, the Josephson supercurrent $I_s(B)$ through an edge junction of height h and width w is found by integrating the resulting supercurrent density over the junction face:

$$I_s(B) = h \int_{-w/2}^{w/2} J_c(y) \sin\left(\frac{2\pi Bt}{\Phi_0}y + \phi_0\right) dy \quad (1)$$

Fig. 1. (**A**) Picture of a typical sample showing a single SRO crystal with four junctions. The black rectangle is the SRO crystal and the gray ribbons are the Pb thin film counterelectrodes. (**B**) Current-voltage characteristic of a typical SRO-Cu-Pb junction, showing typical resistively shunted junction behavior.
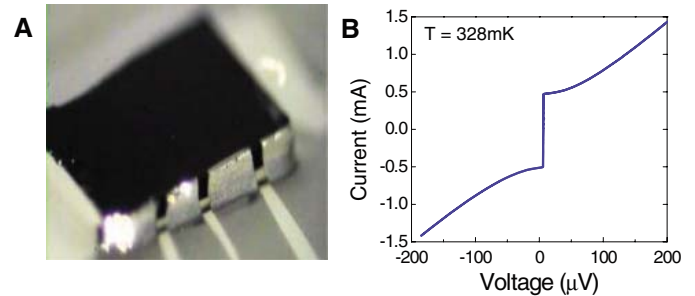
Fig. 2. Examples of diffraction patterns observed in single Josephson junctions on the edge of a SRO crystal: (**A**) Fraunhofer-like pattern, (**B** and **C**) grain boundary–like patterns indicating spatially varying phase differences across the junction, (**D**) pattern taken on the same junction as (C) but on a different thermal cycle (same scale).
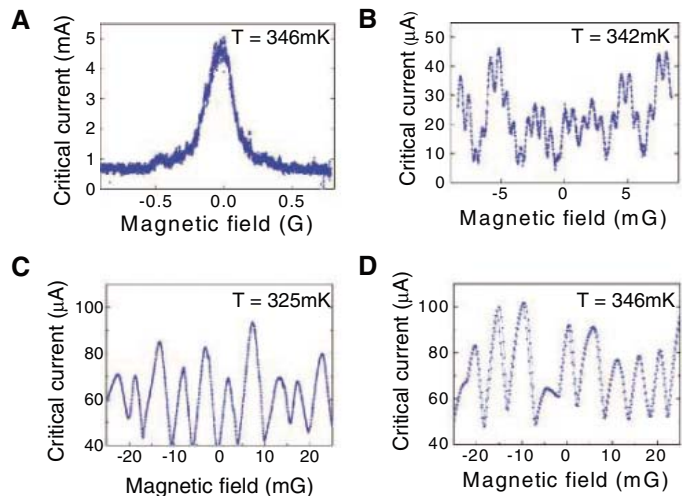
where $J_c(y)$ is the critical current as a function of position along the face of the crystal, and $\Phi_0 = h/2e = 20.7$ G·µm^2 is the magnetic flux quantum. Maximizing this expression with respect to the phase difference ϕ_0 gives the critical current $I_c(B)$.

In the simplest situation, only one order parameter domain would form throughout the entire single crystal. In this case, the order parameter phase is uniform across any junction on a single face. If the critical current density J_c is uniform and small enough that any magnetic fields generated by the tunneling currents can be neglected (the so-called short junction limit), we would expect a Fraunhofer diffraction pattern described by

$$I_c(\Phi) = J_c A \frac{\sin(\pi\Phi/\Phi_0)}{\pi\Phi/\Phi_0} \quad (2)$$

where $A = wt$ is the effective junction magnetic area, and $\Phi = BA$ is the total magnetic flux threading it. Deviations from this pattern can arise from nonuniformity of the critical current density, interface roughness, or inhomogeneity in the applied magnetic field, including that induced by magnetic vortices trapped near the junction. Faceted interfaces cause tunneling at angles that deviate from the intended direction on parts of the junctions, leading to phase interference and asymmetry in the diffraction

pattern. For an order parameter phase that varies continuously with tunneling angle, the amount of interference is relatively small and induces only slight quantitative changes in the diffraction pattern.

However, we would not expect this simple case to apply because domains can nucleate in a chiral system (26, 27). The order parameter for system with chiral symmetry winds from 0 to 2π in k-space and the two winding directions, clockwise and counterclockwise, are degenerate in energy. Moreover, as SRO has a tetragonal crystal structure, the a and b crystal axes are also equivalent. Consequently, four degenerate order parameters can exist: $p_x + ip_y$, $p_x - ip_y$, $p_y + ip_x$, and $p_y - ip_x$. Although the last two forms are topologically equivalent to the first two, a phase-sensitive experiment can differentiate between them: The phase difference between $p_x + ip_y$ and $p_y - ip_x$ for a given tunneling direction is not zero. The superconducting condensation energy is the same in any of these states, but there is an energy cost associated with having a domain wall between regions with different order parameters. This cost is essentially the Josephson coupling energy of the interface, which depends on the critical current density and the relative order parameter phase difference. For this reason, superconducting systems do not usually form order parameter domains. The best example is that of YBCO, a superconductor with $d_{x^2-y^2}$ symmetry characterized by a sign change between orthogonal directions. SQUID interferometry experiments on YBCO (21) have verified that the lobes of a single sign align throughout single crystals and polycrystalline thin films, even in the presence of twinning induced by the orthorhombic crystal structure. This demonstrates that maintaining a single order parameter across twin boundaries is energetically favorable to locking the order parameter locally onto the crystal axes and sustaining a domain wall. However, in SRO the chirality of the material (i.e., the winding of the phase) provides the energy term that tips the balance in favor of domain formation. The order parameter phase gradient is associated with spontaneously generated supercurrents around domain peripheries, and these currents create energetically costly magnetic fields. The situation is analogous to ferromagnetic materials that reduce the energy cost associated with large magnetic moments by breaking up into domains magnetized in different directions. Here, chiral superconductors reduce the field energy associated with chiral currents by forming domains of opposite chirality. In both cases, the ultimate domain structure is a complicated competition among field energies, domain wall energies, surface pinning, nonuniformities, random magnetic fields and defects, and domain nucleation and dynamics during cooling. We make no attempt here to produce an accurate model for domain formation, but rather describe the effects of a domain structure and present the experimental evidence that domains do occur in SRO.

Domain structure. In a crystal with lattice vectors aligned with the x and y directions, the possible domains are of the form $p_x + ip_y$, $p_x - ip_y$, $p_y + ip_x$, and $p_y - ip_x$. Separating these, two distinct types of chiral domain walls can form: (i) parallel domain walls, in which the real parts of the order parameter align but the chirality is reversed (Fig. 4A), and (ii) perpendicular domains, in which the real part of the order parameter changes by 90° and the chirality is reversed (Fig. 5A). Parallel domains are truly degenerate, whereas the degeneracy of perpendicular domains assumes interchangeability between the a and b crystal axes and could potentially be lifted by shape anisotropy, symmetry breaking at the surface, or crystal defects. In general, both types of domain walls can nucleate in a single crystal. However, it is useful to consider the diffraction patterns expected for each type of domain wall formation separately and com-

Fig. 3. (**A** to **C**) Diffraction patterns with different colors indicating sweep directions as shown by the arrows. (**A**) Hysteretic pattern. (**B**) Abrupt switches in the critical current. (**C**) "Telegraph" noise. (**D**) Switching noise in the voltage of a junction biased at a constant current greater than the critical current. The measurement is taken at zero field, but the noise appears only after a field sweep cycle.
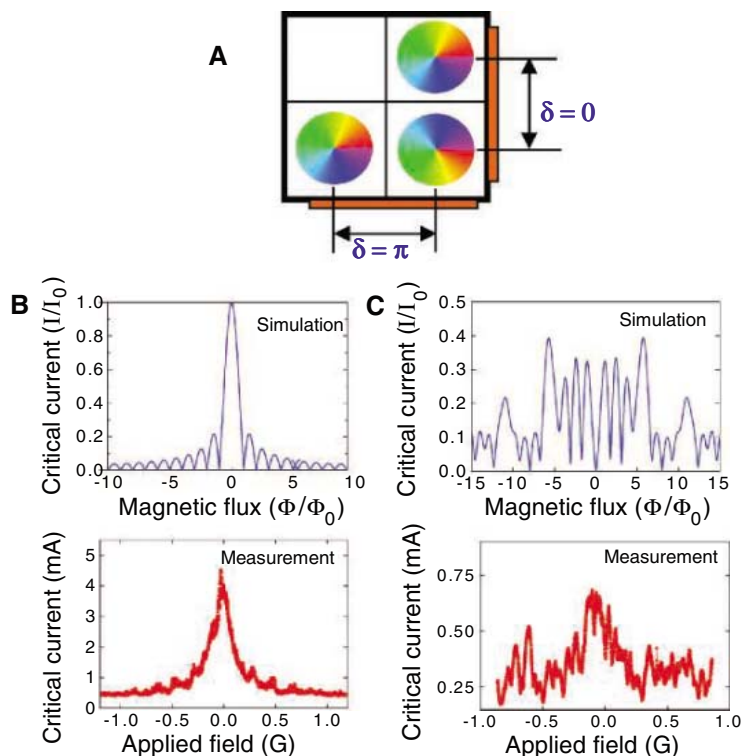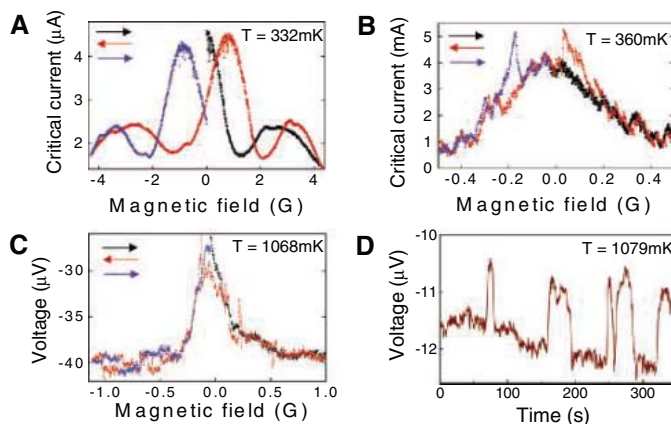
Fig. 4. (**A**) Graphical representation of an SRO crystal with parallel chiral domains showing the order parameter phase winding in opposite directions. The phase difference between domains, δ, is zero in one tunneling direction and π on the orthogonal face. (**B** and **C**) Computer simulations of the diffraction patterns for junctions on orthogonal crystal faces with 10 parallel domains of random size, compared with measurements on those junctions.

pare them to the experimentally obtained diffraction patterns.

If there are only parallel chiral domain walls separating regions of the form $p_x + ip_y$ and $p_x - ip_y$, all domains terminating on the x-face of the crystal have the same phase and a Fraunhofer diffraction pattern is expected. In contrast, on the orthogonal y-faces of the crystal, the $p_x + ip_y$ and $p_x - ip_y$ domains differ by a phase of π because the order parameter vector rotates by $\pi/2$ in opposite directions in each domain. This results in a diffraction pattern that reflects the alternating directions of the tunneling current, whose key characteristics are symmetry with respect to magnetic field polarity, a complicated modulation pattern that characterizes the domain structure, and generally a maximum critical current at a finite magnitude of applied magnetic field. Such patterns are well known in 45°-asymmetric grain boundary junctions in d-wave high-temperature superconducting cuprates (25). In other directions, the diffraction pattern exhibits polarity asymmetry, a direct indication of the broken time-reversal symmetry inherent in the complex order parameter superconductor. In Fig. 4, B and C, we present computer simulations of diffraction patterns expected in different directions for a random spatial distribution of 10 parallel chiral domains. The patterns are calculated from Eq. 1 using a critical current density $J_c(y)$ that characterizes the distribution of chiral domains. The details of the pattern are specific to the random domain configuration chosen for the calculation, but the qualitative features, including the striking differences in the shape and maximum critical current, remain the same.

We measured diffraction patterns consistent with this picture in about half of our samples. Figure 4, B and C, shows examples of these measurements in orthogonal directions in the crystals. The tunneling into one face exhibits a near-Fraunhofer shape with a large critical current near zero field, whereas the critical current in the orthogonal direction is smaller by an order of magnitude and shows a strongly modulated response. This is consistent with domains separated only by parallel domain walls and is direct and compelling evidence for the existence of both p-wave symmetry and a complex order parameter. We also note that the patterns are not perfectly symmetric with respect to magnetic field polarity, which could result from tunneling faces imprecisely aligned with the crystalline axes, self-field effects, trapped vortices that impose a nonuniform contribution to the magnetic field, or the presence of perpendicular domain walls along the junction interface (see below). We note that the field range of the modulations in junctions with sign changes arising from parallel chiral domains gives information about the size of the domains. This is clear in the simulations

in Fig. 4C, in which the envelope of 10 large-scale oscillations of the critical current derives from the distribution of the 10 domains in the junction. Examining the modulation envelopes of all our data yields an estimation of average domain width of ~1 μm. This also sets the spatial scale on which magnetic fields generated by the chiral domain structure could be detected, perhaps explaining why magnetic imaging experiments that typically use sensors of dimensions 5 to 10 μm have not detected them yet (16).

Not all of our measurements show such a clear signature of the complex (broken time-reversal) symmetry. Some samples show complicated modulations and magnetic field polarity asymmetry on both orthogonal crystal faces. This is consistent with the formation of perpendicular chiral domain walls separating regions with orthogonal alignment of the real part of the order parameter. Such domains give phase changes of $\pm\pi/2$ along the junctions on all crystal faces, so that the corresponding diffraction patterns exhibit polarity asymmetry and complicated structure. An example for 10 domains of random sizes with perpendicular chiral domains is shown in Fig. 5, B and C, for the same crystal faces as in Fig. 4. The predicted patterns qualitatively resemble measurements taken in many crystals, such as the examples

shown in Fig. 5, B and C. We have not attempted to make an accurate fit of the observed diffraction patterns, which is complicated by the spatial structure of the domains and their complex phase distribution.

One of the most appealing features of the chiral domain picture is the compelling explanation it provides for the observed hysteresis and switching noise. Because of the Josephson phase interference within the junction, the critical current can be strongly affected by reversing the chirality of a single domain, reorienting the real part of a domain, or moving a domain wall, with the last possibility the most likely. This is demonstrated in Fig. 6A, in which we compare the diffraction pattern for a junction with 10 parallel chiral domains to one for which a single domain wall is slightly displaced. The patterns are quantitatively similar (Fig. 6B), but the critical current at any applied magnetic field value is noticeably changed (Fig. 6C). Reversing the chirality of a single domain has a similar effect. Thus, abrupt switches in the critical current can arise if the domain orientations or domain wall locations change. These can be thermally activated, giving rise to the telegraph switching noise at a fixed magnetic field.

An applied magnetic field can also induce transitions between chiral domain configura-
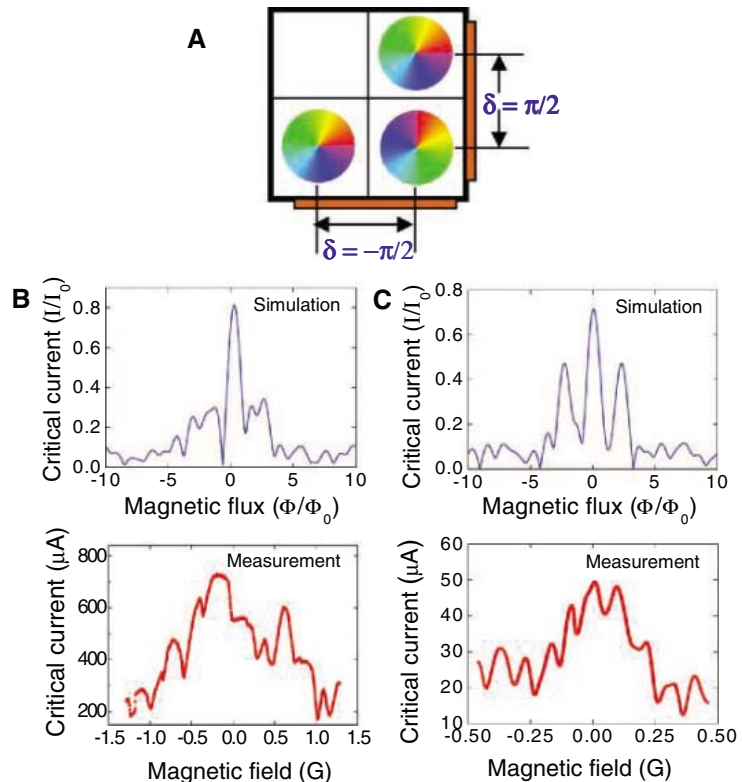
Fig. 5. (**A**) Graphical representation of an SRO crystal with perpendicular chiral domains showing the order parameter phase winding in opposite directions. The phase difference between domains, δ, is $\pi/2$ in one tunneling direction and $-\pi/2$ on the orthogonal face. (**B** and **C**) Computer simulations of the diffraction patterns for junctions on orthogonal crystal faces with 10 parallel domains of random size, compared with measurements on those junctions.

tions. Because magnetic field couples to the chiral order parameter state, an applied magnetic field lifts the degeneracy between chiral domains, causing one of the chiralities to be favored over the other. Hence, the field will cause domain walls to move to enlarge the favored domains. In practice, the domain walls may not move freely because of pinning at defects in the crystal structure, impurities, or regions of weakened superconductivity. When a magnetic field is applied to the sample, the force on the domain walls causes them to move only if it exceeds the domain pinning potential. Once unpinned, the domain walls can either move smoothly or jump from pinning site to pinning site with increasing field, depending on the distribution of pinning sites in the course of motion. Because the domain structure can change as the field is swept, the magnetic field modulations might not correspond to a single domain configuration but instead can be a compilation of many. When the magnetic field is ramped up and then back down, the junction may end up in a distinctly different domain configuration, leading to hysteresis.

A key test of this picture is to determine whether the chiral domains can be aligned by cooling in a magnetic field that favors a particular chiral state. We have done measurements indicating that cooling in even small fields (<1 mG) can enhance the zero-field critical current substantially (by up to a factor of 2) and make the diffraction pattern more Fraunhofer-like. We note that the field scale over which we can explore this effect is very restricted because larger fields induce magnetic vortex entry and trapping in the vicinity of the junctions, creating

local inhomoge)neous fields that modify the diffraction pat)terns. Nonetheless, we do find evidence for coupling of a magnetic field to the domain structure, constituting strong support for chiral symmetry.

We have also considered whether vortex entry and motion could explain all of our data, as this phenomenon shares many of the same properties with domain dynamics: Vortices can distort the diffraction pattern, induce field asymmetry, and move in and out of the junctions. One important difference is that domains are intrinsic to the system and should always be expected to form, whereas vortices arise from external conditions during cooldown so that careful magnetic shielding together with slow cooling should considerably lower their probability of occurrence. To monitor this, we measured each sample after thermal cycling between 5 and 15 times to above the transition temperature. The results showed consistency from one cycle to another, aside from small variations in critical current magnitude and period of modulation and, in some cases, the appearance and disappearance of hysteresis. Also, the dynamics were found to be highly reproducible, which in our experience is not the case for vortices. Another difference is their behavior in a bipolar field sweep. For accidentally trapped isolated vortices, field-induced events are not symmetric for positive and negative field because the vortex has a specific polarity. In the case of domains, different polarities favor different chiralities and both field directions should induce dynamics at the same scale. Data such as those in Fig. 3B are hard to explain with vortices because the switches occur at field values close in magnitude for both polarities. Thus, we are confident that vortices cannot account for our results, but we caution that this effect must always be carefully considered in interpreting Josephson interferometry data.

Concluding remarks. Our results constitute direct evidence for the presence of order parameter domains and domain wall motion in Sr_2RuO_4 through the anomalous behavior of diffraction patterns of Josephson junctions on single faces of the crystal. The result is based on the study of critical current diffraction patterns from 28 Sr_2RuO_4/Cu/Pb junctions, each of which demonstrated some or all of the described unusual features, including complicated modulations characteristic of interference between regions with different phase and size, distinctly different behavior in different crystals and even in different junctions on the same crystal, asymmetry with respect to field direction, abrupt jumps in the critical current, and telegraph switching noise. We propose two families of domains to interpret the data: parallel chiral domains in which only the direction of the phase winding changes, and perpendicular chiral domains in which the chirality and the orientation of the

real part of the order parameter both change. The strikingly different diffraction patterns for junctions on orthogonal faces of the same single crystal confirm both the odd symmetry and the broken time-reversal symmetry of Sr_2RuO_4.

Note added in proof: Xia *et al.* (*28*) have observed evidence for broken time-reversal symmetry in the superconducting state of Sr_2RuO_4 by Kerr effect measurements.

References and Notes

1. Y. Maeno *et al.*, *Nature* **372**, 532 (1994).
2. A. P. Mackenzie, Y. Maeno, *Rev. Mod. Phys.* **75**, 657 (2003).
3. T. M. Rice, M. Sigrist, *J. Phys. Condens. Matter* **7**, L643 (1995).
4. A. P. Mackenzie *et al.*, *Phys. Rev. Lett.* **80**, 161 (1998).
5. K. Ishida *et al.*, *Nature* **396**, 658 (1998).
6. G. M. Luke *et al.*, *Nature* **394**, 558 (1998).
7. I. Bonalde *et al.*, *Phys. Rev. Lett.* **85**, 4775 (2000).
8. S. Nishizaki, Y. Maeno, Z. Q. Mao, *J. Low Temp. Phys.* **117**, 1581 (1999).
9. M. A. Tanatar, S. Nagai, Z. Q. Mao, Y. Maeno, T. Ishiguro, *Phys. Rev. B* **63**, 064505 (2001).
10. K. Ishida *et al.*, *Phys. Rev. Lett.* **84**, 5387 (2000).
11. M. Sigrist, K. Ueda, *Rev. Mod. Phys.* **63**, 239 (1991).
12. M. Sigrist, T. M. Rice, K. Ueda, *Phys. Rev. Lett.* **63**, 1727 (1989).
13. M. Matsumoto, M. Sigrist, *J. Phys. Soc. Jpn.* **68**, 994 (1999).
14. M. Sigrist, D. Agterberg, *Prog. Theor. Phys.* **102**, 965 (1999).
15. A. C. Mota, E. Dumont, A. Amann, Y. Maeno, *Physica B (Amsterdam)* **259**, 934 (1999).
16. P. G. Björnsson, Y. Maeno, M. E. Huber, K. A. Moler, *Phys. Rev. B* **72**, 012504 (2005).
17. D. A. Wollman, D. J. Van Harlingen, W. C. Lee, D. M. Ginsberg, A. J. Leggett, *Phys. Rev. Lett.* **71**, 2134 (1993).
18. V. B. Geshkenbein, A. I. Larkin, A. Barone, *Phys. Rev. B* **36**, 235 (1987).
19. A. J. Leggett, *Philos. Mag. B* **74**, 509 (1996).
20. K. D. Nelson, Z. Q. Mao, Y. Maeno, Y. Liu, *Science* **306**, 1151 (2004).
21. D. J. Van Harlingen, *Rev. Mod. Phys.* **67**, 515 (1995).
22. Z. Q. Mao, Y. Maeno, H. Fukazawa, *Mater. Res. Bull.* **35**, 1813 (2000).
23. See supporting material on *Science* Online.
24. H. Hilgenkamp, J. Mannhart, *Rev. Mod. Phys.* **74**, 485 (2002).
25. W. K. Neils, D. J. Van Harlingen, *Phys. Rev. Lett.* **88**, 047001 (2002).
26. G. E. Volovik, L. P. Gor'kov, *JETP Lett.* **39**, 674 (1984).
27. G. E. Volovik, L. P. Gor'kov, *Sov. Phys. JETP* **61**, 843 (1985).
28. J. Xia *et al.*, *Phys. Rev. Lett.* **97**, 167002 (2006).
29. We thank Z. Mao and H. Yaguchi for preparation of the crystals used in this experiment, and D. Agterberg, M. Sigrist, and Y. Liu for useful discussions. Supported by the NSF grant DMR-01-07253; Department of Energy, Office of Basic Energy Sciences, grant DEFG02-91-ER45439 through the Frederick Seitz Materials Research Laboratory at the University of Illinois at Urbana-Champaign; the Japan Society for the Promotion of Science; and the Japan Ministry of Education, Culture, Sports, Science, and Technology.

Fig. 6. (**A**) Configurations A and B represent chiral domain structures that differ by the displacement of one parallel domain wall. The up and down arrows indicate the chirality of each domain. (**B**) Simulated critical current diffraction patterns for domain configurations A and B. (**C**) Change in critical current for the domain wall shift as a function of applied magnetic flux through the junction.

A Post-Perovskite Lens and *D″* Heat Flux Beneath the Central Pacific

Thorne Lay,[1]* John Hernlund,[2] Edward J. Garnero,[3] Michael S. Thorne[4]

Temperature gradients in a low-shear-velocity province in the lowermost mantle (*D″* region) beneath the central Pacific Ocean were inferred from the observation of a rapid *S*-wave velocity increase overlying a rapid decrease. These paired seismic discontinuities are attributed to a phase change from perovskite to post-perovskite and then back to perovskite as the temperature increases with depth. Iron enrichment could explain the occurrence of post-perovskite several hundred kilometers above the core-mantle boundary in this warm, chemically distinct province. The double phase-boundary crossing directly constrains the lowermost mantle temperature gradients. Assuming a standard but unconstrained choice of thermal conductivity, the regional core-mantle boundary heat flux (~85 ± 25 milliwatts per square meter), comparable to the average at Earth's surface, was estimated, along with a lower bound on global core-mantle boundary heat flow in the range of 13 ± 4 terawatts. Mapped velocity-contrast variations indicate that the lens of post-perovskite minerals thins and vanishes over 1000 kilometers laterally toward the margin of the chemical distinct region as a result of a ~500-kelvin temperature increase.

Heat transfer across Earth's core-mantle boundary (CMB) plays a central role in powering the core's magnetic-field–generating geodynamo and the configuration of mantle convection. Primary constraints on deep Earth temperatures are provided by the interpretation of seismologically detected velocity discontinuities as phase transitions, in which the associated pressures and temperatures can be experimentally and theoretically determined. Phase transitions that account for seismic discontinuities near 410- and 660-km depths and at the inner core–outer core boundary near 5149 km depth provide the few absolute temperature constraints available for the deep interior. There are large (±500 K) uncertainties in extrapolations along adiabats to the CMB at 2891 km depth (*1*). Mineral physics experiments have recently shown that a phase transition occurs in the primary mineral of the lower mantle, $(Mg,Fe)SiO_3$ perovskite (Pv), yielding a post-perovskite (pPv) polymorph (*2, 3*) at pressure and temperature (*P-T*) conditions close to those expected for a seismic velocity discontinuity observed several hundred kilometers above the CMB (*4*). Associating the phase transition with the discontinuity provides direct constraint on absolute temperature in the lowermost mantle, indicating ~2500 K at 2700 km depth (125 GPa) (*2*), but there must be substantial lateral temperature variations.

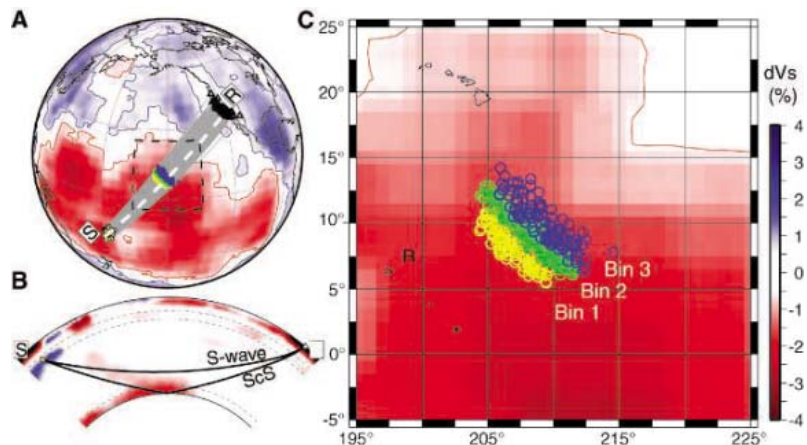The Pv-pPv phase transition is expected to produce a 2 to 4% *S*-wave velocity increase, little change in *P*-wave velocity, and an ~1 to 2% increase in density, which are generally compatible with seismic observations (*2, 3, 5–7*). Experimental determinations of the Clapeyron *P-T* slope Γ for the Pv-pPv phase transition range from 5 to 13 MPa/K (*8, 9*), and theoretical estimates fall within this range (*3, 10*). The phase transition pressure may decrease with increasing bulk FeO content, although the magnitude of this effect is debated (*8–13*), and there is uncertainty in the partitioning coefficients for Fe, which might be influenced by a high- to low-spin transition in Fe^{2+} (*14*). The presence of Al_2O_3 appears to have an opposite pressure effect to that of FeO and may broaden the two-phase region, affecting the seismic reflectivity (*15–18*).

The large positive Γ of the Pv-pPv phase change could potentially allow a rapid increase in temperature at greater depths to reverse the transformation. A strong temperature increase is expected in a thermal boundary layer at the base of the mantle (*1*), and the possibility of a second intersection of the geotherm with the phase boundary has been proposed (*19*). A shear velocity increase overlying a decrease may thus exist in the *D″* region; determining the discontinuity's depths would give two absolute temperature estimates and a temperature gradient based on the phase change *P-T* behavior. Initial investigations relevant to this question (*20, 21*) are subject to other interpretations (*22*). A velocity reduction is intrinsically more difficult to detect than a velocity increase (*23*) and requires waveform stacking of many signals. We conducted a detailed *S*-wave stacking-and-modeling analysis, resolving velocity structures that were consistent with local geotherms having a double intersection with the Pv-pPv phase boundary under the central Pacific. We obtained robust estimates of thermal gradients near the CMB.

Seismic data analysis. We analyzed 736 transverse horizontal-component *S*-wave seismograms from 46 intermediate- and deep-focus Tonga-Fiji earthquakes recorded at broadband seismic stations in California (Fig. 1). We added ~300 seismograms to an earlier data set that sampled the lowermost mantle beneath the central Pacific Ocean (*24, 25*) and used one-dimensional (1D) and 2.5D (axisymmetric spherical) modeling procedures to resolve the regional structure. Our *S* waves traversed a large low-shear-velocity province (LLSVP) imaged by global seismic tomography (*26*) (Fig. 1). Tomography models indicated that the CMB reflected phase (*ScS*) paths sample within the northern margin of the LLSVP, southeast of the Hawaiian hot spot (figs. S1 and S2).

The data have variable waveforms, with amplitude and timing fluctuations over small spatial apertures (figs. S3 to S5), which is con-

[1]Department of Earth and Planetary Sciences, University of California, Santa Cruz, CA 95064, USA. [2]Institut de Physique du Globe de Paris, 75252 Paris, France. [3]School of Earth and Space Exploration, Arizona State University, Tempe, AZ 85287–1404, USA. [4]Arctic Region Supercomputing Center, University of Alaska, Fairbanks, AK 99775, USA.

*To whom correspondence should be addressed. E-mail: thorne@pmc.ucsc.edu

Fig. 1. (**A**) Global map indicating sources (circles near S) and receivers (triangles near R), with ray paths and tomographic shear velocity variations in the *D″* region (*27*). (**B**) Cross section from S to R [dashed white line in (A)] showing *S* and *ScS* ray paths at 79.9° epicentral distance superimposed on the tomography model, where velocity perturbations less than 0.5% are whited out. (**C**) Enlargement of the dashed box in (A), indicating the *ScS* CMB reflection points for the data in bin 1 (yellow), bin 2 (green), and bin 3 (blue). dVs, variation in shear velocity relative to the global average.

sistent with prior work that proposed a laterally varying D'' discontinuity at an average height near 230 km above the CMB in this region (4, 27). Strong lateral gradients in seismic velocity structure are observed in nearby regions of the Pacific LLSVP (28), which suggest an abrupt northern margin similar to its southern margin (29) and the African LLSVP margins (30). In contrast to the southwest-to-northeast (SW-to-NE) regional trend from lower to higher S-wave velocities found in tomographic models, the ScS anomalies involve increasingly delayed arrivals from SW to NE over the small-scale region sampled by the data, along with a gradient in anisotropy (31). Our large data set agrees with previous analyses of various data attributes across the study area, which established that the primary variations are

SW-to-NE, parallel to the Tonga-to-California ray paths.

Source complexity variations were accounted for by deconvolving the signals by averaged source wavelets for each event (fig. S3), which allowed data from different events to be combined. The deconvolved signals had bandwidth from 0.01 to 0.3 Hz. The data were subdivided into three parallel bins, separating ScS CMB reflection points at varying distances from California (Fig. 1). Double-array stacking of all station-receiver combinations sampling each bin characterized the reflectivity relative to height above the CMB. We normalized and aligned the seismograms so that ScS had unity reflectivity at the CMB (figs. S6 to S9). Each bin had several positive and negative peaks in reflectivity (Fig. 2 and fig. S7). Reflectivity more than 400 km

above the CMB could not be confidently constrained as a result of contamination by the direct S phase, which turns at shallower depths.

The data stacks were first modeled with synthetics for localized 1D-layered structures to characterize the basic attributes of the quasi-2D structure. For each bin, a four-layer model, motivated by previous studies of the region (24, 25, 27), was developed to match salient attributes of the data stacks. The synthetics were processed identically to the data, accounting for bandwidth and deconvolution side-lobe effects (figs. S3 to S5).

The resulting models (Fig. 2) indicated a positive velocity increase (reflector U) at depths increasing from 2546 km (bin 1) to 2655 km (bin 2) to 2730 km (bin 3), with shear velocity increases of 1.1, 0.6, and 0.7%, respectively. This feature is similar to the 2 to 3% shear velocity increase detected below circum-Pacific regions commonly associated with the Pv-pPv transition. A small (–0.5 to –0.7%) velocity discontinuity (reflector A) was modeled ~135 to 70 km above reflector U in bins 2 and 3. Although the data did not resolve reflector A in bin 1 because of S-wave interference, a similar structure was assumed to be present with a very small velocity decrease. This feature has no counterpart in models for circum-Pacific regions, and we associated it with the top of the LLSVP in each bin. Below the shear velocity increase, two abrupt velocity decreases were modeled: The shallower decrease (reflector L) was a weak –0.2% jump at 2805 km depth in bin 1, a –0.6% jump at 2800 km depth in bin 2, and a –0.9% jump at 2788 km depth in bin 3; and the deeper decrease (reflector B) was a –4.0% drop at 2874 km in bin 1, a –1.1% drop at 2859 km depth in bin 2, and a –0.6% drop at 2847 km in bin 3. The reflector L velocity decrease was the most unexpected feature in the structures. It is generally consistent with the hypothesis of a second intersection of the geotherm with the pPv phase boundary, involving the conversion of pPv back to Pv, effectively forming a lens of pPv material in D'' above the CMB (Fig. 2). The discontinuity closest to the CMB may be associated with the top of a weak ultra-low-velocity zone (ULVZ), a thin low-velocity layer extensively observed just above the CMB (4, 25, 31). The predicted arrivals for these discontinuities are small (fig. S10); stacking is required to observe them clearly and to suppress scatter and the effects of localized lateral variations.

Our modeling includes the use of ScS and S separately as reference phases, with simultaneous modeling of both ensuring reliable velocity structures (fig. S8). The average S-wave velocity over the lowermost 350 km of the mantle decreases from bin 1 to bin 3 by an amount consistent with the lateral 3- to 4-s increase in ScS travel time delays (31), and this aspect of the data stacks is well modeled by our structures (fig. S8).

Uncertainties in the size of velocity contrasts and depths are ~20% and ±5 km, respectively,
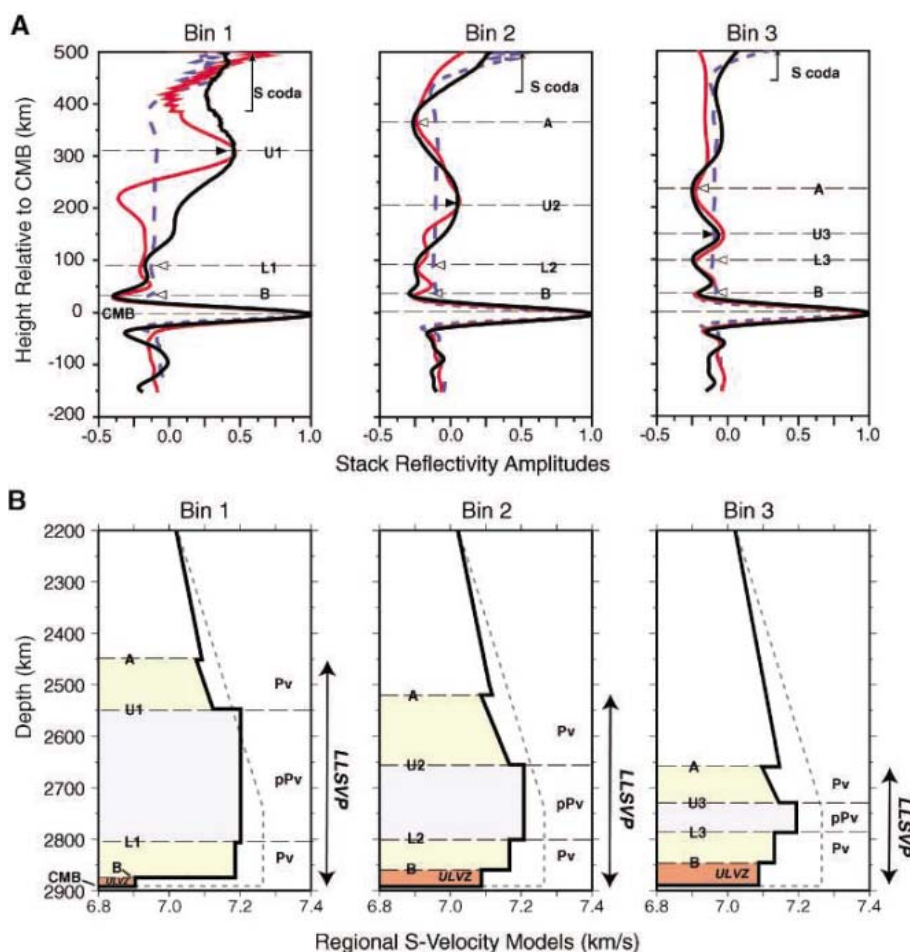
Fig. 2. (**A**) Double-array stacks of horizontally polarized shear wave reflectivity amplitude as a function of height relative to the CMB, normalized to the ScS reflection from the CMB. The numbers of seismograms stacked in each bin are 275 (bin 1), 319 (bin 2), and 142 (bin 3). (**B**) Inferred shear velocity models (solid black lines) and reference model Preliminary Reference Earth Model (PREM) (dashed lines). Stacks of data (solid black lines), synthetics for the inferred layered velocity models (red lines), and synthetics for PREM (dashed blue lines) are shown in (A). The shallow portions of the stacks contaminated by S-coda energy are indicated in (A) with the brackets. Black arrowheads indicate reflections from velocity increases; white arrowheads indicate reflections from velocity decreases. In (A) and (B), the layered structures have reflecting velocity discontinuity boundaries labeled A, Ui (i indicates the bin number), Li, and B. The lowermost layer is designated a ULVZ. The high-velocity layer between Ui and Li is interpreted as a layer of pPv bounded by phase transitions from/to Pv. The region below discontinuity A is designated the LLSVP.

for 1D models, but true uncertainties may be larger in the presence of lateral variations. Modeling with 2.5D finite-difference calculations confirmed that the depth estimates were realistic, but the velocity contrasts tended to be 50 to 100% higher in laterally varying models (figs. S11 and 12) as a result of the lateral termination of the reflecting interfaces. Unresolved small-scale heterogeneity can contribute to amplitude variability, affecting the inferred velocity contrasts (fig. S13).

The S-wave ray paths grazed the lowermost mantle (Fig. 1B). The three data bins spanned only ~4° epicentral distance (240 km at the CMB) along the propagation direction, but the length scale over which the wave fields interact with the structure was several times larger, resulting from the spatial extent of the effective Fresnel zone (300 to 500 km) for the 3- to 4-s dominant periods of the data. 2.5D axisymmetric finite-difference modeling demonstrated that the spatial extent controlling signals in each bin was ~5° epicentral distance; the entire data set sampled structure over about a 15°-wide region in epicentral distance (fig. S11). Energy in the data stacks between reflectors U and L in bins 1 and 2 not reproduced by 1D modeling was due to lateral sampling of adjacent bins. Although the precise structure was not definitively constrained, the basic layering and associated reflectivity are well characterized by the models in Fig. 2, particularly the discontinuity depths, which play a critical role in the following discussion because they provide the connection to pressure.

Thermal models. We focused on the depths of the paired velocity increase and decrease in each bin (reflectors U and L), which we interpreted as double crossings of the Pv-pPv phase boundary. We considered thermal models with mid-mantle adiabats overlying a conductive thermal boundary layer of variable thickness parameterized by an error-function decrease from a peak temperature at the CMB. This choice of model parameterization is discussed in the supporting online material (SOM) text S1. The phase-boundary position in P-T space is not precisely known because of uncertainties in the effects of mixed phases, Fe and Al partitioning in the deep mantle minerals, and experimental error. The position of the phase boundary was parameterized by Γ [ranging from 8 to 13 MPa/K, which spans the range of recent estimates, including those for pyrolitic composition (8, 9, 32)] and $\Delta T_{CMB,pPv}$ [the (positive) temperature difference between the CMB temperature and the pPv phase-boundary temperature at the CMB, ranging from 100 to 400 K].

The seismic models provide three samples of upper and lower intersections with the phase boundary in a laterally varying thermal regime (as required to produce regional topography on the phase boundary). Reflector U varies systematically relative to reflector L as the geotherm changes spatially. The seismic discontinuity depths yield reasonable geotherm fits for the range of Γ and $\Delta T_{CMB,pPv}$ considered, enhancing the plausibility of the double-intersection models. Example geotherms for two choices of Γ and two choices of $\Delta T_{CMB,pPv}$ are shown in Fig. 3 (see also fig. S14). As Γ increases, the radial thermal gradients decrease and, as $\Delta T_{CMB,pPv}$ increases, the gradients increase. The corresponding boundary-layer thickness estimates needed to match seismic observations range from 150 to 400 km (fig. S15).

Estimating heat flux for a given thermal structure requires knowledge of lowermost mantle thermal conductivity K. We adopted the most commonly used estimate, $K = 10$ W/(m·K) (33), noting that this parameter has not been directly constrained and both higher and lower values have been advocated (uncertainty in K is discussed in SOM text S2). The suite of models that fit the data yields average heat flux estimates shown in Fig. 4 and depends directly on the assumed K. The lateral variation in temperature at the depth of reflector U in bin 2 is shown for each set of geotherms. The lateral variation in temperature between the bins is controlled by $\Delta T_{CMB,pPv}$. Fitting the data is difficult for $\Delta T_{CMB,pPv}$ values less than 100 K, whereas unrealistically high heat fluxes are predicted for values more than 300 K. The heat flux estimates, ranging from 60 to 110 mW/m², are on the order of Earth's average surface heat flux (~86 mW/m²) (34). Reducing the uncertainty of Γ and K will directly narrow the range of heat flux estimates.

The core's surface area is ~30% of Earth's surface area, so our result suggests that heat flow through the CMB may be a corresponding fraction of the 44 TW at the surface (34). Assuming that the study region is relatively warm, as indicated by the low S-wave velocities, we estimated a lower bound of 13 ± 4 TW for CMB heat flow for our choice of K. Sub-

Fig. 3. Examples of thermal model fits to the pairs of discontinuity positions for the three bins in Fig. 2, with corresponding labeling of the reflectors. Results for two values of Γ and $\Delta T_{CMB,pPv}$ are shown here, and additional examples are shown in fig. S14.
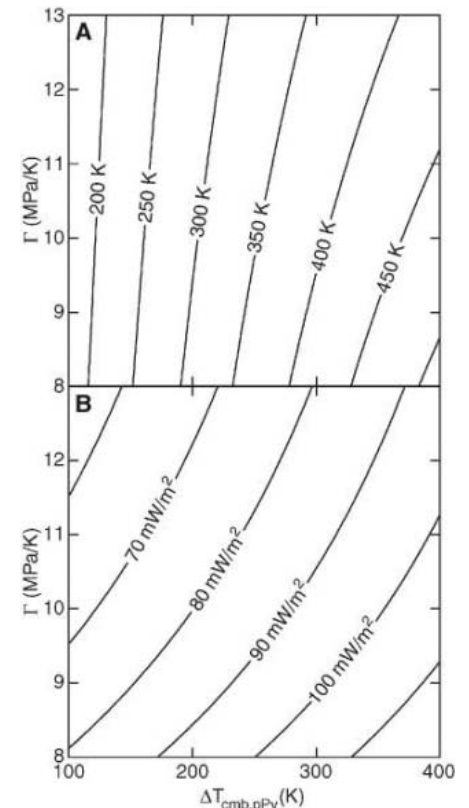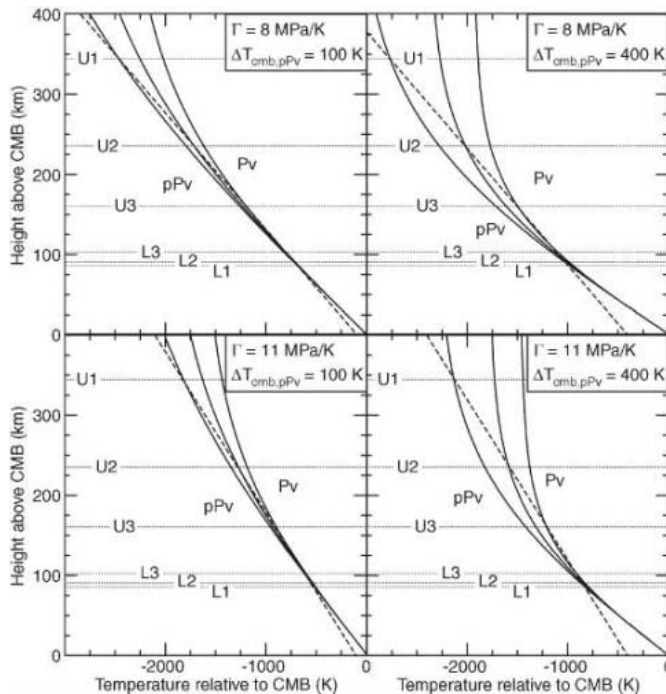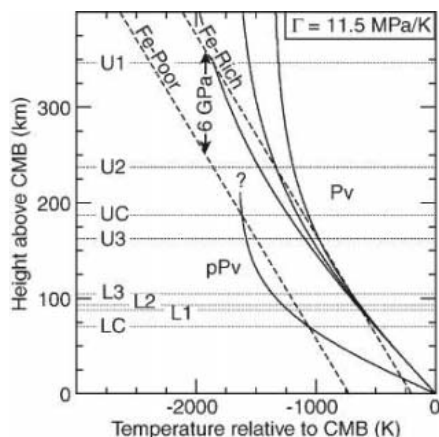

Fig. 4. Characteristics of thermal models fitting the seismic discontinuity data as functions of Γ and $\Delta T_{CMB,pPv}$. The lateral variation in temperature at the depth of the U2 discontinuity is shown at the top (**A**), and the average heat flux for the models is shown below (**B**).

stantially higher heat flux would be estimated if radiative K is high, whereas lower heat flux could result from acutely heterogeneous grain-boundary structures and interstitial impurities that impede phonon conductivity (SOM text S2). Modeling the discontinuity depths for individual bins gives very consistent results (fig. S16). Exploring the effects of the ±5-km uncertainties in the discontinuity depths indicates that the results are most sensitive to the reflector L depths.

The sensitivity to reflector L depths raises the issue of distortion of the phase boundary by dynamical instability. The layer of pPv minerals is expected to be denser (~1 to 2%) than the underlying Pv, and the latter is likely to have strong viscosity reduction resulting from the rapid increase in temperature in the thermal boundary layer. The lower edge of the pPv lens will thus tend to sink, heat up, and convert to Pv, establishing a dynamical equilibrium. This process is difficult to simulate, lacking constraints on the overall size and geometry of the pPv lens and on boundary-layer viscosity structure.

Another implication of these thermal models is that there must be horizontal conduction of substantial heat (on the order of 10 mW/m^2), given the temperature variations between bin models and the horizontal scale of ~1000 km sampled by the seismic waves. This lateral thermal gradient suggests dynamical flow with relatively hot upwelling material toward the northeast (near bin 3).

Chemical piles. We consider the foregoing analysis of thermal gradients under the central Pacific in a global context. The study area is near the northern edge of the LLSVP under the Pacific Ocean, far from recent subduction zones

(35), and is generally considered to be warm (relative to cooler circum-Pacific locations) because of the low shear velocities. Lacking a chemical effect, the Pv-pPv phase boundary should be deeper or absent in warm mantle (36). However, this region appears to be anomalously dense, possibly because of the presence of excess FeO (37, 38), favoring the notion of chemically distinct material swept into a large pile by larger-scale subduction-driven flow in the surrounding mantle. There may be alternate explanations for the density excess, with the accumulation of mid-ocean ridge basalt–enriched mantle being one possibility (39), but this suggestion still invokes a dense, chemically distinct pile of material. Numerical modeling indicates that a dense pile is likely to have an increase in temperature toward its edges as a result of boundary layer separation (40).

Circum-Pacific regions have D'' shear velocities that are 3 to 5% faster than under the central Pacific and stronger shear velocity discontinuities (4). It is widely inferred that the contrast in velocities is partly due to temperatures being 700 to 1200 K lower in the circum-Pacific because of the presence of cool downwellings and partly due to the compositional differences in the dense central Pacific chemical pile. A 10% molar increase of FeSiO$_3$ in pPv can reduce shear velocities by 2.6% (13), which is comparable to the effect of a 1000-K temperature increase at CMB pressure.

Comparing the structure of the double crossing of the Pv-pPv phase boundary in the central Pacific with structure in circum-Pacific regions permits a specific assessment of the effect of chemical variations on the phase boundary. The only circum-Pacific region with evidence for a double crossing is under the eastern Cocos Plate (41): A 1.7% shear velocity increase at 2704 km at the upper Cocos discontinuity (UC) is accompanied by a 1.7% decrease at 2821 km at the lower Cocos discontinuity (LC). The average shear velocity between these depths is 7.55 km/s, ~5% faster than in the pPv lens in the central Pacific. If we assume that the Cocos

Plate and central Pacific environments have the same Γ of 11.5 MPa/K (8) and a 700-K contrast in temperature, we can find a geotherm compatible with the Cocos region velocity discontinuity depths, UC and LC (Fig. 5).

This scenario requires a 6-GPa pressure shift of the phase boundary resulting from an effect such as higher FeO content of the LLSVP, which is consistent with some predictions (9, 11). A 10–mole percent increase in Fe is expected to give a 5- to 10-GPa reduction of the phase-boundary pressure (9). This additional Fe should broaden the phase transition loop, giving a velocity transition rather than a discontinuity and weakening the reflectivity (fig. S17). The velocity discontinuity also diminishes because of the greater reduction of shear velocity with added Fe for pPv (–0.26%/mol % Fe) than for Pv (–0.2%/mol % Fe) (13). For a 10% Fe–enriched region, the shear velocity contrast should be ~0.6% weaker than in a normal region, depending on Fe partitioning coefficients with other phases. The combined effects of added Fe and lateral temperature variations relative to circum-Pacific regions can thus account for the 5% shift of absolute shear velocity and the reduced velocity discontinuity. If the UC phase transition occurs in relatively Fe-depleted MgSiO$_3$ [resulting from the low-spin transition of Fe favoring partitioning into (Mg,Fe)O] at 2500 to 2600 K (2, 9), the CMB temperature for this scenario is ~4100 K.

Conclusions. Seismic reflectivity under the central Pacific is consistent with a laterally vanishing lens of pPv material within and near the margin of a chemically distinct pile (Fig. 6). The pile is probably undergoing internal flow, with shear coupling resulting in hot upwelling on the pile margins, giving a lateral increase in temperature that causes the pPv lens to laterally revert to Pv. The internal transition from horizontal to vertical flow near the edge of the pile can account for an observed gradient in shear wave anisotropy (31). The velocity decrease observed above the U horizon may correspond to the top of an Fe-rich pile. The deeper ULVZ feature

Fig. 5. Comparison of thermal models for the presumed Fe-rich central Pacific discontinuities and the presumed Fe-poor Cocos Plate region, with UC and LC indicating the paired discontinuity depths in the latter region. A common Γ is assumed, and a 700-K lateral temperature shift is imposed. The inferred shift of the phase boundary resulting from the postulated FeO enrichment of the pile is 6 GPa. ? indicates the uncertain position of the mid-mantle geotherm under the Cocos.

Fig. 6. Schematic of the study region, indicating the presence of a pPv lens in the LLSVP under the central Pacific, with colors indicating relative temperature (red is warmest, and blue is coolest). The dotted line indicates the boundaries of the chemically distinct pile. Dashed lines indicate the Pv-pPv phase boundary within the LLSVP and in surrounding mantle. The location of the bins in Fig. 2 is indicated below the pPv lens in the

LLSVP. Schematic ray paths for ScS and SdS (a reflection from the pPv phase boundary) are shown by long dashes. Arrows indicate pattern of mantle flow, and the blackened area indicates the position of the ULVZ. ??? indicates the uncertain nature of the velocity decrease at reflector A in Fig. 2. Internal convection of the pile concentrates hot material near its margin, producing the lateral gradient in temperature that causes the lens to thin laterally. Any pPv in surrounding mantle will thin and disappear toward the hot edge of the pile. Compositional differences cause the phase boundary to have similar depths in warm and cool regions.
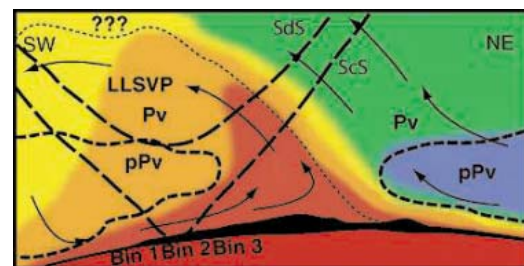
varies on the edge of the pile and is thicker and not as extreme in velocity reduction as observed in some regions (42). The S-velocity reductions are comparable to the P-velocity reductions (27) in this ULVZ. This finding indicates that little or no partial melt accumulated under this edge of the pile, whereas strong ULVZs with partial melting are found on other margins (43).

Thermal modeling gives direct determinations of thermal gradients for the CMB region. Regional heat flux into the base of the LLSVP is 85 ± 25 mW/m^2, close to average surface heat flux, for $K = 10$ W/(m·K). Global extrapolation suggests a lower bound on CMB heat flow of 13 ± 4 TW, subject to large uncertainty in K. These relatively high values favor the sequestration of heat-producing radiogenic elements in the core and a relatively young age for the inner core.

References and Notes

1. Q. Williams, in *The Core-Mantle Boundary*, M. Gurnis, M. E. Wysession, E. Knittle, B. A. Buffett, Eds. (American Geophysical Union, Washington, DC, 1998), pp. 73–81.
2. M. Murakami, K. Hirose, K. Kawamura, N. Sata, Y. Ohishi, *Science* **304**, 855 (2004).
3. A. R. Oganov, S. Ono, *Nature* **430**, 445 (2004).
4. T. Lay, E. J. Garnero, in *The State of the Planet, Frontiers and Challenges in Geophysics*, R. S. J. Sparks, C. J. Hawkesworth, Eds. (American Geophysical Union, Washington, DC, 2004), pp. 25–41.
5. J. Wookey, S. Stackhouse, J.-M. Kendall, J. Brodholt, G. D. Price, *Nature* **438**, 1004 (2005).
6. T. Iitaka, K. Hirose, K. Kawamura, M. Murakami, *Nature* **430**, 442 (2004).
7. T. Tsuchiya, J. Tsuchiya, K. Umemoto, R. M. Wetzcovitch, *Geophys. Res. Lett.* **31**, L14603 (2004).
8. K. Hirose, R. Sinmyo, N. Sata, Y. Ohishi, *Geophys. Res. Lett.* **33**, L01310 (2006).
9. S. Ono, A. R. Oganov, *Earth Planet. Sci. Lett.* **236**, 914 (2005).
10. T. Tsuchiya, J. Tsuchiya, K. Umemoto, R. M. Wentzcovitch, *Earth Planet. Sci. Lett.* **224**, 241 (2004).
11. W. L. Mao et al., *Proc. Natl. Acad. Sci. U.S.A.* **101**, 15867 (2004).
12. Y. Kobayashi et al., *Geophys. Res. Lett.* **32**, L19301 (2005).
13. S. Stackhouse, J. P. Brodholt, G. D. Price, *Geophys. Res. Lett.* **33**, L01304 (2006).
14. J.-F. Lin et al., *Nature* **436**, 377 (2005).
15. S. Akber-Knutson, G. Steinle-Neumann, P. D. Asimow, *Geophys. Res. Lett.* **32**, L14303 (2005).
16. R. Caracas, R. E. Cohen, *Geophys. Res. Lett.* **32**, L16310 (2005).
17. A. R. Oganov, S. Ono, *Proc. Natl. Acad. Sci. U.S.A.* **102**, 10828 (2005).
18. S. Tateno, K. Hirose, N. Sata, Y. Ohishi, *Geophys. Res. Lett.* **32**, L15306 (2005).
19. J. W. Hernlund, C. Thomas, P. J. Tackley, *Nature* **434**, 882 (2005).
20. C. Thomas, E. J. Garnero, T. Lay, *J. Geophys. Res.* **109**, B08307 (2004).
21. C. Thomas, J.-M. Kendall, J. Lowman, *Earth Planet. Sci. Lett.* **225**, 105 (2004).
22. A. Hutko, T. Lay, E. J. Garnero, J. Revenaugh, *Nature* **441**, 333 (2006).
23. C. Flores, T. Lay, *Geophys. Res. Lett.* **32**, L24305 (2005).
24. M. Avants, T. Lay, S. A. Russell, E. J. Garnero, *J. Geophys. Res.* **111**, B05305 (2006).
25. M. Avants, T. Lay, E. J. Garnero, *Geophys. Res. Lett.* **33**, L07314 (2006).
26. S. P. Grand, *Philos. Trans. R. Soc. London Ser. B* **360**, 475 (2002).
27. S. A. Russell, C. Reasoner, T. Lay, J. Revenaugh, *Geophys. Res. Lett.* **28**, 2281 (2001).
28. S.-N. Luo, S. Ni, D. V. Helmberger, *Earth Planet. Sci. Lett.* **189**, 155 (2001).
29. A. To, B. Romanowicz, Y. Capdeville, N. Takeuchi, *Earth Planet. Sci. Lett.* **233**, 137 (2005).
30. S. Ni, D. V. Helmberger, J. Tromp, *Geophys. J. Int.* **161**, 283 (2005).
31. S. A. Russell, T. Lay, E. J. Garnero, *J. Geophys. Res.* **104**, 13183 (1999).
32. K. Hirose, *Rev. Geophys.* **44**, RG3001 (2006).
33. F. Stacey, *Physics of the Earth* (Brookfield, Brisbane, Australia, ed. 3, 1992).
34. H. N. Pollack, S. J. Hurter, J. R. Johnson, *Rev. Geophys.* **31**, 267 (1993).
35. C. Lithgow-Bertelloni, M. A. Richards, *Rev. Geophys.* **36**, 27 (1998).
36. I. Sidorin, M. Gurnis, D. V. Helmberger, *Science* **286**, 1326 (1999).
37. J. Trampert, F. Deschamps, J. Resovsky, D. Yuen, *Science* **306**, 853 (2004).
38. M. Ishii, J. Tromp, *Science* **285**, 1231 (1999).
39. K. Hirose, N. Takafuji, N. Sata, Y. Ohishi, *Earth Planet. Sci. Lett.* **237**, 239 (2005).
40. A. K. McNamara, S. Zhong, *Nature* **437**, 1136 (2005).
41. D. Sun, T.-R. A. Song, D. Helmberger, *Geophys. Res. Lett.* **33**, L12S07 (2006).
42. S. Rost, E. J. Garnero, Q. Williams, M. Manga, *Nature* **435**, 666 (2005).
43. M. Thorne, E. J. Garnero, *J. Geophys. Res.* **109**, B08301 (2004).
44. We thank Q. Williams, K. Hirose, J. Brodholt, and the anonymous reviewers for helpful discussion and comments. We also thank H. Igel and G. Jahnke for help with the 2.5D SHaxi code. This work was supported in part by NSF under grants EAR-0125595, EAR-0453884, and EAR-0453944 and by the French Ministry of Research. Seismic data were obtained from the Incorporated Research Institutions for Seismology, the University of California at Berkeley, and California Institute of Technology/U.S. Geological Survey TRInet data centers. The Arctic Region Supercomputing Center at the University of Alaska at Fairbanks provided computer time.

REPORTS

Radar Imaging of Binary Near-Earth Asteroid (66391) 1999 KW4

Steven. J. Ostro,[1]* Jean-Luc Margot,[2] Lance A. M. Benner,[1] Jon D. Giorgini,[1] Daniel J. Scheeres,[3] Eugene G. Fahnestock,[3] Stephen B. Broschart,[3] Julie Bellerose,[3] Michael C. Nolan,[4] Christopher Magri,[5] Petr Pravec,[6] Petr Scheirich,[6] Randy Rose,[1] Raymond F. Jurgens,[1] Eric M. De Jong,[1] Shigeru Suzuki[1]

High-resolution radar images reveal near-Earth asteroid (66391) 1999 KW4 to be a binary system. The ~1.5-kilometer-diameter primary (Alpha) is an unconsolidated gravitational aggregate with a spin period ~2.8 hours, bulk density ~2 grams per cubic centimeter, porosity ~50%, and an oblate shape dominated by an equatorial ridge at the object's potential-energy minimum. The ~0.5-kilometer secondary (Beta) is elongated and probably is denser than Alpha. Its average orbit about Alpha is circular with a radius ~2.5 kilometers and period ~17.4 hours, and its average rotation is synchronous with the long axis pointed toward Alpha, but librational departures from that orientation are evident. Exotic physical and dynamical properties may be common among near-Earth binaries.

The swarm of near-Earth asteroids (NEAs) whose orbits pass close to that of Earth contains about a thousand objects with effective diameters as large as 1 km. Some 840 of these large NEAs have been discovered, and 28 of them have been found by radar and/or photometry to be binary systems (1, 2), which potentially can offer unique insights into NEA origin and evolution. However, detailed information about the physical configurations and dynamical states of NEA binaries is lacking. Here we present decameter-resolution radar images and a detailed model of one of the largest binary NEAs, (66391) 1999 KW4.

KW4 is one of several dozen NEAs whose orbits cross those of Earth, Venus, and Mercury. The asteroid's May 2001 approach to within 0.032 astronomical units (AUs) from Earth was its closest until 2036, and we conducted extended observations using the Goldstone X-band (8560-MHz, 3.5-cm) and Arecibo S-band (2380-MHz, 13-cm) radar systems (table S1). Goldstone is more fully steerable than Arecibo,

[1]Jet Propulsion Laboratory, California Institute of Technology, Pasadena, CA 91109–8099, USA. [2]Department of Astronomy, Space Sciences Building, Cornell University, Ithaca, NY 14853–6801, USA. [3]Department of Aerospace Engineering, University of Michigan, 1320 Beal Avenue, Ann Arbor, MI 48109–2140, USA. [4]Arecibo Observatory, HC3 Box 53995, Arecibo, PR 00612, USA. [5]University of Maine at Farmington, 173 High Street–Preble Hall, Farmington, ME 04938, USA. [6]Astronomical Institute, Academy of Sciences of the Czech Republic, Fričova 1, CZ-25165 Ondřejov, Czech Republic.

*To whom correspondence should be addressed. E-mail: ostro@reason.jpl.nasa.gov

so the Goldstone image sequences provided our longest continuous coverage (spanning 21 to 29 May, with image sequences up to 6.5 hours long), whereas the Arecibo echoes are an order of magnitude stronger. We also obtained weak, but useful, Arecibo echoes during the asteroid's 0.13-AU approach in June 2002. Our observations used periodic binary phase–coded waveforms to obtain images of the distribution of echo power in time delay (range) and Doppler frequency (line-of-sight velocity) (3, 4). Each of our 279 Arecibo images and 1075 Goldstone images reveal two distinctly separated components (we call the larger one Alpha and the smaller one Beta) and provide excellent orbital phase coverage (Fig. 1).

Alpha's echo bandwidths increased from 21 May to a maximum on 25 May and then decreased through 29 May, indicating that our view was closer to equatorial in the middle of the 9-day experiment. In the Arecibo single-date time exposures (Fig. 1), the 26 May image shows a trailing edge where the echo bandwidth reaches a maximum, but during the next 3 days, as our view migrates away from the equator, we see echoes from increasingly beyond that maximum-bandwidth delay, with the bandwidth of those echoes decreasing. This is the progression one would expect for a flattened (oblate) spheroidal target. Alpha's echo edge frequencies vary by only a few percent during the object's several-hour rotation, indicating a nearly circular pole-on silhouette. Analysis of the day-to-day sequence of Alpha's bandwidths constrains the ecliptic (longitude, latitude) of the object's pole direction to be within 20° of either (150°, 60°) or (330°, −60°). A search for sidereal periods P_A consistent with the reappearance times of feature orientations in images on successive days eliminates the first possibility and constrains P_A to be near 2.765 hours. In images showing the components with their trailing edges at similar ranges [and hence their centers of mass (COMs) presumably at approximately similar ranges], the 21 to 29 May variation in the bandwidth from the middle of Alpha to the middle of Beta increases, peaks, and decreases in a manner commensurate with the pattern for Alpha's bandwidth, suggesting that Alpha's equatorial plane and the system's orbit plane are approximately coplanar. When the components are aligned in Doppler frequency or range, Beta's signature is very symmetrical, with the approaching and receding limbs extending to similar delays. However, away from the conjunctions, Beta's limbs extend to distinctly different ranges, with the pattern as expected if the object is at least slightly elongated and if its longest dimension points toward Alpha (fig. S1).

Although a single radar image can be geometrically ambiguous, the delay-Doppler trajectory of any point on the surface of a rotating rigid body is unique if the radar is not in the target's equatorial plane. Therefore (5), with a time series of images providing enough echo
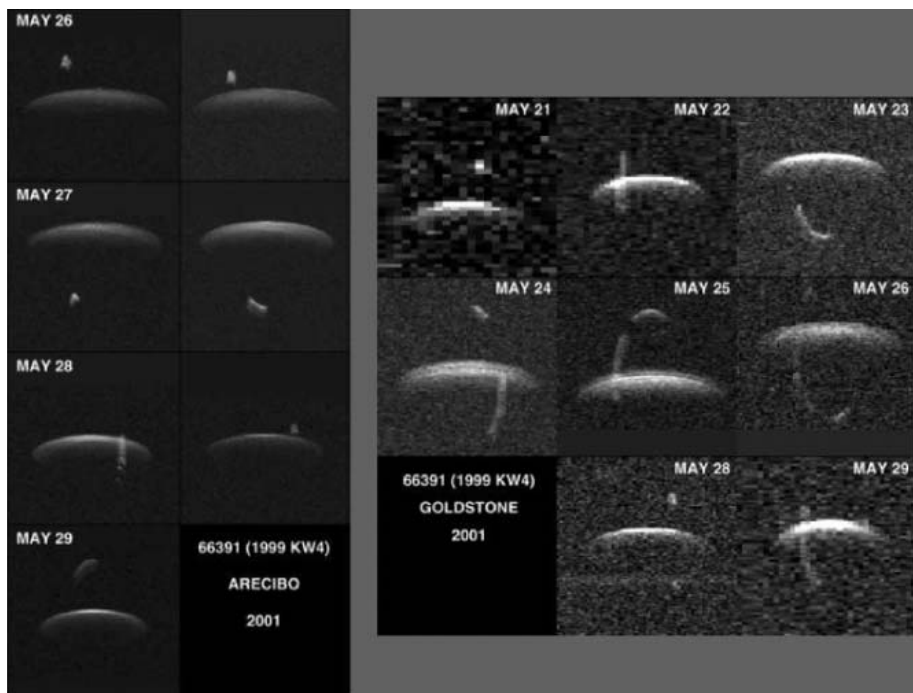
Fig. 1. Single-date, multi-run sums. Sums of delay-Doppler radar images obtained with Arecibo (**left**) and Goldstone (**right**) on each observation date. These sums are long time exposures (table S1) that show the orbital phase coverage of the secondary component (Beta) in each observing sequence. The pairs of Arecibo time exposures on 26 to 28 May correspond to radar setups with slightly different Doppler frequency resolutions (table S1). The radar is toward the top, rotation and orbital motion are counterclockwise, and each image has a height of 5625 m (37.5 μs of roundtrip time delay) and 117.2 cm s^{-1} of line-of-sight velocity (Doppler frequency of 18.6 Hz at Arecibo's 2380-MHz transmitter frequency or 66.9 Hz at Goldstone's 8560-MHz frequency). Vertical smear of the primary component (Alpha) due to motion about the system barycenter is evident in the long Goldstone exposures.

Table 1. Relative orbit of Beta about Alpha. Least-squares estimates of the elements of the average 2001–2002 relative orbit are given in the J2000 equatorial frame along with their standard errors and correlation matrix. The epoch, T, which corresponds to calendar date 26 May 2001 09:55:00.5, represents the time at which Beta is at pericenter. Ω and i correspond to a pole direction at right ascension = 15.4° ± 3° and declination = −66.1° ± 2°. Our estimate of P_{Orbit} from Beta-Alpha delay-Doppler differences, 1045.34 ± 2.16 min, is marginally compatible 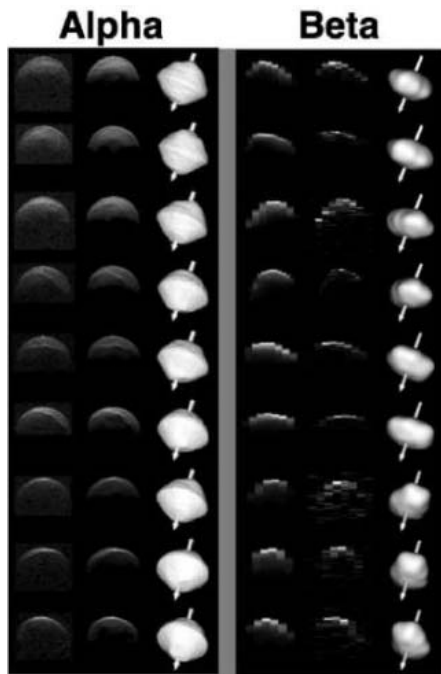with our estimate of P_{Orbit}, 1048.18 ± 1.15 min, from modeling of mutual events observed in optical lightcurves during 3 to 12 June 2001 (2) with the orbital pole fixed at the radar estimate (26). [A decrease in the number of revolutions of Beta around Alpha by one between the 2001 and 2002 epochs of the radar measurements corresponds to an increase in orbital period of 2.04 min. There are solutions that fit the radar data with an orbital period of 1047.38 min, but not without a statistically unacceptable increase (25%) in the chi-square value.] MJD, modified Julian date; arg. peri., argument of perihelion.

Parameter	Estimate	P_{ORBIT}	a	T	Ω	i	ω	e
P_{Orbit} [period (hours)]	17.4223 ± 0.036	1.00	−0.05	−0.02	−0.02	−0.06	−0.02	0.06
a [semimajor axis (m)]	2548 ± 15	−0.05	1.00	0.24	0.52	0.45	0.24	−0.12
T (epoch, MJD)	52055.4132 ± 0.88	−0.02	0.24	1.00	0.18	0.58	1.00	−0.53
Ω [long. asc. node (°)]	105.4 ± 3	−0.02	0.52	0.18	1.00	−0.07	0.18	0.07
i [inclination (°)]	156.1 ± 2	−0.06	0.45	0.58	−0.07	1.00	0.58	−0.30
ω [arg. peri. (°)]	319.7 ± 182	−0.02	0.24	1.00	0.18	0.58	1.00	−0.53
e (eccentricity)	0.0004 ± 0.0019	0.06	−0.12	−0.53	0.07	−0.30	−0.53	1.00
M (total mass)	(2.488 ± 0.054) × 10^{12} kg							

strength, resolution, and orientational coverage, one can estimate the target's three-dimensional shape, spin state, and radar scattering properties, along with the location of the COM in each delay-Doppler frame.

For each component, our shape estimation used images vignetted to exclude the other component. We summed independent images, attempting to strike a balance between maximizing signal-to-noise ratio and minimizing rotational and translational smear (table S1). The latitude-longitude coverage of the image sets used in the modeling is excellent (fig. S2). Our strategy was to start with an ellipsoid model and proceed first to a model in which surface displacement is expressed as a spherical harmonic series and then proceed to a vertex model, in each case adjusting the free parameters to optimize the resemblance between images synthesized from the shape model and the radar images (3, 4). Ellipsoid models, "harmonic" models, and vertex models were realized as polyhedra with triangular sides.

[A triangular polyhedron with V vertices has $(2V - 4)$ faces and $(3V - 6)$ edges. Larger values of V provide greater spatial resolution and, for ellipsoid and harmonic models, sample the mathematical function more densely, but they also slow the estimation.] We used enough vertices to accommodate the most detailed structure revealed in the data (Fig. 2).

To model the components' motion with respect to each other (1), we assumed a Keplerian (two-body, point-mass) orbit of Beta's COM with respect to Alpha's COM and used least squares to estimate the orbit elements from the delay and Doppler offsets of Beta's COM from Alpha's COM as determined in the shape reconstructions. Conservative uncertainties, on the order of several times the image resolution, were assigned to the Beta-Alpha offsets. The best-fit solution [postfit root mean square (rms) residuals of 30 m and 0.75 cm s^{-1} (Table 1)] yields an orbital period $P_{Orbit} = 17.4223 \pm 0.036$ hours and a semimajor axis $a = 2548 \pm 15$ m, with the pole at ecliptic (longitude, latitude) = (326°, −62°) ± 5°. P_{Orbit} and a constrain the system's total mass M by Kepler's third law and yield $M = (2.488 \pm 0.054) \times 10^{12}$ kg (6).

The distances R_A and R_B of the components' COMs from the binary system's barycenter are related to the component masses M_A and M_B by $R_B/R_A = M_A/M_B$. Thus, any candidate mass ratio defines the delay-Doppler location of the barycenter with respect to those of the components'

COMs in any given image, and hence yields estimates of the time-delay and Doppler frequency of hypothetical echoes from the barycenter at the receive-time epoch of the image. We estimated the heliocentric orbit of the asteroid in the absolute reference frame of the planetary ephemerides (table S2), using radar and optical astrometry and evaluating the goodness of fit as a function of M_A/M_B. Fits to optical and Goldstone astrometry (7) (table S3) show a sharp chi-square minimum at $M_A/M_B = 17.4 \pm 2.5$ (fig. S3), which with the results in Table 1 yields the component masses in Table 2, as well as a value for the radius of Alpha's orbit about the barycenter: $R_A = 138 \pm 22$ m.

Alpha's shape (Fig. 3 and fig. S4) is distinguished by a prominent equatorial bulge whose several-hundred-meter vertical extent is defined in the north by a continuous, very abrupt ridge and in the south by more subtle, discontinuous gradations. Much of the surface appears to have subtle structure with perhaps a few decameters of vertical relief. Some concavities might be interpreted as ~100-m impact craters, but most of the structure looks nondescript.

Alpha's bulk density, 1.97 ± 0.24 g cm^{-3}, and rotation period, $P_A = 2.7645 \pm 0.0003$ hours, reveal this object to be in a highly unusual physical state. Alpha spins fast enough so that the "potential low" of the body is located at its equator. That is, particles allowed to freely move across the surface of Alpha would naturally seek out the equator as the lowest-energy

Fig. 2. Examples of images and fit results. Each three-frame horizontal collage shows an Arecibo radar image used in the estimations, the corresponding image synthesized from the shape model, and a plane-of-sky (POS) view of that model. Each three-frame collage consists of three squares with 2.0-km sides for Alpha and 0.8-km sides for Beta. In the delay-Doppler images, the radar is toward the top and the object rotates counterclockwise. In the POS frames, north is toward the top and the arrow represents the spin vector. The Alpha collages (**left**) show images obtained on (top to bottom) 26, 26, 27, 27, 27, 28, 28, 29, and 29 May. The Beta collages (**right**) show images obtained on 26, 26, 27, 27, 28, 28, 29, 29, and 29 May. See (29) for tabulation of all images used in the shape modeling and corresponding three-frame collages.

Table 2. Alpha and Beta model characteristics. The Alpha model has 4586 vertices and 9168 facets, with a mean edge length of 39 m and effective angular resolution of 3°. The Beta model is a spherical harmonics representation of degree and order 8 realized with 1148 vertices and 2292 facets, with a mean edge length of 26 m and an effective angular resolution of 7°. The positive side of Alpha's longest principal axis (+x) is on the plane of the sky and approaching Earth on 25 May 2001 at 12:23:21. We assumed uniform internal density and principal-axis rotation about the z axis. The dynamically equivalent equal-volume ellipsoid (DEEVE) is the homogeneous ellipsoid having the same moment-of-inertia ratios and volume as the model. The assigned standard errors include our assessment of systematic effects. The uncertainties in the components' individual masses include contributions from the uncertainty in the system's total mass (Table 1) and from the uncertainty in the determination of the mass ratio. Uncertainties in densities and other ratios are calculated with Fieller's theorem (27, 28). Our value for Alpha's spin period agrees with the value, 2.7650 ± 0.0004 hours, derived from lightcurves by (2). Digital versions of the models in Wavefront format are available (29).

		Alpha	Beta
Extents along principal axes (km):	x	1.532 ± 3%	0.571 ± 6%
	y	1.495 ± 3%	0.463 ± 6%
	z	1.347 ± 3%	0.349 ± 6%
Area (km^2)		5.744 ± 6%	0.674 ± 12%
Volume (km^3)		1.195 ± 9%	0.048 ± 18%
Mass (10^{12} kg)		2.353 ± 0.100	0.135 ± 0.024
Density (g cm^{-3})		1.97 ± 0.24	2.81 (+0.82, −0.63)
Moment of inertia ratios:	I_z/I_x	1.187 ± 5%	1.74 ± 10%
	I_y/I_x	1.133 ± 5%	1.18 ± 10%
Equivalent diameter (km) of a sphere with the model's volume		1.317 ± 3%	0.451 ± 6%
DEEVE extents (km):	x	1.417 ± 3%	0.595 ± 6%
	y	1.361 ± 3%	0.450 ± 6%
	z	1.183 ± 3%	0.343 ± 6%
Rotation period (hours)		2.7645 ± 0.0003	17.4223 assumed
Pole direction [ecliptic long., lat. (°)]		(326, −65) ± 3	(326, −62) assumed

state (Fig. 3). The equatorial band has a very wide variation in slope, due mostly to the total acceleration of particles on the equatorial band being almost zero, but inward. Thus, in the equatorial region, particles are deposited on the surface in a nearly weightless environment and currently are being retained very tenuously. If Alpha's spin were any faster, loose regolith at certain distinct equilibrium points (8) would be placed in orbit about Alpha and would eventually reimpact Alpha at some other location. The existence of these equilibrium points just at the surface places the system exactly at the boundary of what a rotating body could sustain.

Alpha's radar polarization ratio, SC/OC = 0.45 ± 0.10, indicates more severe decimeter-scale near-surface roughness than on "typical" radar-detected NEAs like 25143 Itokawa and 433 Eros, but specular glints at the leading edges of the images (Fig. 2) show that the surface also possesses a very smooth component. Our modeling used a hybrid, two-term scattering law to accommodate both specular and diffuse scattering, and the parameter values estimated for the specular term correspond to a very shallow rms slope with respect to the model's facets and a near-surface bulk density between 0.6 and 1.2 g cm^{-3}, as might be expected for tenuously held regolith of stony meteoritic material.

The grain density of plausible meteorite matches to the asteroid's S spectral class (9) ranges from about 3.7 g cm^{-3} for ordinary chondrites (10) to about 5.1 g cm^{-3} for stony irons (11). Thus, Alpha's porosity probably is between 40 and 66%, comparable to values for lunar regolith core samples. Our value for Alpha's density is comparable to or lower than other (spacecraft-derived) values for S-class asteroids: 1.95 ± 0.14 g cm^{-3} for the 0.4-km NEA Itokawa (12), 2.67 ± 0.03 g cm^{-3} for the

17-km NEA Eros (13), and 2.6 ± 0.5 g cm^{-3} for the 28-km main-belt asteroid 243 Ida (14). Alpha's porosity apparently exceeds that of the latter two objects but is similar to those of Itokawa and the 58-km C-class main-belt asteroid 253 Mathilde (15) and several other C-class objects (16).

Together, Alpha's size, shape, spin, density, and porosity reveal it to be an unconsolidated gravitational aggregate close to its breakup spin rate, suggesting that KW4's origin involved spin-up and disruptive mass shedding of a loosely bound precursor object (1, 2). The disruption may have been caused by tidal effects of a close encounter with a planet (17–20) or by torques due to anisotropic thermal radiation of absorbed sunlight (the YORP effect) (21). The near-circularity of Alpha's pole-on profile further suggests that the disruption may have produced a quasi-circular disk of particles rather than merely a prolate elongated body (22).

Our Beta shape model (Fig. 3 and fig. S4) is about one-third the size of Alpha and more elongated, flattened, and asymmetrical. Our Beta density estimate, 2.81 (+0.82, −0.63) g cm^{-3}, is about 43% larger than our value for Alpha, presumably due to some combination of Beta's different spin, the circumstances of Beta's formation, and the dynamical and collisional evolution of the KW4 system (22). Beta's disk-integrated radar properties are indistinguishable from Alpha's. Analysis of dual-polarization images reveal a drop in the SC/OC ratio toward Beta's leading edge, suggesting the presence of smooth and rough surface components, as with Alpha. Beta's density allows porosities up to 42% if it resembles ordinary chondrites and from 29 to 58% if it resembles stony irons.

Whereas reconstruction of Alpha was very robust, with Beta our estimations were consistent with rotation periods between 17.3 and

17.5 hours but could not discriminate between specific values in that interval. Moreover, values for Beta's rotation period within the range spanned by the May radar and June optical estimates of P_{Orbit} (Table 1) led to indistinguishable harmonic models for which synthesized images fit the boundaries of the delay-Doppler echo distributions but could not fit image fine structure as well as with Alpha. Vertex models were unable to improve upon the image fits; relaxing the requirement of principal-axis rotation did not help. For certain "conjunction epochs" (with both components' COMs at either the same range or the same Doppler), solutions with any candidate period placed Beta's long axis at least several degrees from the Alpha-Beta line. Experiments in which only short subsets of images were centered on those epochs instead of the full Beta data set yielded smaller angular offsets but still are suggestive of Beta's rotation not being exactly synchronous. These results are at odds with our shape modeling assumption of unforced free rotation and suggest that Beta may exhibit sizable librations in longitude.

The dynamics of the KW4 system have unforeseen complexity (22), potentially involving variations in the orbit and Beta's spin state on a variety of time scales due to dynamical excitation from several possible sources. Consequently, our orbit (Table 1) and rotation parameters (Table 2) represent averages corresponding to the geometrical configurations sampled by the radar observations. The gross dimensions and periodicities of the KW4 system are typical of NEA binaries (2), so many of them may share KW4's physical and dynamical complexity.

Over time scales of tens of thousands of years, variations in KW4's heliocentric orbit due to planetary perturbations produce configurations with ecliptic crossings near the orbits of Mercury, Venus, or Earth. [The eccentricity varies from
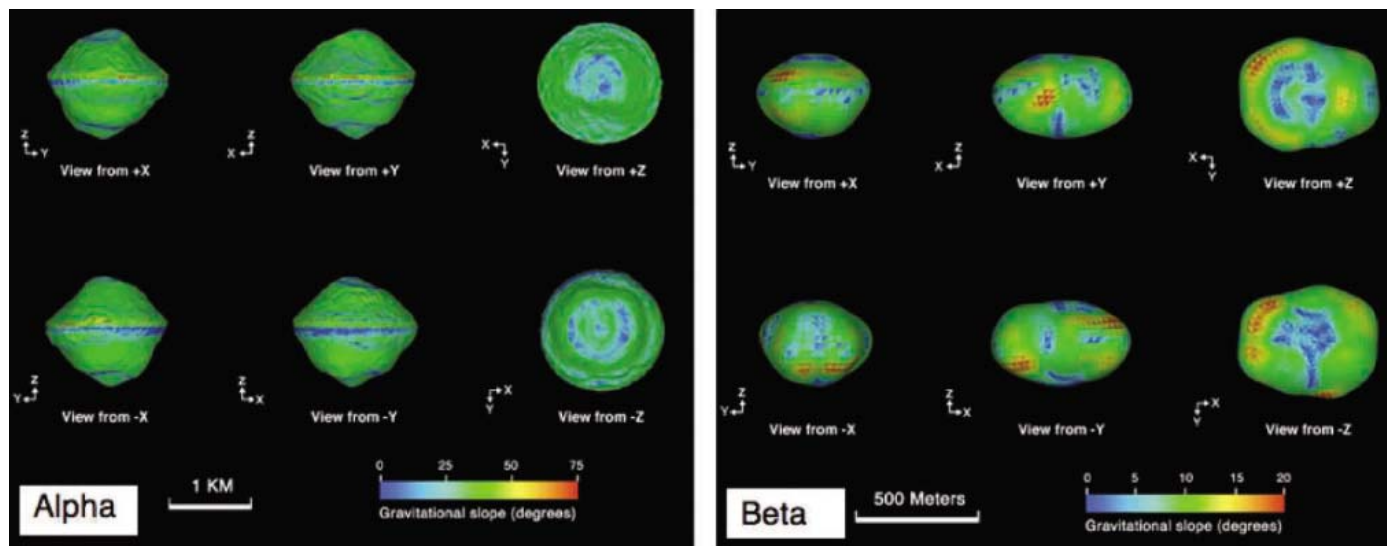
Fig. 3. Principal-axis views of the Alpha (**left**) and Beta (**right**) shape models. Colors indicate effective gravitational slope (the angular deviation from the local downward normal of the total acceleration vector due to gravity and rotation), calculated with the model densities (Table 2). Alpha's slopes average 28° with a maximum of 70°, whereas Beta's average 9° with a maximum of 18°. Beta's +x axis points toward Alpha.

0.68 to 0.81 and the inclination varies from 39° to 14° (23, 24)]. Thus, the KW4 binary system could have originated in a close flyby past any of those planets. Currently, KW4's orbit is close to the (e = 0.68, i = 39°), state and the ascending node is very close to Earth's semimajor axis. Within the nearly two-millennium window (1179 to 2946) of accurate close-approach prediction (table S4) allowed by available radar plus optical astrometry, KW4 makes 186 close Earth approaches and no approaches to any other planet. With Alpha's current pole direction assumed, the sub-Earth latitude at closest approach is generally equatorial, with mean and rms of $-7° \pm 20°$. This geometric configuration conceivably could be the signature of an extremely recent Earth-flyby origin of the system.

References and Notes

1. J. L. Margot et al., Science 296, 1445 (2002).
2. P. Pravec et al., Icarus 181, 63 (2006).
3. Our observational, data reduction, and shape-estimation techniques were nearly identical to those described in reference to asteroid 1580 Betulia by (25).
4. Materials and methods are available as supporting material on Science Online.
5. S. Hudson, Remote Sens. Rev. 8, 195 (1993).
6. Beta-Alpha delay-Doppler differences from our 1 and 2 June 2002 observations are fit acceptably well by an orbit estimated from just the May 2001 observations if we allow for a 189° adjustment to the 2002 orbital phase.
7. The Arecibo delay residuals reveal a systematic bias possibly involving a several-decameter error in the nominal geodetic location of the telescope's reference point. The Goldstone astrometric measurements seem free from such a bias and provide much better orbital-phase coverage and twice the time base of the Arecibo astrometry.
8. D. J. Scheeres, Icarus 110, 225 (1994).
9. R. P. Binzel et al., Icarus 170, 259 (2004).
10. G. J. Consolmagno, D. T. Britt, C. P. Stoll, Meteorit. Planet. Sci. 33, 1221 (1998).
11. J. Wasson, in Meteorites (Springer, New York, 1974), pp. 175–176.
12. S. Abe et al., Science 312, 1344 (2006).
13. D. K. Yeomans et al., Science 289, 2085 (2000).
14. M. J. S. Belton et al., Nature 374, 785 (1995).
15. D. K. Yeomans et al., Science 278, 2106 (1997).
16. D. T. Britt, D. Yeomans, K. Housen, G. Consolmagno, in Asteroids III, W. Bottke, A. Cellino, P. Paolicchi, R. P. Binzel, Eds. (Univ. of Arizona, Tucson, AZ, 2002), pp. 485–500.
17. E. Asphaug, W. Benz, Icarus 121, 225 (1996).
18. W. F. Bottke, H. J. Melosh, Nature 381, 51 (1996).
19. D. C. Richardson, W. F. Bottke, S. G. Love, Icarus 134, 47 (1998).
20. D. C. Richardson, K. J. Walsh, Annu. Rev. Earth Planet. Sci. 34, 47 (2006).
21. D. P. Rubincam, Icarus 148, 2 (2000).
22. D. J. Scheeres et al., Science 314, 1280 (2006); published online 12 October 2006 (10.1126/science.1133599).
23. A. Milani, Near-Earth Objects Dynamic Site: (66391) 1999KW4—Proper elements and encounter conditions (2006); available online at http://newton.dm.unipi.it/cgi-bin/neodys/neoibo?objects:1999KW4;properel;gif.
24. G. F. Gronchi, A. Milani, Icarus 152, 58 (2001).
25. C. Magri et al., Icarus, in press.
26. The radar predictions for the Sun-Earth-Alpha-Beta geometry at the photometric mutual event epochs establish that all the mutual events observed in June were eclipses (of Alpha on 3, 6, and 11 June and of Beta on 7 and 12 June).
27. D. J. Finney, in Statistical Method in Biological Assay (Hafner, New York, ed. 2, 1964), p. 24.
28. S. J. Ostro et al., J. Geophys. Res. 97, 18227 (1992).
29. http://reason.jpl.nasa.gov/~ostro/kw4/index.html
30. We thank the technical staffs of the Arecibo Observatory and the Goldstone Solar System Radar for help with the observations. Some of this work was performed at the Jet Propulsion Laboratory (JPL), California Institute of Technology, under contract with NASA. This material is based in part on work supported by NASA under the Science Mission Directorate Research and Analysis Programs. The Arecibo Observatory is part of the National Astronomy and Ionosphere Center, which is operated by Cornell University under a cooperative agreement with the NSF. Research at the University of Michigan was supported by NASA's Planetary Geology and Geophysics Program, by the JPL/Caltech Director's Research and Development Fund, and by the Air Force Office of Scientific Research. J.L.M. was supported in part by NASA grant NNG04GN31G. C.M. was partially supported by NSF grant AST-0205975. The work at Ondřejov was supported by the Grant Agency of the Czech Republic (grant 205/05/0604).

Dynamical Configuration of Binary Near-Earth Asteroid (66391) 1999 KW4

D. J. Scheeres,[1]* E. G. Fahnestock,[1] S. J. Ostro,[2] J.-L. Margot,[3] L. A. M. Benner,[2] S. B. Broschart,[1] J. Bellerose,[1] J. D. Giorgini,[2] M. C. Nolan,[4] C. Magri,[5] P. Pravec,[6] P. Scheirich,[6] R. Rose,[2] R. F. Jurgens,[2] E. M. De Jong,[2] S. Suzuki[2]

Dynamical simulations of the coupled rotational and orbital dynamics of binary near-Earth asteroid 66391 (1999 KW4) suggest that it is excited as a result of perturbations from the Sun during perihelion passages. Excitation of the mutual orbit will stimulate complex fluctuations in the orbit and rotation of both components, inducing the attitude of the smaller component to have large variation within some orbits and to hardly vary within others. The primary's proximity to its rotational stability limit suggests an origin from spin-up and disruption of a loosely bound precursor within the past million years.

Binary systems in the near-Earth asteroid (NEA) population appear to be common (1). Because of their small sizes, binary NEAs' dynamical states and evolutionary histories may be very unlike those of other binaries in the solar system (the Earth-Moon and Pluto-Charon systems, large mainbelt asteroid binaries, and binary Kuiper Belt objects). Previous analyses of binary-system dynamics (2) have not considered situations with nonspherical components and strong coupling between translational and rotational motion. Radar images have characterized binary NEA (66391) 1999 KW4 in detail (3), and here we explore the full dynamics of the KW4 system with numerical simulations that solve the equations of motion for the coupled evolution of orbit and rotation.

Our simulations model the orbital dynamics as the relative motion between the body centers of mass and model the rotational dynamics using Euler's and attitude kinematic equations for each body (4). The system conserves total angular momentum and energy in the absence of external perturbations but may lose energy through internal dissipation. The coupled rotational and orbital dynamics are driven by the system's mutual gravitational potential, which is an explicit function of the relative position and attitude of the two bodies. The mutual potential between the radar-derived models of KW4's primary and secondary components (Alpha and Beta) are computed using a mutual potential expansion specialized for polyhedral models (5–7). Propagation of the system's dynamical evolution over several-month time scales has been made tractable by using a variational integrator (8) and a parallel computer with up to 256 processors (9).

Ostro et al. (3) find that the average relative orbit is nearly circular with a period of 17.4 hours and a separation of 2.54 km, that Beta's rotation is synchronous on average, and that Alpha's rotation pole and the binary orbit normal are separated by between 0 and 7.5°, with a nominal separation of 3.2°. Our simulations identify an energetically relaxed configuration for the coupled orbit and rotational dynamics, with the orbit and Alpha angular momentum vectors aligned, Beta rotating synchronously with small departures of its long axis from the Beta-Alpha line, and modest dynamical variations (Figs. 1 and 2). The eccentricity of the relaxed orbit, ~0.0113, is nonzero because of the

[1]Department of Aerospace Engineering, University of Michigan, 1320 Beal Avenue, Ann Arbor, MI 48109–2140, USA. [2]Jet Propulsion Laboratory, California Institute of Technology, 4800 Oak Grove Drive, Pasadena, CA 91109–8099, USA. [3]Department of Astronomy, Cornell University, 304 Space Sciences Building, Ithaca, NY 14853, USA. [4]Arecibo Observatory, HC03 Box 53995, Arecibo, Puerto Rico 00612, USA. [5]Department of Natural Sciences, University of Maine at Farmington, 173 High Street, Farmington, ME 04938, USA. [6]Astronomical Institute, Academy of Sciences of the Czech Republic Fričova 1, CZ-25165 Ondřejov, Czech Republic.

*To whom correspondence should be addressed. E-mail: scheeres@umich.edu

nonspherical mass distributions of Alpha and Beta. Nevertheless, the system traces out a nearly circular path as the true anomaly librates about zero with a few degree amplitude, whereas the argument of periapsis increases secularly with a period equal to the orbit period.

A relaxed configuration is expected in the absence of any external perturbations, but during each perihelion passage gravitational perturbations from the Sun excite the system. Numerical simulations indicate that KW4's orbit pole can shift by more than 0.5° per periapsis passage for the current perihelion distance of 0.2 astronomical units (AU) and by more than 1.0° when the perihelion is at 0.12 AU, the minimum perihelion expected as a result of N-body perturbations and the Kozai resonance (10). During each perihelion passage, solar perturbations cause the eccentricity to vary up to 0.002 at a perihelion of 0.2 AU and 0.005 at a perihelion of 0.12 AU, producing excitation in the pole and eccentricity that should persist given the high frequency of perihelion passages. KW4 makes frequent Earth

approaches (3): An approach within 20 Earth radii can excite the system (11), and flybys within 5 Earth radii can disrupt it (12).

An excited energy state can be simulated by parametrically varying the initial osculating eccentricity e. To explore the range of possible excitations, we performed a number of simulations at different initial eccentricities. Figures 1 and 2 show two cases, one chosen with relaxed initial conditions and the other starting from $e = 0$ (to produce an excited state), both of which lie within the uncertainties (3).

Because of the 4% variation in Alpha's equatorial radius, there are fluctuations of the mutual orbit semimajor axis and eccentricity that drive a longer-term oscillation with a period equal to the orbit period (Fig. 1). These excite Beta's free precession, causing oscillations in its rotation and orbit with a period of ~188 hours (about four times Beta's 48-hour free precession period). The oscillation amplitude in Beta's rotation rate changes from near zero to a maximum value, causing the attitude to vary by several degrees

relative to uniform rotation during some orbits but to maintain nearly uniform rotation during others (Fig. 2).

Thus, Beta experiences persistent shaking, with angular accelerations up to 2×10^{-10} rad/s^2 in the relaxed state and substantially more in the excited configurations (Fig. 2), which are much more energetic than that due to free precession (13). Such shaking would drive material toward a minimum-energy, compact configuration, lowering the body's porosity, and possibly producing Beta's low gravitational slopes. This hypothesis is consistent with the fact that Beta's density estimate is larger than Alpha's (3).

The system's total angular momentum budget receives a 75% contribution from Alpha's rotation, 25% from the relative orbit, and less than 0.1% from Beta's rotation. As a result of conservation, the system's total angular momentum vector lies between Alpha's and the orbit's angular momentum vectors, so that the three are in a plane, except for the deviations that Beta allows. Beta's angular momentum is locked
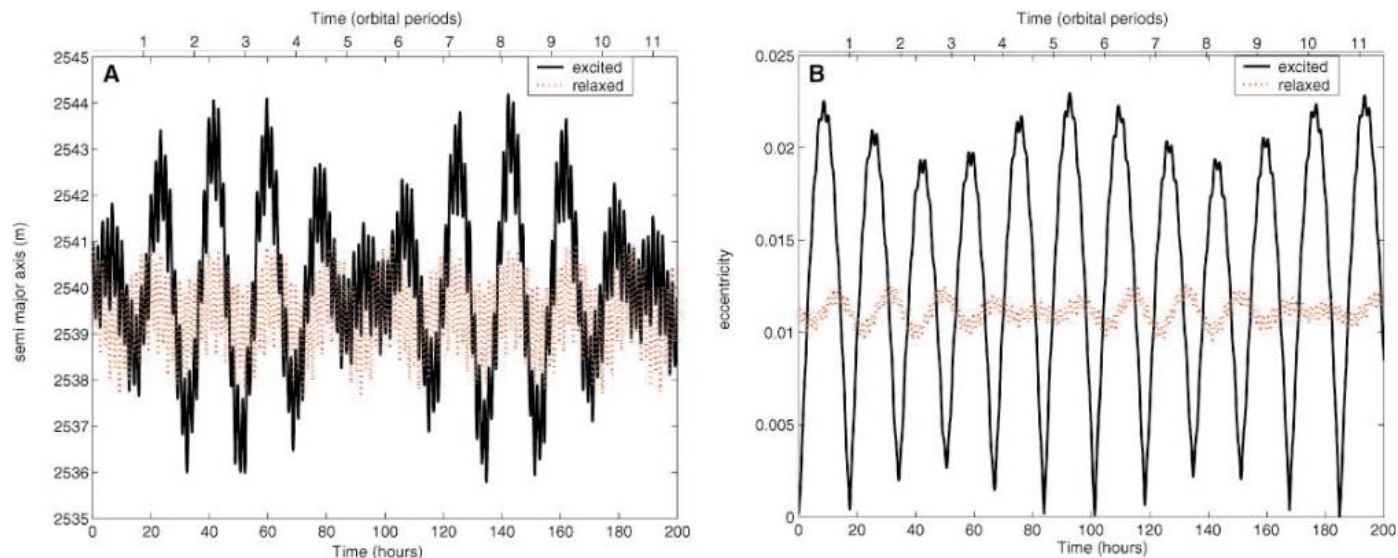

Fig. 1. Evolution of KW4's orbit (**A**) semimajor axis and (**B**) eccentricity over 200 hours, computed for the relaxed and excited system.
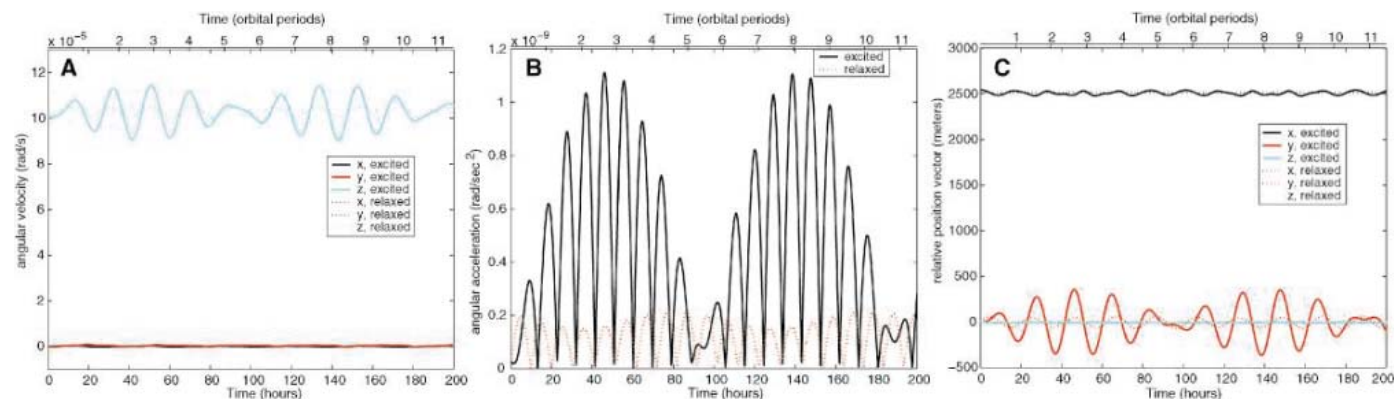

Fig. 2. (**A**) Rotational angular velocity and (**B**) total angular acceleration of Beta, shown in the Beta fixed frame, for the relaxed and excited cases. (**C**) Alpha's orbit in a Beta-fixed frame. The large y variations are due primarily to Beta's attitude libration about the Beta-Alpha line.

within a small-scale variation about the orbit angular momentum vector and is captured on average in a Cassini state (*14*) with fluctuations due to perturbations from the component's shapes. The minimum energy configuration is for the angular momentum vectors to be aligned, consistent with the estimated offset between the vectors of 3.2° with an uncertainty ranging up to 7.5° (*3*). However, solar perturbations at perihelion indicate that a minimum offset on the order of 1° should exist. The actual offset between these vectors will be constant between perihelion passages because the components' mutual potential induces equal precession rates of the orbit plane and Alpha's spin pole (*2, 15*), with a period of ~90 days. Over half a precession period, the inertial directions of the estimated orbit and Alpha poles will vary by 4.8° and 1.6°, respectively, less than the uncertainty in the determined pole direction using data from the 2001 and 2002 observations.

Portions of Alpha's surface are only 7 m from an altitude at which a free particle would be placed into orbit about the body. A rotation period 1.3% shorter would place portions of Alpha's surface at orbital speeds. A particle at such a point would be in a circular synchronous orbit (Fig. 3), and if Alpha rotated faster would be at periapsis of an elliptical orbit and would rise off the surface.

Because of its rapid rotation, Alpha's minimum geopotential is located along the equator rather than at its poles, the usual case for more slowly rotating bodies (*16*), so loose material preferentially migrates toward the equator (fig. S2). Thus, Alpha's equatorial bulge can be understood as the redistribution of loose, unconsolidated regolith toward the lowest point on the object, consistent with recent observations of asteroid Itokawa, where loose regolith was preferentially located in the potential lows of that body (*17*).

At Alpha's high rotation rate, previously compacted granular material could seek out lower-

energy, higher-porosity configurations that do not exist on slowly rotating bodies. Consider an ellipsoid resting on a rotating sphere: For slow rotation, the minimum energy configuration has the ellipsoid's shortest axis normal to the surface and pointing at the body center. For sufficiently rapid rotation, an orientation with the long axis normal to the surface is the minimum energy configuration, increasing the "mean radius" (*18*). Such minimum energy states in an unconsolidated gravitational aggregate can create a porous distribution of material, perhaps producing the lower density found for Alpha (*3*). Furthermore, material on Alpha is subject to minimal compression due to the small surface accelerations (fig. S3) and can exist at high porosities that are impossible on Beta because of its shaking.

We can constrain KW4's formation age by considering the semimajor axis increase due to tides raised on Alpha by Beta. For the nominal KW4 model, if the orbit semimajor axis were 0.238 km (9.4%) smaller, conservation of angular momentum would bring Alpha's surface to the disruption limit. For idealized elastic bodies, the time scales depend linearly on the product μQ, where μ is the shear modulus of the material and Q is the tidal dissipation factor (*19, 20*). Because of evidence for decreased rigidity at small overburden pressures and in fragmented rock (*21*), and because tidal damping is likely to be strong in a gravitationally bound aggregate as a result of friction between constituent particles, we estimate that KW4's formation age is less than 10^6 years (*22*).

The proximity of Alpha's surface to its instability limit may be due in part to the Yarkovsky-O'Keefe-Raszievskii-Paddack (YORP) effect (*23, 24*), in which recoil from thermal reradiation of absorbed sunlight induces a net torque that alters the spin. The YORP effect on Alpha generates rotational accelerations on the order of 3×10^{-11} rad/s per year (*25*) that may induce a cycle of orbiting and reimpacting regolith when Alpha reaches an extreme rotation

rate. Because of the presence of Beta, particles spun off Alpha are trapped within a zero-velocity surface [defined in the context of the restricted three-body problem for the Alpha, Beta, and particle system (*26*)], so neither escape from Alpha nor impact on Beta is allowed. Thus, material spun off Alpha will eventually reimpact and migrate toward the equator, where it may be spun off again. This cycle self-regulates Alpha's spin rate near the surface disruption limit and expands the orbit by transferring angular momentum from Alpha to the orbit. Alpha's surface lies completely outside the rotational Roche Lobe that usually envelopes asteroids (*27*), which is expected if the surface particles fell directly from orbit onto the body surface. At the current rate of YORP acceleration, the semimajor axis expands ~200 m/10^5 years, faster than the estimated time scale for the orbit to evolve as a result of tidal dissipation.

The dynamical and physical characteristics of the KW4 system suggest possible formation and evolution mechanisms but do not point to a single, unambiguous scenario. Below we consider explanations that are consistent with the current system.

Did KW4 form during a close planetary flyby? KW4 seems similar to binaries produced in tidal disruption simulations (*28*); however, such simulations consistently predict primary spin periods ~50% longer than Alpha's 2.8-hour value (*29*). Alpha's rapid rotation could have resulted if a debris disc formed simultaneously with Beta, was trapped inside Beta's orbit, and then collapsed onto Alpha. During tidal acceleration at closest approach to Earth, the largest blocks on the progenitor achieve orbital speeds before smaller particles because, on average, the center of mass of a large block on the surface is farther from Alpha's center and thus has a lower circular speed than a smaller block (*18*). The collapse of a disc returns angular momentum to Alpha and increases its spin: Accelerating Alpha from a period of 4 hours to its current value requires approximately 5% of Alpha's mass to collapse from the current orbit radius of 2.5 km, 10% of Alpha's mass to collapse from 1.4 km, or 20% from 1 km. Such a collapse could leave some of Alpha's surface at the disruption limit and form a raised equatorial structure. Most tidal binary formation simulations to date have employed equal-sized particles with spheres (*28*), ellipsoids (*30*), or simple polyhedra (*31*). Simulations with a distribution of particle sizes are more realistic and may elucidate formation by tidal breakup.

KW4 may have formed by rotational fission, which occurs if the asteroid spins fast enough for the largest blocks on the surface to enter orbit (*32, 18*). KW4's progenitor would need to rotate with a period of 4.2 hours for a block the size of Beta to enter orbit, 3.8 hours if Beta were composed of two equal-sized blocks, 3.5 hours for four blocks, and so forth. Continued acceleration of Alpha from a 3.5-hour period to its current
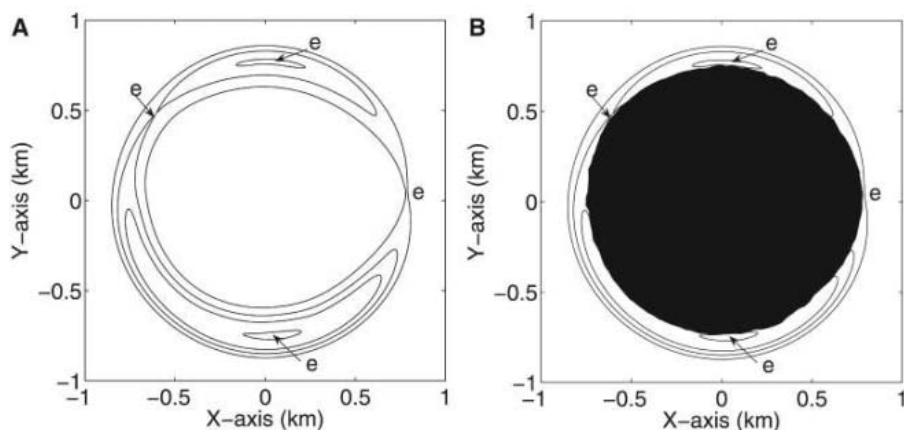
Fig. 3. Curves of constant geopotential about Alpha (**A**) without and (**B**) with Alpha's pole-on shape superimposed. Four equilibrium points, orbits that are stationary in the frame rotating with Alpha, are indicated by "e" and lie just at the body's surface. Alpha's surface lies outside the innermost curve, defined for the equilibrium point with the lowest potential value.

period in less than a million years would require a YORP acceleration rate a factor of five times as high as at present, which is plausible if Alpha's initial mass distribution were less symmetric than it is now. Once Beta formed, continued rotational acceleration of Alpha would be regulated as described previously, the resurfacing making the system more symmetric and diminishing YORP's effectiveness over time.

Could KW4 have formed in the main asteroid belt and subsequently migrated into an Earth-crosser? Recent discoveries reveal a substantial population of small, inner main-belt binaries with characteristics similar to near-Earth binaries (33). Collisions and YORP can form binaries within the main belt, but formation by tidal flybys is extremely unlikely. If KW4 formed in the main belt, then its age must be on the order of 10^8 years and it must have survived multiple close-Earth approaches (3) that could have strongly excited it while avoiding any that could disrupt it. Thus, formation of KW4 in a near-Earth orbit through some combination of tidal and YORP torques seems more likely.

References and Notes

1. J. L. Margot *et al.*, *Science* **296**, 1445 (2002).
2. H. Kinoshita, *Publ. Astron. Soc. Jpn.* **24**, 423 (1972).
3. S. J. Ostro *et al.*, *Science* **314**, 1276 (2006); published online 12 October 2006, 10.1126/science.1133622.
4. A. J. Maciejewski, *Celestial Mech. Dyn. Astron.* **63**, 1 (1995).
5. R. A. Werner, D. J. Scheeres, *Celestial Mech. Dyn. Astron.* **91**, 337 (2005).
6. E. G. Fahnestock, D. J. Scheeres, *Celestial Mech. Dyn. Astron.*, in press.
7. This polyhedral formulation reduces the mutual potential to a series of joint summations over the facets of each model, 9108 for Alpha and 2292 for Beta. The number of operations for each evaluation of the mutual potential, force, and moment is on the order of the product of those numbers, or 21 million.
8. T. Lee, M. Leok, N. H. McClamroch, available at http://arxiv.org/abs/math.NA/0508365
9. The complete equations of motion, model, and an animation are available as supporting material on *Science* Online.
10. Over time scales of 77,000 years, *N*-body gravitational perturbations cause KW4's argument of perihelion to circulate and its eccentricity, inclination, and perihelion distance to oscillate significantly, while its semimajor axis remains approximately constant as a result of a Kozai resonance (34). KW4's heliocentric eccentricity and perihelion vary between current values of $e = 0.68$ and $q = 0.20$ AU to $e = 0.81$ and $q = 0.12$ AU, and its heliocentric inclination varies from 39° (currently) to 14°.
11. P. Farinella, *Icarus* **96**, 284 (1992).
12. W. F. Bottke Jr., H. J. Melosh, *Icarus* **124**, 372 (1996).
13. J. A. Burns, V. S. Safronov, *Mon. Not. R. Astron. Soc.* **165**, 403 (1973).
14. G. Colombo, *Astron. J.* **71**, 891 (1966).
15. A more detailed description is provided in the supplemental material.
16. V. Guibout, D. J. Scheeres, *Celestial Mech. Dyn. Astron.* **87**, 263 (2004).
17. A. Fujiwara *et al.*, *Science* **312**, 1330 (2006).
18. D. J. Scheeres, Stability of Binary Asteroids Formed Through Fission [#1632], abstract presented at the 37th Lunar and Planetary Science Conference (2006).
19. C. D. Murray, S. F. Dermott, *Solar System Dynamics* (Cambridge Univ. Press, Cambridge, 1999), pp. 160–174.
20. Typical values for rocky bodies are $\mu_{rock} = 5 \times 10^{10}$ Nm^{-2} and $Q = 100$.
21. H. He, T. J. Ahrens, *Int. J. Rock Mech. Min. Sci. Geomech.* **31**, 525 (1994).
22. The supporting material provides additional details on this calculation.
23. D. P. Rubincam, *Icarus* **148**, 2 (2000).
24. The effect of solar radiation forces on Beta may also influence orbital evolution via the Binary YORP effect (35). Applying the theory in (35) to the KW4 system predicts that the orbit is shrinking at a rate of 0.8 m per year. Such rapid collapse seems inconsistent with the existence of the system unless it formed very recently.
25. The YORP rotational acceleration is found by applying Rubincam's method (24) to the Alpha model and averaging over one heliocentric orbit period.
26. D. J. Scheeres, J. Bellerose, *Dyn. Syst. Int. J.* **20**, 23 (2005).
27. J. K. Miller *et al.*, *Icarus* **155**, 3 (2002).
28. K. J. Walsh, D. C. Richardson, *Icarus* **180**, 201 (2006).
29. D. C. Richardson, K. J. Walsh, *Annu. Rev. Earth Planet. Sci.* **34**, 47 (2006).
30. F. Roig, R. Duffard, P. Penteado, D. Lazzaro, T. Kodama, *Icarus* **165**, 355 (2003).
31. D. G. Korycansky, *Astrophys. Space Sci.* **291**, 57 (2004).
32. W. F. Bottke Jr., D. Vokrouhlický, D. P. Rubincam, M. Broz, *Asteroids III*, Bottke *et al.*, Eds. (Univ. Arizona Press, Tucson, 2002), p. 405.
33. P. Pravec *et al.*, *Icarus* **181**, 63 (2006).
34. G. F. Gronchi 2006. NEODys Web site. http://newton.dm.unipi.it/cgi-bin/neodys/neoibo?objects:1999KW4;main.
35. M. Ćuk, J. A. Burns, *Icarus* **176**, 418 (2005).
36. Research at the University of Michigan was supported by NASA's Planetary Geology and Geophysics Program, by the Jet Propulsion Laboratory (JPL) California Institute of Technology (Caltech) Director's Research and Development Fund, and by the Air Force Office of Scientific Research. Some of this work was performed at JPL Caltech under contract with NASA. The supercomputers used in this investigation were provided by funding from JPL Institutional Computing and Information Services and NASA Directorates of Aeronautics Research, Science, Exploration Systems, and Space Operations. This material is based in part on work supported by NASA under the Science Mission Directorate Research and Analysis Programs. C.M. was partially supported by NSF grant AST-0205975. J.L.M. was supported in part by NASA grant NNG04GN31G. P.P. and P.S. were supported by the Grant Agency of the Czech Republic, Grant 205/05/0604.

Ongoing Buildup of Refractory Organic Carbon in Boreal Soils During the Holocene

R. H. Smittenberg,[1]* T. I. Eglinton,[2] S. Schouten,[1] J. S. Sinninghe Damsté[1]

Radiocarbon ages of vascular plant wax–derived *n*-alkanes preserved in well-dated Holocene sediments in an anoxic fjord (Saanich Inlet, Canada) were found to be not only substantially older than the depositional age but increasingly so during the Holocene. Assuming that *n*-alkanes serve as a proxy for recalcitrant terrigenous organic matter, this indicates that the accumulation of refractory organic carbon in soils that developed after the deglaciation of the American Pacific Northwest is ongoing and may still be far from equilibrium with mineralization and erosion rates.

Estimated at ~1500 Pg, soil organic carbon (SOC) constitutes the largest active OC pool on the globe (1, 2), and consequently the fluxes of OC to and from this reservoir are important for the carbon budgets in the bio- and geosphere (1, 3). Refractory organic matter makes up approximately half of the SOC pool because of its resistance to degradation (4), and it is this pool that is ultimately responsible for long-term terrestrial carbon storage (1, 5). However, our understanding of the long-term buildup of SOC is largely derived from studies of present-day soils, and there is a paucity of temporal records of SOC dynamics. Because of its complex and heterogeneous nature, the accumulation, erosion, and especially mineralization rates of refractory SOC are hard to determine, which hinders modeling of fluxes to and from this carbon pool (1, 3, 4, 6). For instance, the extent to which the higher-latitude soils and peats have been, or still are, expanding and/or changing in composition after their initial buildup after the most recent deglaciation remains an open question (1, 3, 5, 6). Data to substantiate hypotheses about the global carbon cycle over millennial time scales are very limited, and for the terrigenous component of this cycle, depend mainly on soil chronosequences (7, 8); mass balance studies of various SOC pools, aided by radiocarbon analysis (6); vegetation reconstructions coupled with soil carbon content (9); and models (4). A limiting factor in these studies is that they rely on inventories of biomass and active soil, whose properties have probably changed over time.

Coastal and lake sediments contain a temporal record of soil organic matter delivered from adjacent watersheds, and these records may

[1]Department of Marine Biogeochemistry and Toxicology, Royal Netherlands Institute of Sea Research, Post Office Box 59, 1790 AB, Den Burg, Netherlands. [2]Department of Marine Chemistry and Geochemistry, Woods Hole Oceanographic Institution, Woods Hole, MA 02543, USA.

*To whom correspondence should be addressed. Present address: School of Oceanography, University of Washington, Box 355351, Seattle, WA 98195, USA. E-mail: smitten@u.washington.edu

provide insight into past changes in the refractory SOC pool. We examined sediments of Saanich Inlet, Canada (10), which contain a high-temporal-resolution record spanning the late Holocene, lying above a less-well-resolved early Holocene sequence and late Pleistocene glaciomarine deposits. Because of high sediment accumulation rates (11) and permanent anoxic bottom-water conditions, the sedimentary organic matter and the sediment structure have been well preserved (10, 12), enabling annual dating of the core back to ~6000 years before the present (yr B.P.) by means of varve counting (13). We analyzed the distribution, stable carbon isotopic composition, and radiocarbon composition of vascular plant–derived long-chain n-alkanes from seven well-dated laminated sediment layers ranging from recent to 5500 yr B.P. (14), as well as layers just below the well-dated section and a late Pleistocene layer (Table 1). Both the stable carbon isotopic ($\delta^{13}C$) compositions (table S1) and the distribution of the n-alkanes (Fig. 1), as reflected in the carbon preference index (CPI) (Table 1), suggest that they are predominantly derived from C_3 vascular plant material, admixed with

some fossil alkanes of petrogenic origin, such as from weathering of sedimentary rocks (14, 15). This is in agreement with earlier observations in the Fraser River basin (16) near Saanich Inlet. There is a preponderance of evidence that long-chain n-alkanes are resistant to degradation (17, 18), and previous studies indicate that they can serve as a proxy for the refractory SOC pool (19, 20). The reasons for their recalcitrance, and that of the majority of SOC, may be that they are intimately associated with the mineral fraction (2, 3, 21, 22). The specific surface area of minerals appears to play an important role in OC preservation, with adsorption providing some sort of physical protection against water-soluble microbial enzymes. Such protection may also be provided by the hydrophobic nature of (humified) organic matter or by micropores within soil aggregates (3). Low temperatures and low-oxygen conditions related to waterlogging also decrease OC degradation (3).

The major sources of terrigenous sediment that enters Saanich Inlet are the nearby Cowichan River and the large Fraser River across the Strait of Georgia; this sediment is augmented by material discharged from local streams (11).

Soils in the watersheds of these rivers should thus be the main source of the terrigenous OC, and thereby n-alkanes, in the Saanich Inlet sediments (19). Erosion of the land surface in British Columbia has continued unabated since the last deglaciation, with a dominance of secondary remobilization of Quaternary sediments over primary denudation (23). Because of high flows during the spring freshets and the high topographic relief of the region, most of the fine-grained sediment (silt and clay), and thereby the bulk of eroded SOC (2), experience a relatively short residence time within the river systems (24). Intermediate reservoirs that would delay incorporation of the soil carbon signal into the marine sedimentary record are therefore of limited importance. Besides being derived from soil organic matter, sedimentary n-alkanes may also be derived directly from living vegetation, typically transported by wind after ablation of the leaf waxes (25). Substantial amounts of contemporary n-alkanes from fresh vegetation would result in distinctly higher radiocarbon contents of the odd–carbon-numbered C_{27}-C_{31} n-alkanes deposited after aboveground nuclear weapons testing as compared to "pre-bomb" material. This is not the case (Table 1), which suggests that a direct input from vegetation plays a minor role.

When the calibrated ages of the odd C_{27}-C_{31} n-alkanes are compared with the varve ages of the laminated sediments, it is immediately apparent that there is a discrepancy between these two ages and that this discrepancy increases toward the present (Fig. 2). Such a trend was not observed in marine-derived biomarkers in the same setting (26), indicating that this is clearly a different, exclusively terrigenous signal. For the laminated section, linear regression between the sediment age and the sediment–n-alkane age offset yields a squared correlation coefficient (R^2) of 0.68. The outlier at ~500 yr B.P. may reflect heterogeneities in the nature of the eroded material: Possibly this sample contained an anomalously large fraction of fresh vascular plant detritus. When this outlier is excluded, the R^2 increases to 0.98. Three properties of the

Fig. 1. Measured and modeled distribution and $\delta^{13}C$ values of the n-alkane fraction from the sediment interval corresponding to 2533 to 2702 yr B.P. as a representative of the studied samples. Numbers beginning with n refer to carbon chain length. The modeled data represent the outcome of a mixing model with a fossil (10%) and contemporary vascular plant source (90%) with estimated $\delta^{13}C$ and CPI end-member values (14). Because the model is a simplification of reality, a perfect fit cannot be reached with just two end-members. However, the proportions used give a reasonable estimate. ‰, per mil.
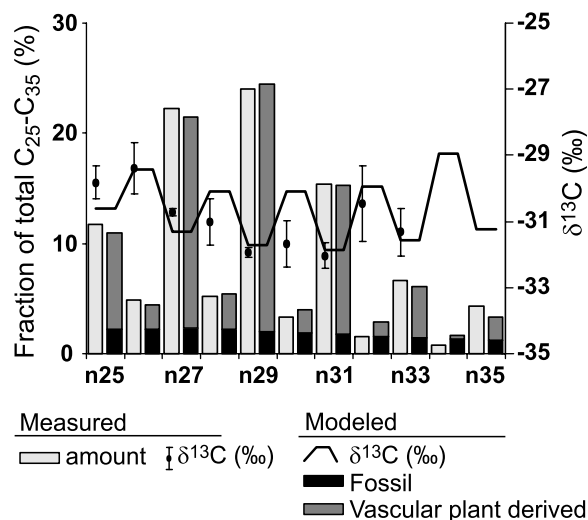
Table 1. Radiocarbon content, calibrated age, and other properties of sedimentary n-alkanes (odd C_{27-31}). cal, calendar.

Sediment age (varve-based) (18)	n-Alkanes $\Delta^{14}C$ (± 8‰)	Calibrated age (cal yr B.P.)*	Concentration (µg/g dry sediment)	CPI†	Fossil fraction (±5%)‡
1984–1998 A.D.	−458	5473 (5599) 5730	4.4	2.7	25
1932–1950 A.D.	−464	5606 (5657) 5844	3.1	4.1	10
568–465 B.P.	−417	4828 (4854) 4893	2.8	4.3	10
1111–977 B.P.	−498	6234 (6290) 6354	2.1	4.9	10
2330–2520 B.P.	−538 ± 40	6666 (6997) 7388	2.2	4.7	10
2707–2533 B.P.	−546	7131 (7215) 7285	1.8	4.8	10
3600–3500 B.P.	−	−	1.8	4.1	10
4940–4840 B.P.	−626	8476 (8617) 8948	0.8	4.8	10
6300–6500 B.P.§	−701 ± 95	10132 (11120) 12339	2.2	4.0	15
11500–13000 B.P.‖	−806 ± 41	15256 (15724) 16374	1.6	4.0	15

*The calibrated age ranges are 1σ confidence intervals. The age in parentheses has the highest probability.   †CPI = 0.5 ×[(C_{25} + C_{27} + C_{29} + C_{31}) + (C_{27} + C_{29} + C_{31}+ C_{33})]/(C_{26} + C_{28} + C_{30} + C_{32}). The average chain length for C_{25}-C_{35} is 28.8 ± 0.3 for all samples.   ‡Estimates based on two end-member models (14).   §Sample from intermittently laminated section. Age was extrapolated using the sedimentation rate of varve-counted sediment above (13).   ‖Glaciomarine silty clay deposited during late deglaciation. The minimum age is based on radiocarbon-dated above-lying sediment (13) and the maximum age on the timing of glacial retreat (27).

regression line are notable: (i) the correlation is linear; (ii) the calculated intercept age (that is, n-alkane age = calendar age) is similar to the time of deglaciation of the area, between 14,000 and 11,500 yr B.P. (27); and (iii) the age offset of 5500 years in the youngest sediments represents about half of the Holocene time span.

The CPI, in conjunction with the δ^{13}C values of the individual n-alkanes, can be used to estimate the relative contribution of fossil (radiocarbon-dead) and Holocene-aged soil n-alkanes (14, 28) (Table 1 and supporting online text). Recalibration to calendar ages after correction of the n-alkane Δ^{14}C value for fossil inputs produces Holocene-sourced n-alkane ages (Fig. 2). The intercept of the regression line comes closer toward the real onset of the Holocene at 11,500 yr B.P. (27). At that time, the entire region became vegetated, although plants had already established themselves in the lowlands of the area as early as 13,500 yr B.P., as evidenced from radiocarbon-dated wood fragments in the Fraser moraines (27). The fossil-corrected n-alkane ages from the older nonlaminated sediments are in agreement with our interpretation. However, uncertainties in dating the n-alkanes and the sediments, together with uncertainties in fossil alkane estimates, make an interpretation of these data tentative, and we therefore refrain from drawing any further inferences from them.

The average age offset of the odd C_{27}-C_{31} n-alkanes of the pre-bomb sediment after a correction for 10% fossil alkanes is ~4700 years (Fig. 2), whereas an equal contribution of n-alkanes aged from 0 to 11,000 yr B.P. would have resulted in an average age offset of 5500 years. This bias toward younger n-alkane ages

suggests that, as expected, some loss of refractory soil carbon by either mineralization or erosion must have occurred, although it is equally feasible that younger topsoils are preferentially eroded as compared to older and more deeply buried material. Regardless, it is evident that the average n-alkane ages have been increasing in a near-linear fashion toward the present, strongly suggesting that any loss due to erosion or mineralization is still largely outpaced by accumulation.

An alternative scenario that would produce the observed n-alkane age profile while allowing for substantially higher erosion and/or mineralization rates is one of continuously decreasing terrestrial primary productivity toward the present. In that case, the stock and concentration of n-alkanes in the drainage basin should diminish, whereas a more steady-state primary production and ongoing accumulation would be reflected by an increasing flux to the Saanich Inlet sediments toward the present. By using varve thickness data (13) in combination with wet bulk density and porosity data (10, 12, 13), we estimated the sediment accumulation rates (Fig. 3) in the laminated section. The accumulation rates of the odd C_{27}-C_{31} n-alkanes to the sediment were then determined from their concentrations (Table 1). The fluxes of the Holocene-aged n-alkanes show an increasing trend toward the present, whereas this is not the case for the bulk sediment accumulation rate. This implies that the primary cause of the increasing odd C_{27}-C_{31} n-alkane accumulation rate in the sediment must be a growing concentration of n-alkanes within the sediment load, which is consistent with a buildup of terrigenous

OC in the area. Postdepositional degradation of n-alkanes within the Saanich Inlet sediment does not appear to be an important factor (12, 17).

Although this study was done using long-chain n-alkanes only, the observed trends are probably valid for a larger range of refractory vascular plant–derived organic compounds (17, 18). These findings indicate that the refractory SOC pool of the Pacific Northwest is still increasing as a long-term response to the last deglaciation. Ongoing accumulation of refractory OC may be a broader phenomenon in boreal soils, or even in other biomes worldwide. However, similar studies to those undertaken here would be needed to verify this, because factors such as mineralogy, climate, and cultivation have an impact on the decomposition and preservation of all organic matter fractions, including the recalcitrant pool (3). Although our results appear to contradict some studies using natural ^{13}C labels (29) that find no evidence of a highly recalcitrant soil carbon pool, they corroborate other findings of old radiocarbon ages of refractory carbon fractions and n-alkanes in a large array of soils (4, 6, 20, 30, 31) and suggest that the turnover time of this carbon pool is 10,000 to 100,000 years or more and not 1000 to 10,000 years as is often used in soil carbon models (4). These findings challenge the notion that the current production of refractory organic matter is balanced by decomposition and erosion after a few thousand years, as inferred via

Fig. 2. Age offset between odd–carbon-numbered C_{27}-C_{31} n-alkanes and sediments. Black diamonds represent offsets calculated with calibrated n-alkane ages given in Table 1. Error bars denote age uncertainty (1σ) after calibration. The data point at ~500 yr B.P. was not used for the regression line. Gray dots represent age offsets of Holocene-aged soil-derived n-alkanes with the sediments after correcting for the fossil fraction given in Table 1. The gray-shaded areas around the non-laminated fossil-corrected values represent their uncertainty based on the original ^{14}C value uncertainties and age constraints. Ka cal BP, thousands of calendar years before the present.
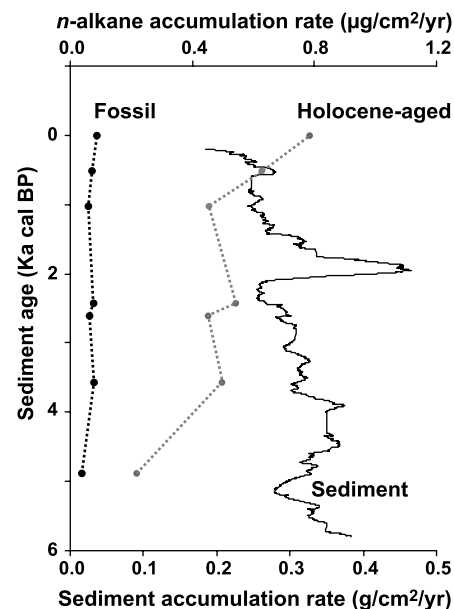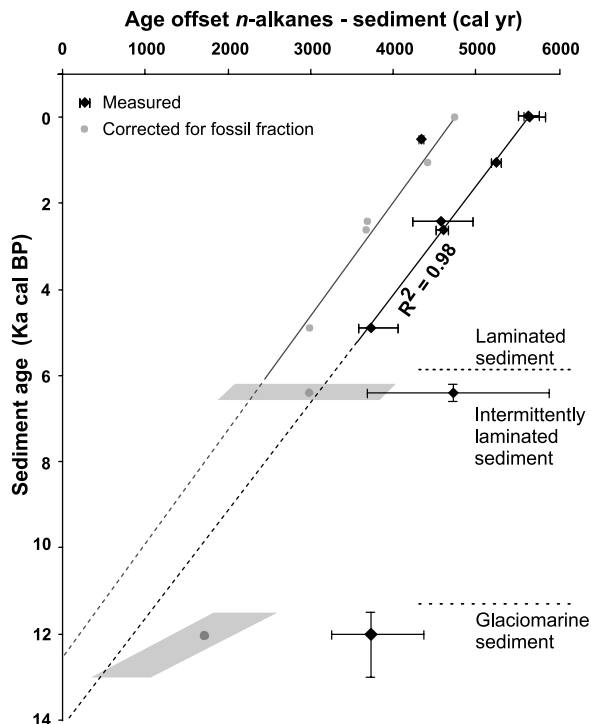
Fig. 3. n-Alkane and sediment accumulation rates of the laminated section of Saanich Inlet. Solid line, sediment; stippled black line, fossil n-alkanes; stippled gray line, Holocene (soil) n-alkanes. n-Alkane accumulation rates were calculated based on varve thickness (13), wet bulk density (10), and porosity data and modeling (10, 11, 13), together with the concentrations and estimated fossil fraction of the n-alkanes listed in Table 1.

chronosequences (7) or soil respiration measurements (31). The assumption that soils are in a steady state is also called into question, especially because it is recognized that refractory OC has been building up in soils exposed since the last glacial (1, 5). This new paradigm likely has its main impact on carbon budget models that calculate sources, sinks, and fluxes within the global carbon cycle on longer time scales (>1000 years). This could be of relevance, for example, to studies that link vegetation type to soil carbon content in order to estimate changing carbon storage on land through time (9). It places the terrestrial biosphere in a more prominent position as a slow but progressively important atmospheric carbon sink on geologic time scales and may even influence current predictions about carbon cycling and soil carbon storage in response to elevated atmospheric CO_2 levels.

References and Notes

1. R. Amundson, Annu. Rev. Earth Planet. Sci. 29, 535 (2001).
2. J. I. Hedges, R. G. Keil, Mar. Chem. 49, 81 (1995).
3. E. A. Davidson, I. A. Janssens, Nature 440, 165 (2006).
4. P. D. Falloon, P. Smith, Biol. Fertil. Soils 30, 388 (2000).
5. J. W. Harden, E. T. Sundquist, R. F. Stallard, R. K. Mark, Science 258, 1921 (1992).
6. E. A. Paul, H. P. Collins, S. W. Leavitt, Geoderma 104, 239 (2001).
7. W. H. Schlesinger, Nature 348, 232 (1990).
8. M. S. Torn et al., Nature 389, 170 (1997).
9. J. M. Adams, H. A. Faure, Global Planet. Change 16-17, 3 (1998).
10. B. D. Bornhold et al., Proceedings of the Ocean Drilling Program, Initial Reports, 169S (Ocean Drilling Program, College Station, TX, 1998), pp. 5–138.
11. S. M. Gucluer, M. G. Gross, Limn. Oceanogr. 9, 359 (1964).
12. M. R. McQuoid, M. J. Whiticar, S. E. Elvert, T. F. Pederson, Mar. Geol. 174, 273 (2001).
13. A. J. Nederbragt, J. W. Thurow, Mar. Geol. 174, 95 (2001).
14. Materials and methods are available as supporting material on Science Online.
15. J. W. Collister, G. Rieley, B. Stern, G. Eglinton, B. Fry, Org. Geochem. 21, 619 (1994).
16. M. B. Yunker, R. W. MacDonald, Org. Geochem. 34, 1429 (2003).
17. F. S. Brown, M. J. Baedecker, A. Nissenbaum, I. R. Kaplan, Geochim. Cosmochim. Acta 36, 1185 (1972).
18. M.-Y. Sun, S. G. Wakeham, Geochim. Cosmochim. Acta 58, 3395 (1994).
19. F. G. Prahl, G. J. De Lange, S. Scholten, G. L. Cowie, Org. Geochem. 27, 141 (1997).
20. Y. Huang, Soil Sci. Soc. Am. J. 63, 1181 (1999).
21. M. J. Kennedy, D. R. Pevear, R. J. Hill, Science 295, 657 (2002).
22. L. M. Mayer, L. L. Schick, K. R. Hardy, R. Wagai, J. McCarthy, Geochim. Cosmochim. Acta 68, 3863 (2004).
23. M. Church, O. Slaymaker, Nature 337, 452 (1989).
24. P. McLaren, T. Tuominen, in Health of the Fraser River Aquatic Ecosystem, a Synthesis of Research Conducted under the Fraser River Action Plan, DOE FRAP 1998-11, C. Colin, T. Tuominen, Eds. (Environment Canada, Vancouver, BC, Canada, 1999), vol. 1, chap. 3.4.
25. M. H. Conte, J. C. Weber, Global Biogeochem. Cyc. 16, 10.1029/2002GB001922 (2002).
26. R. H. Smittenberg et al., Paleoceanography 19, 10.1029/2003PA000927 (2004).
27. D. J. Kovanen, D. J. Easterbrook, Quat. Res. 57, 208 (2002).
28. J. W. Collister, É. Lichtfouse, G. Hieshima, J. M. Hayes, Org. Geochem. 21, 645 (1994).
29. G. Gleixner, et al., Org. Geochem. 33, 357 (2002).
30. E. Lichtfouse et al., Geochim. Cosmochim. Acta 61, 1891 (1997).
31. S. Trumbore, Ecol. Appl. 10, 339 (2000).
32. We thank the staff at the National Ocean Sciences Accelerator Mass Spectrometry Facility at Woods Hole, MA, USA, for help during preparation for ^{14}C analysis; M. Baas, M. Kienhuis (Royal Netherland Institute of Sea Research), and D. Montluçon (Woods Hole Oceanographic Institution) for assistance with the n-alkane isolation; The Ocean Drilling Project for providing subsamples obtained at leg 169S; and M. J. Whiticar (University of Victoria, Canada), for providing the pre- and post-bomb sediments. This research was primarily conducted by R.H.S., supported by a grant to J.S.S.D. from the Research Council for Earth and Life Science (ALW) with financial support from the Netherlands Organization for Scientific Research (NWO), and a grant to T.I.E. from NSF (OCE-0137005).

Recent Greenland Ice Mass Loss by Drainage System from Satellite Gravity Observations

S. B. Luthcke,[1]* H. J. Zwally,[2] W. Abdalati,[2] D. D. Rowlands,[1] R. D. Ray,[1] R. S. Nerem,[3] F. G. Lemoine,[1] J. J. McCarthy,[4] D. S. Chinn[4]

Mass changes of the Greenland Ice Sheet resolved by drainage system regions were derived from a local mass concentration analysis of NASA–Deutsches Zentrum für Luft- und Raumfahrt Gravity Recovery and Climate Experiment (GRACE mission) observations. From 2003 to 2005, the ice sheet lost 101 ± 16 gigaton/year, with a gain of 54 gigaton/year above 2000 meters and a loss of 155 gigaton/year at lower elevations. The lower elevations show a large seasonal cycle, with mass losses during summer melting followed by gains from fall through spring. The overall rate of loss reflects a considerable change in trend (−113 ± 17 gigaton/year) from a near balance during the 1990s but is smaller than some other recent estimates.

Mass changes in the Greenland Ice Sheet are of considerable interest because of its sensitivity to climate change and the potential for an increasing contribution of Greenland ice loss to rising sea level. Observations and models have shown that in recent years Greenland has experienced increased melt (1), thinning at the margins (2–4), and increased discharge from many outlet glaciers (5). At the same time, the ice sheet has been growing in its interior (3, 4, 6).

These recent changes in the Greenland Ice Sheet and the wide range of mass-balance estimates (7) highlight the importance of methods for directly observing variations in ice sheet mass. Moreover, the fact that some regions are shedding mass dramatically, whereas others are not (2–5), indicates a clear need for measurements with a spatial resolution that allows assessment of the behavior of individual drainage systems (DSs). The local mass concentration analysis presented here provides an assessment of mass balance of individual Greenland DS regions, subdivided by elevation, as well as the overall ice sheet mass balance.

Direct measurements of mass change have been enabled by the NASA–Deutsches Zentrum für Luft- und Raumfahrt Gravity Recovery and Climate Experiment (GRACE) mission (8). Since its launch in March 2002, GRACE has been acquiring ultra-precise (0.1 μm/s) intersatellite K-band range and range rate (KBRR) measurements taken between two satellites in polar orbit about 200 km apart. The changes in range rate sensed between these satellites provide a direct mapping of static and time-variable gravity.

Recent GRACE-based mass balance estimates of Antarctica (9) and Greenland (10, 11) have been derived from the monthly spherical-harmonic gravity fields produced by the GRACE project. Although these solutions represent an important advance in the use of gravity measurements to assess ice sheet mass balance, they are limited in their temporal and spatial resolution. For example, the recent results presented in (11) showed sizable mass loss spread over the entire Greenland continent, in contrast with recent studies that indicated loss concentrated on the margins (2–5) and growth in the interior (3, 4, 6). In addition, the fundamental measurements being made by GRACE contain far more information than is currently being exploited by techniques that rely on these monthly

[1]Planetary Geodynamics Laboratory, Code 698, NASA Goddard Space Flight Center, Greenbelt, MD 20771, USA. [2]Cryospheric Sciences Branch, Code 614.1, NASA Goddard Space Flight Center, Greenbelt, MD 20771, USA. [3]Colorado Center for Astrodynamics Research, Cooperative Institute for Research in Environmental Sciences, Department of Aerospace Engineering Sciences, University of Colorado, Boulder, CO 80309, USA. [4]Science Division, SGT Incorporated, Greenbelt, MD 20770, USA.

*To whom correspondence should be addressed. E-mail: Scott.B.Luthcke@nasa.gov

spherical-harmonic fields. Close examination of the KBRR measurements reveals coherent mass variation signals at better-than-400-km full wavelength spatial and 10-day temporal resolution at the mid-latitudes (12) and still better resolution at high latitudes.

Our approach to estimating ice sheet mass changes followed a strategy of preserving the gravity information contained within the GRACE KBRR observations. This was accomplished through an innovative processing of the GRACE intersatellite range-rate measurements (13) and the parameterization of local mass variations as mass concentrations (mascons). Mascons were estimated from short arc solutions of GRACE KBRR data exclusively within a local area of interest (12). The regional solution exploits the fact that the signal from a mass concentration observed in the GRACE KBRR data is centered over the mass concentration and is spatially limited in extent. The mathematical formulation of mascon parameters, the details of the local mascon approach, and the results of a simulation that validate the method are provided in (14). The results of the simulations show that the mascon approach is capable of recovering the spatial distribution and magnitude of realistic and complex ice mass change signal to better than 90% (14).

For our ice sheet analysis, a mascon parameter corresponds to a surplus or deficit of mass in an irregularly shaped DS region (Fig. 1) defined by surface slopes and climatology (15) and subdivided into surface elevation above and below 2000 m. Exterior regions (as outlined in Fig. 1) as well as daily baseline state parameters were estimated to account for mass variations occurring outside our Greenland DS regions of interest (14). The mascon estimates are relative to models of both static and time varying gravity effects (e.g., tides and atmospheric mass redistribution) in order to isolate ice mass change (14).

We derived mascon solutions from GRACE KBRR data for each DS region (Fig. 1) every 10 days from July 2003 through July 2005 (Table 1). The individual elevation-dependent mascon solution time series can be summed over each 10-day interval to produce time series for the six overall DSs (Fig. 2) and time series for regions above and below 2000 m elevation (Fig. 3). The results (Table 1 and Figs. 2 and 3) represent the total observed mass variation, including the trends from glacial isostatic adjustment (GIA). Included separately in Table 1 is the computed GIA trend from ICE-5G using a 90-km lithosphere and VM2 viscosity model (16).

The northern DSs 1 and 2 and the southwest DS 5 are nearly in mass balance (Fig. 2), considering the associated error bars and the GIA noted in Table 1. DSs 3, 4, and 6 all exhibit significant mass loss, with DS 4, the southeast, dominating the overall mass loss. Figure 3 presents our mascon time series for the regions above and below 2000-m elevation. For the 2 years (July 2003 to July 2005), our solutions

(Fig. 3) show a moderate growth of 54 ± 12 Gton/year for the high-elevation Greenland interior, with a significant loss of 155 ± 26 Gton/year occurring in the low-elevation coastal regions. Therefore, we obtain a total Greenland trend of –101 ± 16 Gton/year. These trends have been corrected for GIA and scaled by 1.1 to account for potential signal loss as determined in the simulation analysis (14). Treatment of the associated errors is discussed in (14). The mass loss is dominated by loss in the eastern low-elevation coastal regions and the southeast DS 4. Our overall Greenland mass trend of –101 ± 16 Gton/year is consistent with the GRACE-based analysis by (17), which determined a trend of –118 ± 14 Gton/year for the time period of July 2002 to March 2005. However, these overall trends are nearly a factor of 2 smaller than the recent GRACE-based trend determined in (11). The results presented in (11) show significant

mass loss over the entire continent and therefore are difficult to reconcile with known mass loss concentrated in the low-elevation coastal regions and gain in the interior.

The high-elevation interior region solutions show little annual cycle, with an overall amplitude of 13 ± 9 Gton, whereas in contrast the low-elevation coastal region solutions resolve a significant annual cycle with an amplitude of 150 ± 27 Gton (Table 1 and Fig. 3). The annual cycle of the low-elevation coastal region exhibits significant mass shedding beginning in May-June and ending in October, corresponding to summer melt (Fig. 3). The largest annual cycle is found in the southwest DS 5. A nearly semiannual signal most noticeable in DS 2 is an artifact caused by mismodeled ocean tides (14).

The temporal and spatial resolution of the GRACE mascon solutions provides important insights into the ice sheet behavior and the
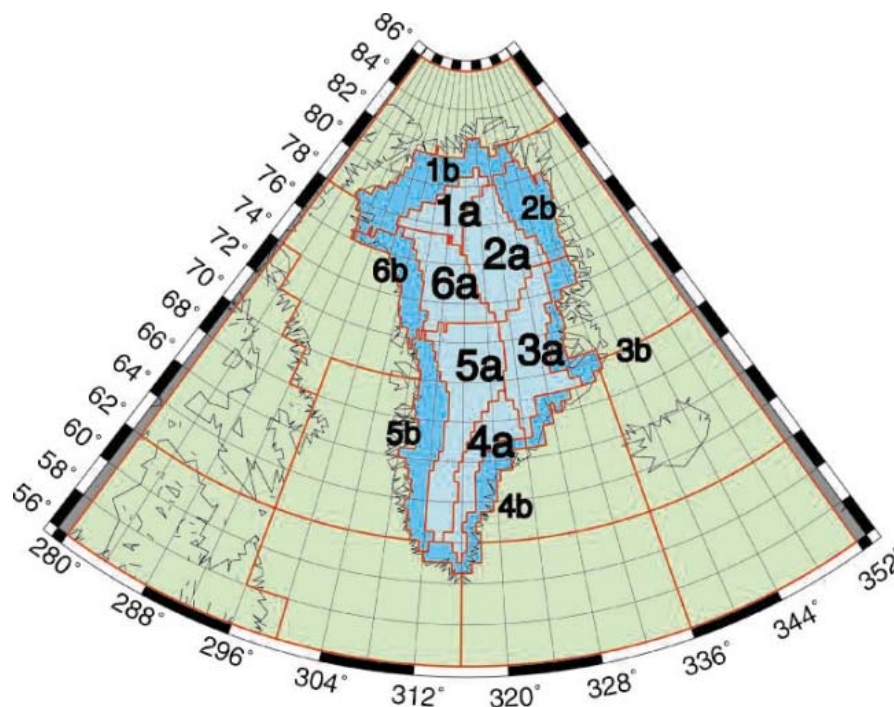
Fig. 1. Greenland DS mascon regions: regions above 2000 m elevation are labeled "a," and those below are labeled "b." Exterior region mascons outside of Greenland are also shown outlined in red.

Table 1. Summary of Greenland drainage system mascon solutions above and below 2000-m elevation (July 2003 to July 2005). GIA calculated from ICE-5G with use of a 90-km lithosphere and VM2 viscosity model (16).

Drainage system	Observed mass change (Gton/year)		GIA (Gton/year)		Annual amplitude (Gton)	
	>2000 m	<2000 m	>2000 m	<2000 m	>2000 m	<2000 m
1	13 ± 2	−4 ± 4	0	2	7 ± 2	34 ± 5
2	40 ± 2	−32 ± 2	−1	2	12 ± 2	11 ± 3
3	50 ± 3	−75 ± 2	−1	0	8 ± 4	24 ± 2
4	−38 ± 11	−33 ± 3	−1	0	12 ± 13	33 ± 3
5	3 ± 3	−3 ± 13	−4	−3	19 ± 3	62 ± 14
6	−27 ± 3	6 ± 5	−1	0	14 ± 3	20 ± 6
Greenland	41 ± 8	−140 ± 24	−8	1	13 ± 9	150 ± 27

quality of the mascon solutions. The moderate growth of the high-elevation interior ice sheet with significant mass shedding of the low-elevation coastal regions is consistent with other recent studies (1–6). In addition, the solutions exhibit a relatively small annual cycle for the high-elevation interior ice sheet, consistent with low temperatures, negligible melting, and small seasonal variation in precipitation. The low elevations show a large annual cycle, with the largest in the southwest DS 5. These results are consistent with warm summer temperatures of the coastal regions in general and, combined with shallow slopes for DS 5 in particular, lead to the most extensive summer melt (18). There-fore, our mascon time series for the low eleva-tions exhibit seasonal characteristics that are very consistent with the well-known net ab-lation during summer melt followed by growth during winter, as shown for example by radar altimeter data (3) and surface mass balance models (19).

Comparison of our 2003–2005 ice mass trends by DS in Table 2 to the 1992–2002 trends computed from satellite radar and airborne laser altimetry (3) provides insights into the evolution of the ice sheet. The changes of the trends with time of the two most northerly DSs, 1 and 2, are not significantly different from zero, which is consistent with the lack of glacier acceleration

(5) or detected icequakes (20) reported for those areas. DS 3 in the east appears to have changed by –20 Gton/year from a slightly negative balance (–5 Gton/year) to a significantly nega-tive overall balance of –25 Gton/year, with very large mass shedding in the low-elevation coastal region and growth at high elevations (Table 1). Although DS 3 had one accelerating glacier (5) and icequakes in two glaciers (20), it has also had a large average annual mass input of 42 Gton/year (3) and is therefore very sensitive to interannual variations or trends in precipitation and ice accumulation. Our largest observed change (–61 Gton/year) occurred in DS 4 in the southeast, whereas the other significant negative change occurred in DS 6 in the west (–32 Gton/year), consistent with glacier accel-erations (5) and increases in icequakes (20) in that system. In particular, the acceleration of three glaciers in DS 4 indicated an increase in the rate of loss in 2005, compared with that in 1996, of –56 Gton/year (5), which is comparable to our change of –61 Gton/year. In DSs 5 and 6, the change from glacier accelerations was –25 Gton/year (5), which compares well with our total change of –37 Gton/year that includes changes in surface balance as well as changes in glacier discharge. Although the extent to which meaningful conclusions can be drawn from a 2-year time series is limited because of the influence of interannual variations, the consist-ency of our results with all other indications of accelerating mass loss (1, 4, 5, 19) strongly sup-ports our interpretation that a significant change in the Greenland mass balance has occurred primarily in DSs 3, 4, and 6.

The high temporal resolution of the mascon solutions provides unprecedented observation of mass change events and provides the opportu-nity to apply filtering techniques to reduce the solution noise. By reliably resolving ice mass change observations into ice sheet DS scales subdivided by surface elevation, the mascon solutions provide the ability to separate the areas of rapid loss [e.g., the southeast DS 4 and the low-elevation coastal regions (Figs. 2 and 3)] from areas of slower loss or even gain (e.g., high-elevation interior regions). The mascon solutions provide a better basis for comparison to passive microwave-derived melt data (18) and surface mass balance models (19) and facilitate the comparison to flux-based methods (5) and altimetric methods (2–4, 6, 21) that examine individual drainage basins.

Our GRACE mascon solutions provide a direct measure of mass changes on the scale of DSs subdivided into regions above and below 2000-m surface elevation. In contrast with other recent gravity-based mass balance estimates (10, 11, 17), our mascon solutions exhibit improved spatial resolution, delineating high-elevation interior region growth and substantial mass loss for the low-elevation coastal regions. In addition, the mascon solutions show improved temporal resolution, delineating the large season-
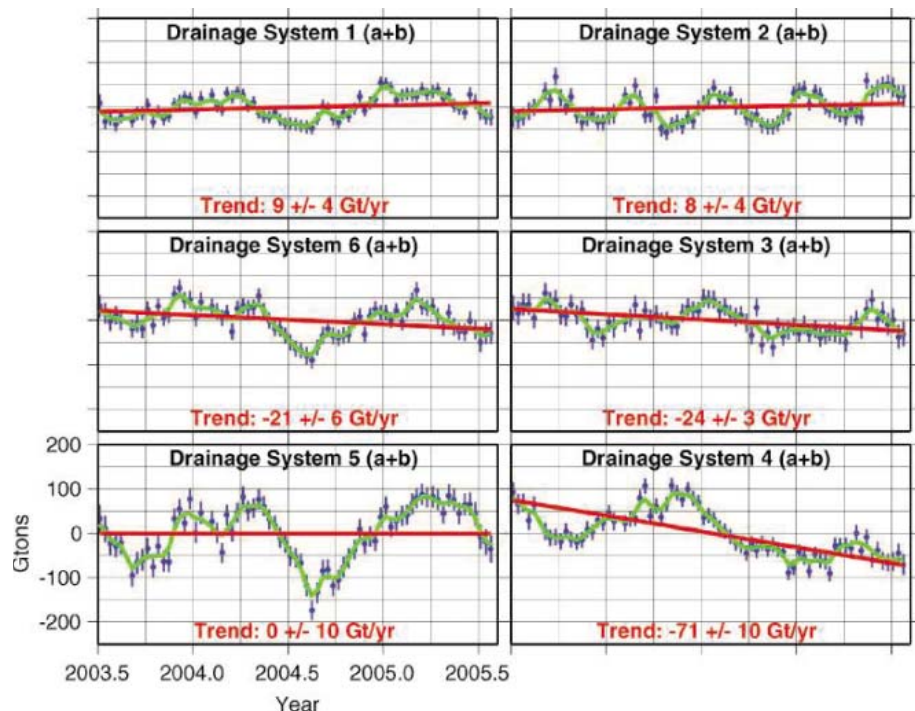
Fig. 2. Greenland drainage systems 2-year (July 2003 to July 2005) mascon time series (summing regions above and below 2000-m elevation for each system) derived from GRACE KBRR data: 10-day estimates (blue dots with error bars); Gaussian 1-day filter with 30-day window applied to 10-day estimates (green line); and trend (red line) recovered from simultaneous estimation of bias, trend, annual and semi-annual sinusoid. Trends have not been corrected for GIA. Error bars indicate 1-σ calibrated uncertainties. Gt/yr, Gton/year.
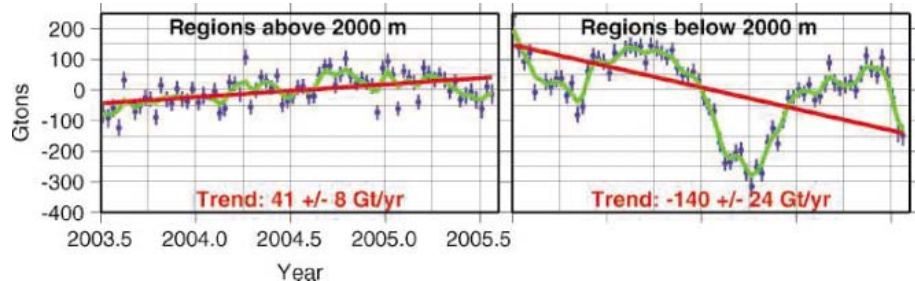
Fig. 3. Time series computed from the sum of mascon region solutions above and below 2000-m elevation: 10-day estimates (blue dots with error bars); Gaussian 1-day filter with 30-day window applied to 10-day estimates (green line); and trend (red line) recovered from simultaneous estimation of bias, trend, annual and semi-annual sinusoid. Trends have not been corrected for GIA. Error bars indicate 1-σ calibrated uncertainties.

Table 2. Comparison of mascon-derived trends with previous values determined from satellite and airborne altimetry (*3*). The mascon-derived trends were corrected for GIA and potential signal loss (~9%) as determined from simulation analysis (*14*). Errors computed as in (*14*) along with assuming 100% error in GIA.

Drainage system	2003–2005 mascon-derived ice mass trend (Gton/year)	1992–2002 altimeter-derived ice mass trend (*3*) (Gton/year)	Delta (2003–2005) − (1992–2002) (Gton/year)
1	8 ± 5	1.6 ± 0.3	6 ± 5
2	8 ± 4	8.8 ± 0.2	−1 ± 4
3	−25 ± 4	−4.9 ± 2.0	−20 ± 4
4	−77 ± 11	−15.7 ± 1.2	−61 ± 11
5	7 ± 13	11.4 ± 0.8	−5 ± 13
6	−22 ± 7	10.5 ± 0.5	−32 ± 7
Greenland	−101 ± 16	11.7 ± 2.5	−113 ± 17

al cycle for the low-elevation coastal regions and observing the summer melt and winter growth cycles. Our finding of an overall mass loss of 101 ± 16 Gton/year for 2003 to 2005 is consistent with the finding of near balance during the 1990s (*3*) and with the recent results on increased melt rates (*1*), acceleration of outlet glaciers (*5, 20*), and the increasingly negative surface balance in recent years (*22*). The Greenland mass loss contributes 0.28 ± 0.04 mm/year to global sea level rise, which is nearly 10% of the 3 mm/year rate recently observed by satellite altimeters (*23*). The observed change from the 1990s of −113 ± 17 Gton/year represents a change from a small growth of about 2% of the annual mass input to a loss of about 20%, which is a significant change over a period of less than 10 years (*24*). This result is in very good agreement with the change in trend of −117 Gton/year from 1996 to 2005 determined from radar interferometry (*5*). During the 1990s, the observed thinning at the margins and the growth inland were both expected responses to climate warming. Our new results suggest that the processes of significant ice depletion at the margins, through melting and glacier acceleration, are beginning to dominate the interior growth as climate warming has continued.

References and Notes

1. An update of (*18*) posted at http://cires.colorado.edu/science/groups/steffen/greenland/melt2005 shows a 31% increase in mean melt area between 1979 and 2005.
2. W. Krabill *et al.*, *Geophys. Res. Lett.* **31**, L24402 (2004).
3. H. J. Zwally *et al.*, *J. Glaciol.* **51**, 509 (2005).
4. R. Thomas *et al.*, *Geophys. Res. Lett.* **33**, L10503 (2006).
5. E. Rignot, P. Kanagaratnam, *Science* **311**, 986 (2006).
6. O. M. Johannessen, K. Khvorostovsky, M. W. Miles, L. P. Bobylev, *Science* **310**, 1013 (2005); published online 20 October 2005 (10.1126/science.1115356).
7. For mass balance within the 1992–2002 time period, the following estimates have been published: +11 ± 3 Gton/year for 1992–2002 (*3*), −46 Gton/year for 1993/4 – 1998/9 (*21*), −72 ± 11 Gton/year for 1997–2003 (*2*), and −83 ± 29 and −127 ± 29 Gton/year for 1996 and 2000, respectively (*5*). If the correction for firn compaction used in the radar altimeter analysis (*3*) is applied to the airborne altimeter estimates (*2, 4, 21*), the difference between the two approaches is reduced by about 23 Gton/year, as reflected by revised airborne values of −4 to −50 Gton/year for 1993 to 1999 (*4*).
8. B. D. Tapley, S. Bettadpur, J. C. Ries, P. F. Thompson, M. M. Watkins, *Science* **305**, 503 (2004).
9. I. Velicogna, J. Wahr, *Science* **311**, 1754 (2006); published online 1 March 2006 (10.1126/science.1123785).
10. I. Velicogna, J. Wahr, *Geophys. Res. Lett.* **32**, L18505 (2005).
11. J. L. Chen, C. R. Wilson, B. D. Tapley, *Science* **313**, 1958 (2006); published online 10 August 2006 (10.1126/science.1129007).
12. D. Rowlands *et al.*, *Geophys. Res. Lett.* **32**, L04310 (2005).
13. S. B. Luthcke *et al.*, *Geophys. Res. Lett.* **33**, L02402 (2006).
14. Materials and methods are available as supporting material on *Science* Online.
15. H. J. Zwally, M. B. Giovinetto, *Ann. Glaciol.* **31**, 126 (2000).
16. W. R. Peltier, *Annu. Rev. Earth Planet. Sci.* **32**, 111 (2004).
17. G. Ramillien *et al.*, *J. Global Planet. Change* **53**, 10.1016/j.gloplacha.2006.06.003 (2006).
18. W. Abdalati, K. Steffen, *J. Geophys. Res.* **106**, 33983 (2001).
19. J. E. Box *et al.*, *J. Clim.* **19**, 2783 (2006).
20. G. Ekstrom, M. Nettles, V. C. Tsai, *Science* **311**, 1756 (2006).
21. W. Krabill *et al.*, *Science* **289**, 428 (2000).
22. E. Hanna *et al.*, *J. Geophys. Res.* **110**, D13108 (2005).
23. A. Cazenave, R. S. Nerem, *Rev. Geophys.* **42**, 10.1029/2003RG000139 (2004). An update is posted at http://sealevel.colorado.edu.
24. For the 1990s, we used the small 11 Gton/year mass gain from (*3*) and noted that the negative balances discussed in (*7*) either would give significantly less negative changes than 113 Gton/year or would give positive changes, in contradiction to the evidence for increases in melt and glacier accelerations. Also, our 113 ± 17 Gton/year is in good agreement with the change in mass flux of 117 Gton/year from 1996 to 2005 from radar interferometry (*5*).
25. We acknowledge NASA's Solid Earth and Natural Hazards Program, NASA's Cryospheric Sciences Program, and NASA's Ice, Cloud, and Land Elevation Satellite and GRACE missions for their support of this research and the quality of the GRACE Level 1B products produced by our colleagues at the Jet Propulsion Laboratory. We thank S. Klosko, T. Williams, and D. Pavilis for their many contributions and the reviewers for their astute commentary.

Abundance Distributions Imply Elevated Complexity of Post-Paleozoic Marine Ecosystems

Peter J. Wagner,[1]* Matthew A. Kosnik,[2] Scott Lidgard[1]

Likelihood analyses of 1176 fossil assemblages of marine organisms from Phanerozoic (i.e., Cambrian to Recent) assemblages indicate a shift in typical relative-abundance distributions after the Paleozoic. Ecological theory associated with these abundance distributions implies that complex ecosystems are far more common among Meso-Cenozoic assemblages than among the Paleozoic assemblages that preceded them. This transition coincides not with any major change in the way fossils are preserved or collected but with a shift from communities dominated by sessile epifaunal suspension feeders to communities with elevated diversities of mobile and infaunal taxa. This suggests that the end-Permian extinction permanently altered prevailing marine ecosystem structure and precipitated high levels of ecological complexity and alpha diversity in the Meso-Cenozoic.

Marine ecosystem complexity is thought to have increased over the past 540 million years, in terms both of the alpha [i.e., local (*1*)] diversity of fossilized assemblages and of the numbers of basic ecological types (i.e., "guilds") (*2–5*). Ecological theory predicts that ecosystem complexity affects relative-abundance distributions (RADs) (*6*). Therefore, if fossiliferous assemblages adequately reflect original communities, then RADs implying interactions and/or a multiplicity of basic ecologies should become more common over time, and

RADs implying simple partitioning and/or limited interaction should become less common. Taphonomic studies show that death assemblages can accurately reflect one aspect of RADs of skeletonized taxa within living communities, namely, rank-order abundance (*7*). Moreover, paleoecological

[1]Department of Geology, Field Museum of Natural History, 1400 South Lake Shore Drive, Chicago, IL 60605, USA. [2]School of Marine and Tropical Biology, James Cook University, Townsville, QLD 4811, Australia.

*To whom correspondence should be addressed. E-mail: pwagner@fmnh.org

studies can detect different model RADs (8, 9). Both findings suggest that the fossil record can test the proposition that marine community structure changed over the Phanerozoic.

RAD evenness (i.e., uniformity of abundances in an assemblage) is greater in the Meso-Cenozoic than in the Paleozoic, which is expected if alpha diversity of Meso-Cenozoic communities is generally greater than that of Paleozoic communities (4). However, evenness is only one aspect of a RAD. Different ecological models for community assembly make more explicit predictions about specific RAD types found in natural communities: (i) geometric or log-series: species entering a community preempt a remaining portion of the available resources without increasing the total resources in the ecosystem (10); (ii) zero-sum multinomial: intrinsic properties affecting migration, origination, and extinction rates affect RADs rather than do ecological interactions among species (11); (iii) Zipf or lognormal: new species increase ecospace, either by facilitating opportunities for additional species (12) or by niche construction (13); and (iv) lognormal: multiple diverse guilds (i.e., groups playing similar general ecological roles) each have their own distributions, but the pool of these distributions is lognormal (6).

Scenarios (iii) and (iv) both require more numerous ecological processes and allow for greater varieties of taxa than do scenarios (i) and (ii). Thus, a shift from ecologically "simple" RADs (i.e., geometric or zero-sum) to ecologically "complex" RADs (i.e., Zipf or lognormal) should accompany an increase in ecological and alpha diversity.

We examined 1176 fossiliferous assemblages of macroinvertebrate marine species with abundance data from the Paleobiology Database (14) to determine whether the frequency of model RADs among Meso-Cenozoic assemblages differs from those of Paleozoic assemblages in a manner consistent with either increased interactions among species shaping community structure and/or elevated diversity of ecological guilds. For each assemblage, we determined the most likely representatives among the four general RAD models [fig. S3 (15)] based on the probability of observing X species with 1… n specimens given a sample size of n [fig. S4]. We then assessed the models using Akaike's weights based on Akaike's modified information criterion [AICc (16)]. We rejected alternative hypotheses if the weight of one hypothesis was 0.89 or greater (17).

Geometric and lognormal are the most common RADs. Considering just these two RADs, geometrics best fit Paleozoic assemblages about as frequently as lognormals do. However, geometrics best fit Meso-Cenozoic assemblages about one-quarter as frequently as lognormals do (Fig. 1A). Limiting the analyses to the 681 significant assemblages given Akaike weights and comparing just simple versus complex RADs shows that, whereas simple and complex

assemblages are equally common in the Paleozoic, complex RADs typically are three to four times as common as are simple RADs in the Meso-Cenozoic (Fig. 1B) (18). The Cambrian might represent a third ratio of simple:complex assemblages. However, few Cambrian assemblages include 10+ taxa, which results in a small number of analyzed assemblages and thus large support bars that overlap those of other Paleozoic periods. Thus, we cannot currently reject the null hypothesis of a consistent Paleozoic ratio.

Because we are examining preserved assemblages rather than original communities, we must consider factors other than original community structure that might account for these results. Numbers of specimens per collection do not differ markedly between analyzed Paleozoic and Meso-Cenozoic collections, which precludes some methodological artifact based on sample size (Fig. 2A) (19). The numbers of classes per analyzed collection typically are higher for Paleozoic collections than for Meso-Cenozoic ones, which contradicts the idea of single-taxon

Paleozoic lists implying overly simple RADs (Fig. 2B). Lithified rocks discourage the sampling of small and aragonitic specimens. Similarly, siliciclastic and carbonate sediments represent both different preservation and general ecological regimes, and siliciclastic sediments become decreasingly common over the Phanerozoic (20).

Fig. 2. Distributions of potential biasing factors over time. Box plots in (A) and (B) encompass 50% and error bars encompass 90% of the data. (**A**) Average numbers of specimens per analyzed assemblage. n, number of assemblages in each geologic period. (**B**) Number of classes present in assemblages. (**C**) Proportions of general preservational and environmental types with binomial error bars (19). "Lithified" gives proportions of analyzed assemblages identified as "lithified" rather than "poorly lithified" or "unlithified." "Carbonate" gives the proportions of analyzed assemblages with carbonate rather than siliciclastic or mixed siliciclastic/carbonate sediments. Lithification and basic sediment type can vary independently.

Fig. 1. Proportions of assemblages that best fit different RAD models. Error bars give one unit of support (18); if support bars do not overlap for the same model(s), then we reject the idea of the same proportions in those intervals. Dashed line separates Paleozoic from Meso-Cenozoic. (**A**) Results for all assemblages showing percentages that fit geometric better than lognormal and vice-versa. (**B**) Results from the 681 significant assemblages where the combined Akaike weights of the two simple (geometric or zero-sum multinomial) or two complex (Zipf or lognormal) models exceed 0.89.

However, the shifts in lithified collections and siliciclastic/carbonate collections do not coincide with the RAD transition (Fig. 2C). Finally, analyses restricted to any one of these partitions replicate the overall pattern (tables S1 to S3 and figs. S5 to S8).

Worker bias also is unlikely given that the assemblages reflect 190 different studies and no single worker or study dominates the whole of either the Paleozoic or Meso-Cenozoic. Shifts in other taphonomic patterns, such as elevated preservation potential of aragonitic skeletons, happen after the Jurassic (21). Our study necessarily omits nonskeletonized organisms that contributed to the original RADs. However, the random removal of taxa from particular RADs tends to encourage a lognormal distribution as well as reduce test power, and thus biases the results against our findings. Moreover, there is no a priori reason to assume that frequencies of soft-bodied organisms occupying the same general habits as skeletonized organisms differed markedly between the Paleozoic and Meso-Cenozoic.

With little support for nonbiological explanations for differences between Paleozoic and post-Paleozoic RAD, our results imply a change in general structure. Ecological theory provides at least two nonexclusive explanations for the shift in RADs, both of which imply elevated ecological complexity in the Meso-Cenozoic. One is a higher diversity of basic ecological guilds in the Meso-Cenozoic (2, 3). Even if taxa within different ecological guilds partition ecospace simply, then averaging across different distributions typically yields a lognormal distribution. Log-series, which are nearly identical to geometrics, better fit RADs for Cenozoic foraminifera in most cases than do lognormals (9), which corroborates this idea.

A second explanation is that guilds and/or taxa that become diverse in the Meso-Cenozoic are more prone to complex RADs. Mobile epifaunal and infaunal macroinvertebrates (especially bivalves and gastropods) that actively seek out nutrients typify major Meso-Cenozoic guilds, whereas sessile organisms (especially brachiopods) that filter nutrients suspended above the sediment-water interface typify major Paleozoic guilds (2, 5). The former taxa also tend to be metabolically buffered from the physical environment to a much greater extent than do the latter taxa (5). Notably, this transition marks a change in dominance as well as in richness (22). For example, "modern" infaunal bivalves and carnivorous gastropods that so pervade later benthic assemblages also occur in the Paleozoic, where they are seldom diverse or common even in collections preserving aragonitic shells. Actively mobile taxa might be more apt to increase ecospace usage either by creating additional ecological opportunities for other taxa or through niche construction and more complex interaction webs than are sessile suspension feeders such as brachiopods or crinoids (13, 23). Indeed, common Meso-Cenozoic sessile suspension feeders such as reef-building corals engineer their environments extensively, whereas living brachiopods and crinoids do not. Similarly, high-metabolism, environmentally buffered organisms might be more capable of inserting themselves into more varied ecosystems. A weak positive correlation does exist between the proportion of specimens that are mollusks and the Akaike weight of the complex RADs among the 43 Paleozoic assemblages with 10+ mollusk species and 100+ mollusk specimens. This is consistent with the idea that molluscan ecology helps drive the pattern. However, sessile brachiopods often dominated Triassic and even Jurassic ecosystems, which is inconsistent with this idea (24).

Increasing frequencies of "complex" RADs have implications for why sampled and inferred alpha diversity apparently increase over the Phanerozoic (4, 25). We typically expect to sample fewer taxa from geometric RADs than from lognormal or Zipf RADs, even when all other parameters (true richness, sample size, and evenness) are the same (26). This might imply that Paleozoic faunas have a greater potential for hiding species than do Meso-Cenozoic ones. However, this mathematical possibility is biologically implausible. Among the 143 Paleozoic assemblages that best fit a geometric RAD, the median model posits 22 taxa with abundance frequencies $(f) \geq 10^{-4}$. This requires thousands of individuals to have even a small population of a 22nd taxon. Among the 376 Meso-Cenozoic assemblages that best match a lognormal RAD, the median model posits 84 taxa with $f \geq 10^{-4}$. Even if one limits comparisons to lognormal assemblages, then one finds that the median parameters posit only 35 taxa with $f \geq 10^{-4}$ for the 122 Paleozoic assemblages that best match the lognormal RAD. Thus, the shift from the Paleozoic to the post-Paleozoic world involves an increase in basic alpha diversity as well as in the frequency of RADs implying complex ecosystems.

Finally, the change in typical RADs coincides with the end-Permian extinction. Our results are consistent with evidence that this mass extinction drastically reorganized the marine ecosystem (27). In particular, the results are consistent with proposals for especially catastrophic causal mechanisms (28) and drastic reorganizations of marine ecosystem structure after the extinction (2, 29). The shift to common "complex" RADs also offers an explanation for the change from extinction-driven to origination-driven diversity dynamics (30). If taxa that require "openings" in ecospace predominate, then diversification should be tied to extinction enabling incipient species to become established. Conversely, if predominant taxa tend to increase interactions and create ecological opportunities for (or facilitate the ecological persistence of) other taxa, then diversification should be a product of the frequency at which incipient species appear and the probability of those species creating a new niche and/or fitting into a potentially open one. Because generic diversification should reflect underlying species diversification, the shift in dominant taxa would affect not just RADs but also macroevolutionary dynamics. Thus, the end-Permian seemingly altered not just taxonomic diversity (27) but also predominant evolutionary and ecological dynamics.

References and Notes

1. R. H. Whittaker, *Taxon* **21**, 213 (1972).
2. R. K. Bambach, in *Biotic Interactions in Recent and Fossil Benthic Communities,* M. Tevesz, P. L. McCall, Eds. (Plenum, New York, 1983), pp. 719–746.
3. W. I. Ausich, D. J. Bottjer, in *Phanerozoic Diversity Patterns-Profiles in Macroevolution,* J. W. Valentine, Ed. (Princeton University Press, Princeton, NJ, 1985), pp. 255–274.
4. M. G. Powell, M. Kowalewski, *Geology* **30**, 331 (2002).
5. R. K. Bambach, A. H. Knoll, J. J. Sepkoski Jr., *Proc. Natl. Acad. Sci. U.S.A.* **99**, 6854 (2002).
6. J. S. Gray, in *Organization of Communities Past and Present,* J. H. R. Gee, P. S. Gillier, Eds. (Blackwell, Oxford, 1987), pp. 53–67.
7. S. M. Kidwell, *Science* **294**, 1091 (2001).
8. T. D. Olszewski, D. H. Erwin, *Nature* **428**, 738 (2004).
9. M. A. Buzas, L.-A. C. Hayek, *Paleobiology* **31**, 199 (2005).
10. R. B. Root, *Ecol. Monogr.* **37**, 317 (1967).
11. S. P. Hubbell, *The Unified Neutral Theory of Biodiversity and Biogeography* (Princeton University Press, Princeton, NJ, 2001).
12. S. Frontier, in *Oceanography and Marine Biology: An Annual Review,* M. Barnes, Ed. (Aberdeen Univ. Press, Aberdeen, 1985), pp. 253–312.
13. K. N. Laland, F. J. Odling-Smee, M. W. Feldman, *Proc. Natl. Acad. Sci. U.S.A.* **96**, 10242 (1999).
14. Paleobiology Database, http://paleodb.org. See (31).
15. Materials and methods are available as supporting material on *Science* Online.
16. AICc = −2 lnL(Hypothesis) + 2K[n/(n − K − 1)], where K is the number of parameters and n is the number of data points (32). This is identical to AIC(Hypothesis) + [2K(K + 1)]/(n − K − 1). Akaike's weight (w_i) for each hypothesis is, $w_i = (e^{-\Delta i/2})/\sum(e^{-\Delta j/2})$, where Δ is the difference between the AICc of the best hypothesis and the hypothesis i.
17. The individual "weight" of each hypothesis is proportional to the probability of the data given that hypothesis, slightly modified by the number of parameters and data points (33). The cutoff of 0.89 is akin to the likelihood testing criterion of rejecting hypotheses when an outcome is eight times (or more) less probable for one hypothesis than for another.
18. A. W. F. Edwards, *Likelihood, Expanded Edition* (Johns Hopkins Univ. Press, Baltimore, 1992).
19. D. M. Raup, in *Analytical Paleobiology,* N. L. Gilinsky, P. W. Signor, Eds. (Paleontological Society, Knoxville, TN, 1991), vol. 4, pp. 136–156.
20. L. J. Walker, B. H. Wilkinson, L. C. Ivany, *J. Geol.* **110**, 75 (2002).
21. M. Kowalewski et al., *Paleobiology* **32**, 533 (2006).
22. M. E. Clapham et al., *Palaios* **21**, 431 (2006).
23. P. D. Roopnarine, *Paleobiology* **32**, 1 (2006).
24. M. Aberhan, *Palaios* **9**, 516 (1994).
25. A. M. Bush, R. K. Bambach, *J. Geol.* **112**, 625 (2004).
26. M. A. Kosnik, P. J. Wagner, *Evol. Ecol. Res.* **8**, 197 (2006).
27. D. H. Erwin, *Extinction: How Life on Earth Nearly Ended 250 Million Years Ago* (Princeton Univ. Press, Princeton, NJ, 2006).
28. A. H. Knoll, R. K. Bambach, D. E. Canfield, J. P. Grotzinger, *Science* **273**, 452 (1996).
29. M. L. Fraiser, D. J. Bottjer, *Comptes Rendus Palevol* **4**, 583 (2005).
30. M. Foote, *Paleobiology* **32**, 345 (2006).
31. Species data were downloaded on 6 November 2005. We limited analyses to marine assemblages with at least 100 specimens and at least 10 invertebrate taxa. The collections reflect 190 publications.

32. K. P. Burnham, D. R. Anderson, *Model Selection and Inference: A Practical Information-Theoretic Approach* (Springer, New York, ed. 2, 2002).
33. R. Royall, *Statistical Evidence: A Likelihood Paradigm* (Chapman and Hall, London, 1997).
34. T. D. Olszewski provided computer code to calculate zero-sum multinomials. R. Bambach, M. Foote, D. Jablonski,

Two Dobzhansky-Muller Genes Interact to Cause Hybrid Lethality in *Drosophila*

Nicholas J. Brideau,* Heather A. Flores,* Jun Wang,* Shamoni Maheshwari, Xu Wang, Daniel A. Barbash†

The Dobzhansky-Muller model proposes that hybrid incompatibilities are caused by the interaction between genes that have functionally diverged in the respective hybridizing species. Here, we show that *Lethal hybrid rescue* (*Lhr*) has functionally diverged in *Drosophila simulans* and interacts with *Hybrid male rescue* (*Hmr*), which has functionally diverged in *D. melanogaster*, to cause lethality in F1 hybrid males. LHR localizes to heterochromatic regions of the genome and has diverged extensively in sequence between these species in a manner consistent with positive selection. Rapidly evolving heterochromatic DNA sequences may be driving the evolution of this incompatibility gene.

Plant and animal hybrids are often sterile or lethal as a result of interspecific genetic divergence. The Dobzhansky-Muller model proposes that hybrid incompatibilities (HIs), which contribute to speciation, evolve as a consequence of interactions between or among genes that have diverged in each of the hybridizing species (*1*). Dobzhansky-Muller incompatibility

genes require three criteria: Each gene reduces hybrid fitness, has functionally diverged between the hybridizing species, and depends on the partner gene to cause HI (Fig. 1A). Major-effect HI genes have been discovered, and functional divergence of single genes has been demonstrated by genetic tests (*2*, *3*) or suggested by patterns of molecular evolution (*4*). Although HI systems composed of complementary factors have been described (*5*, *6*) and interacting genomic regions of hybridizing species identified (*7–9*), no pair of Dobzhansky-Muller genes has been reported. It remains unclear whether HI phenotypes can be explained even in part by two-locus interactions, or alternatively whether HIs require complex multilocus interactions (*10–12*).

Interspecific crosses of *D. melanogaster* females to *D. simulans* males produce no sons.

Department of Molecular Biology and Genetics, Cornell University, Ithaca, NY 14853, USA.

*These authors contributed equally to this work.
†To whom correspondence should be addressed. E-mail: dab87@cornell.edu
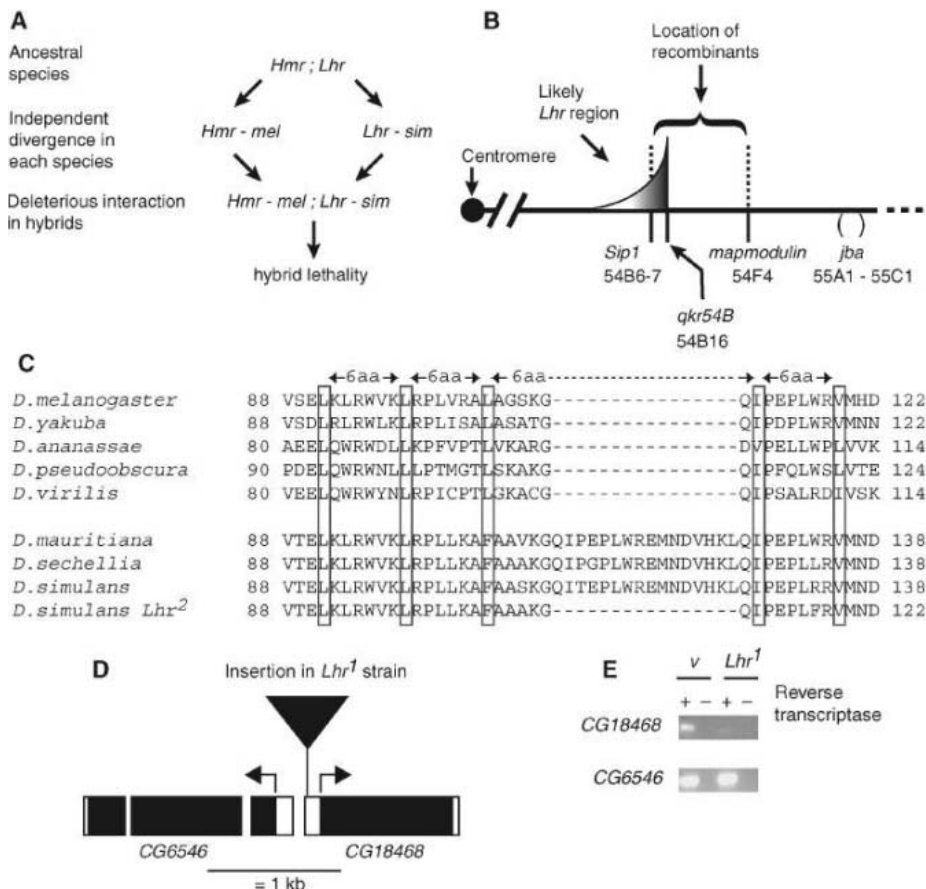
Fig. 1. *CG18468* encodes *Lhr*. (**A**) Model of *Hmr* and *Lhr* functional divergence and the interaction that causes hybrid lethality. Lethality results from the interaction between the *D. melanogaster Hmr* allele (*Hmr-mel*) and the *D. simulans Lhr* allele (*Lhr-sim*). (**B**) Map of *Lhr* region in *D. simulans*. Genetic markers and estimated cytological locations in *D. melanogaster* are shown below the line. Ten recombinants between *jba* and *Lhr* were selected and cross-overs mapped within a region of approximately 480 kb; the most proximal recombinant was between *Sip1* and *qkr54B* (diagram not to scale). (**C**) *CG18468* has a characteristic leucine zipper-like structure in all *Drosophila* species except *D. simulans*, *D. mauritiana*, and *D. sechellia*, which have a 16–amino acid insertion; this insertion is lacking in the *D. simulans* rescue strain *Lhr²*. (**D**) Map of *CG18468* region at 54B7 and insertion in the *Lhr¹* strain. Black boxes, coding regions; unfilled boxes, UTRs; arrows, predicted translation start sites. The large triangle represents an insertion of ~4 kb (triangle not to scale) located between nucleotides 11 and 13 of the predicted *CG18468* mRNA in *Lhr¹*. (**E**) The insertion in *Lhr¹* reduces the level of mRNA of *CG18468* but not of *CG6546*. RT-PCR with larval RNA from a *vermillion* (*v*)–marked *D. simulans* strain and from the *Lhr¹* strain.

The *D. simulans* mutation *Lhr*[1] suppresses the lethality of these F1 hybrid males (*13*). A mutant allele of the X-linked *D. melanogaster* gene *Hmr* similarly suppresses hybrid male lethality (*14*). *Hmr* encodes a rapidly evolving protein with sequence similarity to the myb/SANT-like domain in Adf-1 (MADF) class of DNA binding proteins (*14*). Genetic interaction studies (*15*, *16*) suggested that *Hmr* and *Lhr* interact to cause lethality in a manner consistent with the Dobzhansky-Muller model (Fig. 1A).

Lhr[1] maps 1.7 centimorgans from the visible marker *jba* on chromosome 2R (*17*). We identified recombinants between *Lhr*[1] and *jba* and typed them using molecular markers that distinguish the *Lhr*[1] and *jba D. simulans* strains (Fig. 1B). On the basis of the distribution of recombinants, *Lhr*[1] is likely within several hundred kilobases centromere-proximal to *qkr54B*.

Because of the paucity of visible markers in *D. simulans*, we did not attempt to obtain a proximal limit for *Lhr* by mapping. Instead, we searched preliminary assemblies of the *D. simulans* genome for candidate genes on the basis of similarities to *Hmr*, namely higher-than-average divergence between *D. melanogaster* and *D. simulans* and a possible role in DNA or chromatin binding. Among ~37 genes, we first examined *CG18468* because it contains a boundary element–associated factor 32/Su(var)3-7/Stonewall (BESS) domain. The BESS domain is found in 21 *Drosophila* proteins, often associated with MADF domains, and mediates protein-protein interactions (*18*). *Hmr* is predicted to encode a protein with two MADF domains (*14*), and we detected a putative BESS domain (fig. S1), suggesting a possible functional relationship between *CG18468* and *Hmr*.

Most predicted *D. simulans* proteins are >90% identical to their *D. melanogaster* orthologs. In contrast, CG18468 has only ~80% identity, caused by amino acid divergence and by a 16–amino acid insertion in *D. simulans* (Fig. 1C and fig. S2). The estimated average divergence of *CG18468* is similar to *Hmr* (*14*), measuring 0.078 at nonsynonymous sites (K_A) and 0.106 at synonymous sites (K_S). This K_A value, but not the K_S value, is substantially higher than the average value between *D. melanogaster* and *D. simulans* (*19*). Again similar to *Hmr*, *CG18468* is highly diverged outside the *melanogaster* subgroup (fig. S2), and both genes apparently lack orthologs outside of *Drosophila*.

We discovered that *CG18468* is mutated in the *Lhr*[1] rescue strain, which contains an insertion of ~4 kb in the predicted 5′ untranslated region (UTR) (Fig. 1D) that appears to be a moderately repetitive retrotransposed sequence. This insertion is not found in any of the five strains from which genome sequence is available nor from 11 additional lines we sequenced (*19*). *CG18468* is adjacent to and divergently transcribed from *CG6546* (Fig. 1D), so the insertion in the *Lhr*[1] rescue strain could potentially affect the transcription of either or both of these

genes. Reverse transcription polymerase chain reaction (RT-PCR) products, derived from RNA from the critical early larval stage (*15*), showed that both genes are transcribed in a control strain but that *CG18468* transcription is strongly reduced in the *Lhr*[1] rescue strain (Fig. 1E). These data suggest that the *Lhr*[1] phenotype is caused by reduced expression of *CG18468*.

We cloned the wild-type *CG18468* gene from *D. simulans* and transformed *D. melanogaster* with *P* element vectors containing a *D. simulans CG18468* cDNA under the control of *Saccharomyces cerevisiae* Upstream Activity Sequences (*UAS*), henceforth referred to as *UAS-Dsim\Lhr*. Expression was induced from a second, independently segregating transgene expressing the *S. cerevisiae* transcriptional activator GAL4 (Fig. 2). Control crosses using two different *GAL4*-expressing transgenes suggested that activation of *UAS-Dsim\Lhr* does not cause lethality in *D. melanogaster*, as evidenced by the similar numbers of progeny inheriting the *GAL4* driver ("red eyed" in Table 1) compared to those that did not ("orange eyed" and "white eyed") (Table 1 and table S1).

This result demonstrated that we could introduce both *UAS-Dsim\Lhr* and the *GAL4*-

expressing transgenes into hybrids from the *D. melanogaster* parent (Fig. 2). In contrast to the intraspecific control cross, when the same *D. melanogaster* females were crossed to *D. simulans Lhr*[1] males, only half of the expected hybrid males carrying the *GAL4*-expressing transgene were obtained (Table 1). PCR-based genotyping confirmed our inference that *Lhr*[1]-rescued males carrying only the *GAL4*-expressing transgene are viable, whereas those carrying both transgenes and thus expressing *UAS-Dsim\Lhr* are lethal (table S1). The reduced viability in some crosses of *Lhr*[1]-rescued males containing only the *UAS-Dsim\Lhr* transgene is likely due to maternal inheritance of the GAL4 protein (table S1).

These results suggest that expression of *UAS-Dsim\Lhr* complements the *Lhr*[1] hybrid rescue phenotype. We confirmed that *UAS-Dsim\Lhr* expression is not generally lethal to hybrids compared with *D. melanogaster* pure species by testing for effects in hybrid males rescued by a mutation in *Hmr*. We found that both *D. melanogaster* control males and male hybrids rescued by the null mutation *Df(1)Hmr*− are fully viable when expressing *UAS-Dsim\Lhr* (Table 1). RT-PCR experiments demonstrated that *UAS-Dsim\Lhr* was expressed in these crosses (fig. S3).

$$\frac{w}{w} \; ; \; \frac{P\{w^+, \; UAS\text{-}Dsim\backslash Lhr\}}{+} \; ; \; \frac{P\{w^+, \; GAL4\}}{+}$$

Eye color phenotype:		Expected ratios of genotypes if UAS-Dsim\Lhr expression is viable:	Expected ratios of genotypes if UAS-Dsim\Lhr expression is lethal:
Red	2:	UAS/+ ; GAL4/+ and +/+; GAL4/+	1: +/+; GAL4/+
Orange	1:	UAS/+; +/+	1: UAS/+; +/+
White	1:	+/+; +/+	1: +/+; +/+
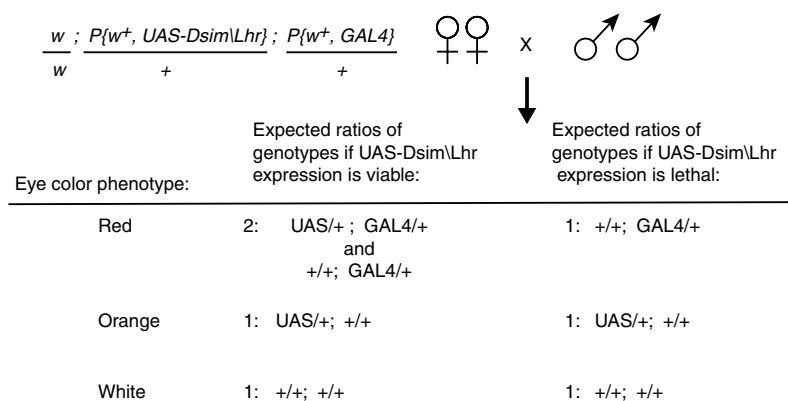
Fig. 2. Complementation crosses to test for suppression of hybrid male rescue. Female parents are heterozygous for both transgenes, each marked with w^+ producing intermediate levels of eye pigmentation. The *GAL4*-containing transformants have darker eye colors and are epistatic to the lighter-colored *UAS*-containing transformants. The red-eyed class is therefore potentially composed of two distinct genotypes.

Table 1. Number of offspring recovered from complementation tests of hybrid rescue mutations by *UAS-Dsim\Lhr* expression. Full parental genotypes and female progeny are shown in table S1, crosses 9 to 12. UAS indicates *D. simulans Lhr* under yeast UAS transcriptional control; GAL4 indicates yeast GAL4 protein driven by the *Actin5C* promoter. In the absence of viability effects, the ratio of red-eyed:orange-eyed:white-eyed males will be 2:1:1. Deviations from this ratio were tested by χ^2 tests. Results for the control cross and the cross with *Df(1)Hmr*− were not significantly different from this ratio ($P > 0.05$). Results for the crosses with *Lhr*[1] and *Hmr*[1] were significantly different from this ratio ($P < 0.001$).

Progeny		*D. melanogaster* control	*Lhr*[1]	*Df(1)Hmr*−	*Hmr*[1]
Phenotype	Genotype				
Red-eyed male	UAS/+;GAL4/+ and +/+;GAL4/+	485	89	169	22
Orange-eyed male	UAS/+;+/+	214	9	82	7
White-eyed male	+/+;+/+	262	94	95	33

We concluded that *UAS-Dsim/Lhr* expression specifically complements the *Lhr¹* mutation in hybrids, that *CG18468* is *Lhr*, and that *Lhr* is a major-effect hybrid lethality gene.

For *Lhr* to fit the Dobzhansky-Muller model of functional divergence, *D. simulans Lhr*, but not *D. melanogaster Lhr*, must cause hybrid lethality (Fig. 1A). Crosses with three different *D. melanogaster Lhr⁻* deletions produced essentially only F1 hybrid females, demonstrating that removal of *D. melanogaster Lhr* does not suppress F1 male lethality (fig. S4 and table S2).

Genetic and molecular analyses have demonstrated that *Hmr¹* retains partial *Hmr* activity (*14*, *15*). In contrast to the results shown in Table 1, which used the null allele *Df(1)Hmr⁻*, we found that rescue of hybrids by the hypomorphic mutation *Hmr¹* is suppressed by *D. simulans Lhr* expression (Table 1 and table S1). These data suggest that the lethal effect of *D. simulans Lhr* requires the presence of *D. melanogaster Hmr* function. The deleterious effects of a *D. melanogaster Hmr⁺* duplication are suppressed by *Lhr¹* (*15*, *16*), results that suggest, based on our characterization of the *Lhr¹* mutation, that *D. melanogaster Hmr* requires a functional *D. simulans Lhr* to cause lethality. These reciprocal genetic interactions are consistent with the model of *Hmr* and *Lhr* forming a Dobzhansky-Muller pair of interacting genes (Fig. 1A).

Functional divergence between species led us to examine the evolutionary forces driving the sequence divergence of *Lhr*. The high K_A/K_S value of 0.731 between *D. melanogaster* and *D. simulans* is consistent with either positive selection or relaxed selective constraint. We sequenced multiple alleles of *Lhr* from *D. melanogaster* and *D. simulans* and performed a McDonald-Kreitman test (*19*). The results of this test rejected the null hypothesis that these genes are evolving neutrally (Fisher's Exact Test, $P = 0.011$) and suggested that there is an excess of nonsynonymous fixations between the species (table S3). Phylogenetic analyses further suggest that the K_A/K_S ratio has increased on branches leading to *D. melanogaster* and its sibling species (fig. S5).

The McDonald-Kreitman and K_A/K_S tests only consider alignable regions of the *Lhr* coding region. *Lhr* from *D. simulans* and its sister species *D. mauritiana* and *D. sechellia* each contain a 16–amino acid insertion, interrupting a potential leucine zipper domain, relative to *D. melanogaster* and outgroup species (Fig. 1C and fig. S2). Notably, we found that this insertion is precisely deleted in a second *D. simulans* stock named *Lhr²*, which also produces viable F1 hybrid males (*20*). Although *Lhr²* contains additional amino acid substitutions relative to *Lhr⁺* alleles, its hybrid rescue phenotype suggests that the functional divergence of *D. simulans Lhr* may be caused by the 16–amino acid insertion.

Heterochromatin Protein 1 (HP1) is a chromodomain-containing protein that localizes to heterochromatic regions of chromosomes and is required to maintain heterochromatic states (*21*). LHR was previously identified (as CG18468) as interacting with HP1 in a yeast two-hybrid assay (*22*). We confirmed this interaction (Fig. 3A), and discovered that *D. simulans* LHR also interacts with *D. melanogaster* HP1 (Fig. 3B). Because *D. simulans* HP1 is nearly identical to *D. melanogaster* HP1 (fig. S6) we hypothesize that *D. simulans* LHR also binds to *D. simulans* HP1. This apparent conservation of HP1-binding function of LHR suggests that the intraspecific function of *Lhr* is conserved between *D. melanogaster* and *D. simulans*, in contrast to the interspecific function for hybrid lethality, which we have shown is specific only to *D. simulans Lhr*.

A *D. melanogaster* LHR–yellow fluorescent protein (YFP) fusion protein accumulated in a small number of foci (usually 1 to 2) in salivary gland nuclei (fig. S7), similar to HP1 (*23*). In polytene chromosomes, HP1 accumulates predominantly in the chromocenter and along the highly heterochromatic fourth chromosome as well as at telomeres and a number of bands along the euchromatic arms (*24*). LHR-YFP has a similar pattern and predominantly colocalizes with HP1 (Fig. 3, C to E). We suggest that *Lhr* may be coevolving with rapidly evolving heterochromatic repetitive DNAs, consistent with the hypothesis that the molecular drive inherent in repetitive DNAs contributes to hybrid incompatibilities and speciation (*25*, *26*).

Hmr and *Lhr* cause F1 hybrid lethality because they are partially or fully dominant. The large number of HI genes estimated from other studies (*27*) may be mechanistically distinct because they are recessive and only cause HI when homozygous in F2 hybrids or in interspecific introgressions. However, our results also show that the interaction of *Hmr* and *Lhr* alone is insufficient to recapitulate hybrid lethality, because control crosses showed that expression of *D. simulans Lhr* does not cause lethality in a *D. melanogaster* pure-species background (Table 1 and table S1). Pontecorvo suggested that an interaction among the *D. melanogaster X* (which contains *Hmr*), *D. simulans* chromosome II (which contains *Lhr*), and *D. simulans* chromosome III causes hybrid lethality (*28*). Hybrid lethality may therefore be enhanced by a multilocus interaction involving additional genes. Alternatively, *Hmr* and *Lhr* may be the only major-effect genes, but their lethal interaction requires a hybrid genetic background. We suggest that altered chromosome morphology and chromatin structure in hybrids due to the

Fig. 3. LHR interacts and colocalizes with HP1. (**A**) *D. melanogaster* LHR interacts with *D. melanogaster* HP1. Yeast two-hybrid interactions were detected by activation of *HIS3* and growth on media lacking histidine; loading controls [complete media (CM) -Leu -Trp] contain histidine. (**B**) *D. simulans* LHR interacts with *D. melanogaster* HP1. (**C** to **E**) Colocalization of *D. melanogaster* YFP::LHR and HP1 on salivary gland polytene chromosomes. Chromosomes from *P{UAS-YFP::Lhr}168-3/+;P{GawB}C147/+* third-instar larvae were incubated with primary antibodies to GFP and HP1, which were detected using rhodamine red-X–conjugated (red) and cyanine-conjugated (green) secondary antibodies, respectively. (C) Antibody to GFP to detect YFP::LHR. (D) Antibody to HP1. (E) Merge with 4′,6′-diamidino-2-phenylindole signal (blue) to detect DNA. A predominant colocalization occurs at the chromocenter (long arrow), fourth chromosome (short arrow), and a telomere (arrowhead).
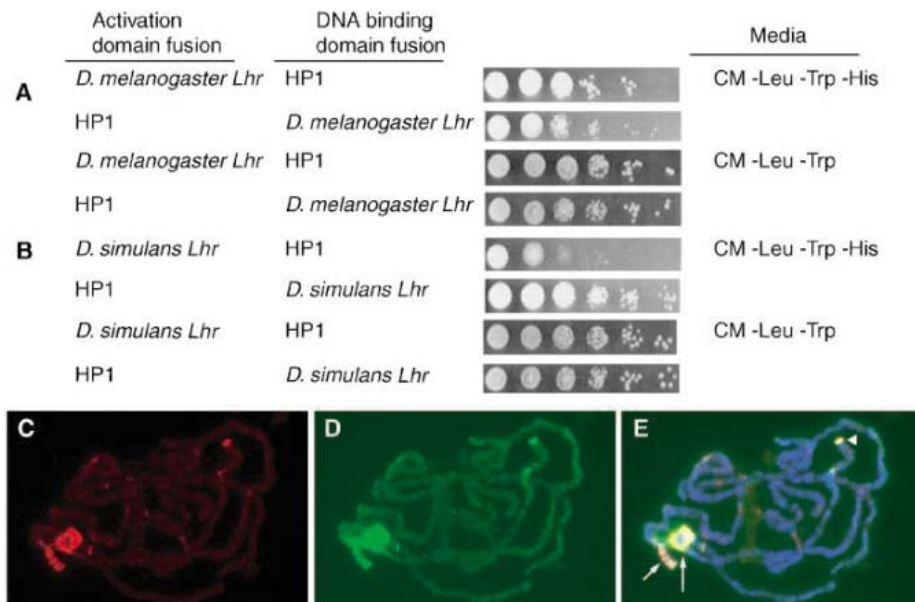
cumulative effects of species-specific differences in satellites, transposable elements, and other repetitive DNAs cause this hybrid genetic background effect.

References and Notes

1. J. A. Coyne, H. A. Orr, *Speciation* (Sinauer, Sunderland, MA, 2004).
2. C.-T. Ting, S.-C. Tsaur, M.-L. Wu, C.-I. Wu, *Science* **282**, 1501 (1998).
3. D. A. Barbash, P. Awadalla, A. M. Tarone, *PLoS Biol.* **2**, e142 (2004).
4. D. C. Presgraves, L. Balagopalan, S. M. Abmayr, H. A. Orr, *Nature* **423**, 715 (2003).
5. J. B. Hutchinson, *J. Genet.* **25**, 281 (1932).
6. P. Christie, M. R. MacNair, *J. Hered.* **75**, 510 (1984).
7. A. R. Carvajal, M. R. Gandarela, H. F. Naveira, *Genetica* **98**, 1 (1996).
8. S. Kazianis *et al.*, *Genes Chromosomes Cancer* **22**, 210 (1998).
9. A. L. Sweigart, L. Fishman, J. H. Willis, *Genetics* **172**, 2465 (2006); published online 16 January 2006.
10. E. L. Cabot, A. W. Davis, N. A. Johnson, C.-I. Wu, *Genetics* **137**, 175 (1994).
11. X. R. Maside, J. P. Barral, H. F. Naveira, *Genetics* **150**, 745 (1998).
12. Y. Tao, Z.-B. Zeng, J. Li, D. L. Hartl, C. C. Laurie, *Genetics* **164**, 1399 (2003).
13. T. K. Watanabe, *Jpn. J. Genet.* **54**, 325 (1979).
14. D. A. Barbash, D. F. Siino, A. M. Tarone, J. Roote, *Proc. Natl. Acad. Sci. U.S.A.* **100**, 5302 (2003).
15. D. A. Barbash, J. Roote, M. Ashburner, *Genetics* **154**, 1747 (2000).
16. H. A. Orr, S. Irving, *Genetics* **155**, 225 (2000).
17. M.-T. Yamamoto, M. Kamo, S. Yamamoto, T. K. Watanabe, *Genes Genet. Syst.* **72**, 297 (1997).
18. V. Bhaskar, A. J. Courey, *Gene* **299**, 173 (2002).
19. Materials and methods are provided as supporting material on *Science* Online.
20. H. A. Orr, personal communication.
21. J. C. Eissenberg, S. C. Elgin, *Curr. Opin. Genet. Dev.* **10**, 204 (2000).
22. L. Giot *et al.*, *Science* **302**, 1727 (2003).
23. J. A. Powers, J. C. Eissenberg, *J. Cell Biol.* **120**, 291 (1993).
24. L. Fanti, M. Berloco, L. Piacentini, S. Pimpinelli, *Genetica* **117**, 135 (2003).
25. G. Dover, *Nature* **299**, 111 (1982).
26. S. Henikoff, K. Ahmad, H. S. Malik, *Science* **293**, 1098 (2001).
27. J. Mallet, *Trends Ecol. Evol.* **21**, 386 (2006).
28. G. Pontecorvo, *J. Genet.* **45**, 51 (1943).
29. We thank the *Drosophila* Genomics Resource Center for cloning vectors; H. A. Orr, M.-T. Yamamoto, and the Bloomington *Drosophila* Stock Center for fly stocks; C. Langley, I. Liachko, T. Schlenke, and J. Werner for helpful discussions; and E. Alani, C. Aquadro, A. Clark, and B. Lazzaro for comments on the manuscript. Supported by NIH grant R01 GM074737-01. Accession numbers mentioned in the manuscript have been deposited in GenBank under the numbers EF044038-62, EF057388-9, and BK005905-14.

Localization of Iron in *Arabidopsis* Seed Requires the Vacuolar Membrane Transporter VIT1

Sun A. Kim,[1]* Tracy Punshon,[1]* Antonio Lanzirotti,[2] Liangtao Li,[3] José M. Alonso,[4] Joseph R. Ecker,[5] Jerry Kaplan,[3] Mary Lou Guerinot[1]†

Iron deficiency is a major human nutritional problem wherever plant-based diets are common. Using synchrotron x-ray fluorescence microtomography to directly visualize iron in *Arabidopsis* seeds, we show that iron is localized primarily to the provascular strands of the embryo. This localization is completely abolished when the vacuolar iron uptake transporter VIT1 is disrupted. Vacuolar iron storage is also critical for seedling development because *vit1-1* seedlings grow poorly when iron is limiting. We have uncovered a fundamental aspect of seed biology that will ultimately aid the development of nutrient-rich seed, benefiting both human health and agricultural productivity.

Iron is the most important yet problematic of the essential elements required by plants. It is needed for life-sustaining processes from photosynthesis to respiration, yet it can be toxic at high levels due to its propensity to form hydroxyl radicals that can damage cellular constituents. Like animal cells, plant cells can safely store iron in ferritin (1). However, unlike animal cells, plant cells also have vacuoles in which iron and other potentially toxic metals can be sequestered. Most efforts to date at increasing the iron content of staple foods have been focused on increasing seed ferritin levels (2–4), but the contribution of the vacuole to seed iron storage has remained largely unexplored.

In yeast, the vacuole serves as the main intracellular storage compartment for iron (5–7). The yeast *CCC1* (Ca^{2+}-sensitive cross-complementer 1) gene encodes an iron/manganese transporter that mediates the accumulation of these metals in the vacuole (8). We have characterized the *Arabidopsis* ortholog of yeast CCC1, VIT1 (vacuolar iron transporter 1; At2g01770), in order to address the role of the vacuole in iron homeostasis. VIT1 shows 62% amino acid similarity to the yeast CCC1 protein, and secondary-structure analysis programs predict five possible transmembrane domains, consistent with the model previously proposed for yeast CCC1. VIT1-like proteins can be found throughout the plant kingdom, with a distinct clustering of dicot and monocot VIT1-like sequences (Fig. 1A).

To determine if VIT1 is a true ortholog of CCC1, we expressed *VIT1* in *ccc1* mutant yeast that are sensitive to high amounts of extracellular iron and thus fail to grow on media containing elevated levels of iron. This sensitivity is due to the inability of the *ccc1* mutant to store iron in the vacuole, leading to increased accumulation of cytosolic iron (8). Expression of *VIT1* sustained the growth of the *ccc1* mutant yeast on high-iron medium (Fig. 1B). When VIT1 was expressed in *ccc1* mutant yeast, vacuolar iron was increased threefold compared to control cells (Fig. 1C). Vacuolar manganese was also increased in yeast cells expressing *VIT1* (Fig. 1D). The increases seen are similar to those conferred by expression of the *CCC1* gene (6). No increases were seen in Zn or Cd. We also examined the effect of *VIT1* expression on iron uptake. Overexpression of CCC1 in yeast cells decreases cytosolic iron levels, leading to increased expression of high-affinity iron transporters in the plasma membrane (9). The iron uptake rate of yeast cells overexpressing *VIT1* was markedly increased relative to *ccc1* cells (Fig. 1E). This result, together with the increased metal content of the vacuole, provides functional proof that VIT1 mediates iron sequestration into vacuoles.

We next investigated the localization of VIT1 using a green fluorescent protein (GFP)–tagged version of the VIT1 protein. The GFP-VIT1 fusion protein complements the *ccc1* mutant phenotype (fig. S1), indicating that GFP tagging does not disrupt the biochemical function or the localization of VIT1. In yeast, GFP-VIT1 colocalizes to the vacuolar membrane with the FM4-64 marker (fig. S1). In transgenic *Arabidopsis* plants that stably express a *GFP-VIT1* gene driven by the 35S promoter, the GFP fluorescence is localized to the vacuolar membrane (Fig. 2, A to D). In Fig. 2, A and C, the VIT1-GFP staining is only seen on the side of the nucleus facing the interior of the cell, that is, distinguishing it from staining of the plasma membrane, which would follow the cell periphery.

[1]Department of Biological Sciences, Dartmouth College, Hanover, NH 03755, USA. [2]Consortium for Advanced Radiation Sources, University of Chicago, Chicago, IL 60637, USA. [3]Department of Pathology, University of Utah School of Medicine, Salt Lake City, UT 84132, USA. [4]Department of Genetics, North Carolina State University, Raleigh, NC 27695, USA. [5]Plant Biology and Genomic Analysis Laboratories, The Salk Institute for Biological Studies, La Jolla, CA 92037, USA.

*These authors contributed equally to this work.
†To whom correspondence should be addressed. E-mail: guerinot@dartmouth.edu

Fig. 1. (A) Phylogenetic tree of plant VIT1 transporters. The deduced amino acid sequences of selected plant VIT1 orthologs were aligned with ClustalW. The tree and bootstrap analyses were performed with MEGA version 2.0 (*25*). Values indicate the number of times (in percent) that each branch topology was found during bootstrap analysis. At, *Arabidopsis*; Le, tomato; Gm, soybean; Bn, rapeseed; St, potato; Vv, grape; Mc, common ice plant; Os, rice; Zm, corn; Ta, wheat; and Hv, barley. The scale bar represents 0.1 substitutions per site. **(B)** VIT1 complements the sensitivity of *ccc1* yeast to extracellular iron. Wild-type (WT) and Δ*ccc1* cells were transformed with either an empty vector or a plasmid containing a *MET25* promoter–regulated cDNA of tomato (*LeVIT1*) or *Arabidopsis* (*VIT1*). Cells were grown in CM-Ura for 16 hours, washed, and spotted onto CM-Ura-Met plates in the presence of different amounts of iron. The plates were incubated at 30°C for 2 days and photographed. **(C to E)** Over-expression of VIT1 increases the accumulation of vacuolar iron and manganese and leads to increased iron uptake in Δ*ccc1*. Δ*ccc1* cells were transformed with either an empty vector or a plasmid containing a *MET25*-regulated *VIT1*. The cells were grown overnight in methionine-free medium, vacuoles were isolated, and the Fe (C) and Mn (D) content of the isolated vacuoles was determined by ICP-MS. The metal content was normalized to vacuolar protein levels. **(E)** Cells were grown for 16 hours in CM-Ura-Met. Cells were washed and incubated with 0.5 μM ^{59}Fe for 15 min, and the amount of cell-associated radioactivity and cell number were determined.
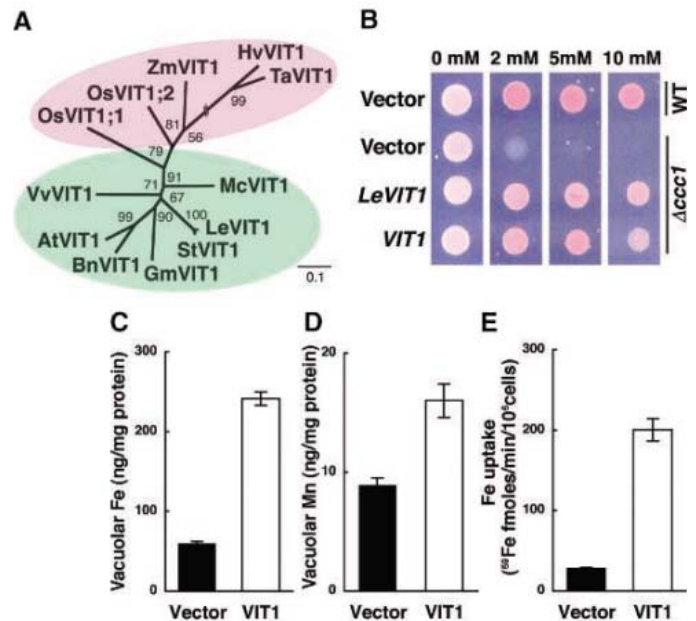
Fig. 2. Subcellular localization, expression, and tissue distribution of VIT1. **(A to D)** GFP-tagged VIT1 localizes to the vacuolar membrane in plant cells. The GFP fluorescence in a root epidermal cell (A) of transgenic *Arabidopsis* stably expressing a *35S::GFP-VIT1* construct was visualized with confocal microscopy. **(B)** The cell walls and nuclei were stained with propidium iodide, shown here by red fluorescence. **(C)** Overlay of green fluorescence and red fluorescence. **(D)** Differential interference contrast image of the observed cell. Scale bar: (A) 10 μm. **(E)** Developmental expression of *VIT1*. mRNA levels for *VIT1* were obtained from AtGenExpress (*9*). The linearized gcRMA values were plotted on a logarithmic scale. The peak value corresponds to seeds at developmental stage 6. **(F to N)** The *VIT1* gene is expressed along the vasculature in developing seeds and young seedlings. The *uidA* gene was expressed under the control of the *VIT1* promoter (1.0 kb upstream of *VIT1* coding sequence). β-Glucuronidase (GUS) assays were performed with either X-GLUC (5-bromo-4-chloro-3-indolyl β-D-glucuronide cyclohexylamine salt) for histochemical staining (F, G, I, J, L to N) or ImaGene Green C12FDGlcU for fluorescent imaging (H and K). [(F to H) and (L)] GUS staining of the developing seeds from transgenic plants. (I to K) GUS staining of wild-type Col-0. (M and N) GUS staining in the seedlings at 0.5, 1, 2, 4, and 6 days after germination. Scale bars: (F to H) 100 μm, (L to N) 1 mm.
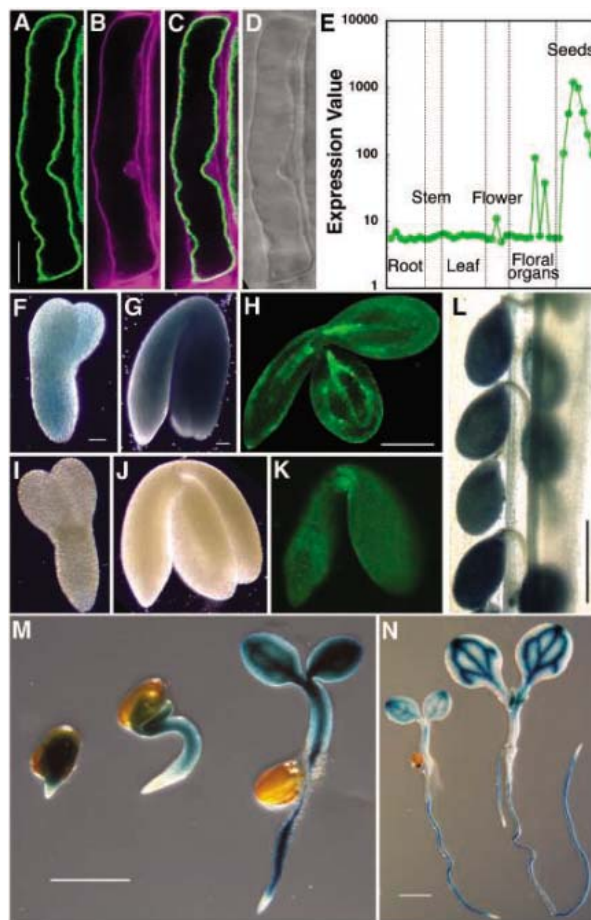
VIT1 is expressed at a low level throughout the plant, but there is a large peak in steady-state levels of *VIT1* mRNA in the developing seed [Fig. 2E (*10*)]. Notably, the peak in *VIT1* expression coincides with vacuole formation in the developing embryo (*11*). *VIT1* expression is not affected by iron availability, unlike other proteins that have been implicated in iron metabolism such as *IRT1*, *FRO2*, *FRD3*, and *FIT1* (*12–15*). To further assess the tissue localization of *VIT1*, we generated transgenic plants that carry a β-glucuronidase (GUS) reporter whose expression is driven by the *VIT1* promoter. Histochemical analysis of GUS activity showed GUS reporter gene expression in the developing embryo and seed (Fig. 2, F to L). Gus staining was also detected in young seedlings, predominantly associated with the vasculature (Fig. 2, M and N).

Because *VIT1* is highly expressed in the developing seed and because seeds are an important food source, we examined the iron content of seeds using inductively coupled plasma mass spectrometry (ICP-MS). However, we found no difference in the iron content of seeds or shoots of *vit1-1* plants compared to wild-type plants (table S1). We next investigated whether there was a change in the distribution of iron in a *vit1-1* mutant, given that VIT1 is expressed in the vascular system and that the vascular system is responsible for the delivery of iron. Previously, metals have been localized in *Arabidopsis* seed by means of electron beam energy-dispersive x-ray spectroscopy, but this technique requires fixation and embedding of samples for electron microscopy [e.g., (*16, 17*)]. Such preparation can alter cellular materials and the location of key associated elements. Synchrotron x-ray fluorescence microtomography requires no sample pretreatment, allows noninvasive examination of

living materials, and can detect elemental abundances in the sub–microgram per gram range with a resolution of 10 μm or less (18). Seeds are ideal samples for x-ray analysis because of their low moisture content and stability over long periods of data collection. Three-dimensional (3D) images and virtual cross sections of the x-ray attenuation or individual elemental fluorescence within the seed can be rendered, allowing visualization of either variability in density or elemental distribution (19). Three-dimensional tomographic reconstructions can be manipulated by computer analysis (in silico), allowing the investigator to look inside the seed, overlay elements of interest, and investigate elemental co-associations. We collected x-ray fluorescence microtomography data from three seeds each of wild-type Col-0 and the vit1-1 mutant (Fig. 3 and fig. S2). Total x-ray absorption allows one to visualize the cellular structure of the seed (Fig. 3, B, C, E, and F) and demonstrates the high resolving ability of the technique such that individual cells in the cortex region can be distinguished. The most notable

difference between the two seed types is in the distribution of Fe, which in wild-type seeds is strongly localized to the provascular strands of the hypocotyl, radicle, and cotyledons (Fig. 3, D and G). In vit1-1 seeds, Fe is completely absent from these cells and is instead located more diffusely in the hypocotyl and radicle, and in the epidermal cells of the cotyledons, in particular, the abaxial (lower) epidermis (Fig. 3, D and H). There is no difference in the pattern observed for Mn between wild-type and vit1-1 mutant seeds, although in vit1-1 mutants, the distribution of Fe is similar to that for Mn, as is apparent in the overlay of the signals for Fe, Mn, and Zn (Fig. 3D). Zinc is found throughout the seed and shows a similar distribution pattern in wild-type and vit1-1 seed (Fig. 3D). Multiple tomograms can be assembled to show the 3D distribution of various metals; Fig. 3G clearly shows that, in wild-type seed, Fe is associated with the provascular system throughout the embryo and additionally shows a region of high Fe concentration associated with the micropylar region (see also Movie S1).

The marked change in metal distribution observed in the vit1-1 mutant implies that most of the iron in the wild-type embryo is stored in the vacuoles of provascular cells. Previous examination of minerals present in electron-dense globoids within protein storage vacuoles from nine different regions of Arabidopsis seed showed the highest Fe levels in the procambium regions of both the hypocotyl-radicle axis and the cotyledons (16), in agreement with our finding that Fe is concentrated in the provasculature. Such a location might allow rapid access to this pool of iron during growth of the germinating seedling. To test whether such localization affects seedling growth, we germinated wild-type and vit1-1 mutants on alkaline (pH 7.9) soil to limit iron availability. vit1-1 seedlings grew poorly compared to wild-type plants (Fig. 4). When plants were grown at pH 5.6, vit1-1 seedlings were indistinguishable from wild-type plants. This finding is very similar to the recently reported phenotype for a nramp3 nramp4 double mutant of Arabidopsis that cannot mobilize iron from the vacuole (20).

Taken together, our results demonstrate that proper localization of iron, as well as an ability to access this store, plays important roles in iron homeostasis. It is important to note that Arabidopsis seed contains a single layer of endosperm and an embryo with two cotyledons and a radicle-shoot axis. The cotyledons serve as the main storage organ, similar to other nonendospermic seeds such as soybean, peanuts, and most Brassica species, in which the endosperm is degraded during the seed development and the cotyledons become the primary storage tissue. This is in contrast to grains like rice and wheat that store materials required for germination of the seedling in a
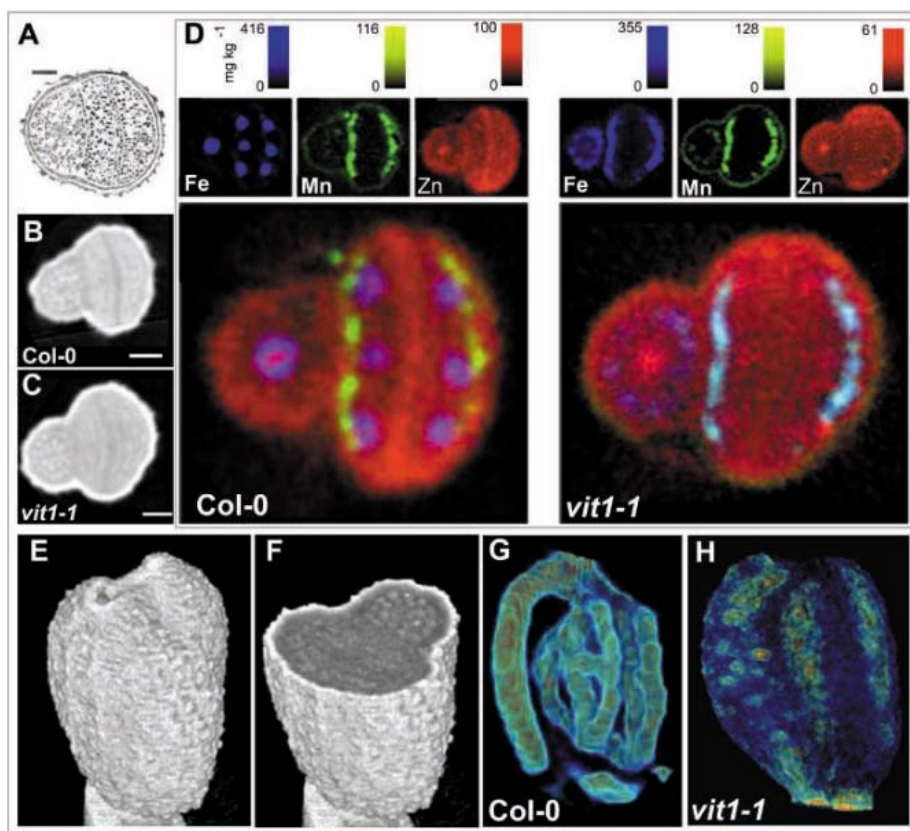
Fig. 3. X-ray fluorescence microtomography of Arabidopsis seed. (A) Light micrograph cross section of a mature Arabidopsis seed [modified from (26) with permission]; bar: 62 μm. (B and C) Total x-ray absorption tomographic slices of Col-0 and vit1-1 seeds; bar: 100 μm. (D) X-ray fluorescence tomographic slices of Fe Kα (blue), Mn Kα (green), and Zn Kα (red) fluorescence lines collected from Col-0 and vit1-1 with metal abundances indicated in mg kg^{-1} (smaller images), and composite images of Fe, Mn, and Zn abundance of Col-0 and vit1-1 (larger images). (E) Three-dimensional rendering of total x-ray absorption of a wild-type Arabidopsis seed. (F) In silico–sectioned (y axis, upper 50% removed) rendering of total x-ray absorption shown in (E). (G and H) Three-dimensional rendering of Fe Kα x-ray fluorescence in Col-0 and vit1-1, respectively, with both seeds identically oriented.
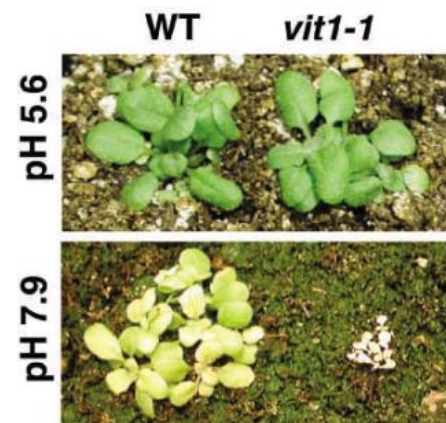
Fig. 4. VIT1 is required for growth on alkaline soil. Wild-type and vit1-1 seedlings were grown for 15 days on either acidic (pH 5.6) or alkaline (pH 7.9) soil. No obvious difference was observed among the plants grown on the acidic soil. Wild-type seedlings developed weak chlorosis on the high-pH soil, consistent with limited iron availability. The growth of vit1-1 was markedly reduced and the leaves of vit1-1 showed severe chlorosis when vit1-1 was grown at pH 7.9.

multilayer endosperm. However, most of the iron in rice seed, for example, is associated with the embryo and the aleurone layer, not the endosperm, suggesting that VIT1-mediated iron storage in the embryo may play the same role in developing endospermic plants as that described here for *Arabidopsis*. Furthermore, unlike other Fe transporters characterized to date such as IRT1, which can transport Cd as well as Fe (*21*), VIT1 does not appear to transport Cd. Cd levels in seeds from lines overexpressing VIT1 were low (< 0.1 part per million), with no significant difference compared to wild-type seeds ($P < 0.05$). Therefore, any potential biotechnological applications of VIT1 will not have to consider unwanted accumulation of this toxic heavy metal.

Our study demonstrates the power of combining mutant analysis with a technique that can both image and determine the elemental composition of living plant material. Although 2D imaging with x-ray fluorescence has been used before to image the distribution of metals in plant tissues (*22*, *23*), including *Arabidopsis* seed (*24*), our ability to render 3D images at high resolution allowed us to determine that Fe was associated with the provascular system throughout the seed and should prompt more studies on spatial distribution of metals in biological samples. Our study also highlights the role of the vacuole in seed iron storage and suggests that the vacuole offers another avenue for increasing the iron content of plant-based diets.

References and Notes

1. C. Curie, J.-F. Briat, *Annu. Rev. Plant Biol.* **54**, 183 (2003).
2. F. Goto, T. Yoshihara, N. Shigemoto, S. Toki, F. Takaiwa, *Nat. Biotechnol.* **17**, 282 (1999).
3. P. Lucca, R. Hurrell, I. Potrykus, *J. Am. Coll. Nutr.* **21**, 184S (2002).
4. L.-Q. Qu, T. Yoshihara, A. Ooyama, F. Goto, I. Takaiwa, *Planta* **222**, 225 (2005).
5. A. Pich, R. Manteuffel, S. Hillmer, G. Scholz, W. Schmidt, *Planta* **213**, 967 (2001).
6. F. Raguzzi, E. Lesuisse, R. R. Crichton, *FEBS Lett.* **231**, 253 (1988).
7. H.-P. Bode, M. Dumschat, S. Garotti, G. F. Fuhrmann, *Eur. J. Biochem.* **228**, 337 (1995).
8. L. Li, O. S. Chen, D. M. Ward, J. Kaplan, *J. Biol. Chem.* **276**, 29515 (2001).
9. O. S. Chen, J. Kaplan, *J. Biol. Chem.* **275**, 7626 (2000).
10. M. Schmid et al., *Nat. Genet.* **37**, 501 (2005).
11. J. L. Bowman, S. G. Mansfield, in *Arabidopsis: An Atlas of Morphology and Development*, J. Bowman, Ed. (Springer-Verlag, New York, 1994), pp. 351–361.
12. D. Eide, M. Broderius, J. Fett, M. L. Guerinot, *Proc. Natl. Acad. Sci. U.S.A.* **93**, 5624 (1996).
13. N. J. Robinson, C. M. Procter, E. L. Connolly, M. L. Guerinot, *Nature* **397**, 694 (1999).
14. E. E. Rogers, M. L. Guerinot, *Plant Cell* **14**, 1787 (2002).
15. E. P. Colangelo, M. L. Guerinot, *Plant Cell* **16**, 3400 (2004).
16. J. N. Lott, M. M. West, *Can. J. Bot.* **79**, 1292 (2001).
17. M. S. Otegui, R. Capp, L. A. Staehelin, *Plant Cell* **14**, 1311 (2002).
18. S. R. Sutton et al., in *Applications of Synchrotron Radiation in Low-Temperature Geochemistry and Environmental Science*, P. A. Fenter, M. L. Rivers, N. C. Sturchio, S. R. Sutton, Eds. (Mineralogical Society of America, Washington, DC, 2002), vol. 49, pp. 429–483.
19. W. H. Stuppy, J. A. Maisano, M. W. Colbert, P. J. Rudall, T. B. Rowe, *Trends Plant Sci.* **8**, 2 (2003).
20. V. Lanquar et al., *EMBO J.* **24**, 4041 (2005).
21. G. Vert et al., *Plant Cell* **14**, 1223 (2002).
22. T. Punshon, A. Lanzirotti, S. Harper, P. M. Bertsch, J. Burger, *J. Environ. Qual.* **34**, 1165 (2005).
23. D. H. McNear Jr. et al., *Environ. Sci. Technol.* **39**, 2210 (2005).
24. L. W. Young, N. D. Westcott, K. Attenkofer, M. J. T. Reaney, *J. Synchrotron Radiat.* **13**, 304 (2006).
25. S. Kumar, K. Tamura, I. Jacobsen, M. Nei, *MEGA2: Molecular Evolutionary Genetics Analysis Version 2.0.* (Pennsylvania and Arizona State Universities, University Park, PA, and Tempe, AZ, 2000).
26. J. S. Busse, R. F. Evert, *Int. J. Plant Sci.* **160**, 1 (1999).
27. We thank F. Ausubel, C. R. McClung, and D. Salt for critically reading the manuscript; B. Lahner and D. Salt for ICP-MS analysis; and A. Lavanway for help with microscopy. This work was supported by grants from the NSF (DBI 0077378 and IBN-0419695 to M.L.G.; DBI 0420126 to J.R.E.) and NIH (DK 30534 to J.K.). T.P. was supported by a training fellowship from the Dartmouth NIH–National Institute of Environmental Health Science Superfund Basic Research Program Project (P42 ES07373) through the Center for Environmental Health Sciences at Dartmouth. A portion of this work was performed at Beamline X26A, National Synchrotron Light Source, Brookhaven National Laboratory. X26A is supported by the U.S. Department of Energy (DOE)–Geosciences and DOE–Office of Biological and Environmental Research, Environmental Remediation Sciences Division.

A NAC Gene Regulating Senescence Improves Grain Protein, Zinc, and Iron Content in Wheat

Cristobal Uauy,[1]* Assaf Distelfeld,[2]* Tzion Fahima,[2] Ann Blechl,[3] Jorge Dubcovsky[1]†

Enhancing the nutritional value of food crops is a means of improving human nutrition and health. We report here the positional cloning of *Gpc-B1*, a wheat quantitative trait locus associated with increased grain protein, zinc, and iron content. The ancestral wild wheat allele encodes a NAC transcription factor (*NAM-B1*) that accelerates senescence and increases nutrient remobilization from leaves to developing grains, whereas modern wheat varieties carry a nonfunctional *NAM-B1* allele. Reduction in RNA levels of the multiple *NAM* homologs by RNA interference delayed senescence by more than 3 weeks and reduced wheat grain protein, zinc, and iron content by more than 30%.

The World Health Organization estimates that more than 2 billion people have deficiencies in key micronutrients such as Zn and Fe and more than 160 million children under the age of 5 lack adequate protein (*1*), leading to an economic burden for society (*2*). The two major types of wheat, tetraploid wheats [diploid cell (2n) = 28], used for pasta, and hexaploid wheats (2n = 42), used primarily for bread, account for ~20% of all calories consumed worldwide. Annual wheat production is estimated at 620 million tons of grain (*3*), translating into approximately 62 million tons of protein. Increasing grain protein content (GPC) has been hindered by environmental effects, complex genetic systems governing this trait, and a negative correlation with yield (*4*). Less progress has been made in increasing Zn and Fe content, the focal point of the HarvestPlus global initiatives (*5*).

Wild emmer wheat [*Triticum turgidum* ssp. *dicoccoides* (DIC)] is the ancestor of cultivated pasta wheat (*T. turgidum* ssp. *durum*) and a promising source of genetic variation in protein, Zn, and Fe content (*6*, *7*). A quantitative trait locus (QTL) for GPC was mapped on chromosome arm 6BS in a population of recombinant inbred lines derived from the *T. turgidum* ssp. *durum* cultivar Langdon (LDN) and the chromosome substitution line LDN (DIC6B) (*8*). This locus was associated with GPC increases of ~14 g kg^{-1} in both tetraploid and hexaploid lines (*8–10*). Olmos et al. (*11*) mapped this QTL as a simple Mendelian locus, *Gpc-B1* (Fig. 1A), which was later located within a 0.3-cM interval (*12*). Molecular markers *Xuhw89* and *Xucw71* within this region flank a 245-kb physical contig, including *Gpc-B1* (*13*).

Tetraploid and hexaploid wheat lines carrying this 245-kb DIC segment show delayed senescence and increased GPC and grain micronutrients (*14*, *15*). The complete sequencing of this region (DQ871219) revealed five genes

[1]Department of Plant Sciences, University of California, One Shields Avenue, Davis, CA 95616, USA. [2]Institute of Evolution, University of Haifa, Mt. Carmel, Haifa 31905, Israel. [3]United States Department of Agriculture, Agricultural Research Service, Western Regional Research Center, 800 Buchanan St., Albany, CA 94710, USA.

*These authors contributed equally to this work.
†To whom correspondence should be addressed. E-mail: jdubcovsky@ucdavis.edu

Fig. 1. Map-based cloning of *Gpc-B1*. (**A**) QTL for grain protein on wheat chromosome arm 6BS (*11*). (**B**) Sequenced B-genome physical contig. The position and orientation of five genes are indicated by arrows. (**C**) Fine mapping of *Gpc-B1*. The x's indicate the positions of critical recombination events flanking *Gpc-B1*. Vertical lines represent polymorphism mapped in the critical lines. A single gene with three exons (green rectangles) was annotated within the 7.4-kb region flanked by the closest recombination events. The open arrowhead indicates the transcription initiation site. (**D**) Graphical genotypes of critical recombinant substitution lines used for fine-mapping of *Gpc-B1*. Blue bars represent LDN markers; red bars represent DIC markers. (**E**) Flag-leaf chlorophyll content of recombinant substitution lines segregating for *Gpc-B1* (*14*). Asterisks indicate significant differences ($P < 0.01$). Phenotypes of critical recombinant substitution lines: (**F**) chlorophyll at 20 days after anthesis (DAA), (**G**) grain protein, (**H**) Zn, and (**I**) Fe concentrations. Blue and red bars indicate the presence of the LDN and DIC alleles at *TtNAM-B1*, respectively. (**J**) First 18 nucleotides of DIC and LDN *TtNAM-B1* alleles and their corresponding amino acid translation. The LDN allele carries a 1-bp insertion (red T) that disrupts the reading frame (indicated by red amino acid residues). Error bars represent standard error of the mean.
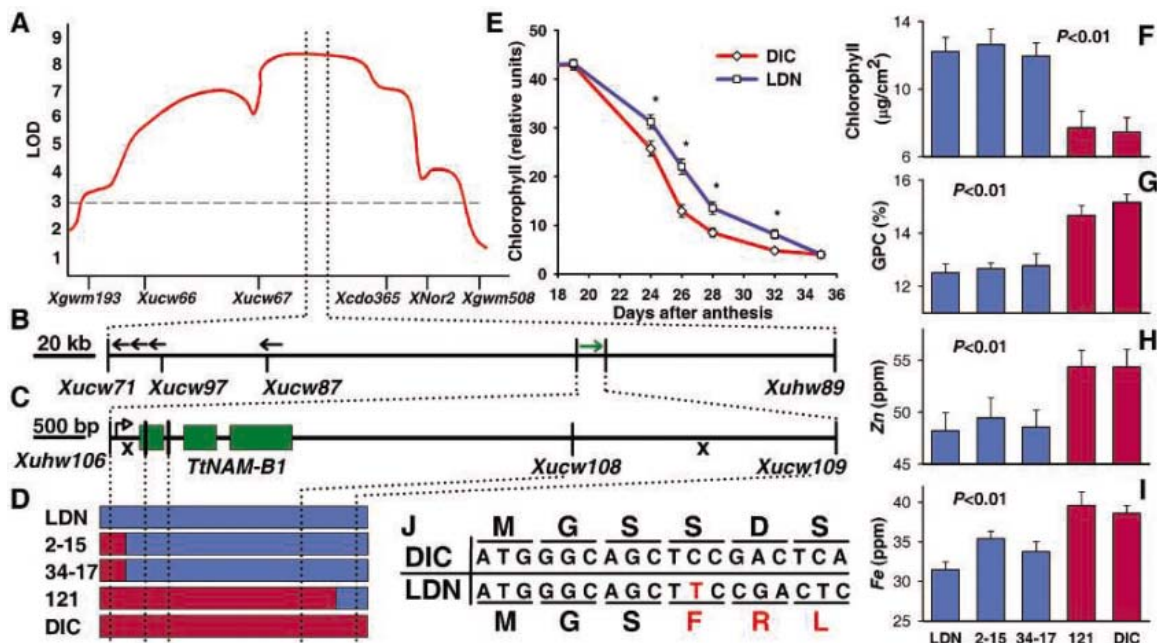
Fig. 2. (**A**) Expression profile of the different *TtNAM* genes relative to *ACTIN* in tetraploid wheat recombinant substitution line 300 carrying a functional *TtNAM-B1* gene. Units are values linearized with the $2^{(-\Delta\Delta CT)}$ method, where CT is the threshold cycle. (**B** and **C**) Relative transcript level of endogenous *TaNAM* genes in T_2 plants (L19-54) segregating for transgenic ($n = 12$, white) and nontransgenic ($n = 11$, black) *TaNAM* RNAi constructs at (**B**) 4 and (**C**) 9 days after anthesis. Asterisks indicate significant differences ($P < 0.05$). (**D**) Flag-leaf chlorophyll content profile of transgenic ($n = 22$ T_1 plants) and nontransgenic controls ($n = 10$ T_1 plants). (**E**) Representative transgenic (left) and nontransgenic (right) plants 50 DAA. (**F**) Main spike and peduncles of representative transgenic and nontransgenic plants 50 DAA. Error bars represent standard error of the mean.
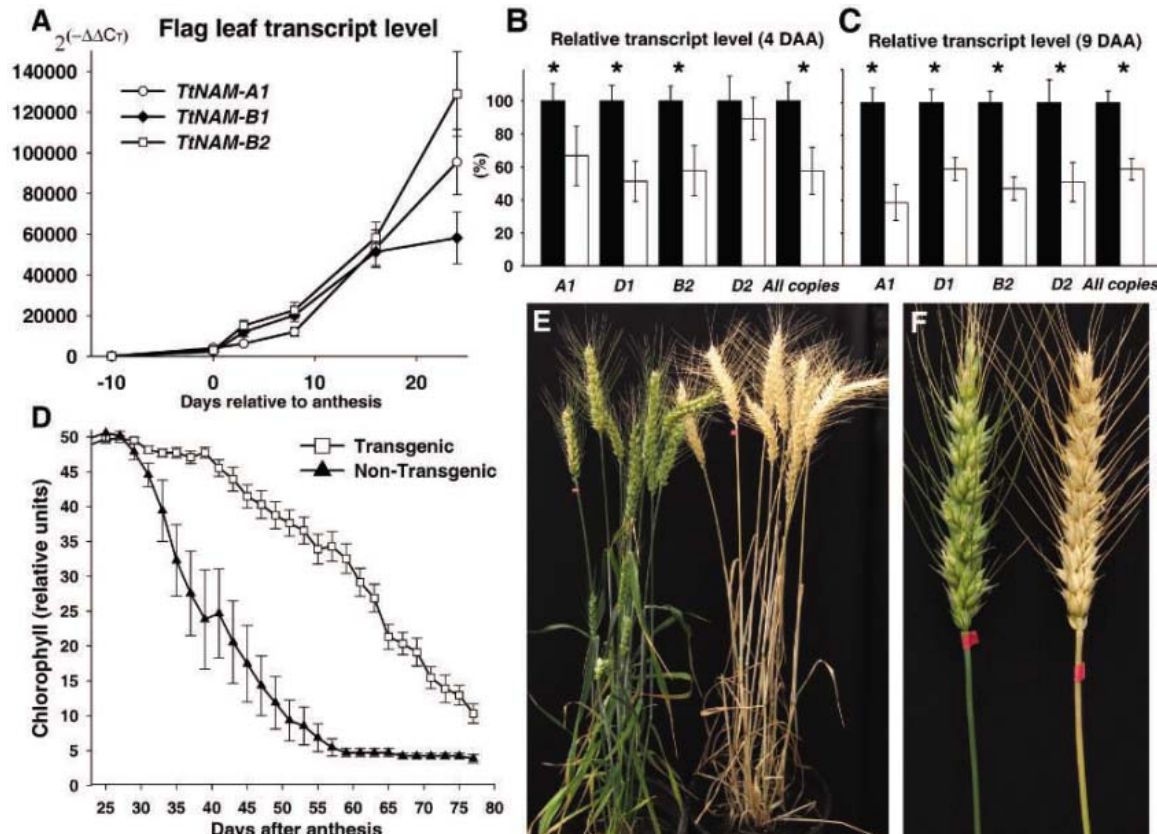
(Fig. 1B) (16). A high-resolution genetic map, based on approximately 9000 gametes and new molecular markers (table S1), was used to determine the linkage between these genes and the Gpc-B1 locus. Three recombinant substitution lines with recombination events between markers Xuhw106 and Xucw109 delimited a 7.4-kb region (Fig. 1, C and D) (16). The recombinant lines carrying this DIC segment senesced on average 4 to 5 days earlier (P < 0.01, Fig. 1, E and F) and exhibited a 10% to 15% increase in GPC (Fig. 1G), Zn (Fig. 1H), and Fe (Fig. 1I) concentrations in the grain (P < 0.01). Complete linkage of the 7.4-kb region with the different phenotypes suggests that Gpc-B1 is a single gene with multiple pleiotropic effects.

The annotation of this 7.4-kb region (Fig. 1C) identified a single gene encoding a NAC domain protein, characteristic of the plant-specific family of NAC transcription factors (17). NAC genes play important roles in developmental processes, auxin signaling, defense and abiotic stress responses, and leaf senescence (18, 19). Phylogenetic analyses revealed that the closest plant proteins were the rice gene ONAC010 (NP_911241) and a clade of three Arabidopsis proteins including No Apical Meristem (NAM) (figs. S1 and S2). On the basis of these similarities, the gene was designated NAM-B1 (DQ869673). To indicate the species source, we have added a two-letter prefix (e.g., Ta and Tt for T. aestivum and T. turgidum genes, respectively).

Comparison of the parental TtNAM-B1 sequences revealed a 1-bp substitution within the first intron and a thymine residue insertion at position 11, generating a frame-shift mutation in the LDN allele (DQ869674, Fig. 1J). This frame shift resulted in a predicted protein having no similarity to any GenBank sequence and lacking the NAC domain.

The wild type TtNAM-B1 allele was found in all 42 wild emmer accessions examined (T. turgidum ssp. dicoccoides) (table S2) and in 17 of the 19 domesticated emmer accessions (T. turgidum ssp. dicoccum). However, 57 cultivated durum lines (T. turgidum ssp. durum) (20) (table S3) lack the functional allele, which suggests that the 1-bp frame-shift insertion was fixed during the domestication of durum wheat. The wild-type TaNAM-B1 allele was also absent from a collection of 34 varieties of hexaploid

wheat (T. aestivum ssp. aestivum), representing different market classes and geographic locations. Twenty-nine of these showed no polymerase chain reaction (PCR) amplification products of the TaNAM-B1 gene, which suggests that it is deleted, whereas the remaining five lines have the same 1-bp insertion observed in the durum lines (table S4).

In addition to the mutant TtNAM-B1 copy, the durum wheat genome includes an orthologous copy (TtNAM-A1) on chromosome arm 6AS and a paralogous one (TtNAM-B2) 91% identical at the DNA level to TtNAM-B1 on chromosome arm 2BS (21) (fig. S3 and table S5). These two copies have no apparent mutations. Comparisons at the protein level of the five domains characteristic of NAC transcription factors (17) revealed 98% to 100% protein identity (fig. S2) between barley, wheat, rice, and maize homologs.

Quantitative PCR (16) showed transcripts from the three TtNAM genes at low levels in flag leaves before anthesis, after which their levels increased significantly toward grain maturity (Fig. 2A). Transcripts were also detected in green spikes and peduncles. The similar transcription profiles and near-identical sequences of TtNAM-A1, B1, and B2 suggest that the 4- to 5-day delay in senescence and the 10% to 15% decrease in grain protein, Zn, and Fe content observed in LDN are likely the result of a reduction in the amount of functional protein rather than the complete loss-of-function of a specific gene.

To test this hypothesis, we reduced the transcript levels of all NAM copies using RNA interference (RNAi). An RNAi construct (16) was transformed into the hexaploid wheat variety Bobwhite, selected for its higher transformation efficiency relative to tetraploid wheat. The RNAi construct targeted the 3′ end of the four TaNAM genes found in hexaploid wheat (TaNAM-A1, D1, B2, and D2), outside the NAC domain, to avoid interference with other NAC transcription factors (fig. S4 and table S6) (22).

We identified two independent transgenic plants (L19-54 and L23-119) with an expected stay-green phenotype. Quantitative PCR analysis of transgenic L19-54 plants showed a significant reduction in the endogenous RNA levels of the different TaNAM copies (22) at 4 and 9 days after anthesis (P < 0.05) (Fig. 2, B and C) compared with control lines. Transgenic plants reached 50% chlorophyll degradation in

flag leaves 24 days later than their nontransgenic sibs (P < 0.001) (Fig. 2D), and their main spike peduncles turned yellow more than 30 days later than the controls (Fig. 2, E and F).

The presence of the RNAi transgene also had significant effects on grain protein, Zn and Fe concentrations. Transgenic plants showed a reduction of more than 30% in GPC (P < 0.001), 36% in Zn (P < 0.01), and 38% in Fe (P < 0.01) concentration compared with the nontransgenic controls (Table 1). No significant differences were observed in grain size (P = 0.41), suggesting that the extra days of grain filling conferred by the reduced TaNAM transcript level did not translate into larger grains in our greenhouse experiments (23). Similar results were obtained for the second transgenic event, L23-119 (fig. S5 and table S7).

These results suggest that the reduced grain protein, Zn, and Fe concentrations were the result of reduced translocation from leaves, rather than a dilution effect caused by larger grains. This hypothesis was confirmed by analyzing the residual nitrogen, Zn, and Fe content in the flag leaves. We analyzed both transgenic events together (due to greater variability in flag leaves compared with the grains) and confirmed higher levels of N (P = 0.01), Zn (P < 0.01), and Fe (P < 0.01) in the flag leaves of transgenic plants compared with the nontransgenic sister lines (table S8). This supports a more efficient N, Zn, and Fe remobilization in plants with higher levels of functional TaNAM transcripts.

These results confirm that a reduction in RNA levels of the TaNAM genes is associated with a delay in whole-plant senescence; a decrease in grain protein, Zn, and Fe concentrations; and an increase in residual N, Zn, and Fe in the flag leaf. These multiple pleiotropic effects suggest a central role for the NAM genes as transcriptional regulators of multiple processes during leaf senescence, including nutrient remobilization to the developing grain.

The differences observed between the transgenic and nontransgenic plants for these traits were larger than those observed between the LDN and DIC alleles. The RNA interference on all functional TaNAM homologs may result in a larger reduction of functional transcripts than the single nonfunctional TtNAM-B1 allele in tetraploid recombinant lines carrying the LDN allele.

The cloning of Gpc-B1 provides a direct link between the regulation of senescence and nutrient remobilization and an entry point to characterize the genes regulating these two processes. This may contribute to their more efficient manipulation in crops and translate into food with enhanced nutritional value.

Table 1. Characterization of grain and senescence-related traits of transgenic Bobwhite T_1 plants (event L19-54) segregating for the presence (transgenic, n = 22 plants) or absence (nontransgenic, n = 10 plants) of the TaNAM RNAi construct. TKW, thousand kernel weight; DAA, days after anthesis.

	GPC (%)	Zn (ppm)	Fe (ppm)	TKW (g)	Dry peduncle (DAA)	Dry spike (DAA)
Transgenic	13.27	52.45	37.40	30.23	72.5	53.0
Nontransgenic	19.08	82.50	60.83	31.27	38.4	37.2
Difference	−5.81	−30.09	−23.42	−1.04	+34.1	+15.8
P value	<0.001	<0.01	<0.01	0.41	<0.001	<0.001

References and Notes
1. World Health Organization, *Meeting of Interested Parties: Nutrition* (2001; http://www.who.int/mipfiles/2299/MIP_01_APR_SDE_3.en.pdf).
2. R. M. Welch, R. D. Graham, *J. Exp. Bot.* **55**, 353 (2004).
3. United Nations Food and Agriculture Organization, *Food Outlook* (4, 2005; www.fao.org/documents).
4. N. Simmonds, *J. Sci. Food Agric.* **67**, 309 (1995).

5. www.harvestplus.org/index.html
6. L. Avivi, "High protein content in wild tetraploid *Triticum dicoccoides* Korn," S. Ramanujam, Ed., 5th Int. Wheat Genet. Symp., New Delhi, Indian Soc. Genet. Plant Breed. (1978).
7. I. Cakmak *et al.*, *Soil Sci. Plant Nut.* **50**, 1047 (2004).
8. L. R. Joppa, C. Du, G. E. Hart, G. A. Hareland, *Crop Sci.* **37**, 1586 (1997).
9. A. Mesfin, R. Frohberg, J. Anderson, *Crop Sci.* **39**, 508 (1999).
10. P. W. Chee, E. M. Elias, J. Anderson, S. F. Kianian, *Crop Sci.* **41**, 295 (2001).
11. S. Olmos *et al.*, *Theor. Appl. Genet.* **107**, 1243 (2003).
12. A. Distelfeld *et al.*, *Funct. Integr. Genomics* **4**, 59 (2004).
13. A. Distelfeld, C. Uauy, T. Fahima, J. Dubcovsky, *New Phytol.* **169**, 753 (2006).
14. C. Uauy, J. Brevis, J. Dubcovsky, *J. Exp. Bot.* **57**, 2785 (2006).
15. A. Distelfeld *et al.*, *Physiol. Plant.*, in press.
16. Materials and methods are available as supporting material on *Science* Online.
17. H. Ooka *et al.*, *DNA Res.* **10**, 239 (2003).
18. A. N. Olsen, H. A. Ernst, L. L. Leggio, K. Skriver, *Trends Plant Sci.* **10**, 79 (2005).
19. Y. Guo, S. Gan, *Plant J.* **46**, 601 (2006).
20. M. Maccaferri, M. C. Sanguineti, P. Donini, R. Tuberosa, *Theor. Appl. Genet.* **107**, 783 (2003).
21. The paralogous *TtNAM-A2* copy was not detected in the LDN tetraploid BAC library or by PCR with 2A genome specific primers derived from *T. urartu*, where the *TuNAM-A2* gene is present.
22. The Bobwhite *TaNAM-B1* gene is deleted as determined by PCR with four sets of independent *NAM-B1* specific primers (table S5). Therefore, no expression data are included for *TaNAM-B1* in the transgenic plants.
23. Field experiments including *Gpc-B1* isogenic lines showed a more variable effect of the DIC chromosome region (including *TtNAM-B1*) on grain size (*14*).
24. We thank G. Hart and L. Joppa for the original mapping materials; L. Li, L. Valarikova, and L. Beloborodov for expert technical assistance; R. Thilmony for critical reading of the manuscript; and the National Small Grain Collection, M. Sanguineti, J. Dvorak, and E. Nevo for germplasm used in this study. This research was supported by the National Research Initiative of USDA's Cooperative State Research, Education, and Extension Service, CAP Grant No. 2006-55606-16629, by BARD, the United States–Israel Binational Agricultural Research and Development Fund, Grant No. US-3573-04C, and by a Vaadia-BARD fellowship. GenBank accession numbers are DQ871219 and DQ869672 to DQ869679.

Evolutionary History of *Salmonella* Typhi

Philippe Roumagnac,[1] François-Xavier Weill,[2] Christiane Dolecek,[3] Stephen Baker,[4] Sylvain Brisse,[2] Nguyen Tran Chinh,[5] Thi Anh Hong Le,[6] Camilo J. Acosta,[7]* Jeremy Farrar,[3] Gordon Dougan,[4] Mark Achtman[1]†

For microbial pathogens, phylogeographic differentiation seems to be relatively common. However, the neutral population structure of *Salmonella enterica* serovar Typhi reflects the continued existence of ubiquitous haplotypes over millennia. In contrast, clinical use of fluoroquinolones has yielded at least 15 independent *gyrA* mutations within a decade and stimulated clonal expansion of haplotype H58 in Asia and Africa. Yet, antibiotic-sensitive strains and haplotypes other than H58 still persist despite selection for antibiotic resistance. Neutral evolution in Typhi appears to reflect the asymptomatic carrier state, and adaptive evolution depends on the rapid transmission of phenotypic changes through acute infections.

Many bacterial taxa can be subdivided into multiple, discrete clonal groupings (clonal complexes, or ecotypes) that have diverged and differentiated as a result of clonal replacement, selective sweeps, periodic selection, and/or population bottlenecks (*1*). Geographic isolation and clonal replacement can also result in phylogeographic differences between bacterial pathogens from different parts of the world (*2*), even within young, genetically monomorphic pathogens (*3*) (supporting online material text) such as *Mycobacterium tuberculosis* (*4*) and *Yersinia pestis* (*5*). Typhi is a genetically monomorphic (*6*), human-restricted bacterial pathogen that causes 21 million cases of typhoid fever and 200,000 deaths

per year, predominantly in southern Asia, Africa, and South America (*7*). Typhi also enters a carrier state in rare individuals [such as Mortimer's example of "Mr. N the milker" (*8*)], who can shed

high levels of these bacteria for decades in the absence of clinical symptoms. Genome sequences are available from strains CT18 (*9*) and Ty2 (*10*), but the global diversity, population genetic structure, and evolutionary history of Typhi were poorly understood. It has been speculated that Typhi evolved in Indonesia, which is the exclusive source of isolates with the z66 flagellar antigen (*11*).

We investigated the evolutionary history and population genetic structure of Typhi by mutation discovery (*12*) within 200 gene fragments (~500 base pairs each) from a globally representative strain collection of 105 strains. The 200 genes included 121 housekeeping genes; 50 genes encoding cell surface structures, regulation, and pathogenicity; and 29 pseudogenes. Size variation of a poly-T_{6-7} homopolymeric stretch within one gene fragment was inconsistent with other phylogenetic patterns (homoplasies) and this fragment was excluded from further analysis. The other 199

[1]Max-Planck-Institut für Infektionsbiologie, Department of Molecular Biology, Charitéplatz 1, 10117 Berlin, Germany. [2]Institut Pasteur, Unité Biodiversité des Bactéries Pathogènes Emergentes, 28 rue du Docteur Roux, 75724 Paris cedex 15, France. [3]Oxford University Clinical Research Unit, Hospital for Tropical Diseases, 190 Ben Ham Tu, District 5, Ho Chi Minh City, Vietnam. [4]The Wellcome Trust Sanger Institute, Wellcome Trust Genome Campus, Hinxton, Cambridge CB10 1SA, UK. [5]Hospital for Tropical Diseases, 190 Ben Ham Tu, District 5, Ho Chi Minh City, Vietnam. [6]Institut National d'Hygiène et d'Épidémiologie, Hanoi 1000, Vietnam. [7]International Vaccine Institute (IVI), Kwanak Post Office Box 14, Seoul 151-600, Korea.

*Present address: GlaxoSmithKline, King of Prussia, PA 19406–2772, USA.

†To whom correspondence should be addressed. E-mail: achtman@mpiib-berlin.mpg.de

Fig. 1. Minimal spanning tree of 105 global isolates based on sequence polymorphisms in 199 gene fragments (88,739 base pairs). The tree shows 59 haplotypes (nodes) based on 88 BiPs, the continental sources of which are indicated by colors within pie charts. The numbers along some edges indicate the number of BiPs that separate the nodes that they connect; unlabeled edges reflect single BiPs. The genomes of the CT18 and Ty2 strains have been sequenced (GenBank accession codes AL513382 and AE014613, respectively). z66 refers to a flagellar variant that is common in Indonesia (*11*).

gene fragments cover 88,739 base pairs, or 1.85% of the genome. Sixty-six were polymorphic as a result of 88 alternative allelic states [biallelic polymorphisms (BiPs)], for a frequency of approximately one BiP per kilobase. Five of the 88 BiPs probably represent three independent recombination events: Four seem to reflect two similar imports spanning 24 to 25 kb from *S. enterica* serovar Typhimurium (fig. S1), and a gene fragment with six single-nucleotide polymorphisms (SNPs) is identical to the corresponding gene fragment in *S. enterica* serovar Paratyphi A. The other 83 BiPs consisted of 37 nonsynonymous SNPs, 3 of which resulted in premature stop codons; 33 synonymous SNPs; 12 SNPs in pseudogenes; and one deletion of 4 base pairs.

We anticipated that housekeeping genes would exhibit diminished levels of nucleotide diversity, π, as a result of purifying selection, and that pathogenicity genes would exhibit elevated levels as a result of diversifying selection. However, π did not differ significantly with gene category ($P >$ 0.05, analysis of variance) (table S1). Purifying selection should result in Ka/Ks (the ratio of nonsynonymous substitutions per nonsynonymous site to synonymous substitutions per synonymous site) values that are less than 1.0 and diversifying selection should result in ratios higher than 1.0. A trend in this direction was observed

(table S1), but it was not particularly strong. We therefore concluded that these 88 BiPs largely reflect the lack of strong selection and are markers of neutral population structure in Typhi. It was somewhat surprising that a supposedly obligate pathogen such as Typhi should possess a neutral population structure, but the population structure of several other bacterial species that occasionally cause disease can also be explained by neutral genetic drift (*13*).

The distribution pattern of the 88 BiPs within Typhi is highly unusual because it is fully parsimonious according to maximum parsimony analysis (homoplasy index = 0). The 88 BiPs defined 59 haplotypes that form a unique path within a single minimal spanning tree of length 88, except for three hypothetical nodes (Fig. 1). These observations suggest that each BiP was caused by a unique genetic event, either a single mutation (83 BiPs) or the three imports described above (5 BiPs). The tree contains 19 informative BiPs that mark the evolutionary history of Typhi plus 69 noninformative BiPs that are specific to single haplotypes. A second, highly unusual feature of this data set is that the ancestral node, haplotype H45, is represented by extant bacteria. H45 must be the ancestral "root" node, because it possesses the identical nucleotides for all 82 SNPs, as did eight genomes of

S. enterica of other serovars, whereas all other haplotypes result from one or more mutations. The general appearance of the tree (Fig. 1) suggests descent from H45 in multiple lineages, followed by diversification during multiple, independent population expansions that resulted in radial clusters of haplotypes containing the noninformative BiPs. For example, one cluster contains all seven Indonesian isolates with the z66 flagellar variant. The z66 cluster radiates from a single haplotype, indicating that it has arisen only once. Hence, z66 isolates cannot represent the evolutionary source of Typhi (*11*), because the z66 cluster is distant from H45.

The haplotype tree has a third, highly unusual feature: Most links between sequential haplotypes consist of single SNPs, and many longer edges, including one hypothetical node, were resolved into steps of single SNPs when additional strains were surveyed (fig. S2). Even within this initial sample of 105 isolates, almost half of the mutational steps during the evolutionary history of Typhi are represented by extant haplotypes, indicating long persistence of individual haplotypes. If ecotypes associated with periodic selection were to exist within Typhi, the genetic continuum between haplotypes implies that ecotypes are subdivisions of haplotypes. Furthermore, haplotypes and haplotype clusters were found in multiple continents. For
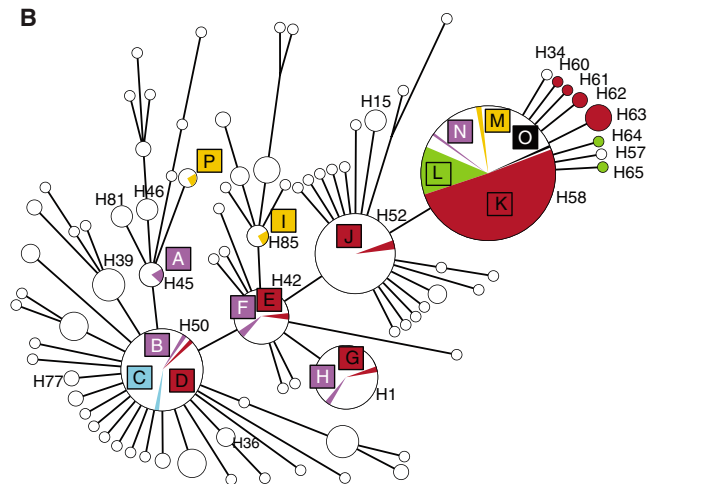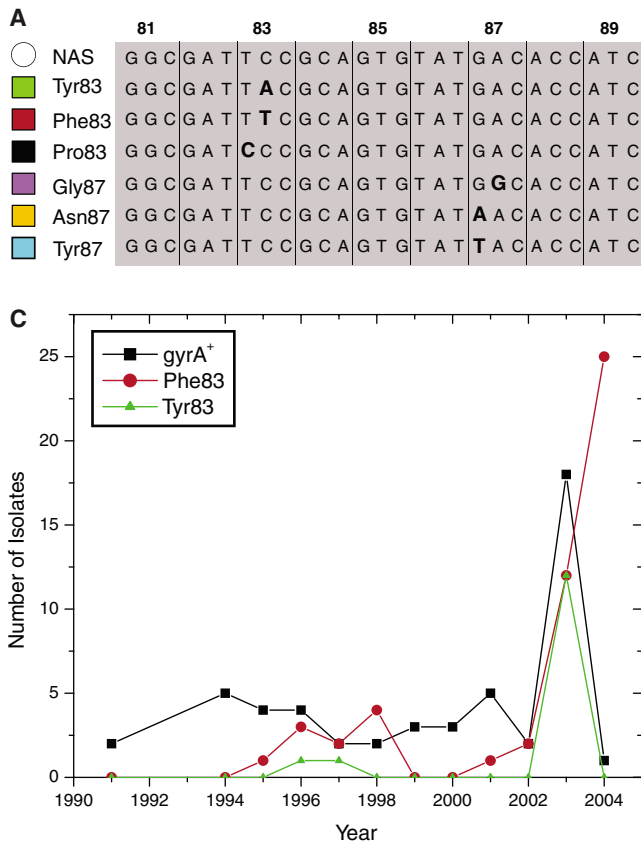
Fig. 2. Selection for mutations in *gyrA* versus a neutral population framework in 483 strains. The strains consisted of 105 global isolates (Fig. 1), 59 older isolates from Africa and Vietnam (1958 to 1967) (fig. S4 and Table 1), and 317 isolates from southeast Asia (1984 to 2004) and other sources. (**A**) Sequence of codons 81 to 89 of *gyrA*, showing all mutated nucleotides (bold) that were detected within a 489–base pair stretch. Each mutation is designated by the name of the resulting amino acid and codon position (left). NAS, nalidixic acid sensitive. (**B**) Minimal spanning tree of 85 haplotypes based on 97 BiPs within 55 polymorphic genes. Sizes of circles and arcs reflect numbers of isolates. Strains without mutations in *gyrA* are shown in white, whereas strains with mutations are indicated by colored arcs that correspond to the colors in (A). The 15 letters indicate independent mutations associated with resistance to nalidixic acid. (**C**) Time course of isolation of 118 isolates of haplotype H58 or its derivative haplotypes H34, H57, and H60 to H65. These isolates were selected for haplotyping and *gyrA* genotyping without prior knowledge of their susceptibility to nalidixic acid. Fifty-two other H58 isolates from Vietnam are not included because they were a nonrandom sample of Nal[R] bacteria. The apparent increase of Phe83 in 2004 is based on a sample from the Mekong Delta province of Vietnam and may represent an outlier.
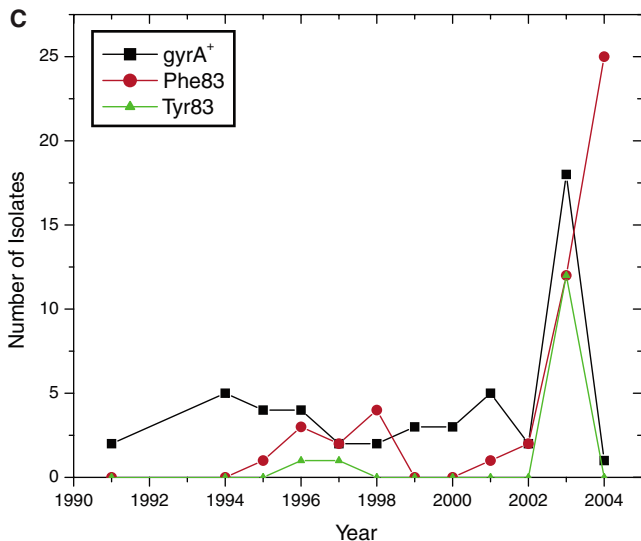
example, it is unclear where H45 evolved, because it has been isolated from five locations in Asia, Africa, and North America (3). Because each BiP is associated with a single, genetic event, each haplotype or haplotype cluster that is present in multiple continents marks at least one independent wave of global transmission. Global transmission has not been previously described for Typhi but is a well-known phenomenon with other human pathogens.

To place the time scale associated with neutral evolution in context, we calculated the time since the most recent common ancestor (tmrca) and the effective population size (N_e) from the selectively neutral data in Fig. 1. These calculations were per-

formed with the use of two estimates of the molecular clock rate, a high rate corresponding to the long-term rate of accumulation of synonymous mutations between *Escherichia coli* and *S. enterica* (5) and a clock rate one-fifth as high, corresponding to the rate of accumulation of all mutations in conserved housekeeping genes between these species (14). For Typhi, tmrca is 10 to 43 thousand years (95% confidence limits of 5.7 to 15.8 thousand years for the high clock rate and 25.5 to 71 thousand years for the low rate) according to both Bayesian skyline plots (15) and maximum likelihood trees (fig. S3). Based on the same clock rates, N_e is currently 2.3×10^5 to 1.0×10^6 (confidence limits of 1.2×10^4 to 9.3×10^5 for the high clock rate and 5.3×10^4 to 4.1×10^6 for the low clock rate) (fig. S3A). Similar values were obtained from the nucleotide variation, θ_w, by an independent method (16) (table S1). The maximum likelihood tree also suggests that H45, the ancestral haplotype, and multiple descendent haplotypes arose after human migrations out of Africa but before the Neolithic period (fig. S3B).

The existence of an asymptomatic human carrier state for typhoid is formally similar to tuberculosis, for which the reactivation of granulomas after decades results in delays of centuries between initial new infections and subsequent epidemic peaks (17). Likewise, we propose that the human carrier state allowed persistence of infection with Typhi during periods of isolation and was essential for transmission between hunter-gatherer groups. Hence, the population structure and geographical distribution of Typhi may largely reflect the frequency of carriers.

The 55 polymorphic coding gene fragments (excluding pseudogenes) were screened by mutation discovery with 59 additional strains that were isolated between 1958 and 1967 from Africa and

Vietnam. All but three strains were assigned to known haplotypes from the global sample (fig. S4). Twelve haplotypes were isolated on multiple occasions over a range of 22 to 44 years from eight countries (Table 1), demonstrating that Typhi haplotypes persist in single countries for decades, or longer. For example, CT18 (9) is a multidrug-resistant (MDR) strain of haplotype H1 that was isolated in Vietnam in 1993, soon after multidrug resistance emerged. However, a Vietnamese isolate from 1967 was also of haplotype H1, showing that H1 was present in Vietnam long before multidrug resistance emerged. The long-term persistence of Typhi may also reflect the carrier state and can help explain why Typhi remains endemic in regions of the world with poor drinking-water quality and limited sewage treatment (18).

Antibiotic-resistant typhoid fever has recently become an enormous public health problem in southern Asia because of the emergence of MDR Typhi followed by nalidixic acid resistance (Nal^R) with concomitant reduced susceptibility to fluoroquinolones (19). Fluoroquinolones were first used for antibiotic therapy in southeast Asia in 1989 (20) and Nal^R Typhi were reported in 1991 (21). Such strong selection should have led to a population expansion of Nal^R Typhi, and possibly to clonal replacement of existing haplotypes within southern Asia. We therefore performed mutation discovery with the 55 polymorphic coding fragments on 295 additional strains of Typhi that were isolated from southern Asia between 1986 and 2004. Again, most strains were assigned to known haplotypes and only a few defined new, peripheral haplotypes (Fig. 2B). However, the relative frequencies of isolates differed from those in the global set of 105 strains (Fig. 1), because most recent isolates from southern Asia, particularly Nal^R isolates, belonged to haplotype H58 (Fig. 2B). Thus, a recent population expansion of H58 seems to have resulted from the general use of fluoroquinolones.

We also investigated the genetic diversity of a 489–base pair fragment of the *gyrA* gene encoding a DNA gyrase subunit, within which nonsynonymous mutations at codons 83 and 87 result in resistance to nalidixic acid (22). All 125 strains that were sensitive to nalidixic acid (Nal^S) and all other strains with unknown resistance to nalidixic acid possessed the ancestral *gyrA*+ sequence. In contrast, all 119 Nal^R strains, most of which were isolated in south central or southeast Asia (table S2), possessed one of six nonsynonymous mutations at codons 83 and 87 of *gyrA* (Fig. 2A), and no other mutations were detected in *gyrA* (or *parC*). We identified 15 independent mutational events (A through O in Fig. 2B) in distinct haplotypes that also possessed *gyrA*+ alleles. Assuming that they all arose between 1991 and 2004 (13 years), the identification of ≥15 mutations in two codons (6 base pairs) yields a minimum frequency of 0.19 per base pair per year, $\geq 2.5 \times 10^8$ greater than the long-term mutation clock rate within *E. coli* (14).

For most haplotypes with *gyrA* mutations, Nal^R strains were detected only once or twice; however,

Table 1. Persistence of haplotypes over decades.

Haplotype	Persistence (years)	Years persisted	No. of isolates
Vietnam			
H1	37	1967–2004	25
H50	37	1959–1996	3
Madagascar			
H15	31	1965–1996	4
H50	33	1967–2000	2
Algeria			
H36	34	1966–2000	3
Ivory Coast			
H39	34	1967–2001	4
H81	35	1967–2002	2
Senegal			
H39	22	1966–1988	4
H52	39	1962–2001	4
Congo			
H46	34	1966–2000	3
Morocco			
H52	34	1966–2000	2
Cameroon			
H77	44	1958–2002	2

Table 2. Geographic sources of haplotypes with *gyr* mutations by haplotype. Where more than one isolate was found in a country, the number of isolates is indicated in parentheses.

Haplotype	*gyrA* mutation (isolates)	*gyrA*+ (isolates)
H45	A: India	Global (4)
H50	B: India	Global (55)
	C: China	
	D: Mexico	
H42	E: India; F: Pakistan	Global (24)
H1	G: Vietnam	Vietnam (23); Laos (7); Bangladesh;
	H: Vietnam	Indonesia
H85	I: India	Morocco, Pakistan, Indonesia
H52	J: India (2)	Global (53)
H58	K: Vietnam (68), Pakistan (5), India (4), Cambodia, Nepal, central Africa;	Vietnam (31), India (12), Laos (5), Pakistan (3), Hong Kong (2), Bangladesh,
	L: India (6), Bangladesh (6), Vietnam (5), Indonesia	Sri Lanka, Morocco
	M: Pakistan (2)	
	N: Vietnam	
	O: Pakistan	
H34, H57, and H60-65	K: Vietnam (8), Bangladesh (2) L: India (2)	Nepal, Laos

Nal^R variants of haplotype H58 and its derivative haplotypes (H34, H57, and H60 to H65) were isolated in Vietnam, India, and Pakistan, and other countries in southern Asia (Table 2). These Nal^R variants represent at least five distinct *gyrA* mutations (K, L, M, N, and O), which arose during or before the mid-1990s (Fig. 2C). The frequency of *gyrA*$^+$ and mutation L has remained fairly constant since the mid-1990s, but H58 isolates with mutation K seem to have become more common in recent years, particularly in Vietnam (Table 2).

These results show that selection for antibiotic resistance has probably led to clonal expansion of H58 and its Nal^R derivatives in southern Asia. These strains have now also reached Africa, given that one MDR H58 strain (isolated in Morocco in 2003) was included among nine rare, recent MDR isolates from Africa and that the sole MDR Nal^R isolate from Africa that was tested (mutation K, isolated in central Africa in 2004) also belonged to H58 (Table 2). Thus, H58 is probably not ethnically restricted to southern Asians, and nalidixic acid–resistant typhoid fever may soon present an additional public health problem in Africa.

Despite the selection for resistance to nalidixic acid in southern Asia, the data do not show complete clonal replacement, which would be expected from periodic selection; about 20% of Typhi isolated in recent years in northern Vietnam and 5% of Typhi from southern Vietnam remain susceptible to nalidixic acid, as are many other recent H58 isolates (Fig. 2C). Furthermore, recent isolates from southern Asia also belong to other haplotypes, where mutations in *gyrA* are rare (Fig. 2B). Thus, the population structure indicative of neutral evolution has not been disrupted by strong selection for resistance to nalidixic acid during the past 15 years, except for the clonal expansion of H58. Possibly *gyrA* mutations in many haplotypes reduce fitness (*23*) or some cases of typhoid fever have not been treated with fluoroquinolones. But still another alternative is that the population structure of Typhi reflects two distinct epidemiological dynamics associated with different time scales: first, the human carrier state permitting slow neutral evolution (millennia), and second, infectious transmission facilitating a rapid response to selection in real time. Outbreaks of infections, similar to the recent expansion of H58 in southeast Asia, may be responsible for independent chains of intercontinental transmission. These, in turn, create a global distribution of carriers for multiple haplotypes. According to this interpretation, it is exactly because the environment selects that everything is everywhere in Typhi, thus inverting a hotly disputed (*24*) tenet of microbial ecology that was proposed by L. G. M. Baas Becking in 1934 (*25*).

The results presented here open multiple avenues for future research. Long-term epidemiology with larger strain collections is now possible on the basis of neutral SNPs (fig. S2), whereas classical microbiological methods do not seem to provide reliable markers for such purposes (table S3). Surveillance of haplotypes is particularly appropriate to provide early warning of the

continued spread of Nal^R H58. Our overview of the current global population diversity in Typhi will allow comparisons of genomic sequences from representative strains without the risk of phylogenetic discovery bias (*26*). Finally, we suggest that the human carrier state may be of much greater importance for neutral evolution and genetic buffering than had been previously appreciated, an interpretation that would demand major changes in public health campaigns to reduce the incidence of typhoid.

References and Notes

1. D. Gevers et al., Nat. Rev. Microbiol. **3**, 733 (2005).
2. P. Zhu et al., Proc. Natl. Acad. Sci. U.S.A. **98**, 5234 (2001).
3. Materials and methods are available as supporting material on Science Online.
4. M. M. Gutacker et al., J. Infect. Dis. **193**, 121 (2006).
5. M. Achtman et al., Proc. Natl. Acad. Sci. U.S.A. **101**, 17837 (2004).
6. C. Kidgell et al., Infect. Genet. Evol. **2**, 39 (2002).
7. J. A. Crump, S. P. Luby, E. D. Mintz, Bull. World Health Organ. **82**, 346 (2004).
8. P. P. Mortimer, Lancet **353**, 1354 (1999).
9. J. Parkhill et al., Nature **413**, 848 (2001).
10. W. Deng et al., J. Bacteriol. **185**, 2330 (2003).
11. G. Frankel, S. M. Newton, G. K. Schoolnik, B. A. Stocker, EMBO J. **8**, 3149 (1989).
12. P. A. Underhill et al., Genome Res. **7**, 996 (1997).
13. C. Fraser, W. P. Hanage, B. G. Spratt, Proc. Natl. Acad. Sci. U.S.A. **102**, 1968 (2005).
14. T. Wirth et al., Mol. Microbiol. **60**, 1136 (2006).
15. A. J. Drummond, A. Rambaut, B. Shapiro, O. G. Pybus, Mol. Biol. Evol. **22**, 1185 (2005).
16. D. J. Funk, J. J. Wernegreen, N. A. Moran, Genetics **157**, 477 (2001).
17. S. M. Blower et al., Nat. Med. **1**, 815 (1995).
18. D. Young, T. Hussell, G. Dougan, Nat. Immunol. **3**, 1026 (2002).
19. M. K. Bhan, R. Bahl, S. Bhatnagar, Lancet **366**, 749 (2005).
20. C. Rodrigues, A. Mehta, V. R. Joshi, Clin. Infect. Dis. **34**, 126 (2002).
21. E. J. Threlfall, L. R. Ward, Emerg. Infect. Dis. **7**, 448 (2001).
22. K. L. Hopkins, R. H. Davies, E. J. Threlfall, Int. J. Antimicrob. Agents **25**, 358 (2005).
23. S. Gagneux et al., PLoS Pathog. **2**, e61 (2006).
24. J. B. Martiny et al., Nat. Rev. Microbiol. **4**, 102 (2006).
25. L. G. M. Baas Becking, Geobiologie of Inleiding Tot de Milieukunde (W. P. Van Stockum & Zoon, The Hague, Netherlands, 1934).
26. T. Pearson et al., Proc. Natl. Acad. Sci. U.S.A. **101**, 13536 (2004).
27. We thank M. Feldkamp and L. Fabre-Berland for technical assistance; K. E. Sanderson, M. Torpdahl, J. M. Collard, and S. Porwollik for DNA; and G. Morelli, B. Linz, Y. Moodley, F. Balloux, and D. Falush for helpful discussions. Support was provided by The Wellcome Trust, UK. Work at IVI was supported by the Diseases of the Most Impoverished Program, funded by the Bill and Melinda Gates Foundation. IVI thanks M. Ali, A.-L. Page, C. M. Galindo, J. D. Clemens, R. L. Ochiai (IVI); B. Dong (Guangxi Center for Prevention and Disease Control, CDC, China); Z. A. Bhutta (Aga Khan University, Pakistan); S. A. Bhattacharya (National Institute of Cholera and Enteric Disease, India); M. Agniti (National Institute of Health Research and Development, Indonesia); V. D. Thiem (National Institute of Hygiene and Epidemiology, Vietnam); A. Naheed (International Centre for Diarrhoeal Disease Research, Bangladesh). GenBank accession numbers: EF070864 to EF070980.

Dissecting the Functions of the Mammalian Clock Protein BMAL1 by Tissue-Specific Rescue in Mice

Erin L. McDearmon,[1,2] Kush N. Patel,[2] Caroline H. Ko,[2,3] Jacqueline A. Walisser,[4] Andrew C. Schook,[1,2] Jason L. Chong,[2] Lisa D. Wilsbacher,[2] Eun J. Song,[1,2] Hee-Kyung Hong,[1,2] Christopher A. Bradfield,[4] Joseph S. Takahashi[1,2]*

The basic helix-loop-helix (bHLH)–Per-Arnt-Sim (PAS) domain transcription factor BMAL1 is an essential component of the mammalian circadian pacemaker. *Bmal1*$^{-/-}$ mice lose circadian rhythmicity but also display tendon calcification and decreased activity, body weight, and longevity. To investigate whether these diverse functions of BMAL1 are tissue-specific, we produced transgenic mice that constitutively express *Bmal1* in brain or muscle and examined the effects of rescued gene expression in *Bmal1*$^{-/-}$ mice. Circadian rhythms of wheel-running activity were restored in brain-rescued *Bmal1*$^{-/-}$ mice in a conditional manner; however, activity levels and body weight were lower than those of wild-type mice. In contrast, muscle-rescued *Bmal1*$^{-/-}$ mice exhibited normal activity levels and body weight yet remained behaviorally arrhythmic. Thus, *Bmal1* has distinct tissue-specific functions that regulate integrative physiology.

Circadian rhythms control many aspects of mammalian physiology and behavior. The suprachiasmatic nuclei (SCN) act as pacemakers required for the generation of circadian behavioral rhythms as well as synchronizers of autonomous peripheral tissue clocks (*1*). Molecular circadian regulation engages a transcription-translation feedback loop comprising the activating proteins CLOCK and BMAL1, which induce expression of the negative feed-

back elements *Per* and *Cry* (*1*). BMAL1 (also known as MOP3) was originally characterized by its high expression in brain and muscle (*2*, *3*) and was identified as a heterodimeric binding partner of CLOCK (*4*, *5*). *Bmal1$^{-/-}$* mice not only lose behavioral circadian rhythmicity but also exhibit a variety of other phenotypes including decreased activity levels and body weight, progressive joint disease, and shortened life span (*6*–*12*). Therefore, in addition to circadian rhythm regulation, BMAL1 appears to play a role in a variety of functions that are potentially dependent on the tissue type in which it is expressed. To determine whether BMAL1 has unique tissue-specific functions, we generated transgenic mice that express *Bmal1* ubiquitously or in distinct tissue types. We then crossed these lines onto a *Bmal1* null background and determined which phenotypes could be rescued by exogenous, tissue-specific *Bmal1* expression.

We first examined the effects of rescuing *Bmal1* ubiquitously by using a transgenic mouse line produced with *Bmal1*-containing bacterial artificial chromosome (BAC) clones (Fig. 1A) (*13*). Because the BAC clones contain the genomic coding and promoter sequence of *Bmal1*, expression of the transgene should occur in all tissues that normally express *Bmal1*. We measured increased *Bmal1* expression in the SCN of BAC transgenic mice at normal peak and trough times of *Bmal1* mRNA [ZT (zeitgeber time) 18 and 6, respectively], and also observed increased *Bmal1* expression during peak times in the liver (ZT 18 to ZT 2) (fig. S1) (*13*). BAC transgenic mice were then sequentially crossed with *Bmal1$^{+/-}$* mice to produce BAC-rescued *Bmal1$^{-/-}$* mice (*13*). Circadian rhythms of locomotor activity were then analyzed in a 12 hour:12 hour light:dark (LD) cycle followed by constant darkness (DD) conditions (Fig. 1C) (*13*).

Whereas *Bmal1$^{-/-}$* mice exhibited no circadian rhythm of activity in DD and showed reduced activity levels, BAC-rescued *Bmal1$^{-/-}$* mice displayed normal circadian rhythm characteristics (free-running period and amplitude of circadian rhythm) and activity levels in LD and DD that were similar to those of wild-type mice (Fig. 1D). In addition, 100% of BAC-rescued *Bmal1$^{-/-}$* mice survived until the end of experimental analysis (≥10 months old) compared to 29% of *Bmal1$^{-/-}$*

mice. Therefore, long-term survival was restored in the BAC-rescued *Bmal1$^{-/-}$* mice, and no gross abnormalities such as low body weight or joint calcification were observed in the BAC-rescued mice. Thus, *Bmal1* BAC transgenes completely rescued the phenotypes observed in *Bmal1$^{-/-}$* mice.

We next determined whether expression of *Bmal1* in brain tissue could restore behavioral rhythms in *Bmal1$^{-/-}$* mice as well as alleviate other phenotypes. To produce the brain-rescued line, we used the tetracycline trans-

activator (tTA) system, which requires two transgenes for expression of the target gene *Bmal1* (Fig. 2A) (*14*, *15*). We used the promoter sequence of *Scg2*, which is expressed in brain and enriched in the SCN (*16*), to drive expression of the tetracycline transactivator (*tTA*) (*13*). The tTA protein binds to the tetracycline operator (tetO) sequence and drives expression of downstream hemagglutinin (HA)–tagged *Bmal1* (*Bmal1-HA*) cDNA. Doxycycline (Dox) inhibits tTA binding to the *tetO* promoter, which halts expression of
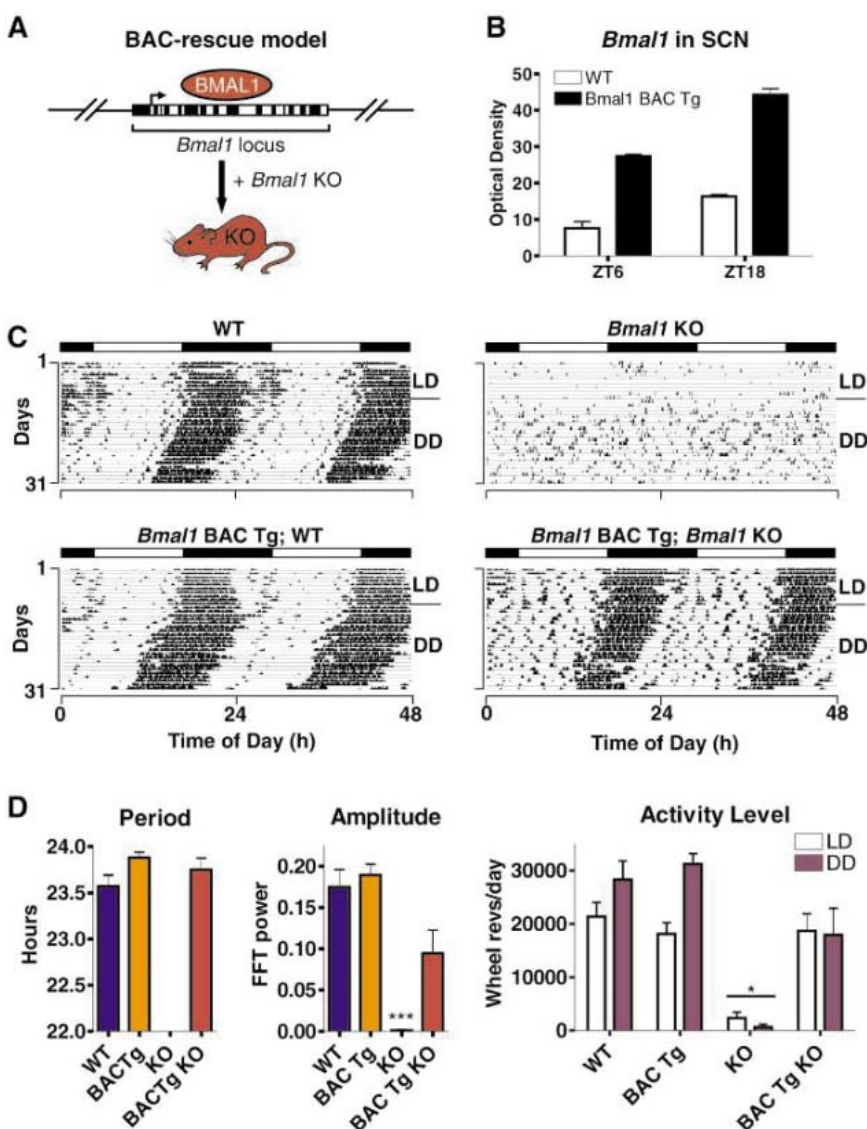
Fig. 1. *Bmal1*-containing BAC transgenes rescue *Bmal1$^{-/-}$* phenotypes. (**A**) *Bmal1* BAC clones were used to create transgenic (Tg) mice, which were consecutively crossed with *Bmal1$^{+/-}$* mice to create BAC-rescued *Bmal1$^{-/-}$* mice. (**B**) *Bmal1* mRNA levels in SCN were examined by in situ hybridization in wild-type (WT) and *Bmal1* BAC Tg mice, killed at ZT 6 and ZT 18 [shown are means ± SEM; significant effect of genotype, generalized linear model analysis of variance (GLM ANOVA)]. (**C**) Representative wheel-running activity records from WT, *Bmal1* BAC Tg, *Bmal1$^{-/-}$* (*Bmal1* KO), or BAC-rescued (*Bmal1* BAC Tg; *Bmal1* KO) mice. Mice were housed in LD and then released into DD for 3 weeks. (**D**) Bar graphs of means ± SEM show that BAC-rescued mice (*n* = 6) exhibit free-running period, amplitude of circadian rhythm, and activity levels that are not significantly different from those of WT. Amplitude is graphed as the peak amplitude of the proportion of the total variance in the time series in the circadian (~24 hours) range (***P < 0.001, one-way ANOVA; *significant effect of genotype, GLM ANOVA).

[1]Howard Hughes Medical Institute, Department of Neurobiology and Physiology, Northwestern University, Evanston, IL 60208, USA. [2]Department of Neurobiology and Physiology, Northwestern University, Evanston, IL 60208, USA. [3]Department of Psychology, University of Toronto, Toronto, Ontario M5S 3G3, Canada. [4]McArdle Laboratory for Cancer Research, University of Wisconsin, Madison, WI 53706, USA.

*To whom correspondence should be addressed. E-mail: j-takahashi@northwestern.edu

Bmal1-HA. In situ hybridization showed strong, specific expression of *Bmal1-HA* in *Scg2::tTA* × *tetO::Bmal1-HA* double transgenic mice only (Fig. 2B) (*13*). The pattern of expression observed is consistent with high *Scg2* expression in the SCN. HA-tagged protein at the correct molecular weight for BMAL1 (~69 kD) was produced specifically in double transgenic mouse brain extracts (Fig. 2C), and HA-tagged BMAL1 was shown to be functional by *Per1::luciferase* reporter gene assays (fig. S2) (*13*). The double transgenic mice were crossed onto a *Bmal1*⁻/⁻ background to create brain-rescued *Bmal1*⁻/⁻ mice, and wheel-running experiments were performed as described above (Fig. 2D and figs. S3 to S5).

Adult (≥8 weeks old) brain-rescued *Bmal1*⁻/⁻ mice exhibited a consistent circadian rhythm of behavior in the initial (pre-Dox) DD period, which was completely abolished after 1 to 2 days of Dox administration and then regained during Dox withdrawal. However, the free-running period of brain-rescued mice was about 1 hour shorter than that of wild-type mice (Fig. 2E). This was likely due to the constitutive bioavailability of BMAL1 protein and/or the lack of peripheral tissue feedback to the SCN (fig. S6). In support of this idea, *Rev-Erbα*⁻/⁻ mice express *Bmal1* in the SCN at consistently high levels and exhibit shortened period length (*17*). In contrast to the restoration of circadian rhythmicity in brain-rescued mice, both amplitude and activity levels were

significantly lower than that seen in wild-type mice (Fig. 2E). Thus, brain-rescued mice exhibit restored circadian rhythms of behavior, but their locomotor activity is still impaired.

Because *Bmal1* is highly expressed in muscle, we investigated whether muscle-specific rescue might restore activity levels in *Bmal1*⁻/⁻ mice. We produced muscle-specific *Bmal1* transgenic mice with the use of a DNA construct consisting of human α-actin–1 (*Acta1*) promoter sequence positioned upstream of *Bmal1-HA* (Fig. 3A) (*13*). HA-tagged protein was specifically detected in transgenic muscle extracts (Fig. 3B) (*13*). Adult muscle-rescued *Bmal1*⁻/⁻ mice did not express circadian rhythmicity of activity (Fig. 3, C and D); however, their level of locomotor

Fig. 2. Reversible restoration of circadian rhythms but not activity levels in brain-rescued *Bmal1*⁻/⁻ mice. (**A**) Mice were created to express *Bmal1-HA* conditionally in brain tissue with the use of the tTA system. (**B**) In situ hybridization was performed with *HA* tag or *Bmal1* probes on brains from WT, *tetO::Bmal1-HA* (tetO), or *Scg2::tTA* × *tetO::Bmal1-HA* double transgenic (DTg) mice killed at ZT 6 (arrow indicates SCN; scale bar, 1 mm). (**C**) Western blot showing HA staining in brain, liver, and skeletal muscle protein extracts from WT or DTg mice killed at ZT 12 (arrow indicates correct size of BMAL1). (**D**) Representative wheel-running activity records from one *Bmal1*⁻/⁻ mouse and two brain-rescued *Bmal1*⁻/⁻ (DTg; *Bmal1* KO) mice. After 3 weeks in DD (Pre), mice were administered Dox for 2 weeks (Dox, highlighted yellow) and then spent an additional 3 weeks without Dox (Post). (**E**) Brain-rescued mice (*n* = 10) display a free-running period of 22.8 hours (Pre) and 22.6 hours (Post) when *Bmal1* is expressed; these values are significantly different from those of WT and DTg groups (*significant effect of genotype, GLM ANOVA). Activity levels of KO and DTg KO mice were significantly reduced relative to WT. Amplitude of circadian rhythm was significantly different in all genotypes relative to WT, and a simultaneous loss of rhythm and decrease in amplitude were observed in DTg KO mice during Dox treatment (†significant effect of time interval). Graphs represent means ± SEM.
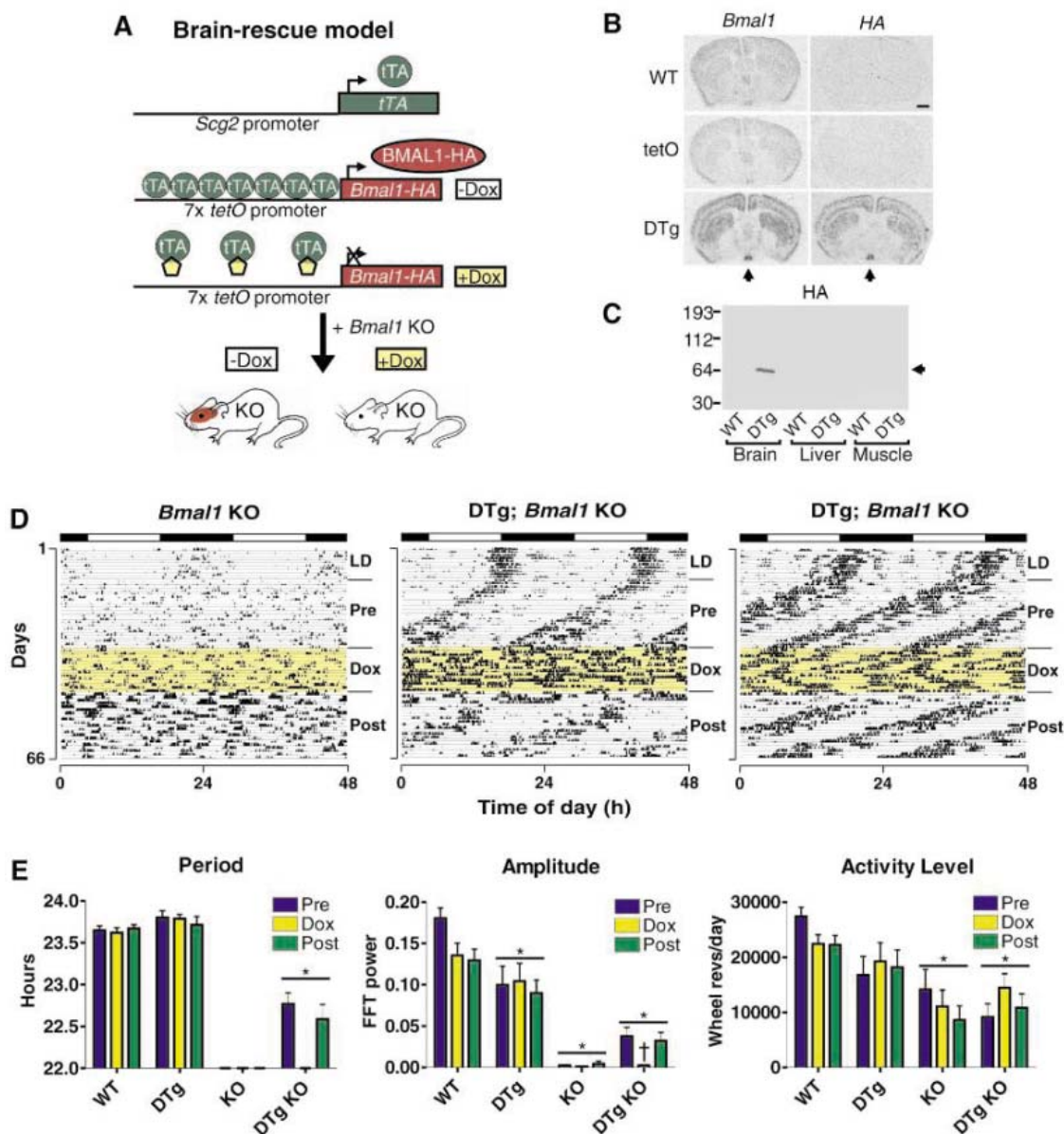
activity was not significantly different from that of wild-type mice (Fig. 3D).

We also found that at 4 to 6 months of age, the $Bmal1^{-/-}$ and brain-rescued mice weighed significantly less than did wild-type mice. In contrast, the body weight of muscle-rescued mice was restored to a level not significantly different from that of wild-type mice (Fig. 4A) (13). Only 75% of brain-rescued mice survived to the end of the experiment, whereas 100% of muscle-rescued mice survived. These results suggest that BMAL1 function in muscle is important for activity as well as for body weight maintenance and longevity. In addition, bone phenotypes were examined by Alizarin Red stain; both brain- and muscle-rescued mice showed significant tendon calcification similar to that seen in $Bmal1^{-/-}$ mice (Fig. 4B). This suggests that $Bmal1$-HA was not expressed in bone in either line and that the calcification observed in $Bmal1^{-/-}$ mice was not improved by restoring BMAL1 expression in muscle or brain. Thus, three distinct patterns of rescue could be observed in these mice, relating to (i) circadian activity rhythms, (ii) activity level and body weight, and (iii) tendon calcification.

Unlike the BAC transgenic line, the brain and muscle transgenic lines were designed to constitutively express BMAL1-HA. To verify this, we measured similar levels of $Bmal1$ mRNA and BMAL1-HA protein at normal peak and trough times in the brain and muscle transgenic lines (figs. S6 and S7) (13). We then examined mRNA levels of the key BMAL1 target genes $Per1$ and $Per2$ (6). Relative to wild-type and brain double transgenic mice, $Bmal1^{-/-}$ mice exhibited consistently low expression levels of $Per1$ in the SCN (fig. S7). In contrast, the brain-rescued mice had increased amplitude of $Per1$ expression, although peak levels remained significantly lower than those of wild-type mice (fig. S7). $Per2$ expression was measured in both muscle and liver from the brain and muscle transgenic lines at normal peak time for $Per2$ (ZT 12) (fig. S8) (13). $Per2$ in muscle of $Bmal1^{-/-}$ mice was significantly reduced to below 50% of wild-type levels at ZT 12. This decreased expression was restored to wild-type levels in the muscle-rescued mice but not in the brain-rescued mice. These data suggest that the presence of BMAL1 is important for proper expression of $Per1$ genes in brain and muscle tissue (but not liver; see fig. S8). Both Rev-$Erb\alpha$ and Dbp exhibited substantial down-regulation in liver and muscle of $Bmal1^{-/-}$ mice at ZT 12 and showed increased expression only in muscle of muscle-rescued mice (fig. S8).

We have shown that all phenotypes of $Bmal1^{-/-}$ mice are alleviated only when $Bmal1$ is rescued ubiquitously, whereas different parameters of behavioral activity (circadian rhythm and activity level), body weight, and
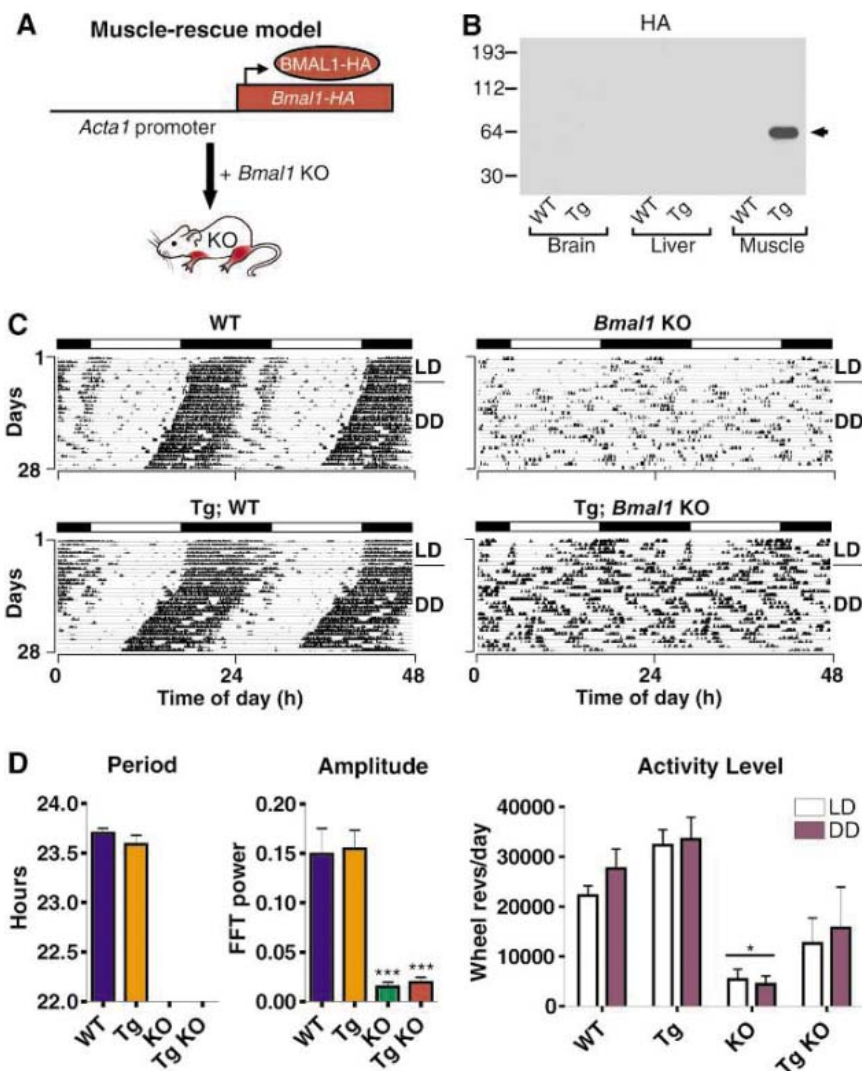
Fig. 3. Muscle-rescued mice exhibit restored activity level but not circadian rhythms. (A) Muscle-specific $Bmal1$ Tg mice were created by fusing the $Acta1$ promoter sequence to $Bmal1$-HA. (B) Western blot shows HA staining in brain, liver, and skeletal muscle protein extracts from WT or Tg mice killed at ZT 12 (arrow indicates correct size of BMAL1). (C) Representative wheel-running activity records are shown from WT, Tg, $Bmal1$ KO, and muscle-rescued (Tg; $Bmal1$ KO) mice. (D) Muscle-rescued mice ($n = 6$) are arrhythmic in DD with significantly reduced amplitude of rhythm (**$P < 0.01$, one-way ANOVA) but display activity levels that are not significantly different from those of WT mice. Graphs show means ± SEM (*significant effect of genotype, GLM ANOVA).
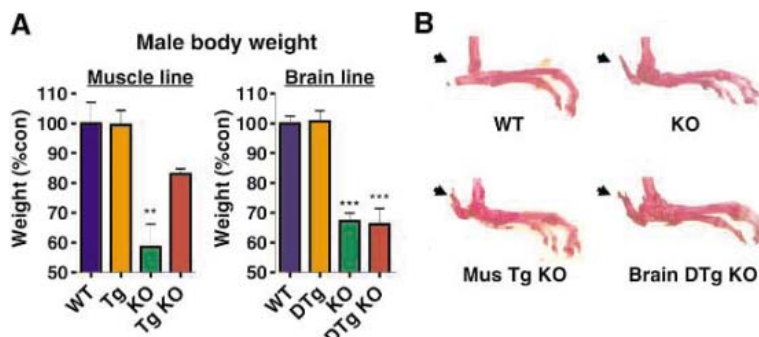
Fig. 4. Effects of tissue-specific $Bmal1$ expression on body weight and tendon calcification. (A) Brain-rescued mice and KO mice in both lines have significantly reduced body weight, whereas muscle-rescued mice exhibit body weight similar to that of WT mice (graphs represent means ± SEM; **$P < 0.01$, ***$P < 0.001$, one-way ANOVA). (B) Photographs of Alizarin Red–stained hindlimbs from WT, KO, muscle-rescued, and brain-rescued KO mice. Arrows indicate calcaneal tendon calcification in all but WT mice.

gene expression can be rescued separately by distinct spatial expression patterns of *Bmal1*. Genome-wide profiling experiments suggest that ~10% of the transcriptome is under circadian regulation; however, the majority of these cycling transcripts are tissue-specific (*18–22*). Our results are consistent with this tissue-specific diversity of circadian expression and further suggest that core circadian clock components may play distinct roles in different tissues, perhaps in addition to their function in regulating circadian rhythms. The restoration of circadian activity rhythms in brain-rescued *Bmal1*$^{-/-}$ mice is consistent with previous SCN transplant studies in rodents (*23, 24*). However, the transgenic approach used here has the advantages of preserving the anatomical integrity of the brain as well as allowing the conditional manipulation of the rescue via Dox treatment. The use of tissue-specific and conditional regulation of circadian clock gene expression should be a valuable method for understanding the molecular-,

cellular-, and systems-level regulation of circadian rhythms in mammals.

References and Notes

1. P. L. Lowrey, J. S. Takahashi, *Annu. Rev. Genomics Hum. Genet.* **5**, 407 (2004).
2. M. Ikeda, M. Nomura, *Biochem. Biophys. Res. Commun.* **233**, 258 (1997).
3. J. B. Hogenesch *et al.*, *J. Biol. Chem.* **272**, 8581 (1997).
4. N. Gekakis *et al.*, *Science* **280**, 1564 (1998).
5. J. B. Hogenesch, Y. Z. Gu, S. Jain, C. A. Bradfield, *Proc. Natl. Acad. Sci. U.S.A.* **95**, 5474 (1998).
6. M. K. Bunger *et al.*, *Cell* **103**, 1009 (2000).
7. R. D. Rudic *et al.*, *PLoS Biol.* **2**, e377 (2004).
8. M. K. Bunger *et al.*, *Genesis* **41**, 122 (2005).
9. A. Laposky *et al.*, *Sleep* **28**, 395 (2005).
10. S. Shimba *et al.*, *Proc. Natl. Acad. Sci. U.S.A.* **102**, 12071 (2005).
11. R. V. Kondratov, A. A. Kondratova, V. Y. Gorbacheva, O. V. Vykhovanets, M. P. Antoch, *Genes Dev.* **20**, 1868 (2006).
12. Y. Sun *et al.*, *J. Biomed. Sci.* 10.1007/s11373-006-9108-4 (2006).
13. See supporting material on *Science* Online.
14. M. Gossen, H. Bujard, *Proc. Natl. Acad. Sci. U.S.A.* **89**, 5547 (1992).
15. P. A. Furth *et al.*, *Proc. Natl. Acad. Sci. U.S.A.* **91**, 9302 (1994).
16. H. Hong *et al.*, paper presented at the biennial meeting of the Society for Research on Biological Rhythms, Sandestin, FL, 21 to 25 May 2006 (www.conferences.uiuc.edu/conferences/conference.asp?ID=292).
17. N. Preitner *et al.*, *Cell* **110**, 251 (2002).
18. B. Kornmann, N. Preitner, D. Rifat, F. Fleury-Olela, U. Schibler, *Nucleic Acids Res.* **29**, E51 (2001).
19. R. A. Akhtar *et al.*, *Curr. Biol.* **12**, 540 (2002).
20. S. Panda *et al.*, *Cell* **109**, 307 (2002).
21. H. R. Ueda *et al.*, *Nature* **418**, 534 (2002).
22. K. F. Storch *et al.*, *Nature* **417**, 78 (2002).
23. M. R. Ralph, R. G. Foster, F. C. Davis, M. Menaker, *Science* **247**, 975 (1990).
24. M. Sujino *et al.*, *Curr. Biol.* **13**, 664 (2003).
25. We thank N. Lampl, A. Jyawook, and A. Falk for technical assistance; members of the Takahashi laboratory and F. Davis for expert advice; and K. Esser, E. Hardeman, and M. Mayford for plasmids. Supported by NIH grants R01 ES005703 (C.A.B.) and P50 MH074924 (J.S.T.).

A Bacterial Protein Enhances the Release and Efficacy of Liposomal Cancer Drugs

Ian Cheong, Xin Huang, Chetan Bettegowda, Luis A. Diaz Jr., Kenneth W. Kinzler, Shibin Zhou,* Bert Vogelstein*

Clostridium novyi-NT is an anaerobic bacterium that can infect hypoxic regions within experimental tumors. Because *C. novyi-NT* lyses red blood cells, we hypothesized that its membrane-disrupting properties could be exploited to enhance the release of liposome-encapsulated drugs within tumors. Here, we show that treatment of mice bearing large, established tumors with *C. novyi-NT* plus a single dose of liposomal doxorubicin often led to eradication of the tumors. The bacterial factor responsible for the enhanced drug release was identified as a previously unrecognized protein termed liposomase. This protein could potentially be incorporated into diverse experimental approaches for the specific delivery of chemotherapeutic agents to tumors.

There is no dearth of drugs that can kill cancer cells. The challenge is killing the cancer cells selectively while sparing the normal cells. Three basic strategies are currently used to achieve this specificity. The first (selective toxicity) uses drugs that have more potent growth-inhibitory effects on tumor cells than on normal cells (*1, 2*). This strategy underlies the success of conventional chemotherapeutic agents as well as those of newer targeted therapies such as imatinib (Gleevec). The second strategy (delivery) uses agents such as antibodies that specifically react with molecules

that are predominantly expressed in tumor cells (*3, 4*). The third strategy (angiogenic) exploits abnormal aspects of the tumor vasculature with agents such as bevacizumab (Avastin) (*5, 6*) or drugs incorporated into liposomes (*7–9*). Liposomes are relatively large particles that can penetrate through the fenestrated endothelium present in tumors and a limited number of other organs (*8, 9*). Once they gain access to tumors, they persist and eventually release their contents and raise local drug concentrations through the enhanced permeabilization and retention effect (*10*). Although each of these strategies has merit, the specificity achieved with any one of them is imperfect, limiting the amount of drug that can be safely administered without causing systemic toxicity.

Here, we describe our efforts to combine all three strategies. We investigated *C. novyi-NT*,

an attenuated strain of the obligate anaerobe *C. novyi*. Similar to other bacteriolytic therapies, *C. novyi-NT* can selectively infect and partially destroy experimental cancers because of the hypoxic nature of the tumor environment (*11, 12*). *C. novyi-NT* is also hemolytic (lyses erythrocytes). Because enzymes that rupture erythrocytes can disrupt lipid bilayers (*13*), we hypothesized that the bacterium's hemolytic properties could be exploited to enhance the release of liposome-encapsulated drugs within tumors. This approach would theoretically increase specificity by combining the selective tumor toxicity of chemotherapeutic agents, the selective delivery of *C. novyi-NT* to tumors, and the selective uptake of liposomes mediated by the abnormal tumor vasculature.

To test this hypothesis, we first treated syngeneic CT26 colorectal tumors in BALB/c mice. *C. novyi-NT* spores were injected intravenously, and once germination had begun in the tumors (~16 hours after injection), we administered a single intravenous dose of liposomal doxorubicin (Doxil). Doxil is a liposomal formulation that encapsulates doxorubicin, a widely used DNA-damaging chemotherapeutic agent. Liposome-encapsulated doxorubicin has been shown to result in improved outcomes compared with unencapsulated doxorubicin (*14*). As previously documented (*15, 16*), treatment with *C. novyi-NT* spores alone resulted in germination and necrosis within the centrally hypoxic region of tumors but left a well-oxygenated viable rim that eventually regrew (Fig. 1A). Neither doxorubicin nor Doxil alone resulted in prolonged therapeutic effects in these mice. The combination of Doxil and *C. novyi-NT* spores, however, resulted in complete regression of tumors in 100% of mice (Fig. 1A), and 65% of the mice were still alive at 90 days (Fig. 1B).

The Howard Hughes Medical Institute and the Ludwig Center for Cancer Genetics and Therapeutics, Johns Hopkins Kimmel Comprehensive Cancer Center, Baltimore, MD 21231, USA.

*To whom correspondence should be addressed. E-mail: sbzhou@jhmi.edu (S.Z.); vogelbe@jhmi.edu (B.V.)

Notably, 100% of the mice treated with *C. novyi-NT* and free doxorubicin at the same dose died within 2 weeks, emphasizing the crucial role of liposomal encapsulation in reducing systemic toxicity (*14*). Similar antitumor effects were observed in experiments with immuno-deficient mice bearing human colorectal cancer xenografts (Fig. 1, C and D). Heat-inactivated *C. novyi-NT* spores did not lead to enhanced tumor regression when injected in combination with Doxil (fig. S1).

We next compared the distribution of doxo-rubicin in mice treated as in Fig. 1. Administration of *C. novyi-NT* spores plus Doxil resulted in tumor drug exposure that was approximately six times the exposure achieved with Doxil alone, without increasing drug concentrations in normal tissues (Fig. 2). This effect was specific to *C. novyi-NT* and not the result of inflammation per se, given that intratumoral injection of the potent inflammatory agent lipopolysac-charide (LPS) before the administration of Doxil did not affect the intratumoral concentration of doxorubicin (fig. S2A). *C. novyi-NT* spores did not enhance the accumulation of unencapsu-lated doxorubicin, excluding the possibility that the increase in accumulation of Doxil was simply due to changes in blood flow asso-ciated with infection (fig. S2B). After treat-ment with Doxil and *C. novyi-NT*, doxorubicin was released from liposomes and was bound to tumor cell nuclei, as revealed by fluorescence microscopy (fig. S3).

We next attempted to identify the mecha-nism through which *C. novyi-NT* enhances in-tratumoral release of liposome-encapsulated doxorubicin. Culture medium conditioned by the growth of *C. novyi-NT* contained substantial liposome-disrupting activity and the concentra-tion of this factor was maximal in late log-phase (fig. S4, A and B). We anticipated that this secreted factor would be a phospholipase, because these enzymes are known to disrupt the lipid bilayers of liposomes as well as those of erythrocytes (*13*). However, hemolytic activity by phospholipases was not required for the liposome-disrupting activity (fig. S5).

To identify the liposome-disrupting factor, we fractionated the growth medium from late log-phase cultures by means of a combination of ammonium sulfate precipitation, ion ex-change chromatography, and gel filtration. A single, major peak of liposome-disrupting activ-ity was observed (Fig. 3, A and B) and SDS-polyacrylamide gel electrophoresis revealed a predominant protein of approximately 45 kD in the active fractions (Fig. 3C). This protein was purified, digested by trypsin, and analyzed by liquid chromatography–tandem mass spectrom-etry. Using the *C. novyi-NT* genome as reference (*17*), we identified the polypeptide as a putative neutral lipase encoded by the NT01CX2047 gene (fig. S6). This gene was not highly homol-ogous to its closest counterpart in other bacteria (50% amino acid identity to a *C. tetani* lipase).
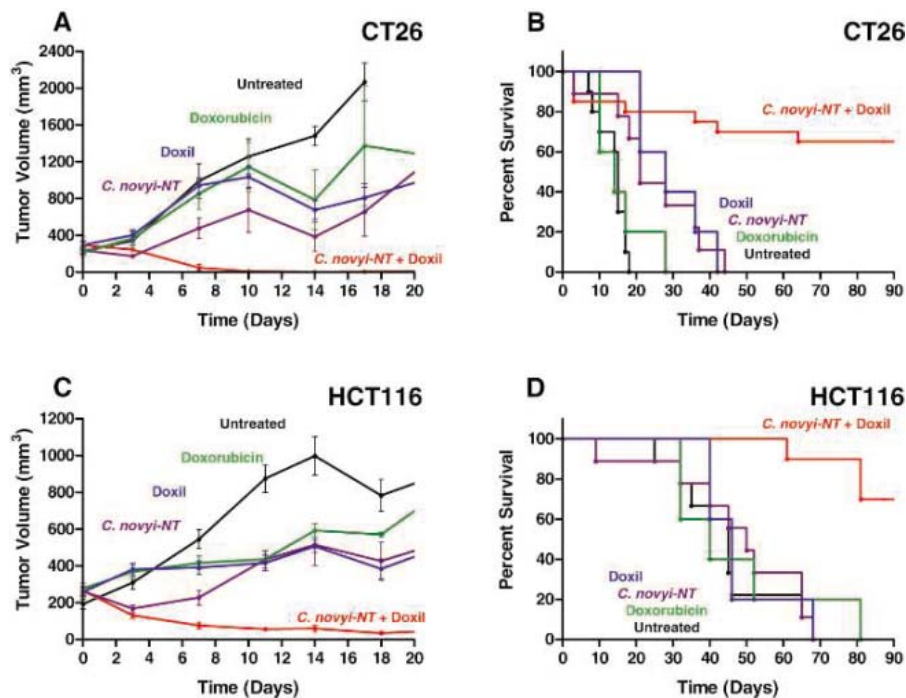
Fig. 1. *C. novyi-NT* treatment enhances the antitumor activity of Doxil in mice. Mice bearing the indicated tumors were treated with various combinations of the indicated agents, and the effects on tumor volume (**A** and **C**) and survival rates (**B** and **D**) were observed. Treatment with doxorubicin plus *C. novyi-NT* spores was toxic and resulted in deaths of all animals within two weeks (not shown). Means and standard errors of data collected from at least five mice per group are illustrated. The differences between *C. novyi-NT* plus Doxil and all other groups were significant ($P \leq 0.0006$, log-rank test) in the survival curves.
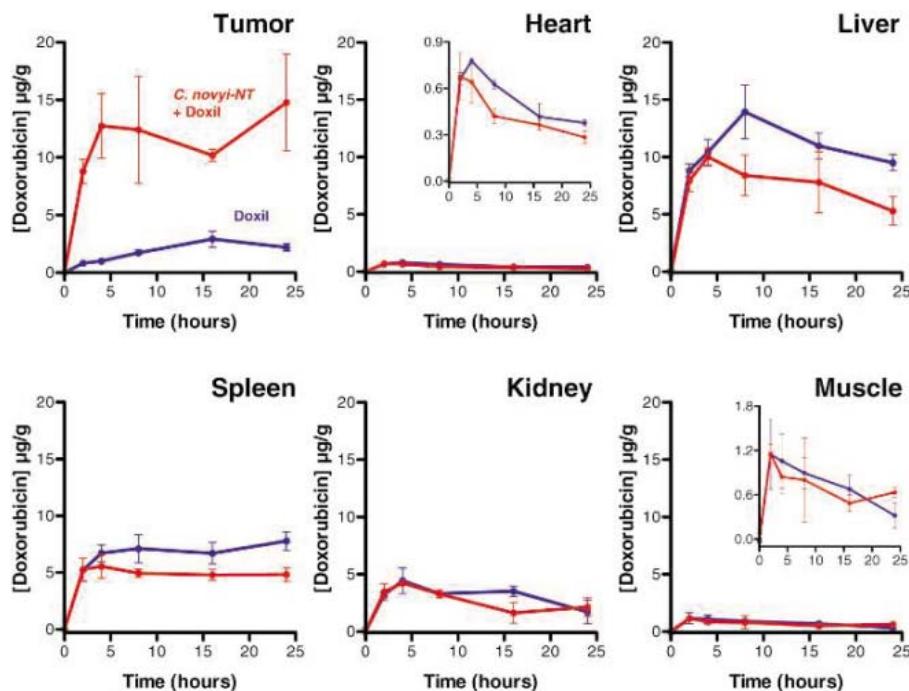
Fig. 2. Pharmacokinetic distribution of doxorubicin after treatment with *C. novyi-NT*. Doxil was administered to athymic nude mice bearing HCT116 tumors that were ~300 mm³ in size. Another group of mice was intravenously injected with *C. novyi-NT* spores 16 hours before Doxil treatment. Mice were sacrificed at the indicated time points after Doxil administration and doxorubicin was extracted from tissues and measured by fluorometry. Means and standard deviations from three mice per time point are shown. Insets in heart and muscle panels were rescaled to show differences.

The identification of the liposome-disrupting factor as the product of NT01CX2047 was consistent with the evidence that this gene was preferentially expressed in late log-phase and was highly expressed in tumors after infection with *C. novyi-NT* (fig. S4C). Additionally, based on its sequence, the product of NT01CX2047 was predicted to be secreted (fig. S6).

To examine the properties of the protein encoded by NT01CX2047, we cloned its open reading frame into an inducible expression vector which was then introduced into a genetically modified *Escherichia coli* strain that permitted expression of *C. novyi-NT* genes (which have a codon usage very different than that of *E. coli*). After induction of protein expression by isopropyl-β-D-thiogalactopyranoside, the transformed *E. coli* cells grew poorly, presumably because the gene product was toxic. Lysates from these cells were tested for lipase activity as measured by hydrolysis of 1,2-dioleoyl-3-pyrenedecanoyl-*rac*-glycerol. The NT01CX2047-expressing clones exhibited lipase activity, whereas clones cured of the vector (*18*) did not (Fig. 4A). As further controls, we generated two mutants: one in which a stop codon was substituted for serine at amino acid 127 (S127X), and another in which this serine was replaced by glycine (S127G). Ser[127] is found within the highly conserved GXSXG lipase motif and was predicted to be the essential catalytic serine responsible for lipase activity (*19*). Both the S127G missense mutant and the S127X truncation mutant were devoid of lipase activity (Fig. 4A), although each was expressed at levels comparable to those expressing the wild-type NT01CX2047 polypeptide (fig. S7). Notably, cells expressing the noncatalytic S127G mutant exhibited the same poor growth as those expressing wild-type NT01CX2047, whereas cells expressing the S127X mutant grew as well as cured cells.

To test the liposome-disrupting activity of these engineered *E. coli* lysates, we incubated them with Doxil. Lysates containing wild-type NT01CX2047 showed potent activity in this assay, whereas lysates from cured cells showed no activity (Fig. 4B). As expected, the S127X truncation mutant had no detectable liposome-disrupting activity, but surprisingly, the S127G mutant, which was devoid of lipase activity, retained substantial liposome-disrupting activity (Fig. 4B). To determine whether this activity was a general feature of lipases or specific to the NT01CX2047 lipase of *C. novyi-NT*, we assayed nine commercially available enzymes with well-defined lipase activity; none had significant liposome-disrupting activity (Fig. 4C).

The absence of a requirement for enzymatic activity implied that the liposome disruption mediated by the NT01CX2047 gene product might be due to a physical process. To investigate this possibility, liposomes containing 1,6-diphenylhexatriene or Laurdan as membrane-sensitive probes were used to investigate the effects of NT01CX2047 on lipid order and membrane polarity, respectively. Lipid order measured by fluorescence polarization significantly decreased with increasing concentrations of NT01CX2047 (fig. S8A). The perturbation of membrane structure by the protein was similar to that mediated by alcohols, although the protein was orders of magnitude more potent on a molar basis (fig. S8A). Membrane polarity measured by fluorometry also increased in the presence of NT01CX2047, indicating greater access of polar molecules to the lipid bilayer matrix (fig. S8B).

Fig. 3. Biochemical purification and identification of liposome-disrupting activity from *C. novyi-NT*. (**A**) *C. novyi-NT* was grown until late log-phase and the medium cleared of cells by centrifugation. After precipitation with 40% saturated ammonium sulfate, ion exchange chromatography was performed and fractions evaluated for liposome-disrupting activity. (**B**) The peak fractions (30 to 31) from (A) were pooled and further fractionated by gel filtration chromatography. (**C**) The peak fractions (29 to 30) from (B) were subjected to SDS-polyacrylamide gel electrophoresis. Silver-staining of the gel revealed a predominant band migrating between protein standards with masses 48.8 and 37.1 kD.
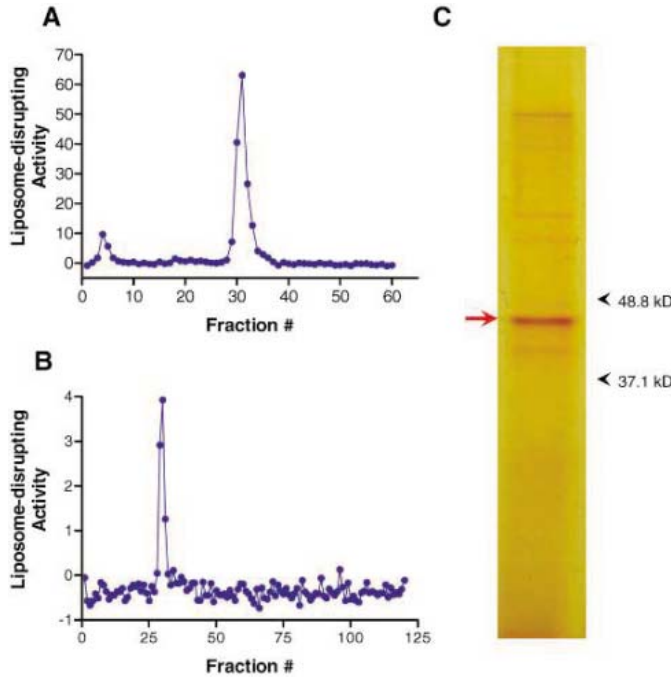
Fig. 4. Functional analysis of the *C. novyi-NT* lipase. Plasmids carrying the wild-type or mutant forms of the NT01CX2047 gene were introduced into *E. coli*. "Cured" bacteria were grown in the absence of antibiotics until the plasmid was lost. Cellular lysates from three independent clones of each strain were assayed for lipase activity (**A**) and liposome-disrupting activity (**B**). (**C**) Liposome-disrupting activities of lipases purified from various organisms were assessed with the use of Doxil. Means and standard deviations of data from at least two independent experiments are shown.
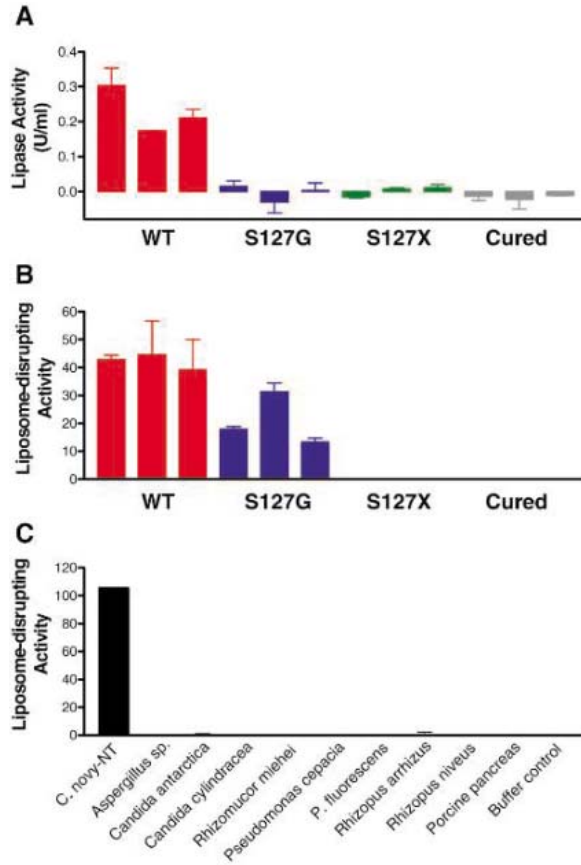
These results suggest that the liposome-disrupting activity of the protein encoded by NT01CX2047 (henceforth termed liposomase) is due to interaction of its lipid-binding domain with the liposomal membrane and the consequent alteration of bilayer structure. This explains why a lipase, which has little phospholipase activity, can disrupt liposomes, which contain phospholipids but no triacylglycerides.

In principle, the approach described here should be applicable to any chemotherapeutic drug that can be encapsulated in a liposome. Indeed, when we repeated the preclinical efficacy experiments with liposomes carrying CPT-11 (irinotecan), a topoisomerase inhibitor widely used in cancer therapy, we obtained results similar to those in the Doxil experiments (fig. S9). Both CT26 mouse tumors and HCT116 human xenografts were relatively resistant to CPT-11 when the drug was administered alone in un-encapsulated or liposome-encapsulated form. However, when liposomal CPT-11 was delivered in combination with *C. novyi-NT* spores, all tumors regressed and more than 60% of the mice survived for at least 3 months (fig. S9). Notably, the combination therapy was effective against small (136 mm^3 in volume) as well as large tumors. In previous studies, small tumors were resistant to bacteriolytic therapies because they had relatively small regions of necrosis (*15*). Importantly, mice treated with *C. novyi-NT* and either Doxil or CPT-11 tolerated the treatments well and did not generally suffer toxicities or weight loss (fig. S10).

We have not excluded the possibility that other secreted factors may contribute to the liposome-disrupting activity. However, the data reported here suggest that liposomase substantially contributes to the therapeutic effects observed in vivo. The identification and cloning of liposomase opens the door to therapeutic strategies in addition to those based on bacteriolysis. For example, liposomase could be attached to antibodies or encoded within vectors used for gene therapy (*3*, *4*). Because virtually any therapeutic agent can be packaged in liposomes and can thereby act as a "prodrug," liposomase offers a number of possibilities for the specific delivery of drugs to tumors.

References and Notes
1. D. D. Von Hoff, A.-R. Hanauske, in *Cancer Medicine*, D. W. Kufe *et al.*, Eds. (BC Decker, London, 2006), pp. 600–616.
2. C. Sawyers, *Nature* **432**, 294 (2004).
3. S. V. Govindan, G. L. Griffiths, H. J. Hansen, I. D. Horak, D. M. Goldenberg, *Technol. Cancer Res. Treat.* **4**, 375 (2005).
4. M. Yamamoto, D. T. Curiel, *Technol. Cancer Res. Treat.* **4**, 315 (2005).
5. R. Kerbel, J. Folkman, *Nat. Rev. Cancer* **2**, 727 (2002).
6. R. K. Jain, D. G. Duda, J. W. Clark, J. S. Loeffler, *Nat. Clin. Pract. Oncol.* **3**, 24 (2006).
7. G. Thurston *et al.*, *J. Clin. Invest.* **101**, 1401 (1998).
8. H. Hashizume *et al.*, *Am. J. Pathol.* **156**, 1363 (2000).
9. D. C. Drummond, O. Meyer, K. Hong, D. B. Kirpotin, D. Papahadjopoulos, *Pharmacol. Rev.* **51**, 691 (1999).
10. J. Fang, T. Sawa, H. Maeda, *Adv. Exp. Med. Biol.* **519**, 29 (2003).
11. R. M. Ryan, J. Green, C. E. Lewis, *Bioessays* **28**, 84 (2006).
12. S. Barbe, L. Van Mellaert, J. Anne, *J. Appl. Microbiol.* **101**, 571 (2006).
13. J. Sakurai, M. Nagahama, M. Oda, *J. Biochem. (Tokyo)* **136**, 569 (2004).
14. D. Papahadjopoulos *et al.*, *Proc. Natl. Acad. Sci. U.S.A.* **88**, 11460 (1991).
15. L. H. Dang, C. Bettegowda, D. L. Huso, K. W. Kinzler, B. Vogelstein, *Proc. Natl. Acad. Sci. U.S.A.* **98**, 15155 (2001); published online 27 November 2001.
16. N. Agrawal *et al.*, *Proc. Natl. Acad. Sci. U.S.A.* **101**, 15172 (2004).
17. C. Bettegowda *et al.*, *Nat. Biotechnol.*, in press.
18. Materials and methods are available as supporting material on *Science* Online.
19. K. E. Jaeger, B. W. Dijkstra, M. T. Reetz, *Annu. Rev. Microbiol.* **53**, 315 (1999).
20. We thank L. Watson for assistance with animal experiments, S. Szabo for sequencing, D. Mamelak for assistance with proteomic analysis, K. Leong for advice on particle sizing, and P. Singh and S. Chandran for advice on fluorescence polarization. This work was supported by the Virginia and D. K. Ludwig Fund for Cancer Research, the Commonwealth Foundation, the Miracle Foundation, and NIH grant CA062924.

Predictive Codes for Forthcoming Perception in the Frontal Cortex

Christopher Summerfield,[1,2]* Tobias Egner,[3,4] Matthew Greene,[1] Etienne Koechlin,[2] Jennifer Mangels,[1] Joy Hirsch[3,5]

Incoming sensory information is often ambiguous, and the brain has to make decisions during perception. "Predictive coding" proposes that the brain resolves perceptual ambiguity by anticipating the forthcoming sensory environment, generating a template against which to match observed sensory evidence. We observed a neural representation of predicted perception in the medial frontal cortex, while human subjects decided whether visual objects were faces or not. Moreover, perceptual decisions about faces were associated with an increase in top-down connectivity from the frontal cortex to face-sensitive visual areas, consistent with the matching of predicted and observed evidence for the presence of faces.

One function of the visual system is to decide what is present in the local environment, resolving potentially ambiguous sensory information into a coherent percept. Models of perceptual decision-making propose that specialized detectors accumulate evidence in favor of a preferred feature or representation, and the output of these detectors is compared in a winner-takes-all fashion at a downstream processing stage (*1*). Accordingly, when subjects are asked to decide whether they perceive stimulus A or stimulus B, cell assemblies in the frontal and parietal cortices track the difference in output of visual neurons collecting evidence in favor of A and B (*2*, *3*).

Prior information may help the brain decide among competing percepts (*4*). According to one view, the brain generates "predictive codes" that dynamically anticipate the forthcoming sensory environment, weighting perceptual alternatives on the basis of this prediction (*5*, *6*). Predictive accounts of decision-making have long been embedded in theories of signal detection, which suggest that subjects compare observed sensory evidence against an internal "template," with a response elicited if the match between the evidence and the template reaches a given criterion (*7*). Moreover, predictive coding offers a parsimonious account for several well-known behavioral phenomena (*8–10*) and recent neurophysiological findings (*11*, *12*). The theory requires that decision-making neurons have access to the set of predicted information (here, we call this "perceptual set") against which to match the sensory data. However, little is known about how—or where—perceptual set might be represented in the decision-making architecture of the brain.

To address this question, we capitalized upon recent work in which functional magnetic resonance imaging (fMRI) was used to identify brain regions responsible for collecting evidence about the presence of faces on

[1]Department of Psychology, Columbia University, 1190 Amsterdam Avenue, New York, NY 10027, USA. [2]INSERM U742, Département d'Études Cognitives, Ecole Normale Superieure, 29, Rue d'Ulm, Paris, 75005, France. [3]Functional MRI Research Center, Neurological Institute, Columbia University, 710 West 168 Street, New York, NY 10032, USA. [4]Cognitive Neurology and Alzheimer's Disease Center, Feinberg School of Medicine, Northwestern University, 320 East Superior, Searle 11, Chicago, IL 60611, USA. [5]Center for Neurobiology and Behavior, Neurological Institute, Columbia University, 710 West 168 Street, New York, NY 10032, USA.

*To whom correspondence should be addressed. E-mail: summerfd@paradox.columbia.edu

Fig. 1. Discrimination task and behavioral data. (**A**) Subjects viewed a sequence of reduced-contrast images of faces, houses, and cars. Four example regressors are shown: for example, F in F (face stimulus in face set block) or C in H (car stimulus in house set block). (**B**) Hit rate was comparable ($P = 0.28$) on face set blocks (left; 70.8 ± 13.4) and house set blocks (right; 66.3 ± 11.9). Moreover, on neither face set blocks ($P = 0.26$) nor house set blocks ($P = 0.92$) did hit rate deviate from pre-established thresholds for discrimination (66%). More false alarms were made on house blocks (25.9 ± 13) than face blocks (13.1 ± 10.5) [$t_{(14)} = 4.52$, $P < 0.001$]. (**C**) Overall percent correct responses varied as expected with degradation level (relative to threshold) for face set blocks (blue lines) and house set blocks (green lines). Each degradation level reflects ~2% loss of contrast information. Bars are standard errors.
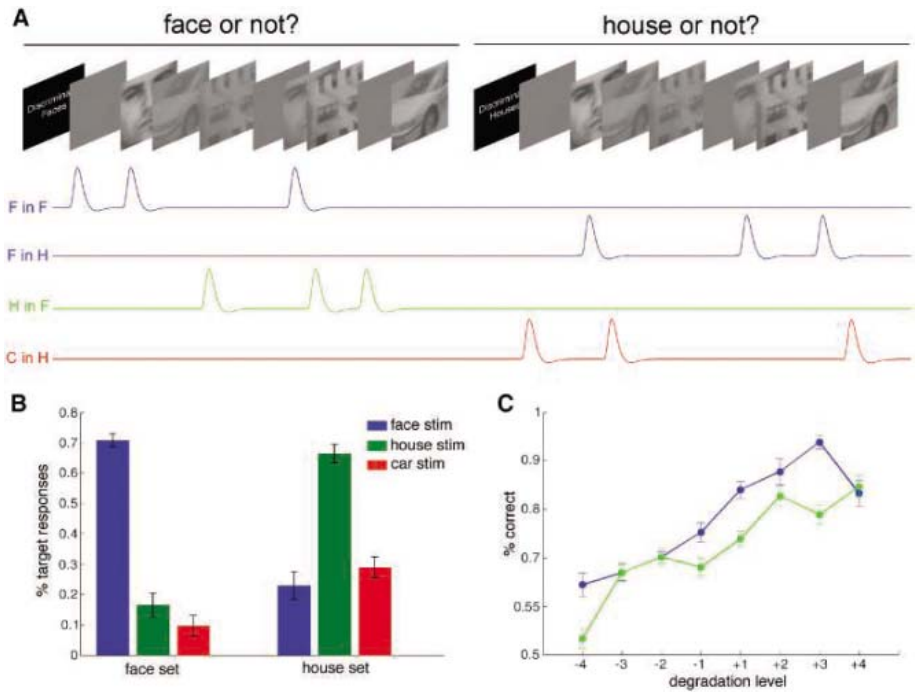
Fig. 2. IOG, FFA, TPJ, and amygdala respond to face stimuli. (**A**) (Top to bottom) Statistic parametric maps showing clusters in the IOG, FFA, TPJ, and amygdala responding to face stimuli > house stimuli at the second (group) level, rendered on a standard brain at a statistical threshold of $P < 0.005$ (IOG, FFA, and TPJ) or $P < 0.01$ (amygdala). Blue crosshairs mark the peak voxel in each cluster. (**B**) Evoked hemodynamic responses from the peak voxel in each cluster to faces (blue lines) and house (green lines), in face set (continuous lines) and house set (dashed lines) conditions. (**C**) Post hoc analyses of variance (ANOVAs) confirmed that a main effect of stimulus was observed in the IOG [$F_{(2,14)} = 10.8$, $P < 0.001$], the FFA [$F_{(2,14)} = 8.4$, $P < 0.003$], and the TPJ [$F_{(2,14)} = 19.0$, $P < 0.0001$]. In the amygdala, we observed an interaction between set and stimulus ($F = 3.7$, $P < 0.04$). Additional t tests performed on the evoked hemodynamic responses revealed an interaction between set and stimulus in the FFA, at ~12 s ($F = 6.0$, $P < 0.03$)
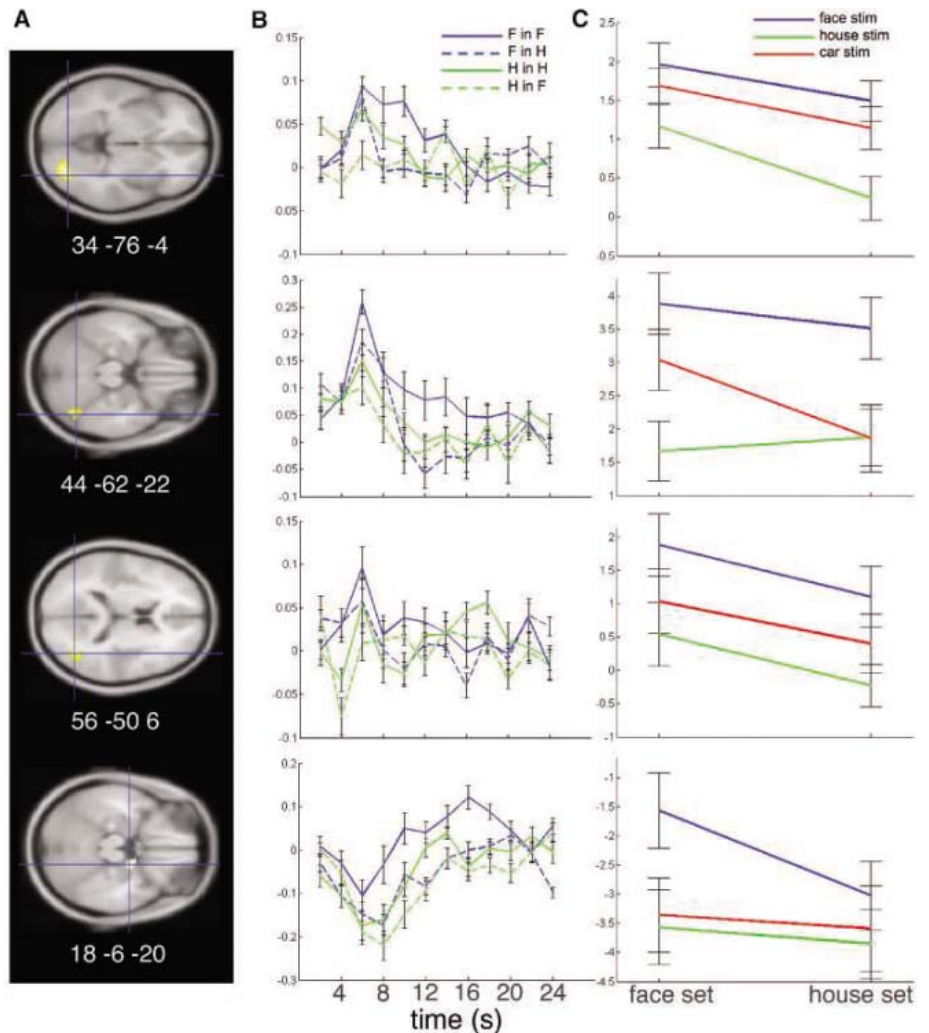
the inferior occipital gyrus (IOG) and the fusiform gyrus, in a region known as the fusiform face area (FFA) (13). The FFA exhibits neural responding that varies with subjects' beliefs about whether the stimulus is a face or not (14, 15), suggesting that it is a target for "set-related" modulation during face perception. Moreover, face perception excites an "extended" network of brain regions beyond the visual cortices (16, 17), including sites on the temporo-parietal junction (TPJ), amygdala, medial frontal cortices (MFCs) (18), and adjacent orbitofrontal cortex (19). This provides a number of candidate regions in which a representation of a face "set" might be observed.

To dissociate between brain regions responsible for detecting the physical presence of the stimuli and those supporting perceptual set, we used a simple task that required subjects to discriminate between randomly intermixed images of faces, houses, and cars (20). Although there were three object categories, subjects used just two buttons to adjudicate between them: on "face set" blocks, they judged whether each object was a face or not, and on "house set" blocks, they judged whether each object was a house or not (Fig. 1A). We also made the task perceptually challenging, by degrading stimuli to match individual thresholds for perception (66.6% correct). These manipulations encouraged subjects to generate a perceptual "set" (corresponding to the target stimulus) on each block. Because face set and house set blocks

were carefully matched within subjects both for the physical characteristics of the stimuli and for discrimination performance (Fig. 1, B and C), the comparison between fMRI activity on face set blocks > house set blocks allowed us to isolate brain activity associated with maintaining a "face set" active—irrespective of whether the physical stimulus was a face, house, or car.

We first explored the effect of stimulus during the discrimination task, by comparing all face stimuli > nonface stimuli, irrespective of perceptual set. Despite the heavy perceptual degradation imposed, selectivity for the physical stimulus was preserved in face-responsive regions such as the IOG, FFA, TPJ, and amygdala (Fig. 2). However, turning to our main comparison of interest (face sets > house sets), a rather different pattern emerged: Face sets elicited greater activation in dorsal (dMFC) and ventral (vMFC) foci within the MFC, irrespective of the physical stimulus presented (Fig. 3). These MFC regions have been previously implicated in face processing in fMRI studies (17, 21), and with single-unit recordings in the macaque (18, 19), and overlapped with regions activated by fully visible faces in a separate experiment (fig. S1).

The images that appeared on face set and house set blocks for each subject were matched for their physical properties, and occurred with equal probability, such that observed differences in fMRI activity for face sets > house sets cannot be accounted for by

the frequency, salience, or visibility of faces. Face-responsive regions of the MFC are thus involved in maintaining a predictive face "set"—information that is relevant for making perceptual decisions about faces. This result squares well with previous findings: first, the responses of face-selective neurons in the MFC are poorly synchronized with the presentation of a face (18), suggesting that they are not passively elicited by face presentation; second, the MFC is particularly responsive to familiar faces, for which a face "template" is presumably more readily available (21); and third, "top-down" generation of face-related contextual information during recall of specific face exemplars excites the vMFC (22). Finally, these two MFC regions are often activated when subjects make a range of perceptual, affective, or social decisions about faces (23, 24).

To rule out alternative explanations of the "perceptual set" effect in MFC, we conducted a number of supplementary analyses. Because the dMFC is involved in monitoring for and detecting errors (25), our results could simply reflect the proportions of errors made on face set versus house set blocks. However, behavioral data (Fig. 1, B and C) indicated that hit rate did not differ between face set and house

Fig. 3. dMFC and vMFC respond to face set. (A) Statistic parametric maps showing dMFC (top) and vMFC (bottom) voxels responding to face set blocks > house set blocks, rendered at a statistical threshold of $P < 0.01$. (B) Evoked hemodynamic responses, as in Fig. 2. Continuous lines are face set trials; dashed lines are house set trials. (C) Post hoc ANOVAs at the peak voxel in each cluster revealed a significant main effect of set [dMFC: 4, 56, 22; $F_{(2,14)} = 22.1$, $P < 0.0004$; vMFC: −6, 56, −16; $F_{(2,14)} = 20.4$, $P < 0.0005$]. No effect of stimulus was observed at either dorsal ($P = 0.70$) or ventral ($P = 0.75$) sites.

Fig. 4. Connectivity analyses. (A) A simple dynamic causal model with hierarchically ordered bidirectional connections between vMFC, amygdala, FFA, and IOG. We modeled face and nonface stimuli as inputs to IOG, and face sets as inputs to vMFC. (B) Statistically significant enhancements in connectivity due to face stimulus (blue lines) and face set (red lines) within this network. Coefficients associated with each line refer to percentage increase in connectivity relative to baseline.

set blocks, and correlation analyses showed that the number of errors made bore no relation to the neural signal in the dMFC ($P > 0.67$) or vMFC ($P > 0.45$). A second alternative account of our data relates to the role of frontal cortex in the detection of target stimuli (25). However, no interactions between perceptual set and response (target or nontarget) were observed in either dMFC or vMFC (fig. S2). Finally, if the MFC were simply responding to task difficulty, then a difference in fMRI signal should be observed between less degraded (easier) and more degraded (harder) trials in this region. However, neither dMFC nor vMFC activity covaried either positively or negatively with stimulus contrast (fig. S3).

Consistent with previous work (14, 15), we also observed set-related effects in the posterior brain, with an advantage for face sets over house sets in the amygdala and FFA (Fig. 2). We reasoned that "top-down" signals from the MFC could sensitize visual regions responsible for collecting evidence about the presence of faces via long-range effective connectivity. To test this hypothesis, we created a simple dynamic causal model (Fig. 4A) of the interactions among visual and MFC regions, basing our model on known interconnectivity from studies of macaque neuroanatomy (26). Treating the brain as an input-state-output system, dynamic causal modeling estimates how (output) hemodynamic activity in a given brain region depends not only on the (input) variables manipulated by the experimenter (such as face stimulus or face set), but also on its interconnectivity with other brain regions whose activity correlates with the task. These inter-regional dependencies can then be parameterized as effective connectivity, allowing confirmatory hypothesis-testing about how brain regions interact during task performance (27).

Face stimulation enabled the flow of information within the posterior and limbic lobes, augmenting feedforward connections linking IOG to the FFA and amygdala. However, feedback connectivity from ventral MFC to the FFA and amygdala was significantly enhanced (by about 11% relative to baseline) on face set trials. By contrast, face set trials had no influence on bottom-up projections from the FFA ($P > 0.17$) or amygdala ($P > 0.19$) to the frontal cortex (Fig. 4B). One appealing interpretation of these data is that top-down signals originating in the vMFC may drive the increased FFA and amygdala response on face set trials—supporting recent reports that vMFC activity correlates with subjective awareness during object recognition (28) and that connectivity between the FFA and the frontal pole is increased when subjects generate mental images of faces (29).

These findings suggest that subjects do indeed deploy predictive information in the service of face perception. If subjects had been solving the three-way discrimination by accumulating evidence in favor of each of the possibilities in an unbiased way, then the comparison between brain activity for face sets and house sets would most likely have failed to yield any differences in brain activity. Moreover, a category-specific perceptual "set" can be visualized in the frontal cortex on a scale gross enough to be detected with fMRI. In supplementary analyses, we identified other frontal regions that were more active on "house set" than "face set" blocks, suggesting that this result may generalize to other categories (fig. S4).

During perceptual inference, discrete neural assemblies in the frontal cortex may come to transiently code for one or more predicted representations and send top-down signals to guide the activation in sensory regions responsible for collecting evidence about the corresponding stimuli. This long-range connectivity may underlie the matching of predictive codes for faces—maintained in the MFC—with incoming sensory data gathered in the face-sensitive zones of the extrastriate cortex, in the service of deciding whether a stimulus is a face or not.

References and Notes
1. P. L. Smith, R. Ratcliff, *Trends Neurosci.* **27**, 161 (2004).
2. J. N. Kim, M. N. Shadlen, *Nat. Neurosci.* **2**, 176 (1999).
3. H. R. Heekeren, S. Marrett, P. A. Bandettini, L. G. Ungerleider, *Nature* **431**, 859 (2004).
4. A. Wald, J. Wolfowitz, *Proc. Natl. Acad. Sci. U.S.A.* **35**, 99 (1949).
5. K. Friston, *Neural Netw.* **16**, 1325 (2003).
6. D. Mumford, *Biol. Cybern.* **66**, 241 (1992).
7. J. Swets, in *Signal Detection and Recognition*, J. Swets, D. Green, Eds. (Wiley, New York, 1964), pp. 164–171.
8. R. N. Henson, M. D. Rugg, *Neuropsychologia* **41**, 263 (2003).
9. R. H. Carpenter, M. L. Williams, *Nature* **377**, 59 (1995).
10. S. Palmer, *Mem. Cognit.* **3**, 519 (1975).
11. J. Sharma, V. Dragoi, J. B. Tenenbaum, E. K. Miller, M. Sur, *Science* **300**, 1758 (2003).
12. M. L. Platt, P. W. Glimcher, *Nature* **400**, 233 (1999).
13. N. Kanwisher, J. McDermott, M. M. Chun, *J. Neurosci.* **17**, 4302 (1997).
14. C. Summerfield, T. Egner, J. Mangels, J. Hirsch, *Cereb. Cortex* **16**, 500 (2006).
15. R. J. Dolan *et al.*, *Nature* **389**, 596 (1997).
16. J. V. Haxby, E. A. Hoffman, M. I. Gobbini, *Trends Cognit. Sci.* **4**, 223 (2000).
17. A. Ishai, C. F. Schmidt, P. Boesiger, *Brain Res. Bull.* **67**, 87 (2005).
18. S. P. Ó. Scalaidhe, F. A. Wilson, P. S. Goldman-Rakic, *Science* **278**, 1135 (1997).
19. S. J. Thorpe, E. T. Rolls, S. Maddison, *Exp. Brain Res.* **49**, 93 (1983).
20. Materials and methods are available as supporting material on *Science* Online.
21. A. Todorov, M. I. Gobbini, K. K. Evans, J. V. Haxby, *Neuropsychologia* (2006).
22. S. M. Polyn, V. S. Natu, J. D. Cohen, K. A. Norman, *Science* **310**, 1963 (2005).
23. T. Singer, S. J. Kiebel, J. S. Winston, R. J. Dolan, C. D. Frith, *Neuron* **41**, 653 (2004).
24. J. P. Mitchell, C. N. Macrae, M. R. Banaji, *Neuron* **50**, 655 (2006).
25. K. R. Ridderinkhof, M. Ullsperger, E. A. Crone, S. Nieuwenhuis, *Science* **306**, 443 (2004).
26. H. Barbas, *Adv. Neurol.* **84**, 87 (2000).
27. K. J. Friston, L. Harrison, W. Penny, *Neuroimage* **19**, 1273 (2003).
28. M. Bar *et al.*, *Proc. Natl. Acad. Sci. U.S.A.* **103**, 449 (2006).
29. A. Mechelli, C. J. Price, K. J. Friston, A. Ishai, *Cereb. Cortex* **14**, 1256 (2004).
30. Financial support was from the William J. Keck Foundation and the NIH (grant R21066129).

Gordon Research Conferences

Session II Meetings

(June-October, 2007)

Visit the GRC web site for programs, fees, and site/travel information: **www.grc.org**

INTERNATIONAL (June - October)

Conference Title	Chair(s)	Dates	Location
Aging, Biology of	H. Brown-Borg, L.D. Thompson & A. Buerkle	Sep 23-28	Les Diablerets
Antimicrobial Peptides	Ylva Engstrom & Yechiel Shai	Apr 29-May 4	Il Ciocco
Atherosclerosis	Michael Rosenfeld & Christopher Glass	Jun 17-22	Il Ciocco
CAG Triplet Repeat Disorders	Diane Merry	May 13-18	Centre Paul Langevin
Cancer Genetics & Epigenetics	En Li & Thomas Jenuwein	May 20-25	Il Ciocco
Cancer Models & Mechanisms	William Kaelin	Aug 26-31	Les Diablerets
Cannabinoid Function in the CNS	O. Manzoni, G. Marsicano & M. Guzman	Sep 30-Oct 5	Les Diablerets
Catecholamines	Jill Becker	Aug 5-10	Magdalen College
Cell Contact & Adhesion	Elisabetta Dejana	May 27-Jun 1	Il Ciocco
Cellular Osmoregulation: Sensors, Transducers & Regulators	Rainer Hedrich & Paul Yancey	Jun 3-8	Centre Paul Langevin
Chronobiology	Till Roenneberg	May 6-11	Centre Paul Langevin
Condensed Matter Physics	Robert Magerle	Aug 19-24	Les Diablerets
Fibronectin, Integrins & Related Molecules	Dean Sheppard	Apr 22-27	Il Ciocco
Floral & Vegetative Volatiles	Eran Pichersky	Oct 7-12	Les Diablerets
Genetic Toxicology	Antony Carr	Jul 29-Aug 3	Magdalen College
Graduate Research Seminar: Catecholamines	K. Smith, J. Becker, C. Furman & S. Hardie	Aug 3-5	Magdalen College
Laser Diagnostics in Combustion	Paul Ewart	Aug 12-17	Magdalen College
Malaria	Kevin Marsh	Sep 9-14	Magdalen College
Matrix Metalloproteinases	Carlos Lopez-otin	Jun 3-8	Il Ciocco
Mechanisms of Cell Signalling	Jonathan Chernoff	Sep 16-21	Magdalen College
Myogenesis	Stephen Tapscott	May 13-18	Il Ciocco
Organic Thin Films	Martien Cohen Stuart & Nicholas Kotov	May 27-Jun 1	Centre Paul Langevin
Protein Transport Across Cell Membranes	Juergen Soll & Carla Koehler	Jun 10-15	Il Ciocco
Quantum Information Science	Robert Schoelkopf & Michel Devoret	Apr 15-20	Il Ciocco
Red Cells	Jon Morrow	May 20-25	Centre Paul Langevin
Solid State Chemistry II	Evgeny Antipov	Sep 2-7	Magdalen College
Staphylococcal Diseases	Harald Labischinski & Mathias Herrmann	Sep 2-7	Les Diablerets
Stress Proteins in Growth, Development & Disease	Peter Walter	Aug 19-24	Magdalen College
Structural, Functional & Evolutionary Genomics	Eugene Koonin	Jul 29-Aug 3	Wellcome Trust
Superconductivity	Nicole Bontemps	Sep 9-14	Les Diablerets
Supramolecules & Assemblies, Chemistry of	John Texter & Dirk Kurth	May 6-11	Il Ciocco
Tuberculosis Drug Development	Valerie Mizrahi	Aug 26-31	Magdalen College

NEW ENGLAND (June - August)

Conference Title	Chair(s)	Dates	Location
Adverse Drug Reactions	Thomas Kawabata	Jun 10-15	Colby College
Amygdala in Health & Disease	Pankaj Sah & Andreas Luthi	Jul 29-Aug 3	Bates College
Analytical Chemistry	Jed Harrison	Jun 24-29	Waterville Valley Resort
Angiogenesis & Microcirculation	Douglas Hanahan	Aug 19-24	Salve Regina University
Apoptotic Cell Recognition & Clearance	Michael Hengartner & Kodi Ravichandran	Jun 17-22	Bates College
Applied & Environmental Microbiology	Kenneth Nealson	Jul 15-20	Mount Holyoke College
Archaea: Ecology, Metabolism & Molecular Biology	Imke Schroeder & Malcolm White	Aug 19-24	Proctor Academy
Atomic Physics	Chris Monroe	Jul 1-6	Tilton School
Barrier Function of Mammalian Skin	Anthony Rawlings & Mike Roberts	Aug 5-10	Salve Regina University
Bioinformatics: from Predictive Models To Inference	Edward Marcotte	Jul 15-20	Proctor Academy
Biological Molecules in The Gas Phase	Albert Heck	Jul 22-27	Bates College
Biomaterials: Biocompatibility / Tissue Engineering	Andres Garcia	Jul 22-27	Holderness School
Bioorganic Chemistry	Blake Peterson & Jessica Friedman	Jun 10-15	Proctor Academy
Bones & Teeth	Pamela Robey	Jul 15-20	University of New England
Calcium Signalling	Indu Ambudkar	Jul 8-13	Tilton School
Carbohydrates	Todd Lowary & Peng Wang	Jun 17-22	Tilton School
Catchment Science: Interactions of Hydrology, Bio. & Geochemistry	Elizabeth Boyer & Heleen De Wit	Jul 8-13	Colby-Sawyer College
Cell Biology of Metals	Andrew Dancis & Jonathan Gitlin	Jul 29-Aug 3	Salve Regina University
Cell Growth & Proliferation	Michael Yaffe	Jun 24-29	University of New England
Cell-Cell Fusion	Diana Myles & Agnès Vignery	Jul 1-6	Colby-Sawyer College
Cellulases & Cellulosomes	Mark Morrison	Jul 29-Aug 3	Proctor Academy
Ceramics, Solid State Studies in	Randall Hay	Aug 5-10	Proctor Academy
Chemical Oceanography	Edward Boyle	Aug 5-10	Tilton School
Chemical Sensors & Interfacial Design	Anthony Coleman	Jul 29-Aug 3	Salve Regina University
Chemistry Education Research & Practice	Christopher Bauer	Jun 24-29	Bates College
Chromosome Dynamics	N. Patrick Higgins	Aug 12-17	University of New England
Clusters, Nanocrystals & Nanostructures	A. Welford Castleman, Jr & Vicki Colvin	Jul 29-Aug 3	Mount Holyoke College
Coastal Ocean Modeling	Francisco Werner	Jun 17-22	Colby-Sawyer College
Collagen	David Birk	Jul 22-27	Colby-Sawyer College
Combinatorial Chemistry	Daryl Sauer	Jun 3-8	Colby-Sawyer College
Computer Aided Drug Design	Richard Lewis	Jul 29-Aug 3	Tilton School
Developmental Biology	Stephen Cohen	Jun 24-29	Proctor Academy
Drug Metabolism	Jae Lee	Jul 8-13	Holderness School
Dynamics at Surfaces	Bret Jackson	Aug 12-17	Proctor Academy
Elastin & Elastic Fibers	Elaine Davis	Jul 29-Aug 3	University of New England
Elastomers, Networks & Gels	H. Henning Winter	Jul 15-20	Colby-Sawyer College

Celebrating our 75th Anniversary on the Frontiers of Science (1931-2006)

Conference Title	Chair(s)	Dates	Location
Electron Distribution & Chemical Bonding	Carlo Gatti	Jul 1-6	Mount Holyoke College
Electronic Materials, Chemistry of	Christopher Chidsey & Gary Taylor	Jul 22-27	Mount Holyoke College
Enzymes, Coenzymes & Metabolic Pathways	Nigel Richards & Squire Booker	Jul 8-13	University of New England
Epigenetics	Steven Jacobsen & Anne Ferguson-Smith	Aug 5-10	Holderness School
Epithelial Differentiation & Keratinization	Paolo Dotto	Jul 29-Aug 3	Bryant University
Evolutionary & Ecological Functional Genomics	Greg Wray	Jul 8-13	Salve Regina University
Excitatory Synapses & Brain Function	Robert Malenka	Jun 10-15	Colby-Sawyer College
Fertilization & Activation of Development	George Gerton	Jul 15-20	Holderness School
Fuel Cells	Bryan Pivovar & Tomoyuki Tada	Jul 22-27	Bryant University
Graduate Research Seminar: Analytical Chemistry	Jed Harrison	Jun 22-24	Waterville Valley Resort
Graduate Research Seminar: Organometallic Chemistry	Nora Radu & Elizabeth Mader	Jul 6-8	Salve Regina University
Graduate Research Seminar: Plant Metabolic Engineering	E. Grotewold, E. Wurtzel & J. Chappell	Jul 13-15	Tilton School
Graduate Research Seminar: Polyamines	C. Hanfrey, M. Phillips, E. Willert & M. Cerrada-Gimenez	Jun 15-17	Waterville Valley Resort
Graduate Research Seminar: Polymer Colloids	W.-D. Hergeth, A. Van Herk, N. Smeets & F. Torres	Jun 22-24	Tilton School
Heterocyclic Compounds	Erik Sorensen	Jun 24-29	Salve Regina University
High Temperature Corrosion	W. Joe Quadakkers	Jul 29-Aug 3	Colby-Sawyer College
Hormone Action in Development & Cancer	Shiuan Chen & Paolo Sassone-Corsi	Jul 15-20	Colby-Sawyer College
Human Genetics & Genomics	James Lupski	Jul 22-27	Salve Regina University
Hydrogen-Metal Systems	Craig Jensen & Klaus Yvon	Jul 8-13	Colby College
Inhibition in the CNS	Chris Mcbain	Jul 22-27	Colby College
Inorganic Chemistry	William Buhro	Jul 15-20	Salve Regina University
Interior of The Earth	Goran Ekstrom	Jun 10-15	Mount Holyoke College
Lipids, Molecular & Cellular Biology of	Charles Martin	Jul 22-27	Waterville Valley Resort
Liquid Crystals	Gregory Crawford	Jun 10-15	Colby-Sawyer College
Liquids, Chemistry & Physics of	David Reichman	Jul 29-Aug 3	Holderness School
Magnetic Resonance	Shimon Vega	Jun 17-22	University of New England
Mammary Gland Biology	Steven Anderson	Jun 10-15	Salve Regina University
Matrix Isolated Species, Physics & Chemistry of	Ara Apkarian	Jul 15-20	Bates College
Mechanisms of Membrane Transport	Peter Maloney	Jun 10-15	Tilton School
Mechanosensory Transduction	Paul Blount & Gloria Muday	Jul 22-27	University of New England
Medicinal Chemistry	George Hartman	Aug 5-10	Colby-Sawyer College
Microbial Adhesion & Signal Transduction	Arturo Zychlinsky & Bonnie Bassler	Jul 22-27	Salve Regina University
Microbial Population Biology	Paul Rainey	Jul 22-27	Proctor Academy
Microfluidics, Physics & Chemistry of	Sabeth Verpoorte	Jul 15-20	Waterville Valley Resort
Molecular & Cellular Bioenergetics	Fevzi Daldal	Jun 17-22	Proctor Academy
Molecular Membrane Biology	Benjamin Glick	Jul 8-13	Proctor Academy
Molecular Therapeutics of Cancer	Phillip Dennis	Jul 22-27	Colby-Sawyer College
Molybdenum & Tungsten Enzymes	Alastair Mcewan & Caroline Kisker	Jul 1-6	Colby-Sawyer College
Motile & Contractile Systems	Margaret Titus	Jul 8-13	Colby-Sawyer College
Mycotoxins & Phycotoxins	Kelly Rein & Kenneth Voss	Jun 17-22	Colby College
Natural Products	David Uehling	Jul 22-27	Tilton School
Neural Circuits & Plasticity	Rafael Yuste	Jul 1-6	Salve Regina University
Neurotrophic Factors	David Ginty	Jun 17-22	Salve Regina University
Nonlinear Science	Anna Lin	Jun 24-29	Colby College
Nuclear Chemistry	Augusto Macchiavelli	Jun 3-8	Colby-Sawyer College
Nuclear Physics	Michael Ramsey-musolf	Jul 15-20	Salve Regina University
Nucleic Acids	Cynthia Burrows & Joseph (Jody) Puglisi	Jun 3-8	Salve Regina University
Nucleosides, Nucleotides & Oligonucleotides	Jyoti Chattopadhyaya	Jul 1-6	Salve Regina University
Oculomotor System Biology	Neeraj Gandhi & Jennifer Groh	Jul 8-13	Bates College
Organic Reactions & Processes	Jos Brands	Jul 15-20	Bryant University
Organometallic Chemistry	Nora Radu	Jul 8-13	Salve Regina University
Origins of Solar Systems	Lee Hartmann	Jul 8-13	Mount Holyoke College
Phagocytes	Joel Swanson	Jun 10-15	Bryant University
Phosphorylation & G-Protein Mediated Signaling Networks	Henrik Dohlman & Joann Trejo	Jun 10-15	University of New England
Photochemistry	Linda Johnston	Jul 8-13	Bryant University
Physical Organic Chemistry	R. Stanley Brown	Jun 24-29	Holderness School
Plant Metabolic Engineering	Erich Grotewold	Jul 15-20	Tilton School
Polyamines	Leena Alhonen & Margaret Phillips	Jun 17-22	Waterville Valley Resort
Polymer Colloids	Alex Van Herk	Jun 24-29	Tilton School
Polymers (East)	Karen Wooley	Jun 17-22	Mount Holyoke College
Proteins	Christopher Hill & Gary Pielak	Jun 17-22	Holderness School
Quantum Control of Light and Matter	Philip Bucksbaum & David Tannor	Aug 12-17	Salve Regina University
Radiation & Climate	Philip Russell & William Collins	Jul 29-Aug 3	Colby-Sawyer College
Radicals & Radical Ions in Chemistry & Biology	James Tanko	Jul 1-6	Holderness School
Small Integrin-Binding Proteins	Cecilia Giachelli & Neal Fedarko	Aug 5-10	University of New England
Thin Film & Crystal Growth Mechanisms	Peter Vekilov	Jun 24-29	Mount Holyoke College
Three Dimensional Electron Microscopy	Phoebe Stewart	Jun 24-29	Colby-Sawyer College
Time-Dependent Density-Functional Theory	Kieron Burke & Carsten Ullrich	Jul 15-20	Colby College
Tissue Repair & Regeneration	Jack Gauldie	Jun 17-22	Colby-Sawyer College
Toxicogenomics	Christopher Bradfield & Cindy Afshari	Jun 24-29	Colby-Sawyer College
Viruses & Cells	Diane Griffin	Jun 3-8	Tilton School
Visualization in Science & Education	Christopher Watters & Roy Tasker	Jul 1-6	Bryant University
Vitamin B12 & Corphins	Wilfred Van Der Donk	Jul 1-6	University of New England
X-Ray Physics	Kenneth Finkelstein	Aug 5-10	Colby-Sawyer College

Conference Title	Chair(s)	Dates	Location
Antigen Cross-Presentation	Matthew Albert & Pramod Srivastava	Sep 2-7	Big Sky Resort
Assisted Circulation	Leslie Miller	Aug 19-24	Big Sky Resort
Atmospheric Chemistry	Douglas Worsnop	Aug 26-31	Big Sky Resort
Detecting Illicit Substances: Explosives & Drugs	Amy Waters & Matthew Brookes	Sep 16-21	Big Sky Resort
Stem Cells & Cancer	Michael Clarke	Sep 9-14	Big Sky Resort

Celebrating our 75th Anniversary on the Frontiers of Science (1931-2006)
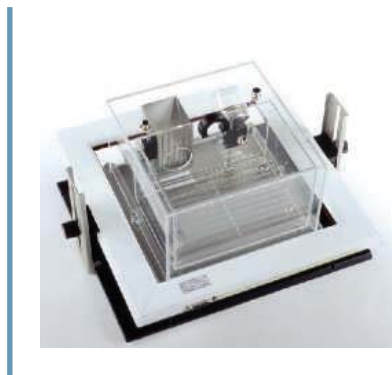
Metabolism Measurement

The Oxylet/Physiocage System is a modular system allowing researchers to measure pulmonary metabolism, feeding, drinking, and spontaneous activity simultaneously. The flexible nature of Oxylet/Physiocage allows researchers to select those components necessary for their specific experiments, and allows them to add other components when they are needed. The extensiometric technology used to monitor activity permits the unit to discriminate minute movements characteristic of knockout, transgenic, and inbred mice, movements that are often missed by infrared beams. Additionally, this technology allows for the continuous assessment of feeding and drinking. The system also makes use of indirect calorimetry to monitor carbon dioxide production, oxygen consumption, and more. Configurations for up to eight mice or rats are available.

Stoelting For information 630-860-9700 www.stoeltingco.com/physio

Automatic Cell Counter

The Cellometer Model Auto T4 cell counter automates cell counting. The Auto T4 has a small footprint of 3.5 inches by 4 inches and is simple to operate. Its patent-pending disposable counting chamber is made of high-quality plastic materials. Samples are pipetted into the chamber and placed into the Auto T4, which connects to a computer via a USB cable. Imaging software automatically measures cell concentration and viability. Cells within a heterogeneous sample with various sizes and morphology can also be measured, providing data not obtained by traditional methods. The disposable chamber handles sample loading easily, requires minimal sample (20 μl), and eliminates washing steps. Because the sample is completely contained within the disposable chamber, the Cellometer Auto T4 is free of cross-contamination and clogging.

Nexcelom Bioscience For information 978-327-5340 www.nexcelom.com

High-Throughput Protein Assay

SPN-htp protein assay is rapid, suitable for as little as 0.5 μg protein, and resistant to the interference of common laboratory agents, such as 2% sodium dodecyl sulfate or reducing agents. The assay is based on the quantitative capture of protein to a proprietary matrix in a 96-well format, with a linear response between 0.5 to 10 μg of protein. The assay is suitable for high-throughput protein estimation and is robotic compatible.

G-Biosciences/Genotech For information 800-628-7730 www.GBiosciences.com

Microplate Solvent Evaporator

The MiniVap is designed to enable researchers to overcome the traditional laboratory bottleneck of solvent evaporation from microplates prior to analysis or reconstitution in buffer. The affordable MiniVap takes just minutes to dry down a plate, replacing traditional techniques that typically take hours to remove solvents from a 96-well microplate. The compact instrument will fit into any standard fume cupboard. It is designed for use in research and development where low numbers of individual plates need drying. Installation simply requires connection to a gas supply and standard mains socket.

Primetek Solutions For information +44 1932 240255 www.porvair-sciences.com

Plasmid DNA Purification System

SNARe Plasmid DNA Purification System offers rapid, cost-effective methods for isolating DNA using DNA Separation Particles. DNA Separation Particles are a suspension of superparamagnetic iron oxide particles that bind double-stranded DNA. Once bound, the DNA-particle complex is stable and can be washed to remove any impurities or unwanted proteins from the sample to provide a clean DNA preparation. The DNA is eluted from the magnetic particles with an elution buffer for use in downstream reactions such as polymerase chain reaction, labeling, sequencing, transfection, cloning, and restriction digest.

Bangs Laboratories For information 800-387-0672 www.bangslabs.com

FailSafe PCR System

The FailSafe PCR System for tough polymerase chain reaction (PCR) amplifications faithfully amplifies the DNA template regardless of its source or sequence. The system includes the FailSafe PCR Enzyme Mix and a set of 12 FailSafe PCR PreMixes that cover a matrix of enzyme-specific PCR conditions that are optimal for amplifying different sequences. The system also includes a patented PCR Enhancer with Betaine.

Epicentre Biotechnologies For information 800-284-8474 www.EpiBio.com/failsafe.asp

OEM Light Detector

The MDE-37 series modular light detectors with integrated amplifier are designed as an OEM (original equipment manufacturer) part configured to end-user specifications for ultraviolet, visible, and near infrared optical radiation monitoring applications. Its rugged black anodized aluminum sensor housing with threaded hole for mounting measures only 37-mm diameter by 20-mm high and includes a cosine diffuser input optic. The sensor can be sealed for waterproof operation. The photodiode type and size and optical filtering can be selected according to the application and associated light signal levels. Temperature stabilization and other control options are available.

Gigahertz-Optik For information 978-462-1818 www.gigahertz-optik.com

---

For more information visit Product-Info, *Science*'s new online product index at *http://science.labvelocity.com*

From the pages of Product-Info, you can:

- Quickly find and request free information on products and services found in the pages of *Science*.
- Ask vendors to contact you with more information.
- Link directly to vendors' Web sites.

POSITIONS OPEN

ASSISTANT PROFESSOR. The Biochemistry and Cellular and Molecular Biology (BCMB) Department at the University of Tennessee, Knoxville (UTK) seeks to fill a tenure-track faculty position at the Assistant Professor level to begin in August 2007, in the following area: computational modeling and simulation of biomolecular structure, dynamics, and function.

The research associated with the appointments will be performed in the Center for Molecular Biophysics at the UTK/Oak Ridge National Laboratory (ORNL) Joint Institute for Biological Sciences at ORNL. The successful candidate for this position will benefit from interactions with strong research groups within the BCMB Department and in other units on campus and at the Oak Ridge National Laboratory in structural biology, neutron sciences, enzyme mechanisms, proteomics, and computational biology. Particularly strong interactions are expected with research undertaken at the new Spallation Neutron Source and the National Leadership Supercomputing Centre, both at ORNL, and with the ORNL Life, Computational and Physical Sciences Programs. The successful applicant will be expected to develop first-class, externally funded research programs, to provide state-of-the-art training for graduate students and postdoctoral researchers, and to contribute to the teaching mission of the BCMB Department at both the undergraduate and graduate levels. Required qualifications include a Ph.D. and postdoctoral experience in relevant areas of computational molecular biophysics, evidence of significant scientific productivity, and a commitment to an integrated program of teaching and research. The University welcomes and honors people of all races, creeds, cultures, and sexual orientations, and values intellectual curiosity, pursuit of knowledge, and academic freedom and integrity. Interested candidates should send a cover letter, a resume, a description of research experience and of the proposed research program, and the names of three individuals who can provide letters of reference to: **Jeremy Smith, Chair, Faculty Search Committee, Biochemistry and Cellular and Molecular Biology Department, M407 WLS, University of Tennessee, Knoxville, TN 37996-0840.** Review of applications will begin on November 17, 2006, and continue until the position is filled.

The University of Tennessee is an Equal Employment Opportunity/Affirmative Action/Title VI/Title IX/Section 504/ADA/ADEA Institution in the provision of its education and employment programs and services.

South Carolina Department of Health and Environmental Control is seeking a **STATISTICIAN III.** Provide overall management of Pregnancy Risk Assessment Monitoring System project, statistical data analysis, grant and report writing, and budget management. Must have a Master's degree in biostatistics, epidemiology, or public health; working knowledge of SAS and SUDAAN, and ability to perform data linkage; demonstrable knowledge of, and experience in, data management techniques and file management. Experience with surveillance system tracking software. Please forward a completed state of South Carolina job application form to: **Jim Ferguson, Division of Biostatistics, 2600 Bull Street, Columbia, SC 29201.**

POSTDOCTORAL FELLOWSHIP in the Section of Atherosclerosis, Department of Medicine, Baylor College of Medicine. Qualified applicants should have a Ph.D. or M.D. and experience in molecular biology with an interest in lipoproteins, inflammation, obesity, and vascular biology. Highly competitive salary will be offered and is negotiable depending upon experience. Eligibility for NIH training-grant position with *U.S. citizenship or residency required.* Reply with curriculum vitae and three references to: **Christie M. Ballantyne, M.D., Fellow of the American College of Cardiology, Professor, 6565 Fannin, M.S. A601, Houston, TX 77030. E-mail: cmb@bcm.tmc.edu.** *Baylor College of Medicine is an Equal Opportunity/Equal Access/Affirmative Action Employer.*

POSITIONS OPEN

TENURE-TRACK ASSISTANT PROFESSOR IN CELL BIOLOGY
University of Dayton, Dayton, Ohio

The Department of Biology seeks applicants with a strong research record for a **CELL BIOLOGIST** position beginning August 2007. Requirements include a Ph.D., relevant postdoctoral experience, and a commitment to excellence in research and teaching. The ideal candidate will have primary research experience in cell biology with a focus in one or more of the following areas: tissue repair, regeneration, and/or neurobiology. The successful candidate will be expected to develop an extramurally funded research program. The individual filling this position will involve Ph.D., M.S., and undergraduate students in his/her research program and teach undergraduate cell biology and another graduate level or advanced lecture/laboratory appropriate to their experience. The Department has expertise in computational biology, microbiology and cell biology, developmental biology, evolution and development, regenerative biology, and stem cell biology. The University of Dayton has a history of interdisciplinary research and has recently established centers of excellence in nanotechnology, and in tissue regeneration and engineering. Recently the University and state of Ohio have invested in a centralized microscopy center which houses state-of-the-art Ramen and atomic force microscopes, X-ray diffraction as well as high resolution transmission electron microscope, scanning electron microscopy (SEM), environmental SEM, low vacuum SEM, and confocal microscopes. Please send curriculum vitae, selected reprints, at least three letters of recommendation, and statements of research interest and teaching philosophy by e-mail to **e-mail: biologysearch@notes.udayton.edu,** or send an electronic copy on CD to: **Dr. John J. Rowe, Chair of Search Committee, Department of Biology, University of Dayton, 300 College Park, Dayton, OH 45469-2320.** Copies of graduate transcripts will be required prior to interviewing. The Committee will begin reviewing applications by December 15, 2006, and applicants will begin to be selected for interview by January 15, 2007. The search will continue until the position is filled.

The University of Dayton is a private comprehensive research University (Carnegie classification) located in the Columbus-Dayton-Cincinnati metroplex. Please visit our **website: http://biology.udayton.edu.**

The University of Dayton, a Comprehensive Catholic University founded by the Society of Mary in 1850, is an Affirmative Action/Equal Opportunity Employer. Women, minorities, individuals with disabilities, and veterans are strongly encouraged to apply. The University of Dayton is firmly committed to the principle of diversity.

The Department of Anthropology at the Pennsylvania State University seeks an **ASSISTANT or ASSOCIATE PROFESSOR** with research interests on the genetic and environmental factors that influence craniofacial and/or brain development and their relation to cognition, in a general evolutionary context. The successful candidate will apply methods of comparative genomics or functional genetic analysis to the development of human cognitive, linguistic, and learning capacities, and the continuum of outcomes from normal to abnormal in these capacities. The position is co-sponsored by Penn State's Children, Youth, and Families Consortium (CYFC), and the candidate will maintain strong interdisciplinary links between the Department of Anthropology and the CYFC, and the Huck Neurosciences Institute, the Rock Ethics Institute, and the Science, Technology, and Society Program here. Application review begins January 26, 2007, but all applications will be considered until the position is filled. Send curriculum vitae and letter of application detailing current and future research projects and plans, and at least three references to: **Wendy Fultz, Search Committee Liaison, Box A, Department of Anthropology, 409 Carpenter Building, Pennsylvania State, University Park, PA16802.** *Pennsylvania State is committed to Affirmative Action, Equal Opportunity, and a diverse work force.*

Positions @ NIH

THE NATIONAL INSTITUTES OF HEALTH

Department of Health and Human Services
National Institutes of Health
Tenure-Track Position

The Division of Intramural Research, National Institute on Deafness and Other Communication Disorders (NIDCD), located in Bethesda, MD, is seeking a tenure-track scientist to establish an independent research program to study molecular and/or cellular mechanisms of hearing and balance. We welcome applications from candidates with a wide range of expertise. Preference will be given to candidates whose experimental approaches complement those of our existing strong programs in the genetics, development and cell biology of hearing. The successful candidate will join a dynamic group of scientists in a growing intramural program that is at the forefront of research on communication disorders.

The NIDCD offers an exceptional working environment including well-equipped research laboratories and numerous opportunities for collaboration. Candidates for this position must possess a Ph.D. and/or M.D., post-doctoral experience, and an outstanding publication record. Salary is commensurate with education and experience.

Please submit a curriculum vitae including bibliography, three reprints of recent relevant publications, statement of research interests, an outline of your proposed research, and the names and addresses of three references to: **Ms. Trudy Joiner, Office of the Scientific Director, NIDCD, 5 Research Court, Room 2B28, Rockville, MD 20850 (joinert@nidcd.nih.gov)**. Applications will be accepted until **December 15, 2006**.

Department of Health and Human Services
National Institutes of Health
National Cancer Institutes

Tenure-Track Principal Investigator, Laboratory of Cellular Oncology and Center for Cancer Research, NCI.

The Laboratory of Cellular Oncology (LCO), Center for Cancer Research, of the National Institutes of Health, invites applications for a tenure track or tenure eligible principal investigator position in the area of research on papillomavirus biology, including vaccines. The LCO, which occupies recently renovated laboratory space, fosters an interactive research environment and the use of diverse experimental approaches and model systems. Applicants should have a Ph.D. and/or M.D. degree, a strong publication record, and demonstrated potential for imaginative research. Salary will be commensurate with education and experience. A one- or two-page statement of research interests and goals should be submitted in addition to three letters of recommendation and a curriculum vitae to: **Theresa Jones, Laboratory of Cellular Oncology, National Cancer Institute, NIH, Building 37, Room 4106, Convent Drive MSC 4263, Bethesda, MD 20892-4263; phone: 301-496-9513; fax: 301-480-5322; email: jonest@DC37A.nci.nih.gov**. Candidates must be U.S. citizens or permanent residents.

Applications must be received by **11/22/06**. The National Cancer Institute is an Equal Opportunity Employer. Selection for this position will be based solely on merit, with no discrimination for non-merit reasons such as race, color, religion, gender, national origin, politics, marital status, physical or mental disability, age, sexual orientations, or membership or non-membership in an employee organization.

Department of Health and Human Services
National Institutes of Health
Clinical Center

Tenure-track Physician
Clinical Center/Nuclear Medicine Department

This position is located in The Warren G. Magnuson Clinical Center, Nuclear Medicine Department (NMD).

We are seeking a research-oriented physician for a possible tenure-track position. An M.D. or M.D./PhD with U.S. Nuclear Medicine Board certification and CT training is needed to provide diagnostic and therapeutic nuclear medicine procedures as well as to participate in clinical research protocols of the NIH Intramural Program. U.S. citizenship or permanent residency status is required.

Please submit your curriculum vitae, bibliography, and a letter describing your clinical, research, and management experience to: **Mrs. Veronica Olaaje, HR Specialist, DHHS, NIH, OD/CSD-E, 2115 E. Jefferson Street, Rm. 2B209 MSC-8503, Bethesda, MD 20892-8503. Phone: 301-435-4748. Email: volaaje@mail.nih.gov**.

Salary is commensurate with experience. This appointment offers a full benefits package (including retirement, health, life and long term care insurance, Thrift Savings Plan participation, etc.). Application packages should be submitted as early as possible, but no later than **December 31, 2006**.

Selection for this position will be based solely on merit, without discrimination for non-merit reasons such as race, color, religion, sex, national origin, politics, marital status, sexual orientation, physical or mental handicap, age or membership or non-membership in an employee organization.

NIDDK

HEALTH SCIENCE POLICY ANALYST

The National Institute of Diabetes and Digestive and Kidney Diseases (NIDDK) is seeking applications from individuals who are currently in post-doctoral positions in biomedical research laboratories, but who wish to make a career change from a laboratory setting. Particularly encouraged to apply are individuals with post-doctoral experience in molecular biology, coupled with demonstrated writing and other communication skills. Incumbent will develop a wide range of documents that analyze and present the scientific accomplishments and plans of the NIDDK to public policy makers, voluntary health organizations, and other lay audiences. Incumbent must thus be able to convey in understandable, scientifically accurate, and meaningful terms the contributions of biomedical research to human health. Total salary is competitive and will be commensurate with the experience of the selectee.

Position requirements and detailed application procedures are provided on Vacancy Announcement Numbers: **NIDDK-07-155678-MP and NIDDK-07-155678-DE**, which can be obtained by accessing **WWW.USAJOBS.GOV**. All applications must be received by **12/14/06**. For additional information contact **Karen Page at (301) 496-4232**.

INTEGRATED MOLECULAR LIFE SCIENCES AND BIOPHYSICS PROGRAM
University of Denver

The Departments of Biological Sciences, Chemistry and Biochemistry, and Physics and Astronomy, are forming the Integrated Molecular Life Sciences and Biophysics (IMLSB) program which will include a multi-departmental graduate program with emphases in biophysics, biochemistry, and neuroscience. At the current time we seek to fill five tenure-track positions that will start September 1, 2007.

• Department of Biological Sciences – IMLSB Program
• Assistant Professor - Cellular/Molecular Biophysics
The Department of Biological Sciences invites applicants for a tenure track faculty position at the assistant professor level for a position in cellular or molecular biophysics to begin September 1, 2007. We are seeking candidates with research interests in cellular biophysics that include, but are not limited to, cytoskeletal motor proteins, protein dynamics, sensory transduction, excitation/contraction coupling or excitation/secretion coupling. The successful candidate will have a Ph.D. and post-doctoral experience in the appropriate field, will develop an extramurally funded research program, will supervise Ph.D. and M.S. students, and undergraduate research projects, and will teach undergraduate and graduate courses in areas of expertise.

• Department of Biological Sciences – IMLSB Program
• Assistant Professor - Neurophysiology/Cell Physiology
The Department of Biological Sciences invites applicants for a tenure track faculty position at the assistant professor level for a position in neurophysiology or cell physiology to begin September 1, 2007. We are seeking applicants that use molecular or cellular approaches to study the physiology of excitable membranes or intracellular signaling mechanisms. The successful candidate will have a Ph.D. and post-doctoral experience in the appropriate field, will develop an extramurally funded research program, will supervise Ph.D. and M.S. students, and undergraduate research projects, and will teach undergraduate and graduate courses in areas of expertise.

• Department of Chemistry and Biochemistry – IMLSB Program
• Assistant Professor - Biochemistry and Biophysical Chemistry (2)
The Department of Chemistry and Biochemistry invites applications for 2 tenure-track faculty positions to begin September 1, 2007. Outstanding candidates at all levels will be considered. Areas of research specialization include but are not limited to, protein conformational dynamics and folding, cell signaling, transport phenomena associated with proteins and membranes, computational and experimental biophysics, and any sub areas of biochemistry. The successful candidate will have a Ph.D. and postdoctoral experience in appropriate fields. These positions will supervise undergraduate and graduate research, teach undergraduate and graduate courses in biochemistry and in inter-disciplinary topics related to the biophysics initiative, and develop an extramurally funded research program.

• Department of Physics and Astronomy - IMLSB Program
• Assistant Professor - Biophysics
The Department of Physics and Astronomy invites applications for a tenure-track faculty assistant professorship beginning September 1, 2007 in areas of theoretical, computational or experimental biophysics. A special emphasis will be given to candidates with research interests in cell signaling, transport phenomena associated with proteins and membranes, and protein conformational dynamics and folding. A B.S. in Physics and Ph.D. in Biophysics or a related discipline are required. Applicants will be expected to teach at both undergraduate and graduate levels and primarily will be expected to support our Medical Physics minor and other interdisciplinary programs. The department offers degrees through the Ph.D.

All candidates must submit their application through **https://www.dujobs.org**. The application should include: a curriculum vitae, and statements of teaching philosophy and research interests. Under separate cover please send two recent publications, three letters of recommendation to: **IMLSB Faculty Search, University of Denver, [the department you are applying to], Denver, Colorado 80208**. The selection process for these positions will begin **December 15, 2006** and continue until the positions are filled. Contact **Prof. Robert M. Dores (rdores@du.edu)** if you have any questions.

The University of Denver is committed to enhancing the diversity of its faculty and staff and encourages applications from women, minorities, people with disabilities and veterans. DU is an EEO/AA Employer.
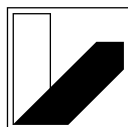
UNIVERSITÄT BAYREUTH

At the University of Bayreuth the following position is open for application at the Faculty of Biology, Chemistry and Geosciences:

Junior Professorship (W1) Biogeographical Modelling

The position will be filled as soon as possible, initially for a period of 3 years, with the possibility of an extension for another 3 years subject to a positive evaluation.

Candidates for this Junior Professorship have received a Ph.D. degree in Biology, Ecology, Geoecology, Geography or any related field during the last three years. The candidate is expected to engage in own independent research programs. Specifically he/she should have experience in biogeographical research. The candidate should be familiar with dispersal models, explorative multivariate statistics and rule based spatially explicit models.

This position will contribute to the research focus on Ecology and Environmental Science at the University of Bayreuth. Integration into existing research groups at the University of Bayreuth is required (e.g. Bayreuth Centre for Ecology and Environmental Research, BayCEER). Documented activities in the acquisition of third-party funding are desired. The teaching will concentrate on the Elite Study Program "Global Change Ecology" (within the Elite Network of Bavaria) but courses for studies in Geography, Geoecology and Biology are expected as well. Teaching language is mainly English.

The successful candidate must hold a university degree, prove his/her potential for scientific work (e.g. by excellent Ph.D.) and teaching skills.

Physically handicapped persons will be favoured, if they are equally qualified. To increase the number of women in science, women are explicitly encouraged to apply. Applications including CV, university certificates and list of publications should be sent before **December 31th 2006** to the:

Dean of the Faculty of Biology, Chemistry and Geosciences; University of Bayreuth; D-95440 Bayreuth, Germany.

TENURE-TRACK FACULTY POSITIONS
CENTRE FOR RESEARCH IN NEUROSCIENCE
McGILL UNIVERSITY

The McGill Centre for Research in Neuroscience (**www.mcgill.ca/crn**) has tenure-track openings to be filled in 2007. The CRN is part of the Research Institute of the McGill University Health Centre in Montreal, Canada. These openings are for investigators at the assistant or associate professor level whose research interests are compatible with our on-going work on neural regeneration/development (synapse formation) and function (synaptic plasticity). We study invertebrate and vertebrate models and have a transgenic mouse facility on-site. We are interested in recruiting either basic scientists or clinician/scientists who wish their time to be largely invested in research. Applicants are expected to develop an independent, innovative research program for which attractive start-up packages are available. Teaching opportunities at the graduate and undergraduate levels are available according to interest at any of several departments at McGill.

The McGill CRN is at the core of a vibrant community of over 100 neuroscience laboratories in Montreal, and therefore we offer excellent prospects for collaboration in basic and clinical research. Montreal is a cosmopolitan city with an attractive and affordable lifestyle.

Please send curriculum vitae, the names of three referees, and a brief statement of research interests to: **Search Committee, McGill Centre for Research in Neuroscience, Montreal General Hospital L7-132, 1650 Cedar Avenue, Montreal, Quebec, Canada H3G 1A4** or **e-mail yvonne.gardner@mail.mcgill.ca**.

Deadline for applications: **15th December, 2006**.

be in touch with science.
we provide the means. you the imagination.

Agency for Science, Technology and Research
SINGAPORE
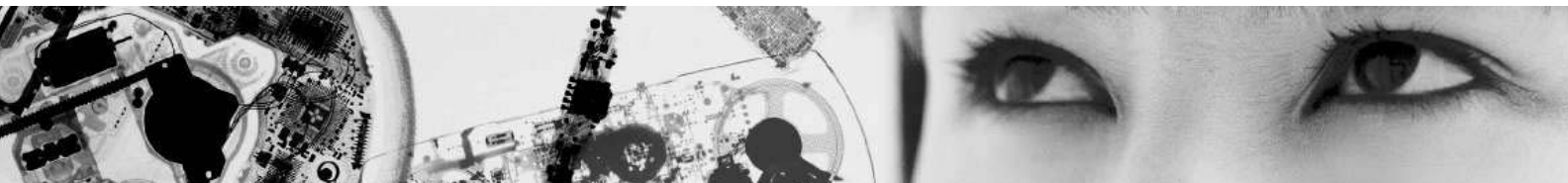
SINGAPORE BIOIMAGING CONSORTIUM (SBIC)

SBIC is a new initiative by A*STAR (Agency for Science, Technology and Research, Singapore) that aims to develop and use latest imaging technologies to pursue biomedical research leading to translational applications. Under the leadership of Professor Sir George Radda, an eminent physiologist and a leader in NMR research, the consortium brings together scientists and researchers from universities, hospitals and commercial laboratories in an integrated, cutting-edge program.

Two laboratories are currently set up within SBIC: Laboratory of Metabolic Medicine (LMM), headed by Professor Sir George Radda and his deputy Dr. Weiping Han, and Laboratory of Molecular Imaging (LMI), by Dr. Xavier Golay.

LMM and LMI are equipped with advanced facilities for conducting biomedical research in molecular genetics, cell biology, physiology, and modern MR imaging. LMM aims to understand the biological basis of metabolic syndromes, to provide molecular targets to treat these diseases, and to offer animal models for evaluation of therapeutic interventions. LMI focuses on the development of a comprehensive program in translational molecular and functional imaging, with long-term aim of providing a platform to shorten the time of new drug development in the fields of neurodegenerative and metabolic diseases.

Successful applicants would be provided with 3-year contracts and internationally competitive packages. The levels of appointment and renumeration packages will be commensurate with the experience of the applicants.

STAFF SCIENTIST

Laboratory of Metabolic Medicine (Position 1)   Ref: SBIC/R/011206/01

Laboratory of Molecular Imaging (Position 2)   Ref: SBIC/R/011206/02

requirements:
- PhD, MD or equivalent in cell or molecular biology, neurobiology, biochemistry, physiology, biomedical engineering or related field (LMM)
- PhD in physics, chemistry or related field with emphasis on NMR spectroscopy (LMI)
- Experience and enthusiasm for research in the field of metabolic medicine and neurodegeneration
- Experience in optical imaging, electrophysiology, molecular biology, animal physiology and/or behavioral studies (LMM)
- Experience with sequence development, data analysis and programming on a Varian spectrometer is an advantage (LMI)
- Publications in international refereed journals

GROUP LEADER

Laboratory of Metabolic Medicine (Position 3)   Ref: SBIC/R/011206/03

Laboratory of Molecular Imaging (Position 4)   Ref: SBIC/R/011206/04

Group Leader will be provided with research support and intramural funding by A*STAR. In addition to the above requirements for Staff Scientist, a Group Leader should meet the following requirements:

requirements:
- At least three years of postdoctoral experience with expertise in the field of metabolism and signaling research (LMM) or MR spectroscopy (LMI) that will complement existing programs
- Submit a brief research proposal of no more than 3 pages

OIST Director Vacancy Announcement

Organization

The Okinawa Institute of Science and Technology (OIST) Promotion Corporation is an Independent Administrative Agency established by the Government of Japan (www.oist.jp). Its aim is to establish a world-class graduate university in science and technology in Okinawa. English will be the language of instruction, and a large segment of the faculty and student population will be international. Currently, 10 Principal Investigators and a total of more than 100 scientists, students, and research support staff are located in temporary OIST Initial Research Project facilities in Uruma, Okinawa. This will expand to 15 Principal Investigators and their teams by the beginning of 2007. OIST is presently constructing a new permanent campus in Onna village, on the west side of Okinawa Island, that will support a major expansion in research activities.

Research Resource Unit Director

Responsibilities

The candidate must be a strong leader able to organize and manage laboratories and technical services and to work effectively with scientists and administrators, in compliance with government rules and regulations. The Research Resource Unit will manage central shared facilities including animal facilities, analysis equipment, electron microscopes, a radioactive materials facility, etc. Specific responsibilities will include:
• Establishment of policies concerning shared laboratory facilities and research space
• Resource and asset management to provide efficient support of scientists' needs
• Effective budget implementation and control
• Management of technical personnel

Qualifications

Specific qualifications include:
• Doctorate degree in a field of science or engineering with a minimum of ten years of experience in managing research facilities.
• International experience strongly preferred, experience in an academic or research institution will be an advantage.
• Excellent written and oral communication skills in English and Japanese.
• In-depth knowledge of modern research facilities and cutting-edge techniques and of related regulations and policies.
• Networking and negotiating skills to build strong working relationships with scientist, administrators, and suppliers.
• Ability and willingness to assume high-visibility institutional roles such as committee participation, and to collaborate with others across the organization.
• A balanced and even-handed disposition; a candid and flexible style.

Compensation

The compensation for this position has been designed to attract a person of significant accomplishment and will be commensurate with experience. This is a 5-year appointment, renewable depending on performance review.

Contact

Please send a cover letter and resume (non-returnable) in English with photo to Mr. Osamu Nonaka, Human Resources Department, Okinawa Institute of Science and Technology, 7542 Onna, Onna-son, Okinawa 904-0411, Japan.
Resumes may also be faxed to: 81-(0)98-966-8717, or emailed to: recruit@oist.jp

Finance Director

Responsibilities

The candidate should have an understanding of Japanese government rules and regulations in proposing budgets and the utilization of public funds. The position requires strong leadership and efficient interaction with both the management and the research team. Specific responsibilities will include:
• Overall policies concerning finance, accounting, budget, and financial planning
• Credit management, tax and public duties, asset management
• Preparation of budget requests and budget negotiation with the Ministry on behalf of OIST PC
• Effective budget implementation and control
• Preparation of financial statements
• Procurement and contracts

Qualifications

• At least a 4-year university degree in a field related to finance, accounting and/or economics with a minimum of ten (10) years of experience working as a senior financial officer.
• International experience is strongly preferred, experience in an academic or research institution will be an advantage.
• Demonstrated leadership, management and mentoring capabilities.
• Certified Public Accountant (CPA) or equivalent will be an advantage.
• Networking and negotiating skills to build a strong working relationship with the Ministry on behalf of OIST PC, and to communicate the value and importance of OIST projects to government agencies.
• Outstanding written and oral communication skills in English and Japanese.
• Ability and willingness to assume high-visibility institutional roles such as committee participation, and to collaborate with others across the organization.
• A balanced and even-handed disposition; a candid and flexible style.
• The highest personal and professional integrity.

Compensation

The compensation for this position has been designed to attract a person of significant accomplishment and will be commensurate with experience. OIST PC is interested in a commitment of not less than three years. This is a full-time permanent position.

Contact

Please send your letter of interest and (non-returnable) resumes in English with photo to Mr. Ferry Toya, Secretary of the Selection Committee, The Office of The President, Okinawa Institute of Science and Technology, 7542 Onna, Onna-son, Okinawa 904-0411, Japan.
Resumes may also be faxed to: 81-(0)98-966-8716, or e-mailed to: ferry.toya@oist.jp

Deadline: December 22, 2006
Confidentiality of all inquiries will be respected.
OISTPC is an Equal Opportunity Employer dedicated to workforce diversity.

Yale University

Yale Stem Cell Program
Yale Human Embryonic Stem Cell Core Facility

Technical Director

We seek to recruit an experienced researcher to establish and manage the Yale Human Embryonic Stem Cell Core Facility. This is a faculty position at the level of Associate Research Scientist or Research Scientist. The Technical Director will oversee and directly participate in the research and training activities of the Facility, including compliance with institutional, state, and federal regulatory requirements. The Facility will serve as a repository, distribution and training center for both federally approved and non-federally approved hES lines, and offer quality assurance, basic characterization, and genetic modification of such lines. In addition, the hESC Core will collaborate with the Yale *In Vitro* Fertilization Laboratory to derive new hESC lines from human blastocysts.

The qualified candidate must have broad expertise in all aspects of hES cell research, including production, characterization and genetic modifications of hES cell lines. S/he will also have in-depth knowledge of regulations regarding hES cells research. Qualifications include a PhD, MD, or MD/PhD degree.

Applicants should mail a three-page research statement and CV, and arrange to have three reference letters sent to:

Haifan Lin, PhD.
c/o Kristin Dugan
Director's Office, Yale Stem Cell Program
P.O. Box 208002, Yale University School of Medicine
333 Cedar Street, New Haven CT 06520-8002

Application deadline is **January 15, 2007**. Follow-up inquiries should be sent to: **StemCell.Search@yale.edu**.

Yale is an Affirmative Action/Equal Opportunity Employer.

Yale University

Yale Stem Cell Program

Faculty Positions

The newly established Yale Stem Cell Program invites applications for faculty positions at the rank of Assistant, Associate, or Full Professor. Rank and tenure will be commensurate with experience. Applicants should have a Ph.D. and/or M.D. degree. Each successful candidate will be expected to develop a vigorous, externally funded research program on fundamental questions related to the biology of embryonic or adult stem cells. Investigators will join a vibrant stem cell research community at Yale with over 40 labs working on various aspects of stem cell biology and medicine, and will have opportunities to compete for Connecticut State funding for stem cell research, including research on non-federally approved human embryonic stem cell lines. Investigators will also contribute to teaching graduate and/or medical students as well as shaping stem cell research at Yale.

Applicants should mail a three-page research statement and CV, and arrange to have three reference letters sent to:

Haifan Lin, Ph.D.
c/o Kristin Dugan
Director's Office, Yale Stem Cell Program
P.O. Box 208002, Yale University School of Medicine
333 Cedar Street, New Haven CT 06520-8002

Application deadline is **January 15, 2007**. Follow-up inquiries should be sent to: **StemCell.Search@yale.edu**.

Yale is an Affirmative Action/Equal Opportunity Employer.

FACULTY POSITIONS
Basic Medical and Behavioral Sciences

The Department of Basic Medical Sciences and related clinical units at the new expansion of the University of Arizona (UA) College of Medicine in Phoenix invite applications for full-time tenure-track (rank open) faculty appointments.

Successful candidates should have a relevant graduate degree (PhD, MD, or equivalent). Candidates must have teaching expertise in one of the following disciplines: behavioral sciences, biomedical informatics, human genetics, microbiology/infectious disease, pathology and pharmacology. Specifically with respect to behavioral sciences, appointments will be made in either Basic Medical Sciences or an appropriate clinical department.

Excellence in teaching is essential, and only accomplished and dedicated medical science educator-scholars will be considered. Candidates should also possess postdoctoral experience and high-quality, peer-reviewed publications evidencing promise of research independence and competitive funding potential. Preferred research qualifications are in the following areas of research emphasis which have been established by The UA College of Medicine-Phoenix: cancer biology, cardiovascular disease, diabetes, neuroscience and bioinformatics/human genetics.

For a full description, qualifications and to apply please go to **Job #36581** at **www.uacareertrack.com**. Online, applicants should provide a letter of interest, complete CV/bibliography, summary of research accomplishments and future plans, and brief statement of teaching experience and philosophy. Applicants should also arrange for three letters of recommendation to be sent to: **Karen Chadderdon, University of Arizona College of Medicine - Phoenix, 550 E. Van Buren, Phoenix, AZ 85004-2230; FAX: 602-827-2130 (kchadder@u.arizona.edu)**. Questions may be directed to: **Dr. Mark R. Haussler, Regents Professor and Head, Department of Basic Medical Sciences, University of Arizona College of Medicine; phone: 602-827-2102 (haussler@u.arizona.edu)**.

As an Equal Opportunity and Affirmative Action Employer, The University of Arizona recognizes the power of a diverse community and encourages applications from individuals with varied experiences and backgrounds. The University of Arizona is an EEO/AA – M/W/D/V Employer.

Featured Employers

Search **ScienceCareers.org** for job postings from these employers. Listings updated three times a week.

Abbott Laboratories www.abbott.com

Elan Pharmaceuticals www.elan.com/careers

Genentech www.gene.com

Institute for One World Health
www.oneworldhealth.org

Invitrogen www.invitrogen.com/careers

Kelly Scientific Resources
www.kellyscientific.com

Novartis Institutes for BioMedical Research
www.nibr.novartis.com

Pfizer Inc.
www.pfizer.com

Pierce Biotechnology, Inc.
www.piercenet.com

If you would like to be a featured employer, call 202-326-6543.

ScienceCareers.org
We know science AAAS

UF | UNIVERSITY *of* FLORIDA

J. Crayton Pruitt Family Chair in Biomedical Engineering Eminent Scholar Professorship

The J. Crayton Pruitt Family Department of Biomedical Engineering in the College of Engineering at the University of Florida invites applications and nominations for a new eminent scholar professorship starting as soon as Fall 2007. Candidates are expected to possess academic credentials sufficient to meet requirements for a full professorship in Biomedical Engineering. Candidates should be leaders in their field capable of making a significant impact through their research. Salary will be competitive and commensurate with qualifications of the candidate.

Candidates from all areas of biomedical engineering are invited to apply. Areas of particular interest include but are not limited to biomedical imaging, biomedical systems analysis, molecular and cellular engineering, biomaterials, and neuroengineering.

With a strong institutional commitment from the University of Florida to create graduate and undergraduate programs, we are building a department where innovation, risk-taking, creativity, interdisciplinary research and collegiality are nurtured and encouraged.

Our proximity to and close ties with the Evelyn F. & William L. McKnight Brain Institute, the National High Magnetic Field Laboratory, the Particle Engineering Research Center, the University of Florida Health Science Center, the VA Hospital, Shands HealthCare at the University of Florida, the University of Florida Genetic Institute, the University of Florida Shands Cancer Center, the Halogen Therapy Center, the Nanoscience Institute for Medical and Engineering Technology, the Howard Hughes Medical Institute and the Scripps Research Center will provide unparalleled opportunities for cross-fertilization and collaborative research.

Review of applications will begin on **January 8, 2007**, and will continue until the position is filled. Candidates should send curriculum vitae with the names of at least four references to:

Dr. Huabei Jiang, Chair of Search Committee
J. Crayton Pruitt Family Department of Biomedical Engineering
University of Florida
130 BME Building/PO Box 116131
Gainesville, FL 32611-6131
Telephone: (352) 846-2950
Email: search2007@bme.ufl.edu
Website: http://www.bme.ufl.edu

The University of Florida is an Equal Opportunity Institution. Women and minorities are encouraged to apply.

THE OHIO STATE UNIVERSITY MEDICAL CENTER

The Ralph W. and Helen Kurtz Endowed Chair in Experimental Pathology
The Ohio State University
Department of Pathology

A Tenure track position at the Rank of Associate Professor or Professor

The Department of Pathology of The Ohio State University is seeking a full-time MD, PhD, or MD/PhD for an endowed faculty position (The Ralph W. and Helen Kurtz Chair in Experimental Pathology). The Department of Pathology is also searching for a Director of the Division of Experimental Pathology. The ideal candidate would hold both positions.

We seek a well funded investigator with a solid track record of funding and high impact publications who can continue their research trajectory, foster research collaboration activities both inside and outside the Department and mentor junior scientists.

The Ohio State University Medical Center is composed of a 923 bed adult tertiary care hospital and a 160 bed cancer hospital and comprehensive cancer center and is internationally recognized for its excellence in hematology, oncology, transplantation, and cardiovascular disease. The department has state of the art resources for image analysis, flow cytometry, immunohistochemistry, in situ hybridization, and electron microscopy. There are active clinical and research programs in cytogenetics, molecular and experimental pathology in cancer metastasis, tumor immunology, neuroscience and imaging. An interest in university-industry collaboration is a plus.

The Ohio State University is an equal opportunity, affirmative action employer. Women, minorities, veterans, and individuals with disabilities are encouraged to apply. Interested individuals should send a copy of their curriculum vitae and the names and addresses of three individuals who can act as references to:

Sanford H. Barsky, M.D.
Senhauser Endowed Chair and Professor
Department of Pathology
Ohio State University Medical Center
129 Hamilton Hall, 1645 Neil Avenue
Columbus, Ohio 43210

The University of Texas at San Antonio
Assistant / Associate Professor – Neuroscience

The Department of Biology at the University of Texas San Antonio invites applications for a tenure-track position at the rank of Assistant/Associate Professor.

Candidates must have a M.D., or Ph.D. or the equivalent in biology or a related discipline, and for appointments as an Assistant Professor, at least 2 years of postdoctoral experience. We are in particular searching for candidates with a record of accomplishment in the study of central pattern generators, especially in invertebrate systems; neuronal control of movement; structure / function studies of ion channels; and/or dynamical changes in neuronal structure whether during development or in adults. Preference will be given to candidates linking experimental and model-based studies.

The successful applicant is expected to establish and maintain an extramurally funded research program, and contribute to undergraduate teaching and graduate supervision. In addition to an attractive startup package and laboratory space, the candidate will also have support from two recently established core facilities, one in computational biology (**http://www.cbi.utsa.edu**) and one with extensive support for imaging studies, including two photon microscopy. The successful candidate will also join a growing group of researchers in Neuroscience at UTSA with an emphasis on experimentally based computational studies.

Candidates please forward via email (**biofacultyad@utsa.edu**) or U.S. Post (**Dr. James M. Bower, Chairman Search Committee, Department of Biology, UTSA, One UTSA Circle, San Antonio, TX 78249-0662**) current curriculum vitae, two or three representative publications, and a brief summary of future research interests and teaching experience. Include contact information (including email addresses) of three references. Applicants who are not U. S. citizens must state their current visa and residency status. Applications will be reviewed starting **December 15, 2006** and will be accepted until the position is filled. For further information contact the chairman of the search committee, **Dr. James M. Bower (bower@uthscsa.edu)**. Pending budget approval.

UTSA is an Affirmative Action/Equal Opportunity Employer. Women, minorities, veterans, and individuals with disabilities are encouraged to apply.

ASSISTANT PROFESSOR
PLANT MOLECULAR BIOLOGY

The Section of Molecular Cell and Developmental Biology at The University of Texas at Austin invites applications for a tenure track position in the general area of plant molecular biology. We are interested in applicants who use molecular and biochemical approaches to investigate fundamental problems in plant genetics, cell and developmental biology and will consider applications at the Assistant Professor level. Areas of particular interest include but are not limited to pathway regulation, signal transduction, and RNA interference. We seek an outstanding investigator who will build an active research program and who will teach effectively at the undergraduate and graduate levels. The successful candidate will also be eligible for affiliation with the Institute for Cellular and Molecular Biology, which provides state-of-the-art facilities and supports an excellent graduate program. The molecular biology community at UT Austin is in an exciting phase of growth with recent hires in cell biology, developmental biology, genomics and related areas.

Applications will be considered from **December 1, 2006**, until the position is filled. Applicants should send their curriculum vitae, statement of research and teaching interests, representative publications, as well as arrange for three letters of recommendation to be sent to:

**Chairman, Plant Molecular Biology Search Committee
ATTN: Maureen Meko
Section of Molecular Cell and Developmental Biology
University of Texas at Austin
BIO 311, 205 W 24th St
Austin, TX 78712-0183**

Home pages: **http://www.biosci.utexas.edu/MCDB/**
and **http://www.icmb.utexas.edu/**

Austin is located in the Texas hill country and is widely recognized as one of America's most beautiful and livable cities.

The University of Texas at Austin is an Affirmative Action/ Equal Opportunity Employer. Qualified women and minorities are encouraged to apply.

TENURE-TRACK FACULTY POSITION

The Department of Biochemistry and Molecular Biology, University of Texas Medical School, Houston plans to appoint a tenure-track Assistant Professor starting Fall 2007. Appointment as Associate Professor will be considered for exceptional candidates. We will consider applicants from any area of biochemistry, cell and molecular biology. The successful candidate will be expected to establish an externally funded research program, and participate in team-taught biochemistry and molecular biology courses offered to medical and graduate students. Applicants must have a Ph.D., at least two years of postdoctoral research experience, and evidence of significant research accomplishments.

Send curriculum vitae, statement of research interests (1-2 pages), the names, addresses, e-mail addresses of three references to:

**Dr. Ann-Bin Shyu, Chair
Faculty Search Committee
Department of Biochemistry and Molecular Biology
University of Texas Medical School at Houston
P.O. Box 20708
Houston, TX 77225**

Application deadline is **January 15, 2007**, or thereafter until the position is filled. For additional information, please see: **http://med.uth.tmc.edu/departments/biochemistry/**.

The University of Texas Health Science Center at Houston is an EO/AA employer. M/F/D/V. This is a security sensitive position and thereby subject to Texas Education Code § 51.215. A background check will be required for the final candidate.

SPECIAL POST- DOCTORAL RESEARCH FELLOWSHIP IN PHYSICS

SCUOLA NORMALE SUPERIORE

TELECOM ITALIA Progetto Italia

'Progetto Italia Fellowship at the Scuola Normale Superiore'

The Scuola Normale Superiore of Pisa invites interested, talented candidates to apply for a special Post-Doctoral Research Fellowship in Physics (Progetto Italia Fellowship), offered for the first time thanks to generous support provided by the *Telecom Italia Group*.
The Fellowship will be awarded for two years; candidates must hold a PhD in physics or an equivalent diploma and must be less than 35 years old. The amount of the fellowship is €100,000. Applications for participation in the selection, addressed to the *Direttore della Scuola Normale Superiore di Pisa, Piazza dei Cavalieri n.7, 56100 Pisa,* must arrive by 15 December 2006. Further information: **http://www.sns.it/en/borse/asscon/contratto/progettoitalia/**

Scuola Normale Superiore, since its establishment in 1810, has been characterized by a special procedure for student selection and a unique mixture of research and education. It is the university of Presidents of the Italian Republic, Prime Ministers, researchers and world-famous scientists such as the Nobel Prize winners Enrico Fermi and Carlo Rubbia.

There are more than 100 faculty members for fewer than 600 students, all working together in close contact in a unique research environment. The Faculty of Sciences offers classes in Physics, Chemistry, Biology, Mathematics and Information Sciences. Activity is accompanied by research in 14 different laboratories and research groups and aided by a library with specifically earmarked funds.

Established in 2003, in its first four years **Progetto Italia**, wholly-owned by Telecom Italia, has run a large number of cultural, charitable, educational and sports projects, involving millions of Italians, public and private institutions, local government and associations in a different kind of contact with their country. Its aim is to work to give its contribution to the growth of the country. The Company's **Advisory Board** brings together internationally-renowned figures such as Susanna Agnelli, Tara Gandhi Bhattacharjee, Peter Sutherland, Umberto Veronesi. For further information: **www.telecomprogettoitalia.it**

ENERGY FOR THE FUTURE
TWELVE FACULTY POSITIONS AT THE UNIVERSITY OF CALIFORNIA, DAVIS

The University of California, Davis, announces the establishment of a new initiative on Energy for the Future. This initiative strengthens and expands existing campus efforts in energy science, technology, and policy to address energy challenges of the 21st century.

UC Davis seeks highly motivated and qualified persons to fill 12 tenure-track faculty positions in the following energy areas:

Bioconversion Engineer
Biofuels Engineer
Bio-inspired Approaches to Energy Generation
Catalysis and Photovoltaic Materials
Efficient Energy Systems, Renewable Energy
Energy Efficiency in Buildings, Energy Systems Analysis or Energy and Transportation Logistics
Experimental Condensed Matter Physicist
New Materials for Energy Applications
Plant Biologist
The Ultra-Fast Frontier in Energy Research
Transportation Economics (recruitment in 2007)

Positions are available for individual or joint appointments within the departments of Biological and Agricultural Engineering, Chemical Engineering and Materials Science, Chemistry, Civil and Environmental Engineering, Economics, Mechanical and Aeronautical Engineering, Physics, and Plant Sciences.

UCDAVIS

Faculty applicants must have a Ph.D. degree or equivalent. Successful applicants will be required to develop strong research and teaching programs of relevance to the initiative. Senior faculty appointments may be considered for highly distinguished individuals for some positions.

For more information or to apply, visit the Energy for the Future initiative on-line at: **http://energy.ucdavis.edu**.

The University of California, Davis is interested in candidates who are committed to the highest standards of scholarship and professional activities, and to the development of a campus climate that supports equality and diversity.
The University of California is an Affirmative Action/Equal Opportunity Employer.

OAKLAND UNIVERSITY
DEPARTMENT OF BIOLOGICAL SCIENCES

TENURE-TRACK FACULTY POSITIONS
IN MICROBIOLOGY AND IMMUNOLOGY

The Department of Biological Sciences at Oakland University invites applications for two tenure-track positions to be filled by August 2007, one in **Microbiology** and one in **Immunology**. We seek candidates who are interested in key molecular/biochemical questions in their fields, using state of the art approaches and techniques. A Ph.D. and post-doctoral experience are required as well as a strong research track record evidenced by publications. Appointments will be at the assistant professor level; outstanding candidates with appropriate experience and long-term funding may be considered for appointment as associate professor. Each successful candidate is expected to develop a vigorous, extramurally funded research program, to teach effectively at the undergraduate and graduate levels, and to mentor graduate students in doctoral programs.

The Department of Biological Sciences (**http://www2.oakland.edu/biology/**) is a modern, well equipped, and research oriented department. The department has active graduate programs at the Master's and Ph.D. levels. Oakland University is a state-supported institution of 17,000 students situated on a beautiful 1,600-acre campus 25 miles north of Detroit.

Review of Applications will begin on January 15, 2007, and continue until the position is filled. Applicants should submit a curriculum vitae, statement of research plans and teaching philosophy, key reprints, and arrange to have at least three letters of reference sent to:
Arik Dvir, Chair
Department of Biological Sciences
Oakland University
Rochester, MI 48309-4401

Or by email: **biology1@oakland.edu**

Oakland University is an Affirmative Action/Equal Opportunity Employer and encourages applications from women and minorities.

FACULTY POSITION IN BIOLOGICAL CIRCUITS

Caltech invites applications for a tenure-track position in the broadly-construed area of engineering biological circuits.

We are interested in areas such as synthetic and systems biology, circuit design and analysis, biomolecular information processing, and bionanotechnology. Candidates pursuing wet, dry, in vivo, in vitro, analytic, synthetic, experimental, and/or theoretical research will be considered. A strong commitment to excellence in teaching and mentoring is also expected. The successful candidate will have a primary home in Bioengineering, Applied Physics, Computation and Neural Systems, Computer Science, Control and Dynamical Systems, Electrical Engineering, or Applied and Computational Mathematics, as well as the possibility of a joint appointment in Biology, Chemical Engineering, Chemistry, or Physics. Participation in the Center for Biological Circuit Design, part of Caltech's Information Science and Technology initiative, will provide access to an active research community with opportunities for interdisciplinary collaborations. Strong preference will be given to applicants at the assistant professor level, but exceptional candidates at the associate or full professor levels will be considered. The term of the initial appointment at the assistant professor level is normally four years, and is contingent upon completion of a Ph.D.

Applicants should apply online at http://www.eas.caltech.edu/bio-circuits by submitting a letter of application; a brief statement of research accomplishments, interests, and goals; a brief statement of teaching interests; curriculum vitae; and up to three selected reprints or preprints. Applicants should arrange to have four letters of reference sent directly to bio-circuits-search@caltech.edu. Application review will commence on December 31, 2006 and continue until the position is filled.

CALIFORNIA INSTITUTE OF TECHNOLOGY
Division of Engineering and Applied Science

Caltech is an Equal-Opportunity/Affirmative-Action Employer.
Women, minorities, veterans, and disabled persons are encouraged to apply.

DEPUTY DIRECTOR, BIOMEDICAL LABORATORY R&D
DEPUTY DIRECTOR, CLINICAL SCIENCE R&D
Veterans Health Administration

The Veterans Affairs Office of Research and Development is accepting applications for two positions, Deputy Director, Biomedical Laboratory R&D Service (BLRDS) and Deputy Director, Clinical Science R&D Service (CSRDS).

VA provides health care for veterans through a network of over 150 hospitals and 850 outpatient clinics and supports an intramural research program. The BLRDS focuses on preclinical investigations in a wide range of areas, including neuroscience, cancer, cardiovascular disease, infectious and immune diseases, and mental health. The current annual VA budget for BLRDS is $173,000,000. The CSRDS focuses on clinical investigations including multisite clinical trials. The current annual VA budget for CSRDS is $90,000,000.

The Deputy Directors, working closely with the Director, are responsible for the overall management of the intramural research program carried out through the BLRDS/CSRDS, including training, research centers, individual investigator-initiated research, and conduct of large clinical trials. The Deputy Directors must have a strong research background and strong management skills. The successful candidate must have an appropriate doctoral degree, typically an M.D., Ph.D., or both. Salary is commensurate with experience.

All applicants should submit a letter indicating interest in the position, a career synopsis, current curriculum vitae with complete bibliography, and the names and addresses of five references by December 20, 2006, to: **Sara Clark, Office of Research & Development (121), Veterans Affairs Central Office, 810 Vermont Avenue N.W., Washington, DC 20420.**

FACULTY POSITIONS IN PHARMACEUTICS/DRUG DELIVERY
Department of Pharmaceutical and Biomedical Sciences
College of Pharmacy
University of Georgia

The Department of Pharmaceutical and Biomedical Sciences at the University of Georgia, Athens, invites applications for two full-time, tenure-track faculty positions (one **ASSISTANT PROFESSOR** and one **ASSOCIATE/FULL PROFESSOR)** in the areas of biopharmaceutics, drug delivery/nanotechnology, pharmaceutical technology, or drug targeting/drug transport. Applicants should possess a Ph.D. or Pharm.D./Ph.D. or equivalent degree in pharmaceutical sciences or a closely related area as the focus of their graduate education and research training. Each successful applicant is expected to have or to develop a dynamic, extramurally funded research program in an area identified above. Excellent communication skills and the ability to teach basic pharmaceutics and drug delivery concepts at both the Pharm.D. and Ph.D. levels are required. A highly competitive salary, modern research space, and excellent startup funds will be provided. To be assured of full consideration, applications should be received by February 1, 2007. Interested qualified applicants should submit a letter of application, curriculum vitae, a research plan, and three confidential letters of recommendation to: **Chair, Faculty Search Committee, Department of Pharmaceutical and Biomedical Sciences, R.C. Wilson Pharmacy Building, University of Georgia, Athens, GA 30602-2352.** Applicants may also apply online to **e-mail: pbssearch@rx.uga.edu.** *The University of Georgia is an Equal Employment Opportunity/Affirmative Action Employer. Applications from qualified women and minority candidates are encouraged.*

CHAIR IN AUTISM RESEARCH

The Department of Pediatrics at the University of Pennsylvania School of Medicine seeks candidates for an **ASSOCIATE or FULL PROFESSOR** position in either the tenure track or the nontenure clinician-educator track. Track and rank will be commensurate with experience. The successful applicant will be accomplished in the area of autism. Applicants must have an M.D. or Ph.D. or M.D./Ph.D. degree and have demonstrated excellent qualifications in education, research, and/or clinical care.

We are seeking a scientist of international renown to occupy a newly established **CHAIR IN AUTISM RESEARCH.** The successful applicant will be qualified to participate actively in ongoing research in complex neurodevelopmental and neuropsychiatric disorders at the Children's Hospital of Philadelphia and University of Pennsylvania, including cutting-edge programs in developmental neurobiology, genetics/genomics, cognitive neuroscience, neuroimaging, and treatment. The holder of the Chair should bring a research program that will complement and enhance these multidisciplinary activities. The applicant should demonstrate a history of successful collaboration with clinicians who treat patients with autism and/or related neurodevelopmental disabilities and be prepared to play a major role in the training of junior researchers, medical students, and clinical investigators.

Please submit curriculum vitae, a letter of interest, and three reference names to: **Susan E. Levy, M.D., Clinical Professor of Pediatrics, University of Pennsylvania, School of Medicine, Chair, Search Committee, The Children's Hospital of Philadelphia, Children's Seashore House Building, Room 231, 3405 Civic Center Boulevard, Philadelphia, PA 19104.**

The University of Pennsylvania is an Equal Opportunity, Affirmative Action Employer. Women and minority candidates are strongly encouraged to apply.

The University of Michigan Department of Internal Medicine, Division of Infectious Diseases seeks Ph.D., M.D., or M.D./Ph.D. candidates for tenure-track positions at the **ASSISTANT, ASSOCIATE, or FULL PROFESSOR** rank to develop and conduct independently funded basic and/or translational research programs in the field of viral or bacterial pathogenesis. Investigators will join a growing and interactive group of researchers with close ties to both basic science and clinical departments within the University, and joint appointments within graduate departments of the University of Michigan are available. Physician-scientists who are Board-certified/eligible in infectious diseases are encouraged to apply and will be provided protected time to conduct their research. Interested individuals should submit curriculum vitae, summary of research and career goals for junior applicants, and contact information for three references to: **Powel Kazanjian, M.D., Professor and Chief Division of Infectious Diseases, Department of Internal Medicine, 1500 E. Medical Center Drive, 3120 Taubman Center, Ann Arbor, MI 48109-0378.** *The University of Michigan is an Equal Opportunity Employer, women and other minorities are encouraged to apply.*

POSTDOCTORAL SCIENTIST
Immunology

Requirements: A Ph.D. in microbiology, immunology, or infectious disease with a strong background in immunology and previous specific experience in the separation of T cell subsets and flow cytometry techniques. Send curriculum vitae along with names and contact information for three professional references to:

Imtiaz A. Khan, Ph.D.
Department of Microbiology, Immunology and Tropical Medicine
The George Washington University
Ross Hall, Room 745
2300 I Street N.W.
Washington, DC 20037
Telephone: 202-994-2863
Fax: 202-994-2913
E-mail: mtmixk@gwumc.edu

TENURE-TRACK FACULTY POSITION
Plant Field Biology

The Department of Biology at the University of Central Arkansas (UCA) invites applications for a tenure-track faculty position in plant field biology. This appointment will be at the **ASSISTANT PROFESSOR** level and will begin August 15, 2007.

Applications are sought from outstanding individuals who value quality teaching and are dedicated to developing active research programs involving both undergraduate and graduate students. The individual hired will teach upper-division plant courses and contribute to our lower-division majors or non-majors curriculum. Preference will be given to candidates working at the community or systems level. The successful candidate will have opportunities to develop and teach other upper-division and graduate courses and to be involved in our interdisciplinary Environmental Science Program. For additional information, please visit **website: http://www.uca.edu/biology/.**

Candidates should submit curriculum vitae, statement of teaching philosophy, an outline of research plans indicating where students may participate, and the names and contact information for three references to: **Dr. Steven Runge, Department of Biology, 180 Lewis Science Center, University of Central Arkansas, Conway, AR 72035-5003.** Ph.D. required; recent Ph.D.s are encouraged to apply. Review of applications will begin on December 12, 2006, and continue until the position is filled. *University of Central Arkansas is an Equal Opportunity/Affirmative Action Employer.*

GENETICS AND MOLECULAR BIOLOGY
Biology, University of North Carolina

The University of North Carolina at Chapel Hill invites applications for a tenure-track position at the rank of **ASSISTANT PROFESSOR** in the Department of Biology to be effective on or after July 1, 2007. We encourage applications from individuals using genetic and molecular approaches in genetically tractable systems to investigate modern problems in the biosciences. Please submit curriculum vitae, statements of research plans and teaching interests, up to three publications, and four letters of recommendation to: **Dr. Kerry Bloom, Chair, Genetics and Molecular Biology Search Committee, Department of Biology, CB#3280, University of North Carolina-CH, Chapel Hill, NC 277599-3280.** See **website: http://www.bio.unc.edu/news/faculty/search** for details. Closing date: until filled; review of applications begins December 15, 2006. *The University of North Carolina is an Equal Opportunity Employer.*

Duke University has an opening for a **POST-DOCTORAL RESEARCH ASSOCIATE** in computational structural biology. The successful candidate will have a Ph.D. in computer science, computational biology, statistics, or other relevant mathematical science; experience applying his or her strong computational/mathematical skills to problems in structural or molecular biology, biophysics, or protein biochemistry; and enthusiasm for working within a world-class multi-institutional consortium toward an understanding of antibody-mediated neutralization of HIV and the discovery of novel vaccination strategies. He or she will work with **Professors Scott Schmidler** (statistical sciences) and **Tom Kepler** (biostatistics and bioinformatics, immunology) and the Gates Foundation Vaccine Discovery Antibody Consortium (VDAC). Review of applications will begin February 1, 2007, and continue until position is filled.

Please send curriculum vitae, letter of research interests, and three letters of recommendation to **Mr. Harrison Daniels (e-mail: harrison.daniels@duke.edu).**

FACULTY POSITION

The Department of Materials Science and Engineering at MIT invites applications for a tenure-track faculty position at the **ASSISTANT/ASSOCIATE PROFESSOR** level, to begin June 2007. Applicants should hold a Ph.D. in materials science and engineering or a related science or engineering discipline. The successful candidate will be expected to develop a vibrant research program at the forefront of the field, and to harness his/her expertise in curriculum development and teaching at the undergraduate and graduate levels. Research areas of interest include, but are not limited to: materials for energy applications, including novel solar energy systems, electrocatalysis and electrochemistry; materials processing, including green materials processing; crystal chemistry; materials chemistry; combinatorial materials science; clinical biomaterials; soft materials, including modeling; and electronic materials.

Applications received by February 15, 2007, will receive full consideration.

Applications submitted should include two copies of the following: complete curriculum vitae, a three to five-page statement of research and teaching interests, no more than three publications, and complete contact information for three references. Applications should be addressed to: **Department of Materials Science and Engineering, Attn: Esther Greaves Estwick, Room 8-328, Massachusetts Institute of Technology, 77 Massachusetts Avenue, Cambridge, MA 02139-4307.**

MIT has a strong and continued commitment to diversity in engineering education, research and practice, and especially encourages applications from women and minorities.

EXECUTIVE VICE PRESIDENT

National Disease Research Interchange (NDRI), a not-for-profit company providing scientists with human biomaterials for research, invites applications for Executive Vice President. The Executive Vice President will possess strong financial and organizational competencies with a minimum of ten years of experience working in a scientific environment requiring business management skills. Requires demonstrated success in negotiating sponsored research agreements, supervising technology joint ventures, and evaluating new science and technology.

Qualified candidates with an advanced degree in medicine or a Ph.D. in the biological sciences or medicine in molecular biology, immunology, genetics, pathology, or a related field are expected to have submitted successful grant applications to NIH and be familiar with NIH reporting requirements and leadership. Superior communication skills required. Computer expertise to include advanced spreadsheet, database, and reporting skills. Must have excellent analytic, writing, and presentation skills. An energetic team player committed to organizational growth and identification of new opportunities is required. Competitive salary and excellent benefits. E-mail curriculum vitae to **e-mail: smcgovern@ndriresource.org,** or fax to **S. McGovern** at **fax: 215-557-7154,** or mail to:

**Attn: S. McGovern
1628 John F. Kennedy Boulevard
8th Floor, 8 Penn Center
Philadelphia, PA 19103**

BIOLOGIST/PHYSIOLOGIST. Tenure-track, **ASSISTANT BIOLOGY PROFESSOR,** fall 2007. Ph.D. and commitment to teaching undergraduates required; postdoctoral research preferred. Responsibilities include teaching human anatomy and physiology, upper-level animal physiology and a course of candidate's choice, as well as supervising undergraduate research/internships. Submit letter of application, curriculum vitae, undergraduate and graduate transcripts, statements of teaching philosophy and research interests, and three letters of recommendation to: **Dr. Mary Mulcahy (e-mail: biology@upb.pitt.edu), Search Committee Chair, University of Pittsburgh at Bradford, 300 Campus Drive, Bradford, PA 16701 (website: http://www.upb.pitt.edu).** Review of completed applications will begin immediately, and continue until the position is filled. *Women and minorities are encouraged to apply. Affirmative Action/Equal Opportunity Employer.*

SWARTHMORE

The Department of Biology at Swarthmore College invites applications for two different one-year faculty leave replacement positions at the **ASSISTANT PROFESSOR** level, each beginning September 2007. Applicants should have a Ph.D., teaching experience, and a strong commitment to undergraduate education. All application materials should be received by January 10, 2007.

Evolutionary biology: Teaching responsibilities include a broadly based, intermediate-level course in evolution with weekly laboratories, an advanced seminar with laboratory in some area within evolutionary biology, and participation in the Department's team-taught introductory course in organismal and population biology. Applicants should submit curriculum vitae, three letters of recommendation, and a statement of teaching and research interests to: **Dr. Colin Purrington, Evolutionary Biology Search, Department of Biology, Swarthmore College, Swarthmore, PA 19081-1390.**

Developmental biology: Teaching is expected to include an intermediate-level laboratory course in developmental biology as well as an intermediate level course in one's area of special interest. Such a course would be expected to complement the Department's offerings during the fall semester in areas such as genomics, immunology, or stem cell biology. Interested persons should submit curriculum vitae, three letters of recommendation, and a statement of teaching and research interests to: **Dr. Scott Gilbert, Developmental Biology Search, Department of Biology, Swarthmore College, Swarthmore, PA 19081-1390.**

Swarthmore College is an Equal Opportunity Educator and Employer and specifically invites and encourages applications from women and minorities.

FACULTY POSITIONS
Environmental and Molecular Toxicology
EPV: 01-100-0605

The Department of Environmental and Molecular Toxicology at North Carolina State University (NCSU) is seeking two new faculty members. Two tenure-track positions are available, one at the **ASSISTANT PROFESSOR** level and one at the **ASSISTANT or ASSOCIATE PROFESSOR** level; rank will be commensurate with experience and training. Research areas of interest are those that complement the existing strengths in molecular/cellular and environmental/ecological toxicology, particularly neurotoxicology, molecular epidemiology, developmental/reproductive toxicology, and the application of omics technologies. Applicants must have a Ph.D. and postdoctoral experience. The successful candidate will develop or currently have a strong, independent, extramurally funded research program and contribute to graduate education/training. The Department is housed in a new, state-of-the-art research facility and offers Ph.D. and M.S. degrees. NCSU is located in the Research Triangle Park area, a world center for environmental health research.

To apply for this position: Submit an online application with your curriculum vitae, cover letter, statements of research and teaching goals, and the names and addresses of three references. Follow the instructions on the attached **website: https://jobs.ncsu.edu/applicants/jsp/shared/frameset/Frameset.jsp?time=1128453484872.**

Additional information about the Department can be found at **website: http://www.tox.ncsu.edu.** Review of applications will begin on December 15, 2006; search will remain open until positions are filled.

NC State University is an Equal Opportunity Employer/Affirmative Action Employer. Women and minorities are encouraged to apply. NC State welcomes all persons without regard to sexual orientation. ADA accommodations: Call the **Office of Equal Opportunity, telephone: 919-515-3148.**

THE RICHARD STOCKTON COLLEGE OF NEW JERSEY

Stockton is a nationally ranked public liberal arts college located on 1,600 acres in southern New Jersey about one hour from Philadelphia, two hours from New York City, and 20 minutes from Atlantic City. The College has a diverse array of programs and provides vast opportunities for interdisciplinary academic, pedagogic, and scholarly development in the sciences and mathematics. We are seeking outstanding candidates who show spark, insight, and commitment to both teaching and research to join us in September 2007, to meet the challenges of the 21st century as the College is about to embark on the design and construction of a 170,000 square-feet Unified Science Center. Applications are invited for tenure-track positions in the following programs of the Division of Natural Sciences and Mathematics: biology - **ASSISTANT PROFESSOR** in microbiology; chemistry - **ASSISTANT PROFESSOR** in physical chemistry; computational science - **ASSOCIATE/FULL PROFESSOR** in the physical sciences or mathematics.

For further information, please view employment opportunities at our **website: http://www2.stockton.edu.**

Screening will begin in early December 2006. Send a letter of application indicating the position of interest, resume, a brief statement about your teaching philosophy and research interests, and have three letters of recommendation sent to: **Dean Dennis Weiss, Natural Sciences and Mathematics, The Richard Stockton College of New Jersey, P.O. Box 195, AA29, Pomona, NJ 08240.** *Stockton is an Affirmative Action/Equal Opportunity Employer.*

TRAINING OPPORTUNITY IN BIONANOTECHNOLOGY

Funding is available to support **POSTDOCTORAL FELLOWS** and graduate students in an NIH roadmap funded Nanomedicine Development Center at Purdue University **(website: http://nihroadmap.nih.gov/nanomedicine/fundedresearch.asp).** Research includes engineering of biomotors, bionanotechnology, viral DNA packaging, RNA biochemistry, single molecule imaging and lipid/lipisome chemistry. Contact: **Peixuan Guo, Professor and Director, Bionanotechnology Interdisciplinary Graduate Program, and Principal Investigator of the Nanomedicine Development Center, Purdue University (e-mail: guop@purdue.edu).** *Purdue is an Equal Opportunity/Equal Access/Affirmative Action Employer. Women and minorities are strongly encouraged to apply.*

POSTDOCTORAL POSITIONS:
STEM CELLS IN NORMAL DEVELOPMENT AND CANCER

Two Postdoctoral Positions are immediately available to work on the role of neural stem cells in normal brain development and cancer. For examples of recent research projects, see the **website: http://www3.mdanderson.org/~genedev/majumder.html.** Experience in one of the following areas is required: mouse transgenic/knockout technology or culture and characterization of embryonic or neural stem cells. Please send curriculum vitae and names and addresses of three references to: **Sadhan Majumder, Department of Cancer Genetics, The University of Texas M.D. Anderson Cancer Center, Houston** by **e-mail: smajumder@mdanderson.org.**

The Office of Science, Department of Energy is seeking a motivated and highly qualified individual to serve as the **ASSOCIATE DIRECTOR,** Office of Biological and Environmental Research. As such, you will provide leadership and direction in establishing vision, strategic plans, goals, and objectives for the research activities supported. You may apply through two different methods, one is for a **SENIOR EXECUTIVE SERVICE** appointment and the second is for an **INTERGOVERNMENTAL PERSONNEL ACT** appointment. The announcement number is SES-SC-HQ-005. The announcement opens on November 6, 2006, and closes on December 21, 2006. Visit **website: http://www.usajobs.opm.gov/** for more information and for instructions concerning application procedures.

7th IBRO World Congress of Neuroscience

Melbourne, Australia
Melbourne Exhibition and Convention Centre

12-17 July 2007

Deadline for abstract submission 31st January 2007

Full program at www.ibro2007.org

EIGHT Plenary Lectures
Peter Agre
Norio Akaike / Lily Jan / Herta Flor
Edvard Moser / Simon Gandevia
Mu-Ming Poo / Mandyam Srinivasan

SIXTY FOUR Symposia
Workshops / Posters / Social events
Plus:
SEVENTEEN Satellite meetings

FIVE DAYS of
Top-class Brain
Science
Down Under!

Organising Committee Secretary: A.Lawrence@hfi.unimelb.edu.au
Conference Secretariat: ibro2007@sallyjayconferences.com.au

ETH
Eidgenössische Technische Hochschule Zürich
Swiss Federal Institute of Technology Zurich

Science City: International Sustainability Competition

ETH Zurich is pleased to announce the "International Sustainability Competition Science City". This is a global competition for interdisciplinary teams to provide ideas for how Science City can realize its vision of a new model for the sustainable integration of science and society. Teams from academic institutions are particularly encouraged to participate. Entrants will be asked to combine competencies from different fields, for example spatial planning, urban development, mobility, sociology, arts and culture, economics and management, and must demonstrate sound knowledge and experience in sustainability-related topics.

With Science City, ETH Zurich establishes a university campus where science and society can meet and which serves as a model for sustainability. Science City, located at Hoenggerberg near the center of Zurich, is much more than a conventional university campus. Science City embodies the vision of an urban neighborhood where people not only teach, study and conduct research, but where they also live, shop, socialize, exercise, attend cultural events and much more. It represents a culture of thinking and dialogue.

Information:
www.sciencecity.ethz.ch/internationalcompetition

Organisation/Contact:
Novatlantis – Sustainability at the ETH Domain
Tanja Lütolf, Tel: +41 44 305 94 65, **luetolf@novatlantis.ch**

Santa Fe Institute
2007 Complex Systems Summer Schools

SANTA FE: June 3-29, 2007, in Santa Fe, New Mexico, USA. Director: Dr. Dan Rockmore, Dartmouth College and SFI. Administered by the Santa Fe Institute (SFI).

BEIJING: July 8 to August 4, 2007, in Beijing, China. Sponsored by SFI in cooperation with The Institute of Theoretical Physics, the Chinese Academy of Sciences (CAS). Co-directors: Dr. David P. Feldman, College of the Atlantic and SFI, and Dr. Chen Xiao-song, Institute for Theoretical Physics, CAS.

The Complex Systems Summer School offers an intensive four-week introduction to complex behavior in mathematical, physical, living, and social systems for graduate students and postdoctoral fellows in the sciences and social sciences. The schools are for participants who want background and hands-on experience to help prepare them to do interdisciplinary research in areas related to complex systems.

Each school consists of an intensive series of lectures, laboratories, and discussion sessions focusing on foundational ideas, tools, and current topics in complex systems research. These include nonlinear dynamics and pattern formation, scaling theory, information theory and computation theory, adaptation and evolution, network structure and dynamics, adaptive computation techniques, computer modeling tools, and specific applications of these core topics to various disciplines. In addition, participants will formulate and carry out team projects related to topics covered in the school.

Applicants are welcome from all countries. Participants are expected to attend one school for the full four weeks. All activities will be conducted in English at both schools. No tuition is charged, and some support for housing and travel expenses is available. Enrollment is limited.

TO APPLY: Applications are welcomed from graduate students and postdoctoral fellows in any discipline. Some background in science and mathematics is required, as well as English language proficiency; see out website for specific requirements for each school. You may apply to either the Santa Fe or Beijing school, regardless of home country; however, placements may be influenced by restrictions in U.S. foreign visitor policies.

APPLICATION DEADLINE: All application materials must be electronically submitted or received at SFI no later than **January 19, 2007**.

For complete eligibility requirements and application instructions see http://www.santafe.edu/csss07.html, or e-mail summerschool@santafe.edu.

Women, minorities, and citizens of developing countries are especially encouraged to apply. These schools are partially supported by the National Science Foundation.

FACULTY POSITION IN DEVELOPMENTAL BIOLOGY/BIOLOGY ASSISTANT PROFESSOR
(Position Number 2-39370)

The Department of Biology at Auburn University, Montgomery, invites applications for a full-time tenure-track position at the Assistant Professor level to begin in August 2007. The position is for a nine-month appointment with the possibility of summer employment. Candidates must have an earned Ph.D. in developmental biology or a related field. *Foreign nationals should be authorized to work in the United States.* The faculty member will teach anatomy and physiology and other biology courses on a regular basis and developmental biology and other senior level courses on alternate years, advise students, perform departmental and University responsibilities, and engage in research. The Department promotes excellence in teaching and provides opportunities for research in biology. Research published in refereed journals will be required in order to obtain tenure and promotion.

Please submit a letter of application, current curriculum vitae that includes the names, addresses, and telephone numbers of at least three professional references, a statement of teaching philosophy, and a brief research outline to: **Dr. Nathan O. Okia, Department of Biology, Auburn University Montgomery, P.O. Box 244023, Montgomery, AL 36124-4023;** or via **e-mail: nokia@mail.aum.edu.** Review of applications will start immediately and continue until the position is filled. An official transcript will be required from individuals selected to interview for the position. *Auburn University Montgomery is an Affirmative Action, Equal Opportunity Employer.*

GENETICS AND MOLECULAR BIOLOGY
Department of Biology/Program in Molecular Biology and Biotechnology
University of North Carolina at Chapel Hill

The University of North Carolina at Chapel Hill invites applications for a tenure-track position at the rank of **ASSOCIATE or FULL PROFESSOR** in the Department of Biology and the Program in Molecular Biology and Technology, which is affiliated with the School of Medicine to be effective on or after July 1, 2007. We encourage applications from individuals using genetic molecular or biophysical approaches in genetically tractable systems to investigate modern problems in the biosciences. Please submit curriculum vitae, a statement of research plans and teaching interests, up to three publications and four letters of recommendation to: **Dr. Jeff Dangl, Chair, Senior Faculty Search Committee, Genetics and Molecular Biology, Department of Biology, Coker Hall, CB#3280, University of North Carolina-CH, Chapel Hill, NC 27599-3280.** See **website: http://www.bio.unc.edu/news/faculty/search** for details. Closing date: until filled; review of application begins December 15, 2006. *The University of North Carolina at Chapel Hill is an Equal Opportunity Employer.*

Two **OPTICAL MAPPING** positions are available for **POSTDOCTORAL/RESEARCH ASSOCIATE/RESEARCH ASSISTANT PROFESSORS** in cardiovascular MERIT research program. Research facilities include a state-of-the-art dual-channel high-speed imaging setup, whole organ and tissue culture facilities, and dedicated laboratory personnel. Interactions with the clinical cardiovascular medicine programs at the Veterans Affairs Medical Center and faulty in State Univesity of New York Downstate Physiology and Pharmacology Department are available. The candidates must have practical experience in optical mapping of biological signals using fluorescent dyes and background of biophysics of bioengineering. *The candidate must be a U.S. citizen or a permanent resident.*

Please send curriculum vitae and references to:
Nabil El-Sherif, M.D., Veterans Affairs Medical Center, 800 Poly Place, Brooklyn, NY 11209. Fax: 718-630-3740. E-mail: nelsherif@aol.com.

PURDUE UNIVERSITY, CROP SCIENCE, ASSISTANT PROFESSOR; Department of Agronomy (tenure-track, academic year appointment).
West Lafayette, Indiana. (Purdue posting 001724-2006.) Position available August 2007.

The Department of Agronomy seeks to fill a tenure-track faculty position in crop science. The successful candidate will provide leadership and scholarship in crop science teaching, research, and outreach. Emphasis will be on the creation of innovative approaches to crop science teaching and development of a nationally recognized, high-impact education program. The successful candidate is expected to teach courses in crop science (including the introductory crop science course each semester), mentor undergraduate and graduate students, and provide national leadership in curriculum and course development. A robust set of resources is available to support these activities including the Teaching Academy, the Purdue Discovery Learning Center, the Center for Instructional Excellence, and the Instructional Development Center. The Department has long recognized and rewarded the scholarship of teaching and learning.

Teaching responsibilities are to be complemented by collaborative, interdisciplinary, and externally funded crop science research. Potential research topics include, but are not limited to: precision agriculture; crop ecology, management, or physiology; seed science; crop breeding/genetics. Integration of economic analysis into teaching and research activities is expected. Collaborative work with biological and physical scientists and economists in the college of Agriculture and elsewhere is encouraged. The successful candidate is expected to disseminate agronomic and educational research findings through refereed journals and other peer-reviewed publications.

Candidates must have a Ph.D. in crop science, agronomy, or a closely related field, and have a demonstrated record of excellence in teaching and research. Candidates also must possess the interest and ability to interact with diverse groups of students and clientele. Experience in international dimensions of crop science is also desirable.

Salary is commensurate with education, training, and professional experience. Excellent fringe benefit package that includes TIAA-CREF retirement program, medical, life, and disability insurance, and sabbatical leave program.

Qualified individuals are requested to send a letter of application including a statement of teaching philosophy, research goals, curriculum vitae, and contact information for four references to: **Dr. Lee Schweitzer, Department of Agronomy, Purdue University, 915 W. State Street, West Lafayette, IN 47907-2054; telephone: 765-494-4774 (voice); fax: 765-496-2926, e-mail: lschweit@purdue.edu.** Application review will begin January 10, 2006, and continue until a successful candidate is identified. For more information, please contact: **Department Head, Craig Beyrouty (e-mail: beyrouty@purdue.edu)** or **Search Committee Chair, Lee Schweitzer (e-mail: lschweit@purdue.edu).** *Purdue University is an Affirmative Action/Equal Access/Equal Opportunity Employer. Women and individuals in underrepresented groups are encouraged to apply.*

We deliver — customized job alerts.

ScienceCareers.org
We know science — AAAS

THE STANFORD BIO-X FELLOW PROGRAM

The Stanford Bio-X Program is an interdisciplinary bio-related research program connected to biology and medicine. The Bio-X Fellow Program attracts young, highly talented researchers after their Ph.D. or first postdoctoral experience to start an independent, yet integrated research program with the potential of groundbreaking impact on biosciences. The Fellows are expected to creatively make use of the interdisciplinary resources of the Bio-X program and community. In this solicitation we are seeking a Fellow with research goals focusing on microbial systems.

For details of the posting please see **website: http://biox.stanford.edu/grant/pdf/fellow-program.pdf.**

Please send applications including curriculum vitae, plan research, and names of references to: **Professor Alfred M. Spormann (e-mail: spormann@stanford.edu).** Application deadline is December 3, 2006.

BRAIN TUMOR RESEARCH GRANTS
One-Year $100,000 Grants
Two-Year $200,000 Grants
Available in the United States and Canada
Letter of Intent Deadline: January 16, 2007

The Brain Tumor Society (BTS) is awarding grants to fund basic scientific and translational research directed at finding a cure for brain tumors. Grants are awarded annually at a maximum of $100,000 per year. Grants may be used for startup projects or supplementary funding. Funds cannot be used for indirect costs. Clinical projects will not be funded.

Letter of intent packets available on **website: http://www.tbts.org.**

BTS proudly announces a funding opportunity for specific research focused on juvenile pilocytic astrocytoma and other pediatric low-grade astrocytomas. Deadline for applications is February 15, 2007.

For more information and application packets visit **website: http://www.tbts.org.**

The world's most outstanding cancer research conferences

In the Forefront of Basic and Translational Cancer Research

January 21 - 25, 2007
Hilton Waikoloa Village, Waikoloa, HI
AACR/JCA 7th Joint Conference
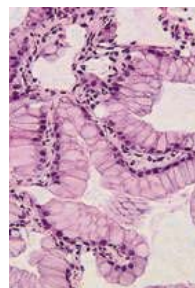
Advances and Challenges in Aerodigestive Epithelial Cancer Research: Genetics, Diagnosis, and Therapy

February 6 - 9, 2007
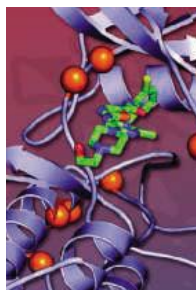Charleston Place Hotel, Charleston, SC

Oncogenomics 2007: Dissecting Cancer through Genome Research

January 31 - February 3, 2007
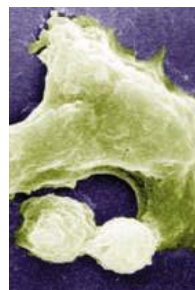Pointe Hilton Tapatio Cliffs, Phoenix, AZ

Translational Research at the Aging and Cancer Interface

February 20 - 23, 2007
Omni San Diego Hotel, San Diego, CA

Chemistry in Cancer Research: A Vital Partnership

February 4 - 7, 2007
Sheraton San Diego Hotel and Marina,
San Diego, CA
Joint conference with the American
Chemical Society

Advances in Proteomics in Cancer Research

February 27 - March 2, 2007
Amelia Island Plantation,
Amelia Island, FL

Visit our Web site at www.aacr.org
to register or for more information

AACR CENTENNIAL
1907 - 2007

*American Association
for Cancer Research*